Characterising microglial activation: refinement and validation of primary *in vitro* models

Sama Al-Shaheeb

Thesis submitted to Keele University for the degree of Doctor of Philosophy

June 2019

Abstract

Background: Neuroinflammation is common to many neurodegenerative conditions and is principally mediated by microglia. Microglia maintain homeostasis, respond to trauma/infection and can promote repair. This is achieved by switching between surveillance (M0), pro-inflammatory (M1) and pro-repair (M2) phenotypes. However, inappropriate phenotype switching contributes to neurodegeneration, through failure to clear harmful substances or even direct tissue damage. How inappropriate switching occurs is not fully understood. Therefore, identifying a model for assessing phenotypic changes would provide a powerful tool to investigate the roles of microglia in disease, and develop therapies based on microglial immunomodulation. Nanoparticles (NPs) may be key to delivering immunomodulatory drugs to the brain, but it is unknown whether NPs will provoke inflammatory microglial responses.

Methods: RT-qPCR was used to detect differences in gene expression for primary rat microglia, in response to various culture conditions and stimuli, including differently formulated NPs (e.g., PEGylated 'stealth' NPs and dextran 'control' NPs).

Results: Three microglia reference genes were validated for qPCR (*Gapdh*, *Usp14* and *Rpl32*). The presence of serum did not alter microglial activation state, compared to two commercially-available serum-free media. Cardinal M1 markers (*Il-6*, *Il-1β* and *Tnf-α*) were well-characterised in response to a wide range of lipopolysaccharide (LPS) concentrations, and at three different time points (2, 6 and 24 h). Unexpectedly, several pro-M2 stimuli (Il-4, Il-13 and Tgf-β) failed to alter M2 markers, even with multiple changes to the protocols. Microglia exhibited uptake of several NP types without inflammatory responses.

Conclusions: An *in vitro* model of microglial switching has been refined and validated for M1 responses. Further refinement is necessary for study of M2 switching. The NP data suggest that NPs could be used without unintended inflammatory responses.

Acknowledgements

With boundless love and appreciation, I would like to extend my heartfelt gratitude and appreciation to the people who helped me bring this thesis into reality. First and foremost, I would like to express my sincere gratitude to my supervisors Dr. David Morgan and Dr. Stuart Jenkins, whose expertise, consistent guidance, ample time spent, patience and consistent advice that helped me bring this thesis into success; my advisor Dr. Clare Hoskins for her supportive comments.

I owe a huge thanks to my country, Iraq and particularly my sponsor, the Higher Committee of Education Development in Iraq (the HCED)- Prime Minister Office- for providing the funding for this scholarship.

In addition, I owe a big thanks to Dr. Jan-Herman Kuiper, for his kind advices with statistical analysis. I would like to thank Professor Divya Chari, for providing the nanoparticles. Also to all her group Dr. Christopher Adams and Farhana Chowdhury for all the help and support during the laboratory work. Thanks are due to several students who assisted with some basic cell counting and morphological analysis of immunostained cells: Anna Biju (Nuffield summer project student, school level), Tiggs Gholamian (medical undergraduate, Keele University School of Medicine) and Bukunmi Okude (Masters student, Keele University School of Pharmacy).

I am grateful to all staff at Keele University School of Life Sciences and a special thanks to Jayne Bromley, Nigel Bowers and Chris Bain. I am thankful to many people in the School of Pharmacy, who created a wonderful working environment.

I owe a big thanks to my colleague Dr. Mohammed Aladul, who been a great friend, and provide constant support, you are one of the most beautiful things happen to me during this PhD. Also, I express my gratitude to the following people for their friendship and

scientific help during the project work: Dr. Jacqueline Tickle, Dr. Arwa Al-Shakli and Dr. Rawaa Salim Al-Mayyahi.

Lastly and personally, big thanks to my long-suffering husband, Athir Mohammed, thank you for all your patience and help throughout this crucial time of my life. Thank you, Athier, for always being my biggest supporter. Thank you to my wonderful daughter Shadan, who have kept me motivated and smiling through the highs and the lows of my PhD. Thank you all for bearing me even with my mood swings and being my greatest supporters. There are no proper words to convey my deep gratitude to my parents, my constant source of inspiration. Particularly, my forever interested, encouraging and always enthusiastic my mother, she was always keen to know what I was doing and how I was proceeding and big thank to my father (God bless his soul), who couldn't see me finish this PhD, I hope you are proud of me. Massive thanks to my sister and my brother for their long distance support and unconditional love. Words cannot explain how grateful I am to my family.

"Winners are not those who never fail, but those who never quit"

(Edwin Louis Cole)

Table of contents

List of figures

List of tables

List of abbreviations

Abbreviation	Meaning
AAV	Adeno-associated virus
ACTB	Beta-actin
AD	Alzheimer's disease
ADCF	Animal-derived component free
AGM	Aorta gonad mesonephros
AMPK	AMP-activated protein kinase
ANOVA	Analysis of variance
APCs	Antigen presenting cells
APP	Amyloid precursor protein
Arg1	Arginase-1
ATP	Adenosine triphosphate
BBB	Blood brain barrier
CCL	Chemokine (C-C motif) ligand
CD200	Cluster of differentiation 200
CD200R	CD200 receptor
CD45	Cluster of differentiation 45
cDNA	Complementary deoxyribonucleic acid
CMX	Carboxymethyl dextran
CNS	Central nervous system
COX-2	Cyclooxygenase 2
CPPs	Cell-penetrating peptides
CRP	C-reactive protein
Cq	Quantitation cycle
CSF	Cerebrospinal fluid
CSF1R	Colony stimulating factor 1 receptor
CX3CR1	Fractalkine receptor
CXCL	Chemokine (C-X-C motif) ligand
DAMPs	Damage-associated molecular patterns
DIV	Day *in vitro*
DMEM	Dulbecco's modified Eagle's medium
E	Embryonic day

ECM	Extracellular matrix
EDTA	Ethylene diamine tetraactic acid
ELISA	Enzyme-linked immunosorbent assay
EMP	Erythromyeloid progenitor
FBS	Fetal bovine serum
FcγR	Fc receptor for immunoglobulin G
FDA	Food and drug administration
Fizz1	Resistin-like molecule alpha
GA	Glatiramer acetate
GAPDH	Glyceraldehyde-3-phosphate dehydrogenase
gDNA	Genomic deoxyribonucleic acid
GOI	Genes of interest
GSK3	Glycogen synthase kinase 3
GSK3β	Glycogen synthase kinase-3 β
HAPI	Highly aggressively proliferating immortalised cell line
HDACs	Histone deacetylases
HMGB1	High-mobility group box-1
HSCs	Haematopoietic stem cells
Iba1	Ionized calcium binding adaptor molecule 1
IC	Immune complexes
IFN-γ	Interferon gamma
IGF-1	Insulin-like growth factor I
IgG	Immunoglobulin G
IL-	Interleukin-
iNOS	Inducible nitric oxide synthase
IRF8	Interferon regulatory factor 8
JAK2	Activating Janus kinase-2
LBP	Lipopolysaccharide-binding protein
LPS	Lipopolysaccharide
LRP	Low-density lipoprotein receptor-related protein
M0	Inactivated (default) microglial phenotype
M1	Initial reactive phenotypes
M2	Alternatively activated microglia
MAPKs	Mitogen-activated protein kinases

MDM	Monocyte-derived macrophages
MHC II	Major histocompatibility complex protein II
MIQE	Minimum information for publication of quantitative Real-Time PCR experiments
MMP	Matrix metalloproteinase
MMP-3	Matrix metallopeptidase 3
MNPs	Magnetic nanoparticles
Mo’	Priming microglia
MPS	Mononuclear phagocytise system
MPs	Myeloid precursors
MRI	Magnetic resonance imaging
MS	Multiple sclerosis
MYB	Transcriptional activator MYB
NADP	Nicotinamide adenine dinucleotide phosphate
NDS	Normal donkey serum
NED	N-(1-Naphthyl) ethylenediamine
NF-κB	Nuclear factor kappa-light-chain-enhancer of activated B cells
NO	Nitric oxide
NO^{2-}	Nitrite
NOD	Nucleotide binding oligomerisation domain
NPs	Nanoparticles
NSCs	Neural stem cells
PBS	Phosphate buffered saline
PD	Parkinson's disease
PDL	Poly-D-lysine
PEG	Polyethylene glycol
PET	Positron emission tomography
PFA	Paraformaldehyde
PPAR-γ	Peroxisome proliferator-activated receptor γ
PU.1	Transcription factor PU.1
qPCR	Quantitative polymerase chain reaction
RES	Reticuloendothelial system
RNA	Ribonucleic acid
RNA-seq	Ribonucleic acid sequencing
RNS	Reactive nitrogen species

ROS	Reactive oxygen species
RT	Reverse transcription
RUNX1	Runt-related transcription factor 1
SCI	Spinal cord injury
S.E.M.	Standard error of the mean
SF	Serum-free
STAT	Signal-transducers and activators of transcription
TBE	Tris-borate EDTA
TBI	Traumatic brain injury
TGF-β	Transforming growth factor β
Th1	T helper cells 1
THP-1	Tohoku Hospital Pediatrics-1 Macrophages cell line
TLRs	Toll-like receptors
TNFR	Tumour necrosis factor receptor
TNF-α	Tumour necrosis factor alpha
YM1	Chitinase 3-like protein 3

Note: Nomenclature and abbreviations differ among species, for this reason we have used *italic* for gene names while protein names in normal font. Similarly, uppercase and lowercase were used to distinguish between species: generally, for mouse and rat, gene names are written with an uppercase first letter and the rest in lowercase; for humans are written with all capital letters.

Chapter 1 : General introduction

1.1 Neurodegenerative disease: need to model and develop therapies

A major societal and economic concern for the world is the increasing prevalence of neurodegenerative diseases (e.g. dementia) as shown in Figure 1-1 for Europe (Prince *et al.* 2013). This represents a substantial burden for healthcare systems, estimated to cost $1 trillion worldwide, requiring expensive long-term treatment and personal care (WHO & Alzheimer's 2012). There are no cures, and current treatments are palliative and often needed until death (Alzheimer's Association 2018). So, better treatments are required to ease these burdens and ideally cure/reverse these diseases.

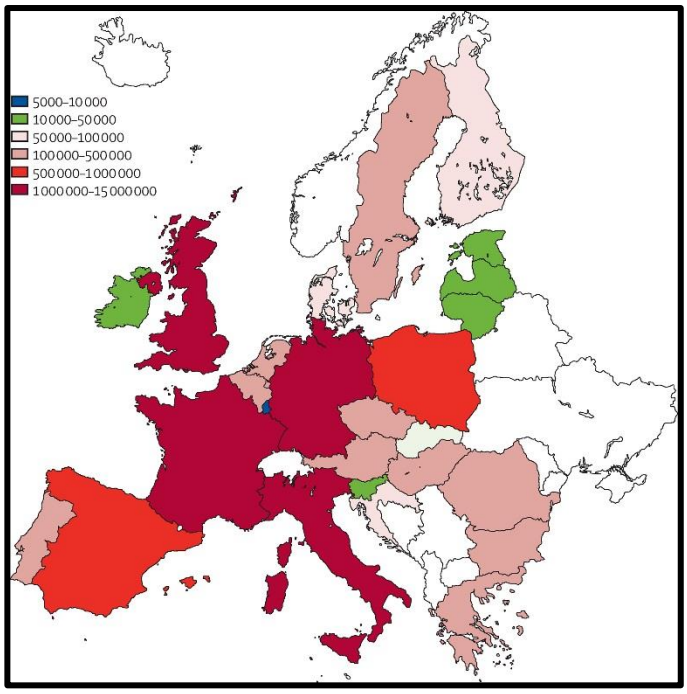

Figure 1-1: Prevalence of dementia in Europe. Adapted from Winblad *et al.* (2016)

Neuroinflammation is a term used to describe inflammation in the central nervous system (CNS; brain and spinal cord). It may be triggered by pathological events such as infection, trauma or disease associated molecules: e.g., amyloid β (Aβ) or α-synuclein misfolding/aggregation. Similar to peripheral inflammation, neuroinflammation can be acute or chronic. Acute neuroinflammation (e.g., CNS injury/trauma) is defined by brain's

immune cells response, production of inflammatory mediators (e.g., chemokines and cytokines) and phagocytic activity. Even though acute inflammation may lead to the production of destructive molecules, such as reactive oxygen and nitrogen species, this is usually short-lived and unlikely to damage healthy tissue (Buckley *et al.* 2001). Acute neuroinflammation is essential for minimising the adverse effects of injury and promoting recovery of the injured tissue.

In contrast, chronic neuroinflammation can cause neural tissue damage, and is a major feature of traumatic brain injury (TBI) and neurodegenerative diseases, such as multiple sclerosis (MS), Alzheimer's disease (AD) and Parkinson's disease (PD). Acute inflammation should resolve itself through anti-inflammatory signalling, restoring homeostasis to the tissue (Medzhitov 2008). However, failure to resolve, results in chronic pro-inflammatory activation. The destructive features of this can ultimately damage healthy neural tissue, which causes more release of pro-inflammation cytokines, continuing a feedforward loop. As opposed to the acute neuroinflammation, chronic neuroinflammation can have harmful outcomes in the brain.

Studies have provided a lot of evidences that chronic neuroinflammation has roles in the development and progression of many neurodegenerative diseases. For example, AD is usually associated with chronic neuroinflammation and increased levels of many pro-inflammatory cytokines (Qiao *et al.* 2001). In AD, it has been suggested that neuroinflammation might be a crucial link between Aβ deposits, tau pathology and clinical symptoms (Boon *et al.* 2018). In another study, results from analysis of the cerebrospinal fluid (CSF) sample of patients with AD indicated a high level of inflammatory markers being strongly associated with Aβ-positive individuals (Janelidze *et al.* 2018) (discussed in section 1.7.1). The inappropriate expression or overexpression of these pro-inflammatory cytokines can lead to neuronal dysfunction and death in neurodegenerative disease (Modi *et al.* 2010).

Neuroinflammation in neurodegenerative diseases has been suggested to be mediated at least in part by the microglia, as evidence suggested an increased accumulation of these cells in neurodegenerative tissue (Ransohoff, 2016). Microglia have important roles in maintaining CNS homeostasis, however a change in activation state in neurodegeneration from proactive helpful to harmful state, might ultimately play a critical role in disease pathogenesis (Dorothée 2018). Therefore, microglia could provide an attractive therapeutic target for the treatment of neurodegenerative diseases.

1.2 The role of microglia in brain homeostasis and proteopathy

Microglia are specialised form of immune cells in the CNS (Stollg & Jander 1999). In healthy tissue, microglia are similar to macrophages that scan their environment and engulf invading pathogen, therefore, microglia are considered the brain's first line defence and are essential for its homeostasis (Hefendehl *et al.* 2014). The initial understanding of microglia came from macrophages. Therefore, a growing body of evidence suggests that like macrophages, microglia can be activated to adopt different states/phenotypes depending on challenging stimuli (Carson *et al.* 2007; Hanisch & Kettenmann 2007; Colton 2009; Varnum & Ikezu 2012; Tang & Le 2015). Macrophages are activated in response to microbial infection or innate danger signals by producing toxic substances (e.g., nitric oxide, NO), this activation state typically called M1 (mirroring T-helper cell 1, Th1) (Italiani & Boraschi 2014). The M1 activation state is typically followed by the repair state, typically called M2 (mirroring T-helper cell 2, Th2) (Mantovani *et al.* 2004). The repair action could be explained by arginine/NO pathway since this pathway would decrease the amount of arginine available for NO synthesis and the pathway itself produces ornithine which feeds into the downstream of polyamine and proline syntheses pathways. Polyamine and proline are important for proliferation and tissue repair (Rath *et al.* 2014). As originally established

in macrophages, the initial microglial pro-inflammatory M1 phenotype may converts to repair-orientated activity profiles (alternatively activated microglia; M2) (Liu *et al.* 2012). Under normal conditions, microglia should eventually return to the resting state M0 (Blaylock & Maroon, 2011) (Figure 1-2).

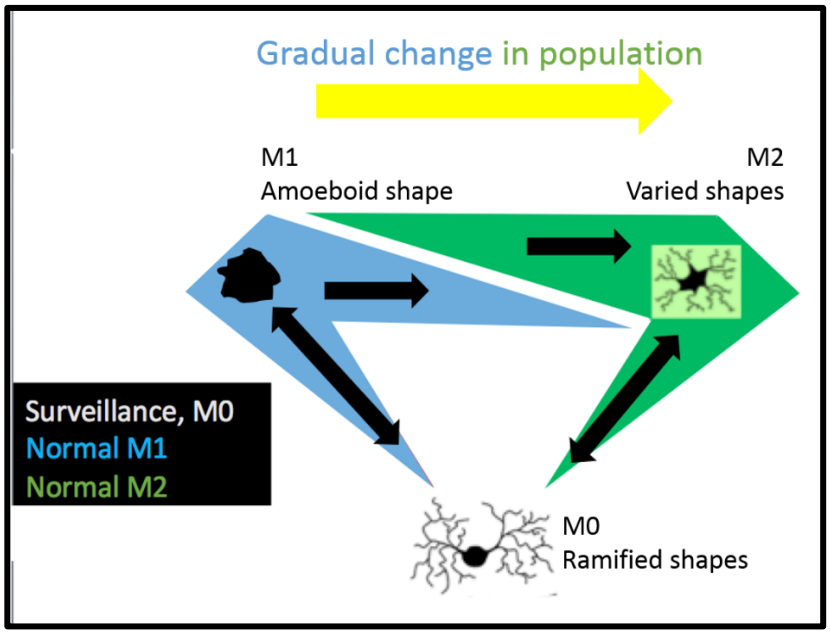

Figure 1-2: Schematic diagram illustrating proposed microglia phenotype switching: activation and expected return to 'resting' or 'surveillance' state. This illustrates population-level changes, not an individual cell. For example, 50 % the microglia may exhibit an M1 phenotype, while the other 50 % may exhibit an M2 phenotype.

Appropriate changes between phenotypes are important for coping with disease. For example, M1 activation in injury produces pro-inflammatory responses to kill damaged cells, preventing damage from propagating neighbouring cells, but should typically be followed by the M2 phenotype to phagocyte cell debris, enhance tissue repair, and produce anti-inflammatory factors that end the neuroinflammation (Tang & Le 2015). Sometimes, cells fail to resolve back to M0 state, as a result of lost specific function (e.g., ineffective phagocytosis) or undergoing inappropriate activation (e.g., aggregated α-synuclein in PD or Aβ plaques in AD, which could induce a chronic M1 activation, that eventually leads to an irreversible neuronal death (Lee *et al.* 2013)). Therefore, developing a therapy that has the

ability to resolve the activation, restore microglial function and/or phenotype switching would be of great benefit in this field.

1.3 Microglial origins and phenotypes

Although microglia are developed from different progenitor cells and within a unique environment compared to other innate immune cells, microglia are frequently called 'brain macrophages'. Furthermore, microglia share functional similarities with macrophages resident in peripheral tissues. Early histological observations noted that microglia could exhibit ramified or amoeboid morphologies (Figure 1-2). A wider variety of phenotypes have been described, based on markers and behaviours similar to those of macrophages. This led to the adoption of similar terminology for both. The inactivated (default) microglial phenotype, present throughout the 'healthy' CNS, is often described as 'resting'. However, this term failed to reflect the high levels of activity displayed by these cells, which actively survey their local microenvironment using highly motile processes (video file submitted with thesis, Video 1; internet link: youtube.com/watch?v=OVE1AL7xmwE). Here, this phenotype will be termed M0, with the activated phenotypes being referred to as M1 (also known as 'classically activated') or M2 ('alternatively activated'). These major phenotypes would be described in the sections 1.4.1, 1.4.2 and 1.4.3.

1.3.1 Microglial development: features unique to parenchymal microglia

While all other resident cells in the CNS are derived from the neuroectoderm (Kang *et al.* 2010), microglial precursors are developed from myeloid progenitors in the yolk sac and make a journey into the brain early in embryonic development (Figure 1-3) (Kierdorf *et al.* 2013). Although sharing similarities with macrophages from other sources, microglia are a distinct population, with properties that differentiate them from other tissue-resident immune cells (Figure 1-4). In the mature CNS, microglia are not typically replenished from bone

marrow cells (as peripheral immune cells are) but can self-renew from mature microglia as required (Bruttger *et al.* 2015).

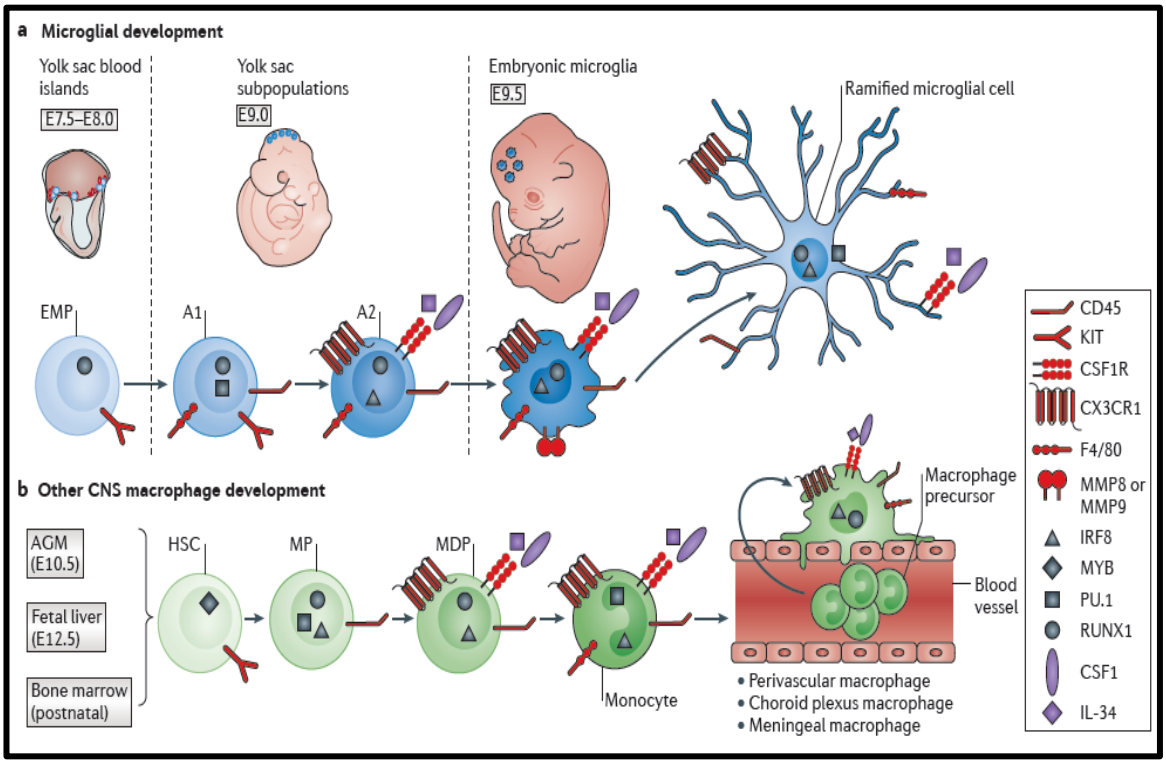

Figure 1-3: Microglial precursors originate in the yolk sac, and express similar markers to peripheral macrophages during development. (a) Microglia are specialised immune cells found throughout the CNS parenchyma. (b) Some brain macrophages (e.g., pericytes, which are associated with blood vessels) are proposed to be generated by infiltration from the periphery, although this is likely limited to perivascular areas, including the choroid plexus and meninges. AGM, aorta gonad mesonephros; CD45, cluster of differentiation; CSF1R, colony stimulating factor 1 receptor; CX3CR1, fractalkine receptor; E, embryonic day; EMP, erythromyeloid progenitor; HSCs, haematopoietic stem cells; IL-34, interleukin-34; IRF8, interferon regulatory factor 8; MMP, matrix metalloproteinase; MPs, myeloid precursors; MYB, transcriptional activator MYB; PU.1, transcription factor PU.1; RUNX1, runt-related transcription factor 1. Adapted from Prinz & Priller (2014).

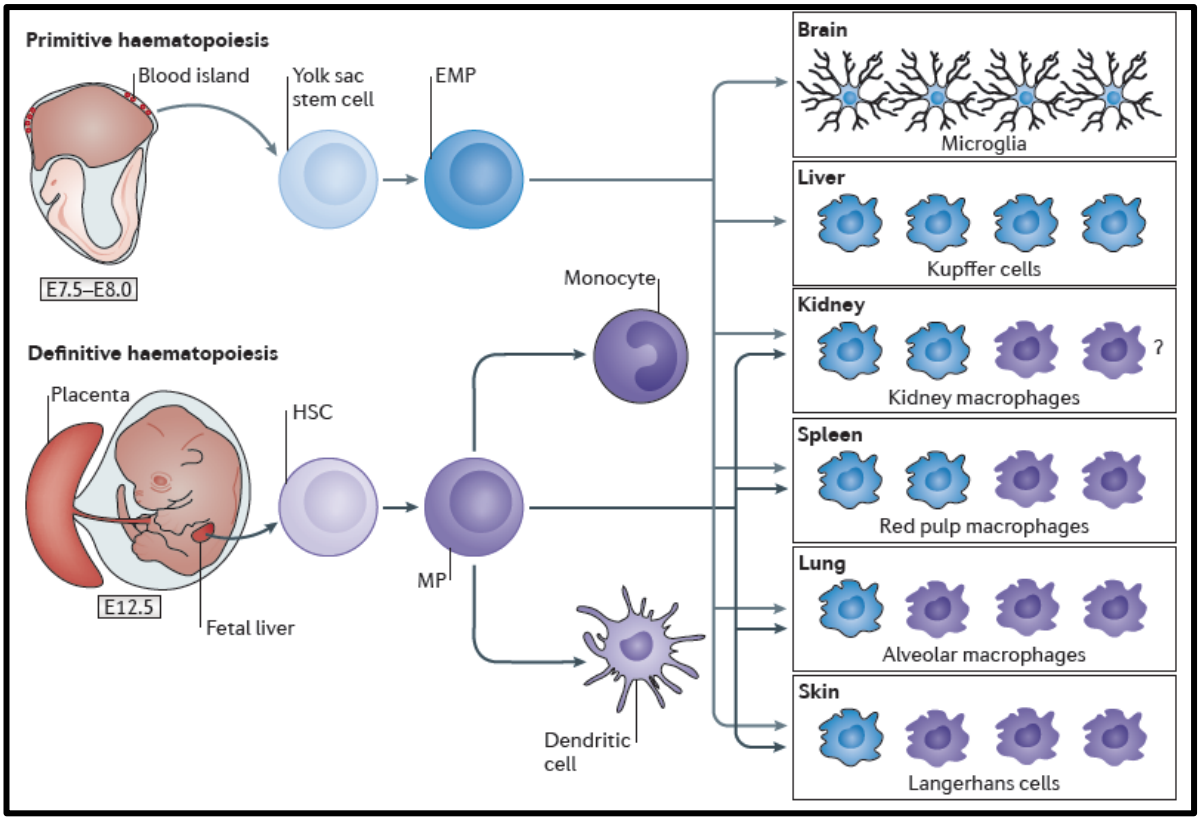

Figure 1-4: Development of resident macrophages in different tissues . Tissue-resident macrophages in the brain are predominantly microglia, derived from the yolk sac. Immune cells from both yolk sac and 'definitive haematopoiesis', which occurs in the foetal liver, typically populate other tissues. This difference contributes to the unique profiles and behaviours of microglia compared to other macrophages. For example, microglia have greater longevity and capacity for self-renewal. E, embryonic day; EMP, erythromyeloid progenitor; HSCs, haematopoietic stem cells; MPs, myeloid precursors. Adapted from Prinz & Priller (2014)

Although microglia are considered to be macrophages, with similar immune regulatory functions (surveillance and debris removal), and share macrophages-specific markers such as ionized calcium binding adaptor molecule 1 (Iba1) and fractalkine receptor (Cx3cr1) (Prinz & Priller 2014). Studies have identified a number of signature genes expressed only in microglia and not in other macrophages, such as *Sall1, P2ry12* and *Tmem119* (Hickman *et al.* 2013; Bennett *et al.* 2016; Koso *et al.* 2016). Parenchymal microglia have a self-renewal ability, but most other tissue-resident macrophages (Figure 1-3) can be renewed from monocytes (immune cells from bloodstream) which in turn are constantly replenished by the differentiation of hematopoietic stem cells (HSCs). This

explains why microglia are more prone to becoming senescent than peripheral macrophages, the same pool of cells makes new microglia throughout life, and they are not renewed from bone marrow. So, microglia and macrophages can be represented as two distinct populations (Prinz *et al.* 2011). Therefore, it is important to study microglia, not just assume literature on peripheral immune cells will predict microglia behaviour.

1.4 Microglial activation is poorly understood (M1/M2 model system)

Microglia exhibit a wide variety of behaviours mainly intended to destroy foreign matter and remove debris, with roles in brain development and remodelling, infection and trauma. To achieve these effects, microglia can reversibly alter their phenotypes between an 'inactivated' state and various 'activated' states including a pro-inflammatory phenotype that induces neuroinflammation. Microglia are activated in response to different pathological states within the CNS including injury, ischemia and infection. The subsequent neuroinflammation produces pro-inflammatory cytokines such as interleukin (Il)-1β, Il-6 and tumour necrosis factor alpha (Tnf-α), although this pro-inflammatory response is important in fighting infections and removing damaged "self" cells, it could be toxic to other healthy neural cells (Smith *et al.* 2012). Tnf-α may directly mediate apoptosis by interaction with tumour necrosis factor receptor (TNFR). The actions of Il-1 in inducing apoptosis are less clearly defined but appear to be dependent on the presence or absence of additional cytokines and signalling molecules. For example, Il-1 has been shown to promote cell death when combined with either interferon gamma (IFN-γ) or TNF-α in primary human neuron cultures (Chao *et al.* 1995). Pro-inflammatory cytokines can also contribute to damage of neurons and glia by promoting the transfer of peripheral immune cells into the CNS.

Some markers have been reported for the identification of microglial activation state, but it has become obvious that more detailed analyses are required. As different microglial phenotypes can perform different functions, an assessment that involves the

identification of specific microglial phenotypes is required. Inactivated M0 microglia have few unambiguous markers/hallmarks. Activated microglia have been classified broadly into M1 and M2 phenotypes, but a number of M2 subtypes have also been proposed, based on a wide variety of markers. Although considerable researches have been devoted to establishing which markers most reliably identify each phenotype, M1 and M2 are *in vitro* phenotypes and the *in vivo* situation is not fully clear cut.

Table 1-1: Microglial phenotypes, roles and proposed markers.

Subtype	Induced by	Cytokines	Chemokines	Phenotypic markers	References
M0	Cd200		Cx3cr1	Cd200R	(Ponomarev *et al.* 2005; Li *et al.* 2007; Zhang *et al.* 2011)
M1	Ifnγ, LPS–TLR4 signalling	Il-1, Il-6, Il-12, Il-15, Il-23, Tnf-α.	Ccl8, Ccl15, Ccl19, Ccl20, Cxcl9, Cxcl10, Cxcl11, Cxcl13.	Il-6, Il-1β, Tnf-α, Cox-2, iNos.	(Kaneko *et al.* 1989; Masliah *et al.* 1991; Letiembre *et al.* 2009; Chhor *et al.* 2013; Kobayashi *et al.* 2013; Brites & Vaz 2014; Szulzewsky *et al.* 2015; Walker & Lue 2015)
M2a	Il-4 or Il-13	Tgf-β, Il-10, Il-1Ra, fibronectin 1, Igf-1.	Ccl13, Ccl14, Ccl17, Ccl18, Ccl22, Ccl23, Ccl24, Ccl26.	Arg1, Ym1, Fizz1.	(Martinez *et al.* 2006; Chhor *et al.* 2013; Lisi *et al.* 2014; Peferoen *et al.* 2015; Walker & Lue 2015)
M2b	Immune complexes (binding of fcγR) and Il-1β or LPS	Il-10, Tnf-α, Il-1 β, Il-6.	Ccl1, Ccl20, Cxcl1, Cxcl2, Cxcl3.	Il-10^{high}, Il-12^{low}, MHC II, Cd86.	(Chhor *et al.* 2013; Lisi *et al.* 2014; Gensel & Zhang 2015)
M2c	Il-10, Tgf-β or glucocorticoids	None known	Ccl16, Ccl18, Cxcl13.	Tgf-β, Arg1, Cd163, Cd206.	(Mantovani *et al.* 2004; Chhor *et al.* 2013; Novak & Koh 2013; Pey *et al.* 2014; Mecha *et al.* 2015)

Arg1, Arginase 1; Ccl, Chemokine (C-C motif) ligand; Cd86, Cluster of differentiation 86; Cd163, Cluster of differentiation 163; Cd200, Cluster of differentiation 200; Cd200R, Cluster of differentiation 200 receptor; Cd206, Cluster of differentiation 206; Cox-2, cyclooxygenase 2; Cx3cr1, fractalkine receptor; Cxcl, Chemokine (C-X-C motif) ligand; FcγR, Fc receptor for immunoglobulin G; Fizz1, Resistin-like molecule alpha; Ifn-γ, interferon-γ; Igf-1, insulin-like growth factor 1; Il-, interleukin-; iNos, inducible nitric oxide synthase; LPS, lipopolysaccharide; MHC II, Major Histocompatibility Complex Protein II; Tgf-β, transforming growth factor β; TLR, Toll-like receptor; Tnf-α, tumour necrosis factor; Ym1, chitinase 3-like protein 3. Table adapted from David & Kroner (2011).

1.4.1 Resting microglial (M0)

1.4.1.1 Actions of M0 microglia

The resting/quiescent microglial phenotype M0 is also called 'ramified microglia', because it is characterised by a small soma with many fine branched (ramified) cellular processes (Brites & Vaz 2014). Although described as 'inactive' or 'resting', M0 microglia are physiologically active, showing pinocytosis (uptake) activity and a high degree of process motility (Fetler & Amigorena 2005). The classical thought was that the main purpose of this phenotype is to provide a constant amount of microglia to sense and fight infection (Aloisi 2001), with their processes screening the environment, making them the monitor of the CNS (Vinet *et al.* 2012). However, the published evidence reports that M0 microglia have active roles in development, homeostasis and brain remodelling. For example, microglia can secrete neurotrophic factors (Saijo & Glass 2011) and also play an important part in neuronal activity, including structural and functional plasticity (Tremblay *et al.* 2010).

1.4.1.2 Mediators and markers characteristic of M0 microglia

The M0 phenotype has a fewer reported markers than other phenotypes. Bertolotto *et al.* (1995) reported that keratan sulphate epitope is expressed by ramified microglia in adult rats (recognised by monoclonal antibody 5D4) on their surface, unlike peripheral macrophages and other microglial phenotypes. Thiamine pyrophosphatase is another selective marker for ramified microglia (Glenn *et al.* 1992). Major histocompatibility complex protein II (MHC II) is present in M0 microglia, but as co-stimulatory molecules are not present, M0 microglia cannot function as antigen presenting cells (Li *et al.* 2007) (microglia antigen presentation is discussed in section 1.6). Although few markers have been suggested to be M0 markers, from my review of the literature nobody has attempted to characterise this phenotype.

1.4.1.3 Presence of M0 phenotype

M0 microglia are present in a normal healthy condition, and so are considered to be the default phenotype, rather than an 'activated' form (Vinet *et al.* 2012). *In vitro*, untreated microglia are often considered to be M0, but this should be investigated in greater detail, as the derivation process can be expected to provide activating stimuli, and culture conditions may also lead to activation (Butovsky *et al.* 2014). Microglia maintain the M0 state through cluster of differentiation 200 (Cd200), which is expressed by neurons and acts on the Cd200 receptor (Cd200R) (Zhang *et al.* 2011). This Cd200-Cd200R signalling may play an important role in keeping the microglia in the resting state, as neuronal loss leads to loss of this signal and subsequent microglial activation (Gorczynski *et al.* 2004). Similar to Cd200-Cd200R signalling, signals such as fractalkine (Cx3cl1), which is expressed by neurons, and interacts with microglial fractalkine receptors (Cx3cr1) to maintain them in the M0 phenotype (Verge *et al.* 2004).

1.4.1.4 Controlling M0 microglia

In healthy conditions, M0 is the dominant microglial phenotype (Nimmerjahn *et al.* 2005). M0 changes to other microglial phenotypes in response to various stimuli, e.g., neuronal 'distress' signals, trauma, injury, neurodegenerative diseases (Haynes *et al.* 2006). It has been suggested that resting microglia do not convert to an active state directly, but they might pass through a 'primed' M0 stage first (Blaylock 2013). Furthermore, resting microglia can be stimulated through damage-associated molecular patterns (DAMPs) (DAMPs are endogenous molecules released from cells into cytoplasm after CNS injury) or pathogen-associated molecular patterns (PAMPs) such as lipopolysaccharide (LPS), which interact with adenosine triphosphate (ATP) receptors or Toll-like receptors (TLRs) (Mosser & Edwards 2008). Upon receiving these signals, microglia direct their processes towards the site of injury then retract the processes and become motile cells travelling to that location

(Davalos *et al.* 2005), often adopting an amoeboid morphology (Hailer *et al.* 1999). Depending on which signal is received, microglia can shift to either M1 phenotype (e.g., in response to LPS) or M2 phenotype (e.g., in response to interleukin 4, Il-4) (Gordon & Martinez 2010).

1.4.2 Activation microglial (M1)

1.4.2.1 Actions of M1 microglia

Microglia in classical activation state (M1 microglia) are an important player in defence against most foreign substances (Ridolfi *et al.* 2013). M1 microglia produce redox molecules such as reactive nitrogen species (RNS) (e.g., NO and inducible nitric oxide synthase, iNos) and reactive oxygen species (ROS) (Liao *et al.* 2012). However, an excessive amounts of these substances could damage cell membranes of neuron and other glia cells.

M1 response also includes an expression of pro-inflammatory cytokines such as Tnf-α, Il-1β, Il-12, Il-1α, Il-6 and Il-23. These cytokines play an important roles; Tnf-α plays a role in the control of neuronal survival (Gururaja *et al.* 2007). Collectively, Il-1β, Il-6 and Tnf-α impart neuroprotection both *in vivo* and *in vitro* (Carlson *et al.* 1999). However, the mechanism of action of these proinflammatory cytokines is not fully clear and there is increasing evidence to suggest that pro-inflammatory cytokine might have a role in neuronal degeneration (Smith *et al.* 2012).

Furthermore, M1 microglia have the ability to produce inflammatory chemokines (C-C motif) ligand e.g., Ccl8, Ccl20 and Ccl15 (Orihuela *et al.* 2016), which are produced during infections or as a response to an inflammatory stimulus and facilitating immune response. Chemokines attract microglia to the infection site to destroy the pathogens (Ramesh *et al.* 2013).

Additionally, M1 microglia can act as antigen presenting cells (APCs) due to their expression of co-stimulatory molecules (e.g., Cd86) on the surface of the cell (Taylor & Sansing 2013). Together, MHC II and Cd86 expression in M1 microglia can activates T-cells (discussed in section 1.6).

M1 microglia are proposed to exhibit phagocytosis (discussed in section 1.5), enabling the engulfment of dead cells, debris and pathogens, which is critical in reconstruction and reorganisation of neuronal networking, e.g., in the case of brain injury (Mantovani *et al.* 2002). Other reports suggested that phagocytosis is also performed by M2 phenotypes, making phagocytosis less useful as a phenotype marker (Fumagalli *et al.* 2015).

1.4.2.2 Mediators and markers characteristic of M1 microglia

Despite a wealth of literature describing microglia M1 phenotype markers (e.g., Cd86 (Kobayashi *et al.* 2013), Il-1β, Il-6 and Tnf-α (Brites & Vaz 2014)) however, the most reliable marker seems to be iNos (Chhor *et al.* 2013) (see section 5.1.2 which further explains the role of these markers). The significance of these contradictory reports might reveals the limitations of the current discrete classification system; therefore, it has been proposed that activated microglia can adopt phenotypes along a spectrum, and so simultaneously display 'markers' of multiple phenotypes (Chhor *et al.* 2013).

1.4.2.3 Activation of the M1 phenotype

Physiologically, M1 is associated with ageing, infections and neurodegenerative diseases (Harry 2013). In the laboratory, M1 activation is reliably induced by exposure to LPS and/or Interferon gamma (Ifn-γ) (Walker & Lue 2015), which leads to activation of TLR4 or Ifn-γ receptors 1 and 2, respectively. For both stimuli, this causes stimulation of NF-κB and signal-transducers and activators of transcription 1 (STAT1), increase in iNos, secretion of pro-inflammatory cytokines, chemokines, and overflow of ROS and RNS

(Orihuela *et al.* 2016). These responses can recruit other immune cells (including by antigen presentation) and destroy foreign pathogens (Orihuela *et al.* 2016).

1.4.3 Alternative activation microglial (M2)

The M2 microglial phenotype is usually referred to as 'alternatively activated', and broadly described as anti-inflammatory. However, it has recently been proposed that M2 microglia could be divided into several subtypes: M2a, M2b and M2c. Each subtype is reported to perform different functions and express a different combination of genes/proteins, although there is substantial overlap between these. Many published articles continued to refer to M2 microglia, without distinguishing between these subtypes. Microglia routinely adopt M2 phenotypes upon resolution of inflammatory events, and possibly under other circumstances such as in early stage of AD (Tang & Le 2015).

1.4.3.1 M2a

1.4.3.1.1 Actions of M2a microglia

M2a is an alternate activation phenotype. M2a microglia secrete a range of anti-inflammatory molecules (e.g., Il-1Ra and Tgf-β) (Chhor *et al.* 2013). Therefore, the main function of this phenotype is inflammatory suppression (Cherry *et al.* 2014) by decreasing M1 microglia cytokines and other pro-inflammatory mediators (Mosser & Edwards 2008). Furthermore, M2a microglia have the ability to promote tissue repair (Walker & Lue 2015) via production of repair-promoting molecules such as Arginase-1 (Arg1), Chitinase 3-like protein 3 (Ym1) and Resistin-like molecule alpha (Fizz1). The proline and polyamine produced in Arg1 pathway has a high impact in tissue repair . Ym1 has an important roles in the protection of the extracellular matrix (ECM) especially during injury (Hung *et al.* 2002). M2a also produces insulin-like growth factor 1 (Igf-1) that helps in the resolution of

inflammation and enhances neuronal survival and phagocytosis (see section 1.5) (Cherry *et al.* 2013; 2014). Furthermore, M2a could be a neuroprotective phenotype (Chhor *et al.* 2013). There are some evidences to suggest that M2a microglia function may be impaired with age (as discussed in section 6.1.2), and this may have consequences for late-onset metabolic and neurodegenerative diseases (Fenn *et al.* 2014).

1.4.3.1.2 Mediators and markers characteristic of M2a microglia

Reports showed that Arg1, Fizz1 and Ym1 can be considered as a M2a microglia markers (Chhor *et al.* 2013; Orihuela *et al.* 2016). Furthermore, M2a microglia have been reported to produce macrophages mannose receptors: Cd206 and Cd209 (Peferoen *et al.* 2015), and chemokines Ccl22, Ccl13, Ccl17 and Ccl23 (Martinez *et al.* 2006). However, Arg1 is the most commonly used marker for M2a phenotype identification (Lisi *et al.* 2014).

1.4.3.1.3 Activation of M2a phenotype

M2a microglia are activated in response to extracellular stimuli such as spinal cord injury (SCI), and potentially play a role in survival, repair and growth processes (David & Kroner 2011). Walker & Lue (2015) *in vitro* study, showed that M2a microglia are reliably induced in response to Il-4 or Il-13. Both Il-4 and Il-13 interact with Il-4R to induce several processes that lead to effective anti-inflammatory functions, such as Arg1 up-regulation, inhibition of NF-κB isoforms and production of scavenger receptors for phagocytosis (Cherry *et al.* 2014).

1.4.3.2 M2b

1.4.3.2.1 Actions of M2b microglia

M2b is an immune regulatory phenotype (Chhor *et al.* 2013). M2b microglia are unique in their ability to produce high levels of anti-inflammatory cytokine Il-10 and low

level of Il-12 (Mosser 2003). Furthermore M2b microglia have the ability to produce pro-inflammatory cytokines such as Tnf-α, Il-6 and Il-1β (David & Kroner 2011). This suggests that M2b expresses the same genes as M1 and M2c, and explains their ability to adopt complex function of both inflammation and tissue repair (Fenn *et al.* 2012).

1.4.3.2.2 Mediators and markers characteristic of M2b microglia

Available evidence indicates that no specific markers for M2b exists since this phenotype is capable of producing both pro- and anti-inflammatory cytokines (e.g., Il-1β, Il-6, Tnf-α, MHC II, Cd86, Il-10 and Cd163; see Table 1-1) (Chhor *et al.* 2013; Lisi *et al.* 2014; Gensel & Zhang 2015). Therefore, it has been suggested that a high cytokine Il-10 with low Il-12 might be a M2b marker.

1.4.3.2.3 Activation of the M2b phenotype

Although, few studies have reported the induction of M2b, it has been suggested that a combination of either immunoglobulin G (IgG), TLR agonists and Il-1R or immunoglobulin Fc gamma receptor (FcγRs: Cd16, Cd32 or Cd64) ligands can be used to generate M2b microglia *in vitro* (Chhor *et al.* 2013). Furthermore, only one study has suggested that adult microglia adopt M2b (as indicate by high level of Il-10 and low level of Il-12) (Fenn *et al.* 2012).

1.4.3.3 M2c

1.4.3.3.1 Actions of M2c microglia

The acquired-deactivating (M2c) phenotype has an immunosuppressive function (Gensel & Zhang 2015). Microglial morphology in this phenotype has been suggested to be "round with multiple microspikes" (Mecha *et al.* 2015). The M2c microglia are sometimes

referred to as deactivated , however this description seems to be unhelpful, since M2c appears to be associated with tissue remodelling, matrix deposition after inflammation (Cherry *et al.* 2014), involved in the innate immune response suppression (Mandrekar-Colucci & Landreth 2010) and debris scavenging (David & Kroner 2011). Additionally, M2c microglia can increase neural stem cell (NSC) proliferation (Kiyota *et al.* 2012), down-regulate pro-inflammatory microglia (Varnum & Ikezu 2012), up-regulate cytokine Tgf-β (Appel *et al.* 2010) and down-regulate factors that contribute to APC function, such as MHC II (Gordon 2003).

1.4.3.3.2 Mediators and markers characteristic of M2c microglia

Reports have shown that M2c have several markers such as Cd206 (Gensel & Zhang 2015), Cd163 (Pey *et al.* 2014), scavenger receptor A and B and Cd204 (Table 1-1) (Varnum & Ikezu 2012). But the key marker in this phenotype is Tgf-β (Novak & Koh 2013).

1.4.3.3.3 Activation of the M2c phenotype

Physiologically, apoptotic cells are capable of increasing microglial Tgf-β expression and secretion and shift the microglia phenotype toward M2c (Spittau *et al.* 2015). Il-10, Tgf-β and glucocorticoids are used to induce M2c microglia *in vitro* by downregulating STAT1 and NF-κB (Chhor *et al.* 2013; Mantovani *et al.* 2004).

1.4.4 Microglia and resolution of neuroinflammation

The loss of M1 microglia, and reversion to M0 microglia, is described as the resolution of inflammation. The general assumption was that inflammatory (M1) microglia should convert to the anti-inflammatory/wound healing M2 phenotype, and then the same cells would revert to the M0 phenotype. But even from *in vitro* data, it is not clear that this

is the case. Some studies do suggest that M1 microglia alter their phenotype to become M2 (same cells) (Polazzi & Monti 2010). Other studies suggested that M1 inflammatory state might undergo apoptosis, with different M0 microglia generating a replacement population of M2 cells (Lobo-Silva *et al.* 2016). Furthermore, there is some indication that after M1 activation, an individual microglial cell may not fully resolve to the M0 phenotype. Rather, it could retain a low level of 'activation', or at least remain long-term/permanently altered (e.g., in the literature some theories suggested a 'primed' microglial phenotype: M0') (Torres-Platas *et al.* 2014). M1 microglia is the most widely studied phenotype, but its resolution is not fully understood.

As M2a is the disease/injury resolved phenotype it could be expected that it following the resolution of inflammation, M2a microglia revert to the M0 phenotype (Varnum & Ikezu 2012). However, it has been suggested that resolution may involve phenotype switching of some microglia from M1 to M2a and then M2c, since M2c is the wound healing phenotype, playing important roles in further deactivating of microglial inflammation (Mantovani *et al.* 2004).

M2b microglia are the least understood phenotype, and its existence *in vivo* is controversial. *In vitro,* it has been suggested that this phenotype might be associated with M1 as it works on removal of ROS and RNS during M1 activation, as M2b could be induced by combination of immune complexes (IC)+LPS (Mantovani *et al.* 2004). However, Mosser (2003) study showed that M2b cells had protected mice against LPS toxicity. Furthermore, another study showed that, in the last proliferative stage of M2b microglia, there is as increase in the production of both Il-10 and Tgf-b, and this signal converts M2b microglia to M2c phenotype (Novak & Koh 2013). Also, an *in vivo* study showed that adult mouse microglia have been switched from M2b to M2c, 24h after LPS injection (Fenn *et al.* 2012).

Although, few authors have described the M2 subtypes (as discussed previously), these reports were contradictory with a lot of overlaps between these subtypes. Therefore, this thesis will study M2 in general.

In summary, the resolution of microglial inflammation needs further study both *in vivo* and *in vitro*. Understanding why neuroinflammation fails to resolve, and how resolution may be triggered, will be of great benefit for developing treatments for neurodegenerative diseases. In particular, how microglia switch between appropriate phenotypes should allow modulation of microglial function.

1.5 Microglia are the principal phagocytic cells in the brain

Phagocytosis is the ability of cells (usually specialised phagocytises, including microglia) to identify, engulf and degrade invading organisms, debris and apoptotic cells (Mukherjee *et al.* 1997). Active microglia play an important role in maintaining the homeostasis of the brain through phagocytosis (Neumann *et al.* 2009). In the phagocytosis process, first microglia recognise surface signals (so-called eat-me signals) (Zitvogel *et al.* 2010) such as phosphatidylserine (PS), which is a component of the inner surface of the cellular membrane and is everted when cells undergo apoptosis (Sambrano & Steinberg 1995). Secondly, microglial receptors interact with eat-me signals to initiate phagocytosis. Microglial phagocytosis depends mainly on two receptors: TLRs, which have a high affinity for foreign microbial pathogens (Veerhuis *et al.* 2011); and PS receptors (Green & Beere 2000), which identify apoptotic cells. There are several other phagocytosis-related receptors such as: complement receptors, pyrimidinergic receptor (P2Y), scavenger receptors (SR) (Lucin & Wyss-Coray 2009), LPS receptor CD14 (Liu *et al.* 2005), and low-density lipoprotein receptor-related protein (LRP) receptor, which also take part in microglial clearance of apoptotic cells and dead neurons in both acute and chronic brain injury (Smith

1999). So, microglia sense eat-me signals, engulf cells by binding to these signals and forming vesicles called phagosomes, which then go through a series of events leading to digestion of the pathogen/debris when phagosomes merge with lysosomes (vesicles containing degradative enzymes at low pH; Figure 1-5) (Fu *et al.* 2014).

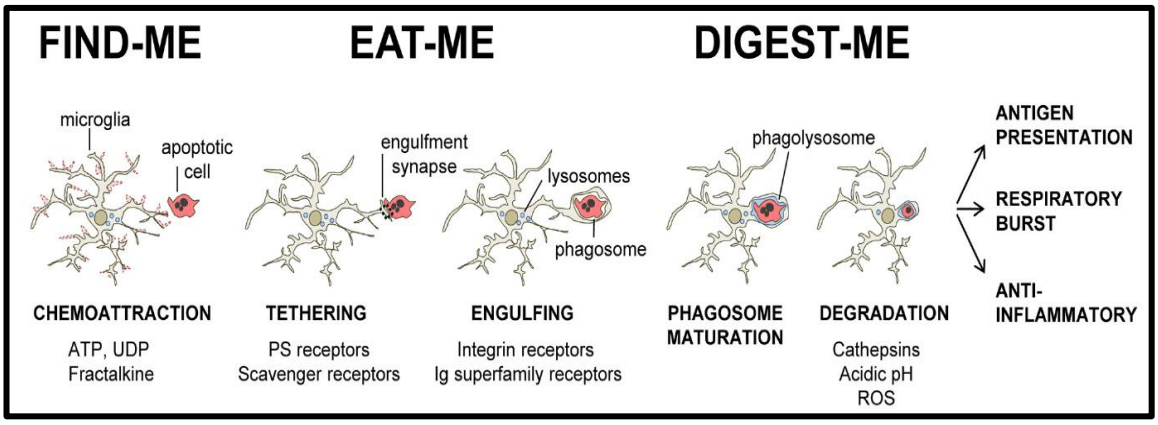

Figure 1-5: Microglia-signalling pathway in phagocytosis. Microglia membrane recognises the apoptotic cell, then microglia processes surround the target and engulf it. The target will be internalised and merged with the lysosome. This process could lead to an antigen presentation and M1 activation of other cells. Adapted from Sierra *et al.* (2013).

1.6 Microglia can engage in antigen presentation

Antigen presentation may be defined as the process that takes place in the immune cells to generate T-cell protective responses against pathogens or other foreign structures. The APCs must have the ability to phagocytose the foreign body and express MHC II on the cell surface. The T-cells recognise the MHC II, which leads to activation of T-cell and initiates the immune response (Becher *et al.* 2006).

Studies have shown that in normal brain, microglia have the ability to be APCs by having MHC II and co-stimulatory molecules (e.g., Cd40 and Cd86) on their surface (Williams *et al.* 1995), which bind to CD4+ (T-cell receptor) (Almolda *et al.* 2011). Antigen-presenting microglia can cause CD4+ T-cells to differentiate into helper T-cells (either Th1 or Th2 subtypes), which modulates their activity, for example by increasing production of

pro-inflammatory cytokines such as Ifn-γ in Th1 or anti-inflammatory cytokines such as Il-4 in Th2 (Aloisi *et al.* 1998). Furthermore, it has been suggested that MHC II upregulation in microglia is an early sign of microglial activation in CNS injuries (Kreutzberg 1996). In early MS lesion, increased MHC II expression in microglia suggest that microglia are responsible cells for presenting the myelin to CD4+ T-cells and sustaining the inflammatory process (Li *et al.* 1996). An *in vitro* study on both primary microglia and microglia cell line, showed a timed response of *MHC II* gene expression when microglia were treated with Ifn-γ and that expression decreased when the cells further treated with Tgf-β, Il-4 or Il-10 (O'Keefe *et al.* 1999).

It has been suggested that T-cells might promote M1 microglial activation, as part of $CD4^+$ Th1 cells response; these cells start to produce Ifn-γ, which induces M1 microglial activation (Mount *et al.* 2007). Furthermore, studies suggested that activated microglia and $CD4^+$ T-cells might play a role in neuroinflammatory disease progression (e.g., PD and amyotrophic lateral sclerosis) but probably not in disease initiation (Appel *et al.* 2010).

1.7 Microglial roles in neurodegenerative diseases

1.7.1 Microglia in Alzheimer's disease

Alzheimer's disease is characterised by accumulation of Aβ plaques (Ballard *et al.* 2011). Aβ is a fragment of a protein known as amyloid precursor protein (APP), which can be cleaved to produce amyloid protein, and the Aβ fragment. The main function of amyloid protein is neurotrophic factor in undifferentiated neurons and it is neurotoxic to mature neurons (Lorenzo *et al.* 1994). Aβ function depends on two factors: the concentration of Aβ and the age of the neurons so high concentrations of the protein in mature neurons could cause neuronal degeneration as in AD (Yankner *et al.* 1990).

Normally, Aβ are soluble proteins but insoluble Aβ are characteristic of several neurological conditions including: AD. Amyloid plaques do not seem to have a definite pattern of deposition, perhaps due to the many mechanisms able to clear these extracellular proteins, including microglial phagocytosis (Webster *et al.* 2000). Microglia have a role in degrading Aβ. But failure to either degrade / misfolding / aggregation (still unclear) leads to insoluble aggregates, associated with AD.

In the early stage of AD, microglia are present in increased numbers, and may delay disease progression through clearance of Aβ before senile plaque formation (Webster *et al.* 2000). But, increased Aβ accumulation even in the presence of microglia suggests that microglial ability/capacity to phagocytose Aβ may diminish with increasing age and progression of AD (Hickman *et al.* 2008). In a human study, evidence has shown increased numbers of pro-inflammatory M1 microglial markers (e.g., IL-1β, IL-6 and TNF-α) (Sastre *et al.* 2006), and similar observations have been made in mouse models (Sarlus & Heneka 2017). Several studies have confirmed that Aβ can interact with TLR4 and suggested that TLR4 mediates microglial-induced neurotoxicity both *in vitro* and *in vivo* (Lehnardt *et al.* 2003; Carty & Bowie 2011).

Healthy neurons express CD200 at the cell membrane, which interacts with CD200R (in microglial membrane), to maintain an M0 phenotype (Lynch 2014). Age-dependent decline of CD200 leads to the activation of microglia (Varnum & Ikezu 2012). In AD, evidences from both human and rodent brain tissue suggested that there is more rapid decrease in CD200 expression (Lyons *et al.* 2007). Sudduth *et al.* (2013) showed that in early stage AD, there are two distinct patient populations, based on analysis of microglia in brain tissue. One-half of the early AD cases showed a bias toward a pro-inflammatory, M1 phenotype, whereas the other half of the early AD cases show a bias toward the M2 phenotype (Sudduth *et al.* 2013). In contrast, the late-stage AD patients were more

homogeneous, and all of them showed a similar complex neuroinflammatory state, with markers of M1 and M2 all being elevated (Sudduth *et al.* 2013). It would be fascinating to know the role of different microglia phenotype in AD as in normal healthy brain, microglia phagocytose Aβ which may suggest the presence of M2. It is not clear why microglia lose this ability and increasingly exhibit an M1 phenotype. However, to investigate this a better *in vitro* model with known phenotype characteristic should be developed.

It is important to unravel the factors that contribute to the apparent inability of microglia to phagocytise Aβ aggregates. Many studies suggested different mechanisms, e.g., Hickman *et al.* (2008) in their mouse model, indicate that microglia promote Aβ clearance in early AD, but as the disease progresses, pro-inflammatory cytokines produced (i.e. M1) in response to Aβ deposition down-regulate genes involved in Aβ clearance. A second study demonstrated that microglial activation in AD can, in turn, activate astrocytes, which can inactivate microglial phagocytosis, which could be through down-regulation of microglial scavenger receptors or altered levels of phagocytosis related trophic factors (Liddelow *et al.* 2017). A third study on AD brain showed that microglial Aβ phagocytosis dysfunction may be caused by high mobility group box protein 1 (HMGB1), a chromosomal protein that inhibits phagocytosis. HMGB1 may bind to Aβ and inhibit Aβ degradation by microglia (Takata *et al.* 2012). Given these and other reports, it remains unclear how effective microglial phagocytosis of Aβ is, and how a loss of this capability may contribute to AD pathophysiology.

A really well-defined model will allow better understanding at an *in vitro* level; this allows the generation of hypothesis which can be tested in more complex models.

1.7.2 Microglia in Parkinson's disease

Parkinson's disease is characterised by degeneration of dopaminergic neurons in the substantia nigra pars compacta and development of Lewy bodies (a pathologic hallmark) in

dopaminergic neurons (Lue *et al.* 2001). The most important molecule in PD is α-synuclein (Papadopoulos *et al.* 2018). Although α-synuclein has been suggested to be neuroprotective, there are abundant data implying its role in the regulation of presynaptic secretory function (Chandra *et al.* 2005). In PD, α-synuclein levels are changed by overexpression, mutations, or chemical modifications (such as increased dopamine quinone formation, oxidation, nitration, phosphorylation and exposure to metal ions or toxins) (Sulzer 2007). These conditions can lead to an increased oxidative environment around dopaminergic neurons, which ultimately leads to neuronal death (Obeso *et al.* 2010).

In post-mortem analyses of the brains of PD patients, high numbers of activated microglia are found near the degenerating dopaminergic neurons (Ferreira & Romero-Ramos 2018). Also, *in vivo* positron emission tomography (PET) imaging of patients diagnosed with PD showed increased microglial numbers in the substantia nigra (Sulzer *et al.* 2017). This is to be expected, as damaged and dying dopaminergic neurons would produce pro-M1 signals (such as α-synuclein aggregates, ATP, matrix metallopeptidase 3 (MMP-3) and neuromelanin), which activate microglia (Kim *et al.* 2007). However, it is not clear whether microglial activity slows disease progression, or whether chronic over-activation contributes to the pathology, causing further damage through the release of neurotoxic factors (Manocha *et al.* 2017). Some animal model studies suggested that microglia play an important role in the disease process at an early stage (Liu 2006).

The role of microglia in PD is not entirely understood; but their potential modes of participation might include cell death (that produces DAMPs which interacted with ATP receptor inducing M1 microglia phenotype as discussed in 1.4.2), increased α-synuclein levels (α-synuclein M1 microglia phenotype through NF-κB, and alters microglia phagocytosis (Zhang *et al.* 2017)) and loss of neuronal signals, such as CD200 and fractalkine, which are known to be important in the maintenance of the M0 phenotype; and

increased protease production, which is thought to activate microglia by outline mechanism (Moehle *et al.* 2012). Disorder of CD200-CD200R signalling might increase microglial activation during PD, as this removes a stimulus that usually induces the M0 phenotype (Nayak *et al.* 2014). Zhang *et al.* (2011) reported that inhibition of this pathway increased inflammation, neuronal cell death and neurological dysfunction in a rat model of PD. Because CD200-CD200R signalling physically couples microglia and neurons in the healthy CNS, helping maintain an inactivated microglial state, disruption of this pathway during a neurodegenerative disease such as PD could result in chronic microglial activation (Zhang *et al.* 2011). A study showed that the chronic production of ROS and pro-inflammatory molecules (e.g., Tnf-α, Il-1β and Ifn-γ) from microglia in the brains of PD patients (Brochard *et al.* 2009), can subsequently cause damage to midbrain neurons, including dopaminergic neurons (Lysle *et al.* 1999), which feeds this vicious cycle.

M1 and M2 Microglia phenotype has been poorly studied in PD. Autopsy of PD brain showed cytokine markers of both M1 and M2 (Rojo *et al.* 2010), however, other study suggested that α-synuclein induces M1 microglia phenotype (Zhang *et al.* 2017). Furthermore, some study suggested that different M1/M2 polarisation state depends on the stage and severity of the disease. Therefore, understanding stage-specific switching of microglial phenotypes could be beneficial for PD therapy (Subramaniam & Federoff 2017).

A well-defined *in vitro* microglia system will allow better understanding of PD multiple factors on microglial activation state and the role of each phenotype in PD progression; this allows the generation of hypothesis which can be tested in more complex models.

1.7.3 Microglia in traumatic brain injury

It has been suggested that microglial activation plays an important role in the neuroinflammation and secondary injury after TBI (Loane & Kumar 2016). A good

understanding of microglia phenotype/function could contribute to the treatment of neuroinflammatory brain injury.

One of microglia's important function (as discussed in section 1.5) is to remove the debris through their phagocytic ability. In the case of brain injury with damaged neurones, microglia play neuronal protective roles through phagocytosis, production of neurotrophic factors and anti-inflammatory cytokines (Witcher *et al.* 2015). Which might suggest that microglia in the early stage of TBI are adopting M2 phenotype (Loane & Kumar 2016). However, TBI causes neuronal death, in turn these damaged cells release DAMPs, ROS, pro-inflammatory chemokines and cytokines, which suggests that these signals might drive microglia toward M1 phenotype. As discussed in section 1.4.2, M1 microglia produce important pro-inflammatory markers that are essential in host defence mechanism via ATP release and activation of purinergic receptors. Therefore, it has been suggested that both M1 and M2 microglia work together after TBI, although their roles in brain injury progression and repair were not fully determined.

However, experimental and clinical studies showed that chronic M1 phenotype lasts for months to years after TBI with low tissue repairing ability, mainly in moderate and severe TBI (Nagamoto-Combs *et al.* 2007; Smith *et al.* 2013; Loane *et al.* 2014). *In vivo* studies, using animal models of spinal cord and brain injury have shown that within the site of injury, there were mixed M1 and M2 phenotypes. But M2 phenotype response is short-lived and there is a phenotypic shift towards M1 microglia phenotype within 7 days of injury (Kigerl *et al.* 2009; Hu *et al.* 2012). Which decreases the microglia phagocytic ability, and increased pro-inflammatory production that could contribute to the injury and pathology (David & Kroner 2011). Furthermore, it has been suggested that after one month of brain injury, microglia show priming phenotype (there is

further discussion on this phenotype in section 1.8) with hyper M1 response to second stimuli (LPS) (Fenn *et al.* 2014).

It has been suggested that M2 microglia have important roles in neuronal repair and regeneration after TBI (Loane & Kumar 2016). Therefore, a better understanding of M1/M2 mechanisms in TBI might help in developing a future therapeutic targeting microglia phenotypic switching to enhance functional recovery after TBI (Figure 1-6).

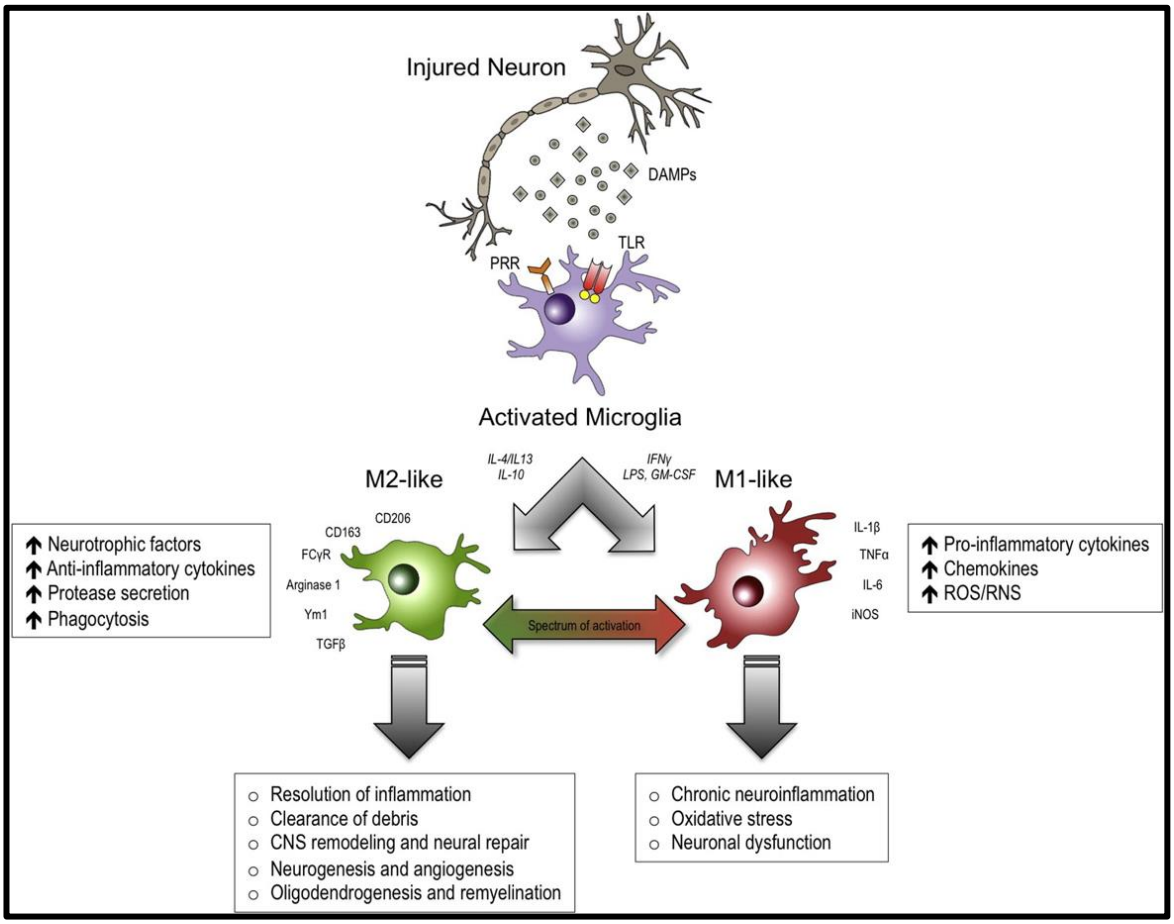

Figure 1-6: M1 and M2 microglia phenotype/ function in TBI. DAMPs produce by injured neuron could lead to microglia activation, microglia phenotype depends on the extracellular signals released by injured neurons. M1 microglia produce pro-inflammatory markers such as IL-1β, TNFα, IL-6 and iNOS, chemokines and free radicals. In contrast, M2 microglia upregulate markers such as CD206, CD163, FCγR, arginase 1, Ym1, and TGFβ and produce neurotrophic factors, anti-inflammatory cytokines, enhance protease production and phagocytosis ability. DAMPs, danger-associated molecular patterns; PRR, pathogen recognition receptors; TLR, toll-like receptors. Adapted from Loane & Kumar (2016).

1.8 The theory of microglial 'priming'

It has been proposed that the extent and type of microglial activation in response to a given stimulus might be altered by the environment in which these microglia have pre-existed (Wolf *et al.* 2017). It has been suggested that some M1 microglia do not go back to M0 but instead adopt a 'primed' phenotype. The definition of primed (M0') microglia, is that they exhibit an exaggerated inflammatory response (hypersensitive pro-inflammatory phenotype) to a second stimulus, after prior exposure to an initial (priming) stimulus. The initial stimulus could be a systemic illness or infection (i.e. not necessarily in the brain), but still lead to modified microglial responses to subsequent disease or injury, adversely affecting disease outcome (Haley *et al.* 2017) see Figure 1-7.

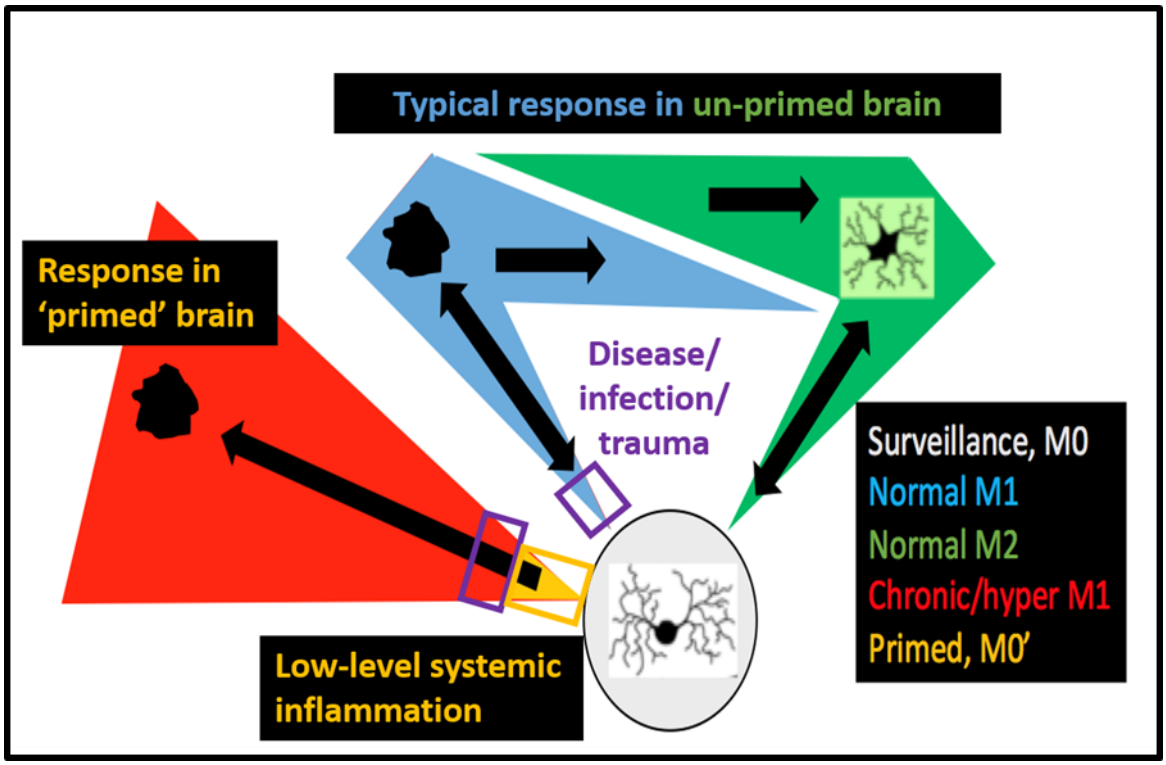

Figure 1-7: Schematic diagram illustrating the priming theory. Low level of inflammatory signal may not be enough to induce full M1 activation, but it could put microglia in the primed state. M0' microglia 'over-react' to subsequent activation with prolonged pro-inflammatory activation.

One of the first studies done on the priming of microglia was by using an animal model of prion disease where it was shown that microglia from animals with prion disease produce more pro-inflammatory cytokines when treated with LPS in comparison with naïve microglia (Combrinck *et al.* 2002). Later on, similar work has been done using prion disease and LPS (Cunningham *et al.* 2005; Cunningham *et al.* 2009) or polyinosinic:polycytidylic acid (poly I:C) (Fielda *et al.* 2010). Also, clinical and pre-clinical studies have shown that aged microglia are primed and present an exacerbated response to acute inflammatory challenge (Wolf *et al.* 2017; Godbout *et al.* 2005). In a recent study, d'Avila *et al.* (2018) showed that aged microglia produced a higher levels of pro-inflammatory cytokines (Il-1β and Il-6) in comparison with younger microglia when both young and aged mice have been treated with systemic inflammation (LPS). This might be due to the less sensitivity of microglia – neuronal signal such as fractalkine–CX3CR1 and CD200–CD200R1 with aging (Hanisch & Kettenmann 2007). However, the real mechanism behind priming microglia is not fully understood.

It has been suggested that peripheral infection might contribute to neurodegenerative disease, and the link between peripheral and neuronal disease might be through priming microglial cells in the brain. It is well known that peripheral viral or bacterial infection usually associate with sickness behaviour (controlled by the brain) such as loss of appetite, depression and loss of concentration (Dantzer *et al.* 2008). Peripheral infection and chronic disease are associated with increased production of pro-inflammatory markers (Il-6, Il-1β, Tnf-α, RNS and ROS) by peripheral immune cells. These markers might reach the brain and cause the sickness behaviour (van Dam *et al.* 1992). The actual mechanism that explains how these markers enter the brain is not fully explored, however there are different suggestions. Vitkovic *et al.* (2000) suggested that cytokines might affect neurons, which in turn affect microglia. While Dantzer *et al.* (2008) suggested that cytokines overflow in

systemic circulation can cross the blood-brain barrier (BBB) to the brain through transport system. The presence of these markers could partially activated or primed microglia.

M0' microglia theory provides a molecular and cellular pathway on how the systemic inflammation could contribute in neurodegenerative disease progression. Furthermore, the increase in pro-inflammatory marker expression could damage neurons, M0' microglia may respond to the further stimulation by altering the receptor properties in ways which have highly important consequences. In mouse models of neurodegenerative disease, peripheral inflammation led to increased microglial Fc-type immunoglobulin receptor expression higher than these with neurodegenerative or systemic inflammation alone.

Many preclinical studies provide evidence that M0' microglia and their subsequent inflammatory response might lead to damage the tissue in animal models of prion disease (Perry 2010), AD (Kitazawa *et al.* 2005), PD (Pott Godoy *et al.* 2010), stroke (McColl *et al.* 2007) and MS (Moreno *et al.* 2011).

1.8.1 Systemic inflammation can influence neuroinflammation

Systemic inflammatory signals can travel through the bloodstream, reaching the majority of tissues, except some 'immunoprivileged' sites, such as the eyes, testicles or placenta (Padrós *et al.* 2018; Ramos Robles *et al.* 2018; Schooten *et al.* 2018). For a long time, the brain was also considered immunoprivileged, due to the presence of the BBB. However, it is now clear that immune related molecules such as inflammation factors can cross the BBB, for example receptors for Il-1β, Il-6 and Tnf-α are expressed on cerebral endothelium and systemic Il-1β and Tnf-α cause cerebral endothelial activation (Skelly *et al.* 2013). Also, cells can cross the BBB to some extent such as lymphocytes in response to systemic inflammation (Banks *et al.* 2012). Ultimately, they influence neuroinflammation (Galea *et al.* 2007). The BBB does greatly limit the levels of

cytokines and antibodies within the brain, compared to the blood, and neuroinflammation is not a guaranteed consequence of systemic inflammation.

The mechanisms by which systemic inflammation may lead to neurodegeneration or neuroinflammation have been studied in many rodent models, by using administration of a peripheral stimulus (i.e. LPS) and/or pro-inflammatory cytokines (such as Il-1β, Il-6 and Tnf-α) (Dantzer *et al.* 2008; Andersson & Tracey 2012). Results showed that systemic inflammation (low doses of LPS) can cause microglial activation in both humans and animal models (Brydon *et al.* 2008; Harrison *et al.* 2009; Hannestad *et al.* 2012). The systemic effects seem to be mediated by increased production of NF-κB (Li *et al.* 2012), which is first observed in the microglia, but is later also observed in neurons (Zhang *et al.* 2013).

Findings from both humans and animal models of obesity support the idea that a high-fat diet and obesity are associated with neuronal damage in the hypothalamus and this is associated with altered microglial activation (Thaler *et al.* 2012). Age-related activation of microglial cells within the hypothalamus could, therefore, partly explain the relationships between chronic systemic inflammatory conditions, such as diabetes and obesity and the development of the age-related neurodegenerative disease (Balakrishnan *et al.* 2005; Donath & Shoelson 2011).

In summary, there are some circumstances in which systemic inflammatory signals can affect the CNS, including microglial phenotype switching in particular. These effects may influence disease onset and progression and warrant further study.

1.9 Immunomodulation as a therapy

Although it is not yet fully understood which events lead to inappropriate microglial activation, their roles in neurodegenerative conditions, such as AD, PD and TBI, are clearly important. It has been shown previously that microglia adopt different phenotypes in the different stages of neurodegenerative disease. In fact, in the early phase of some

neurodegenerative disease, microglia may adopt a neuroprotective M2 state and later become pro-inflammatory (M1), contributing to neurodegeneration (Kempuraj *et al.* 2016). Therefore, some strategies aimed to use immunosuppressive drugs to reduce microglial numbers, and/or convert M1 microglia to M0. However, it could be argued that a more effective approach could be used. Instead of immunosuppression, immunomodulation could be used to switch the microglial phenotype from M1 to M2, offering a better solution to treat neurodegenerative diseases. In this case, the unwanted M1 activity would be reduced, but also protective M2 activity would be promoted. Immunomodulatory drugs have been tested in *in vitro* and *in vivo* models of neurodegenerative diseases and showed some promising results.

Fingolimod (Gilenya®) was the first Food and Drug Administration (FDA) approved MS treatment, based on its ability to modulate microglia phenotypes. *In vitro,* fingolimod modulates microglial activation, by increasing neurotrophin production and decreasing Tnf-α, Il-6 and Il-1β release, which switch microglia towards a neuroprotective phenotype (Noda *et al.* 2013). Two independent phase-III clinical trials have approved its effectiveness (NCT02139696, NCT00340834) (Pawate & Bagnato 2015; Peña-Altamira *et al.* 2016).

Glatiramer acetate (GA) (Copaxone®), is another immunomodulatory drug to treat MS, approved by FDA in 2014 (English & Aloi 2015). *In vitro* and *in vivo* studies have demonstrated that microglia are the key mediator in the neuroprotective effect of GA in MS, mainly by inducing the M2 phenotype (Giunti *et al.* 2014). *In vitro* study showed that GA leads to reduced release of pro-inflammatory cytokines by microglia (Chabot *et al.* 2002). Also, GA causes an elevated Il-10 levels and promotes phagocytic activity in microglia (Pul *et al.* 2011).

Many other possible cellular and molecular targets have been identified such as HMGB1, AMPK, GSK3β, HDACs and peroxisome proliferator-activated receptor γ (PPAR-

γ) for their potential role to immunomodulate microglia (Table 1-2) (Peña-Altamira et al. 2016). This is an interesting therapeutic target, however further studies are needed. Therefore, the development of an in vitro microglia system will allow better understanding of these mechanisms and allow the generation of hypotheses which can be tested in more complex models.

Table 1-2: Potential molecules and targets for microglia immunomodulation.

Immunomodulatory molecule	Potential targets for immunomodulation	The modulation effect	References
Ethyl pyruvate (EP)	High-mobility group box-1 (HMGB1)	Dopaminergic neurons are protected by regulating microglial activation	(Huh *et al.* 2011)
Inflachromene (ICM)	HMGB1	Blocks microglial-mediated inflammation and stimulate microglial-mediated neuroprotection	(Lee *et al.* 2014)
5-amino-4-imidazole carboxamide riboside (AICAR)	AMP-activated protein kinase (AMPK)	Inhibits the expression of pro-inflammatory cytokines and iNos in microglia, by reducing NF-κB activation	(Giri *et al.* 2004)
Metformin	AMPK	Promotes functional recovery and tissue repair after stroke through the switch of microglia phenotype from M1 to M2	(Jin *et al.* 2014)
GSK-3β inhibitors	Glycogen synthase kinase-3 β (GSK3β)	Reduces microglial M1-like activation, without affecting M2-like activation	(Prati, De Simone, *et al.* 2015)
HDAC inhibitor trichostatin A (TSA)	Histone deacetylases (HDACs)	Decreases histone acetylation, modulating chromatin condensation and gene expression driving microglial phenotypic shift	(Suuronen *et al.* 2003; Suuronen *et al.* 2006)
Pioglitazone	Peroxisome proliferator-activated receptor γ (PPAR-γ)	Modulates microglia towards a more neuroprotective phenotype	(Masciopinto *et al.* 2012; Barbiero *et al.* 2014)

1.10 Drug delivery to the CNS is hindered by the blood-brain barrier

Developing therapies for modulating neuroinflammation with high specificity and low side effects may be critical to treating neurodegenerative diseases. As described in section 1.9, there is a substantial evidence that immunomodulatory drugs have a high therapeutic potential. However, many immunomodulatory drugs cannot currently be used to treat CNS conditions, because of the presence of the BBB, preventing or severely limiting drug delivery to the brain (Löscher & Potschka 2005).

1.10.1 Blood brain barrier structure and functions

The main function of the BBB is the regulation of transport of molecules and cells into and out of the CNS (Saraiva *et al.* 2016). The neurovascular unit is the functional unit of the BBB, comprising astrocytes, pericytes (the smooth muscle-like cells), endothelial cell, neurons and microglial cells (Figure 1-8) (ElAli *et al.* 2014). The BBB is a physical and enzymatic barrier (Lalatsa & Butt 2018). It inhibits the passage of many drugs and biomolecules (proteins, carbohydrates and insoluble lipid) from the endothelial capillaries to the brain parenchyma (Upadhyay 2014). The BBB function comes from :

- Tight junctions between the endothelial cells that are responsible for providing a physical barrier between the brain–blood compartments, and the selective transport of important ions (Abbott *et al.* 2010).
- Efflux/influx transporters that are responsible for the transport of nutrients and hormones, and the removal of metabolic waste, foreign substances and excess neurotransmitters via the ATP-binding cassette (ABC) transporters (Thurgur & Pinteaux 2018).

- Detoxifying and scavenging enzymes that are responsible for supplying trophic factors and hormones for brain maturtion, and the protection of the brain fluid environment (Abbott & Friedman 2012).

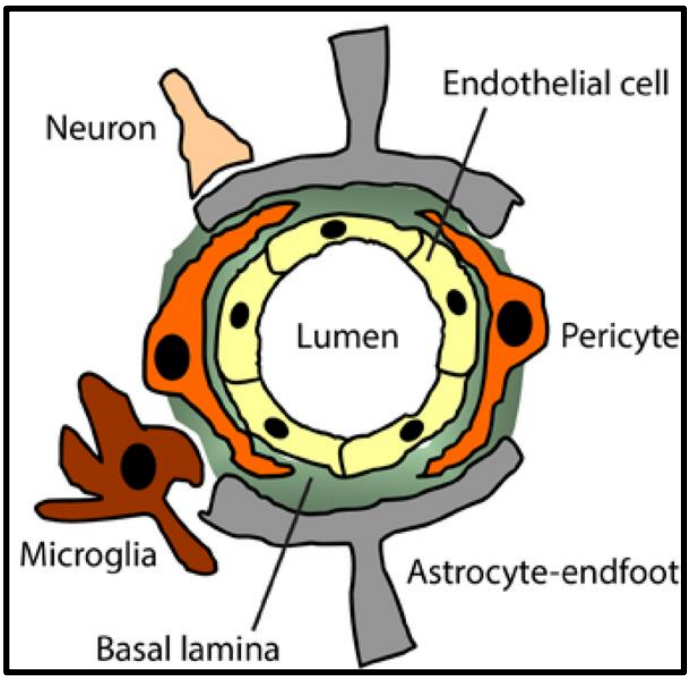

Figure 1-8: Blood brain barrier functional unit (neurovascular). Comprises of astrocytes, pericytes, endothelial cells, neurons and microglial cells. Adapted from ElAli *et al.* (2014)

In summary, the BBB is a major challenge to immunomodulatory therapies targeting microglia. It may be necessary to identify novel drugs with the ability to cross the BBB and reach microglia. However, an alternative approach would be to modify microglial activity, but the inability to cross the intact BBB, so that the modified form reaches the brain parenchyma. Various approaches are being investigated and may involve drug modification (conjugating particular molecules), or packaging of the drug within a delivery system so that it can cross the BBB.

1.10.2 Strategies to cross the blood brain barrier

There are different transport methods for substances to cross the BBB (Table 1-3). The strategies to cross the BBB either through the paracellular pathway (between adjacent

cells) such as ions, which could cross the BBB by simple diffusion, this usually occurs from the high to the low concentration side (Gjedde & Crone 1983) alternatively there is a transcellular pathway (through the cells) which includes mechanisms such as receptor-mediated transport and transcytosis (Dong 2018). Despite the nature of the BBB, the transport of substances across the BBB depends on different factors such as their lipid solubility, molecular size, electrical charge and affinity for a carrier molecule (De Lange 2012).

Table 1-3: Representation of known transport mechanisms at the blood brain barrier.

Type of transport	Sub-type	Mechanism of action	References
Paracellular	Simple diffusion	Transport of the substances depends on their concentration on each side of the barrier	(Gjedde & Crone 1983)
Transcytosis	Influx transport	Transport gradient by carriers from the blood into the brain	(Ohtsuki & Terasaki 2007)
	Efflux transport	Transport gradient by carriers from the brain into the blood	(Scherrmann 2005)
Vesicular transport	Receptor-mediated endocytosis	Transport of the substance occurs by endocytosis of the materials out of the plasma membrane at the blood side of the BBB, then, moving through the cytoplasm of the endothelial cell, followed by exocytosis in the brain	(Temsamani & Vidal 2004)
	Absorptive-mediated endocytosis	Transport of the substances depends on electrostatic interactions with anionic sites of the plasma membrane surface that trigger adsorptive endocytosis	(Hervé *et al.* 2008)

Although the BBB used to be a major problem for treating CNS diseases effectively because of its selective permeability (as discussed previously), methods to cross the BBB and deliver therapy to the brain are being investigated currently such as cell-mediated delivery, cell-penetrating peptides (CPPs), receptor-mediated transport (RMT) and hyperthermia techniques (Pandey *et al.* 2016). Although all of these techniques have promising results and

are now under clinical trials, they still have some disadvantages (Table 1-4). Therefore, another way has been proposed that is 'nanotechnology'.

Table 1-4: Pros and cons of different strategies to cross the blood brain barrier. Adapted from Pandey *et al.* (2016).

Strategy	Pros	Cons	Clinical trial
Cell penetrating peptides (CPPs)	Excellent penetrating ability	Fast Removal	Phase II
	Low cellular toxicity	Non-specificity	
		Immunoresponsive	
Hyperthermia	Easy to perform	Increase intracranial pressure	Phase II
	Drug compatible	Necrosis	
		Tissue damage	
Cell-mediated delivery	Low cytotoxicity	Require high cell quantity	Phase I
	Controlled drug release	Cell injury	
	Targeted transport		
Receptor-mediated transport (RMT)	Site-specific	Low dissociation rate	Phase III
		Rapid cargo degradation	
		Possible toxicity	

1.10.3 Nanotechnology to cross the blood brain barrier

Nanotechnology is a material or a device that has at least one dimension on the nanometer scale range from a few to about 1000 nm. Nanoengineered materials and devices aimed at biological applications and medicine in general, and neuroscience in particular, are designed fundamentally to interact with cells at the molecular level. One particularly important area of nanotechnology application to CNS is the development of approaches for delivering drugs, genes, and contrast agents across the BBB. The ability to cross the BBB to deliver the drugs to the target site may face several challenges. First, the nanodelivery drug should avoid the clearance by the immune system in the body as the mononuclear

phagocytise system (MPS) (Dobrovolskaia *et al.* 2008). Second, they should be able to cross the BBB. Finally, they should be able to reach the target cells.

A body of work has been aimed to overcome these challenges to cross the BBB by a specific mechanism such as opening the tight junctions between the endothelial cells (Borlongan & Emerich 2003), disrupting the tight junctions by using the osmotic shock which leads to shrinking the endothelial cells (Doolittle *et al.* 2000). However, these methods might cause extra damage since they may lead to the presence of unwanted blood components in the brain which could lead to neuronal damage/death. Therefore, using nanotechnology s facilitator to cross the BBB (Lipinski *et al.* 2001).

Another challenge for the drug to reach the CNS is that most of these drugs are intravenously (i.v.) administered which leads to recognising them by the MPS in the body, causing a major loss of the injected dose (>50 %) within a few hours after an i.v. injection (Li & Huang 2010). Therefore, a modification to the surface of the drug/ drug carrier should be made to avoid the clearance by the MPS and increase the half-life of the drug in the circulating system which increase the changes to reach the CNS, and that is why some drugs have been coated with poly(ethylene glycol) (PEG) (Verrecchia *et al.* 1995; García *et al.* 2014). Nanotechnology also used the PEGylated coating especially in term of treatment and imaging CNS cancers (Malam *et al.* 2009; Bae & Park 2011). PEGylated nanoparticles (NPs) are often mentioned as "stealth" NPs, because of their ability to escape the surveillance of MPS better than the non-stealth nanoparticles.

Research is focusing on using PEGylated nanoparticles for the delivery of drugs that have poor solubility under physiologic conditions and require specific carriers. In a MS model, PEGylated nanoparticles showed the ability to cross the BBB and accumulate at high concentration in the brain (Calvo *et al.* 2002). In a rat model of PD, a tyrosine hydroxylase

expression plasmid was delivered to the striatum of adult rats using PEGylated NPs to normalise tyrosine hydroxylase (TH) expression levels. By using specific antibodies to transferrin receptors conjugated to the nanoparticles, TH plasmids were shown to be expressed throughout the striatum (Zhang *et al.* 2003).

There are increasing number of researches interested in using PEGylated NPs in treatment and diagnosis, and an increasing body of work indicates that PEGylated NPs could escape clearance by the MPS (Zhu *et al.* 2017; Shen *et al.* 2018), and increased crossing of the BBB, but even after entering the CNS there is another immune cell with phagocytosis ability (microglia). Microglia could engulf NPs, which may or may not be useful, depending on the intended target of the drug payload. If drugs are intended to activate surface receptors, it would be preferable to avoid cellular uptake. But if intracellular delivery to microglia is intended, then this uptake may be beneficial. However, there is limited research into the fate of NPs within the brain, and also with respect to interactions between NPs and microglia, in particular.

1.10.4 Microglia response to nanoparticles

Some studies have evaluated microglial response to NPs, including these that may be encountered accidentally (e.g., through pollution), or these intended for research of therapeutic purposes. These studies will be discussed here.

The effect of NPs' toxicity on microglia have been studied using NPs with different composition such as SiO_2, TiO_2, Fe_3O_4, Ag and Au NPs, although none of these NPs used as drug-delivery vehicles, none of these NPs cause any toxic effect on microglia especially in the low to moderate concentration (Xue *et al.* 2012; Söderstjerna *et al.* 2014). Although NPs did not cause a direct toxic effect on microglia, further studies have been performed to understand their effect on microglial activation state.

In vitro studies regarding the inflammation caused by NPs used to treat microglia have primarily suggested an increased ROS and RNS in NPs treated microglia (Long *et al.* 2006; 2007; Choi *et al.* 2010; Wang *et al.* 2011). Fe_3O_4- and TiO_2-NPs have been shown to induce ROS and RNS generation in BV-2 microglia cell line (Long *et al.* 2007; Wang *et al.* 2011), and similar observation has been made when primary microglia culture have been treated with Si-NPs (Choi *et al.* 2010). However, Xue *et al.* (2012) reported no increase in RNS production or *iNos* gene expression by microglia when treated with SiO_2-NPs or Fe_3O_4-NPs.

Few studies have tried to understand the effect of NPs on pro-inflammatory factors produced by microglia such as Tnf-α and Il-1β (Choi *et al.* 2010; Wang *et al.* 2011; Xue *et al.* 2012). Choi *et al.* (2010a) reported that silica NPs (ranging from 150 to 200 nm in diameter) induced the expression of Tnf-α, Il-1β and cyclooxygenase 2 (Cox-2) in primary microglia. Xue *et al.*, (2012) reported that Fe_3O_4-NPs also induced the protein production of Tnf-α, Il-1β and Il-6 in primary microglia. In contrast, Wang *et al.* (2011) observed that microglia treated with Fe_2O_3 NPs did not lead to elevation of the levels of inflammatory cytokines Tnf-α, Il-1β and Il-6.

In summary, microglia can internalise a variety of NPs, with no obvious toxic effect. These NPs could lead to alternative microglial response. A better understanding of microglial response will be necessary, if NPs are to be considered as a drug delivery method for manipulating microglial functions.

1.11 Greater understanding of microglial phenotype switching is required

An understanding of neurodegenerative diseases will be greatly enhanced by a full understanding of microglial phenotype switching. As discussed above, it is widely speculated that events such as inappropriate M1 activation, loss of phagocytic function or

microglial priming are key to disease onset or progression (Gao & Hong 2008). If this is true, then determining the stimuli that lead to these events could offer valuable insight into currently untreatable and devastating diseases. Such insights could inform the development of effective therapies based on neuroimmunomodulatory drugs and harnessing the protective/regenerative abilities of microglia.

Studying microglial phenotype switching is important, since microglial response varies to different stimuli, refined phenotypes (M0, M1, M2) were proposed. Microglia phenotype identification is usually based on the different markers that these phenotypes produce, for example M1 microglia are associated with pro-inflammatory cytokines, while, M2 microglia produce anti-inflammatory markers. Microglia phenotype will depend on CNS environment which is complex and hard to define precisely. The mechanism behind the *in vivo* phenotype switching is not fully understood. However, some reports suggested the ability to drive microglia from one phenotype to another, which could be a good target for treating neurodegenerative diseases.

While the *in vivo* environment is too complex to study, *in vitro* models may be viewed as overly reductionist. However, such models will allow the mechanisms crucial to switching of microglial phenotype to be defined to develop hypotheses with regards these mechanisms, which can be tested in more complex models.

The available researches on microglia phenotype often lack to full characterising the model. These studies usually depend on using only one concentration of the stimuli, which makes it difficult to know if the microglia response is the highest response. Also, they depend on only one-time point. Such limitations in the current studies make these models not the best option to study microglial phenotype switching in disease and on testing

different treatments. Therefore, increasing the knowledge in these areas will require suitable models to study microglial phenotype switching.

1.11.1 Gene expression studies require greater rigour

Gene expression is of interest to microglial researchers (Bennett *et al.* 2016Plastira *et al.* 2016; Rey *et al.* 2016; Yang *et al.* 2017), and is likely useful for identifying phenotypic changes (Satoh 2017). Furthermore, characterising an exclusive gene expression signature of different microglia state would be of great importance for both understanding microglia biology behaviour in healthy brain and developing microglia-targeted therapy for different neurodegenerative diseases.

There are different assays for gene expression analysis such as quantitative polymerase chain reaction (qPCR), microarray and RNA sequencing (RNA-seq). qPCR (referred to as real-time PCR) is a widely used assay to determine relative transcript numbers in biological samples. qPCR is a robust, highly reproducible and sensitive method to quantitatively study gene changes across varying environmental or experimental conditions. Furthermore, reverse transcription analyses are now combined with qPCR methods (RT-qPCR), offering a powerful tool for quantifying gene expression (in terms of relative quantities of mRNA transcripts). Microarray is used to measure DNA expression levels of thousands number of different genes at the same time. RNA-seq also has the abilty to look at differential expression at the same time and even discover new genes or alternative splice variations; however RNA-seq is expensive and represents a challenge in the planning stage. qPCR has a wide dynamic range and low quantification limits in comparison to microarrays or RNA-seq.

Most microglial RT-qPCR studies have used glyceraldehyde-3-phosphate dehydrogenase (*Gapdh*) or *ACTB* as the sole reference gene. However, their suitability as

reference genes is questionable, because of their potential involvement in a wide range of physiological conditions. Furthermore, the minimum information for publication of quantitative real-time PCR experiments (MIQE) guidelines highly recommend using multiple reference genes for reliable qPCR data (Bustin *et al.* 2009). Therefore, it is surprising that, to date, no study has been performed to identify the reference gene(s) for normalisation of transcript levels in microglia.

1.12 Modelling microglial phenotype switching

Models for studying microglial phenotype switching that offer greater control are needed, and the ability to measure phenotype-relevant changes. But, widely-used microglial models have various drawbacks.

Human data for live microglia are limited due to the difficulty to study the microglia in human before death. Although, there has been some progress in *in vivo* imaging of microglia, it is impossible to study phenotypes in detail in living patients. Although neuroinflammation could be detected, implying M1, current techniques cannot reliably identify microglial phenotype.

Human tissue samples are available with some limitations such as ethical approval and high biosafety requirement to deal with such samples. There is no regular source of live microglia from humans that could be studied *in vitro*. Furthermore, cells sometimes are available, but not on a regular basis, that make it possible to study microglia phenotype in neurodegenerative diseases. Post-mortem samples are available from tissue banks; from patients with neurological diseases. However, characterising microglia phenotype in fresh brain is more challenging than assessing fixed brains or fixed blocks.

Furthermore, the fixation and storage of these tissues may not always be perfect for preserving markers. Also, it is difficult to reliably get mRNA/gene expression data for

human microglia and to have control groups. In addition, access to the patient's disease history is limited and it is difficult to definitively know whether the human source had or was developing specific diseases.

Live animal models offer some advantages, including the presence of the BBB, all cell types being present, …, etc. But microglia are difficult to monitor in live animals; it is more difficult to control experimental conditions *in vivo*, with experiments being time consuming, low throughput and requiring more training, compared to cell culture. Furthermore, animal models are limited due to the legal restrictions on their availability and use, particularly for therapy development projects.

Therefore, *in vitro* microglial cultures can overcome many of these problems, representing a valuable tool to study microglial phenotypes. *In vitro* studies enable assessment of secreted factors, cell motility, allow testing of more concentrations/times and other important components that characterise microglia, which cannot be appropriately studied *in vivo*.

Microglial cell line has been widely used in studying microglia, but one of big cell line's problem is the immortalised cell lines ability to genetically drift or select for certain phenotypes, as they are passaged many times over. This may explain why the same treatment (stimuli) lead to different response. Cheepsunthorn *et al.* (2001) and Horvath *et al.* (2008) studies showed different results when treated highly aggressively proliferating immortalised cell line (HAPI; microglia cell line) with LPS. Cheepsunthorn *et al.* (2001) found an increase in Tnf-α release in the culture media, while, Horvath *et al.* (2008) found no release of Tnf-α into the media at either 24 or 48 h.

Ultimately, it would be of high value to the research community to develop an *in vitro* microglial model that reliably predicts/measures phenotype switching. Such a model

would allow the study of pathological stimuli, and the screening of immunomodulatory drugs. This may be particularly useful in the context of drug delivery systems that employ novel biomaterial-based technologies.

1.13 Aims and objectives of the experimental Chapters

This thesis will describe studies to develop an *in vitro* model of microglial phenotype switching, focussed on gene expression analysis.

1.13.1 Objectives

- To develop an *in vitro* microglial culture system, to study phenotype switching. Identify and validate multiple reference genes for microglial qPCR studies.
- To collect detailed gene expression changes in response to a widely-used M1 stimulus.
- To collect detailed gene expression changes in response to a widely-used M2 stimulus.
- To assess whether nanoparticles alter the expression of M1 and M2 markers genes and the activity of inducible nitric oxide synthase system.

1.13.2 Experimental studies descriptions

Chapter 3: Validating culture system and methods for microglial studies

Validation of primary microglial culture and qPCR methods was the aim of this Chapter. The purity of microglia derived from primary mixed glial culture was assessed. qPCR primers for multiple reference genes and genes of interest were designed and validated. Yield of mRNA from microglia was assessed. Sex-dependent differences in microglial gene expression were studied.

Chapter 4: Characterising primary microglia culture in serum-free media

The possibility that serum may alter 'baseline' microglial activation, or maximum response, was tested in this Chapter. Serum-free media were tested for maintaining microglial cultures.

Chapter 5: Characterising microglial responses to pro-inflammatory activation

The primary aim for this Chapter was to characterise microglial responses to a range of concentrations of an M1 stimulus, and at different time points. These data would permit the calculation of the maximum response and EC50 values, which will be useful in understanding microglial behaviour in disease. These data would allow the comparison between different stimuli, including pathology-associated molecules. They would also be useful for determining the effects of potential microglia-targeted drugs. The secondary aim was to investigate whether microglia may exhibit behaviours consistent with 'priming', in this *in vitro* model.

Chapter 6: Characterising microglial responses to anti-inflammatory activation

The aim for this Chapter was to characterise microglial responses to a range of concentrations of M2 stimuli. Calculating the maximum response and EC50 values, as

previous chapter, would be useful in understanding microglial responses in different phenotypic states, and potentially aid development of immunomodulatory therapies targeting microglia.

Chapter 7: Microglial response to different nanoparticle formulations, including 'stealth' coat

The primary aim of this Chapter was to study whether NPs induce inflammatory responses in M0 microglia, and whether a 'stealth' coating may limit any such responses. A 'control' NP was compared to a stealth NP, identical except for the coating. NP toxicity and levels of uptake were compared for both. The secondary aim was to investigate if M1 (pre-activated) microglia have their inflammatory responses exacerbated by interaction with NPs, including stealth NPs.

Chapter 2 : Materials and methods

2.1 Experimental design

In comparison with *in vivo*, *in vitro* studies provide methodological benefits for high-throughput screening of microglial response, including greater experimental control (e.g., direct application of treatments, with identical local concentrations), and ease of monitoring. *In vitro* experiments also use fewer animals and produce larger numbers of microglia with high purity (Schmid *et al.* 2009). Multiple doses and time points can be studied with cells derived from the same source, reducing noise due to biological variation between animals. Rodents were chosen as a model organism because their genetic and biological characteristics closely resemble these of humans (Galatro *et al.* 2017). Also, there is evidence that the immune system in rat shares many characteristics with that of human (Guerrero & Reiter 2002; Azizi *et al.* 1998).

2.2 Reagents and equipment

Unless otherwise stated, culture plastics, media and reagents were from SLS, Sigma-Aldrich and Fisher, UK. End-point PCR used a thermocycler (Bibby Scientific, UK), qPCR was performed using a PrimePro48 machine (Techne, UK).

2.3 Primary microglial culture

The care and use of all animals in the production of cell cultures were in accordance with the Animals Scientific Procedures Act of 1986 (UK) with approval by the local ethics committee.

Primary mixed glial cultures were prepared from the cortices of postnatal day 0-3 rat (McCarthy & de Vellis 1980). Briefly, the cortices have been dissected in 1 M HEPES with HBSS and 2 % penicillin–streptomycin and removal of the meninges, the cortices were chopped into small pieces and subsequently mechanically dissociated. Dissociated cortices

were maintained in D10 media [Dulbecco's modified Eagle's media (DMEM) supplemented with 10 % fetal bovine serum (FBS), 50 U/ml penicillin, 50 µg/ml streptomycin, 1 mM sodium pyruvate and 2 mM Glutamax] in poly-D-lysine (PDL) coated flasks until confluent (37 °C; 5 % CO_2; 95 % humidified air; 7-10 days). Cultures were maintained in D10 media with a 50 % D10 refresh every 2-3 days. Microglia were isolated by mechanical shaking (ThermoScientific, USA) (200; 37 °C; 90 min; Figure 2-1). Medium enriched with microglia was collected, cells pelleted by centrifugation (300 g, 5 min), counted then plated in D10 (6 x 10^5 cells/cm^2; PDL-coated coverslips or 12 well plates or 24 x 10^5 cells/cm^2; PDL-coated T25 flasks). The plating density have been increased from 6 to 24 x 10^5 cells/cm^2 to increase the amount of RNA extracted from microglia cells. The day after plating, cultures were treated.

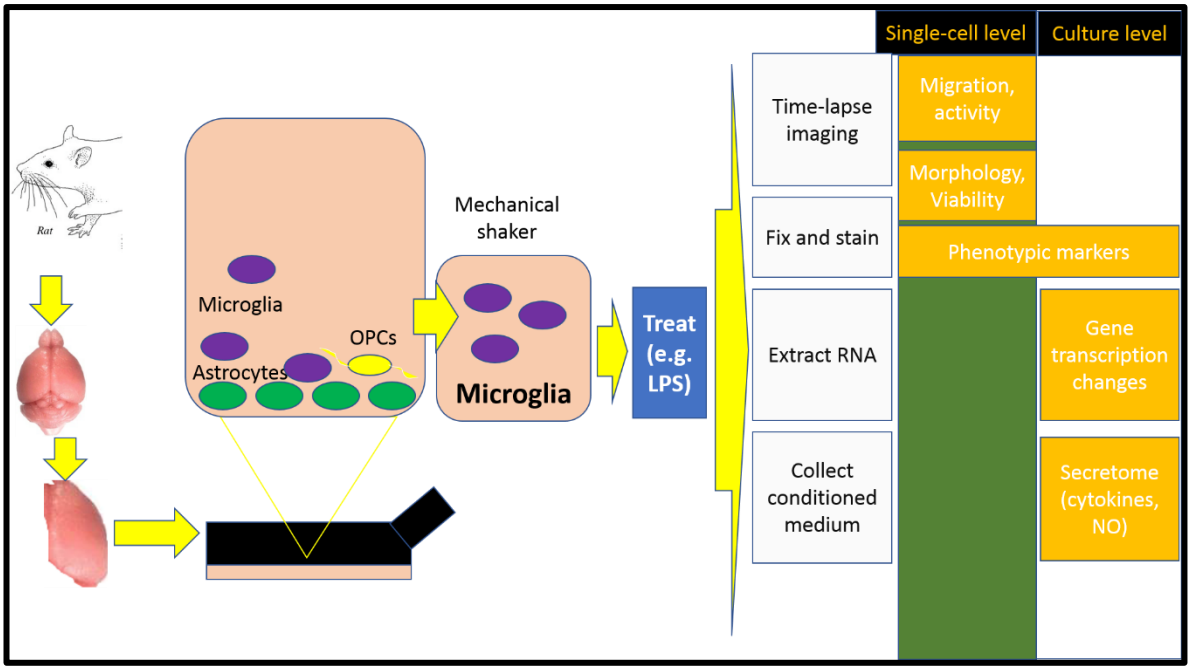

Figure 2-1: Schematic diagram illustrating the main procedures for the preparation of purified microglia from mixed glial cultures. Neonatal cortex is dissociated and cultured in flasks until confluent. Once confluent, astrocytes force microglia and oligodendrocyte precursors to form an upper layer of cells. Simple shaking can then release microglia, which can be plated in high purity culture. After experimental treatment (e.g., LPS to induce M1 phenotype), cells can be imaged live or fixed and stained. In parallel, mRNA can be extracted from cultures for qPCR analysis. Finally, culture media can be collected to assess what cytokines have been secreted and/or detect products of reactive nitrogen species. Adapted with permission from Dr Stuart Jenkins (Keele University) Jenkins (2013).

2.4 RNA extraction and quantification of gene expression by qPCR

2.4.1Selecting genes of interest and reference genes

The literature search identified several genes that could serve as markers for different microglial phenotypes (Table 2-1). A panel of three reference genes (*Gapdh, Usp14 and Rpl32*) was used for the quantitation of changes of gene expression (see section 3.1.3).

Table 2-1: List of microglial phenotypic markers. Upregulation or down–regulation of each gene (marker) helps in the distinction between different phenotypes.

Phenotype	Genes (markers) with altered expression	References
M0	Cd200R	(Zhang *et al.* 2011; Butovsky *et al.* 2015)
M1	Il-1β, Il-6, Tnf-α and iNos	(Ling & Wong 1993; Chhor *et al.* 2013; FreILich *et al.* 2013; Orihuela *et al.* 2015)
M2	Fizz1, Arg1, Il-10, Tgf-β and Ym1	(Chhor *et al.* 2013; Kobayashi *et al.* 2013; Cherry *et al.* 2014; Orihuela *et al.* 2015)

2.4.2 RNA extraction and RNeasy columns

Total RNA was purified according to Qiagen RNeasy instructions. Before RNA extraction, supernatant (conditioned media) was collected and stored at -80 °C until analysis of nitrite levels. Cells were washed twice with diethylpyrocarbonate (DEPC; used to inactive RNase enzyme) containing phosphate buffered saline (PBS), homogenised in lysis buffer and transferred to eliminator spin columns to remove gDNA (genomic DNA). Then, three wash steps (RW1 and RPE buffers) removed salts and biomolecules (e.g., carbohydrates, proteins, fatty acids, …, etc.). RNA was eluted using RNase-free water, then the RNA

concentration and purity level was quantified using Nanodrop (NanoDrop Technologies, USA) then stored (-80 °C).

2.4.3 Reverse transcription

Total RNA was reverse transcribed into complementary DNA (cDNA) using the iScript™ cDNA synthesis kit (BIO RAD, UK), according to kit instructions. 1-2 µg of RNA was combined with reaction mix and reverse transcriptase in a thermal cycler (Prime thermal cycler, Bibby Scientific) (5 min, 25 °C; 30 min, 42 °C; 5 min, 85 °C). Negative controls (RT; this control assesses the amount of DNA contamination present in an RNA preparation) omitted the reverse transcriptase enzyme.

2.4.4 Primer design

Primer pairs were designed to generate amplicons between ~75 and 300 base pair (bp) since short PCR products are typically amplified with higher efficiency than longer ones (Ma & Chung 2014). An amplicon should be at least 75 bp to easily distinguish it from any primer-dimers that might form (primer dimers are short non-target PCR products, formed from partial complementarity of the primers with non-target templates, or among the primers themselves) (SantaLucia 2007) and to cross at least one intron so that products amplified from gDNA will be a different size to these amplified from mRNA. The search algorithm was set to keep guanine cytosine (GC) content between 50-60 % (for optimum PCR efficiency as clusters of G's or C's can cause non-specific priming) and melting temperatures close to 60 ^{o}C (because primers with melting temperatures above 65 ^{o}C have a tendency for secondary annealing). The primers designed with NCBI Primer Blast software. Table 2-2 lists the sequences and NCBI references of used primers for RT-qPCR (SantaLucia 2007; Ma & Chung 2014).

Table 2-2: List of primers used for real-time reverse transcription polymerase chain reaction (RT-qPCR). References to literature indicate sequences derived from published papers. All other primer pairs were designed as part of this project. bp = base pairs.

Gene	NCBI references	Forward primer	Reverse primer	Amplicon length (bp)
Arg1	NM_017134.3	TCGGAGCGCCTTTCTCTAAG	ATCCCCGTGGTCTCTCACAT	125
Arg1 (Louveau *et al.* 2015)	NM_017134.3	CCAACTCTTGGGAAGACACCA	GTGATGCCCCAGATGACTTT	173
ATP6AP2	NM_001007091.1	CGCCAGGGTCTGTTGTTTTC	GGAATAGGTTGCCCACAGCA	138
Gapdh	NM_017008.4	CAGGGCTGCCTTCTCTTGTG	GGTGGTGAAGACGCCAGTAG	256
Gusb	NM_017015.2	GAGCGAGTATGGAGCAGACG	GGCACTGAACCGTAACCTCT	306
Il-10	NM_012854.2	CCTGGTAGAAGTGATGCCCC	GATGCCGGGTGGTTCAATTT	281
Il-1rn	NM_022194.2	GGGGACCTTACAGTCACCTA	ACTTGACACAAGACAGGCACA	279
Il-1β	NM_031512.2	TGGCAACTGTCCCTGAACTC	ACACTGCCTTCCTGAAGC TC	192
Il-6	NM_012589.2	CACTTCACAAGTCGGAGGCT	TCTGACAGTGCATCATCGCT	114
Itgam, Cd11b, Cr3	NM_012711.1	TGCTGAGACTGGAGGCAAC	CTCCCCAGCATCCTTGTTT	101
Mtco2	GenBank: S67722.1	TGGCTTACAAGACGCCACAT	TGGGCGTCTATTGTGCTTGT	156
Rpl22	NM_031104.1	CACTTCCGAGGAGCCTTTCT	TCGTAGCTCTCCTTGCTGTTG	117
Rpl32	NM_013226.2	GGTGAAGCCCAAGATCGTCA	ATCTTCTCCGCACCCTGTTG	125
St13	NM_031122.1	GAGCCATCGAGTGAGGAGAG	AAACACTGGCTCTCTTGGCA	256
Tgf-β	NM_021578.2	CTGGAAAGGGCTCAACACCT	AGAAGTTGGCATGGTAGCCC	172
Tnf-α	NM_012675.3	ACCATGAGCACGGAAAGCAT	GTTTGCTACGACGTGGGCTA	297
Usp14	NM_001008301.1	TCCAGCCAGCCAGACAAAAA	GAGCATCTGCTGACCCCATC	117

2.4.4.1 Endpoint PCR

Standard polymerase chain reaction was performed for each primer pair to produce a high copy number of each PCR product for assessing the primers efficiency using MyTaq Red Mix (Bioline, UK), according to the kit instructions. 200 ng of cDNA was combined with 1 µl primer and 25 µl MyTaq Red Mix, and after 1 min initial denaturation, went through 40 PCR cycles (15 s denaturation at 95 ^{o}C, 15 s at 55 ^{o}C, 10 s extension at 72 ^{o}C). The final product was either used for primer efficiency (the fraction of target molecules that are copied in one PCR cycle (Svec *et al.* 2015)) or run on agarose gel to detect the amplicon length.

2.4.4.2 Gel electrophoresis

Two microliter of each standard PCR product was mixed with 4 µl loading buffer (Bioline). The mixture was electrophoresed on 2 % agarose gel (prepared from dissolve agarose powder in trisborat-ethylene diamine acid (TBE) buffer and visualised using ethidium bromide) for one hour at 100 Volt then imaged using UV transillumination and digital photography. The size of each unknown primer pair was calculated with the standard curve equation derived from the ladder (hyper ladder 100 pb, Bioline).

2.4.5 RT-qPCR

Reverse transcription quantitative polymerase chain reaction (RT-qPCR) was performed for each sample using SYBR Green Supermix (Bio-Rad) for 40 cycles with a 2-step program (5 s at 96 °C (denaturation) and 10 s at 60 °C (annealing temperature)). Amplification specificity was assessed by melt curve and electrophoresis analyses. Two qPCR controls were run with each qPCR plate RT- and NTC (no template control; general

control for extraneous nucleic acid contamination), which helps in detecting any contamination.

2.5 Time-lapse microscopy

Dynamic time-lapse transmitted light allowed real-time assessment of microglial numbers, behaviours and morphologies. Images captured at a frequency of 1 frame/120 s over a period of 24 h.

2.6 Immunocytochemistry

For immunocytochemistry 300 µl (6 x 10^5 cell/ml) microglia were plated onto glass PDL-coated coverslips, incubated in 37 °C, 5 % CO2, 95 % humidified air overnight and then treated according to the experiment condition. Microglia cultures were gently washed three times with PBS (5 min; room temperature) then fixed [4 % w/v paraformaldehyde (PFA) in PBS; 20 minutes; room temperature; in fume hood]. Fixed cells were washed three times with PBS (5 min; room temperature), non-specific staining was blocked (blocking solution: 5 % normal donkey serum (NDS) and 0.3 % Triton in PBS) for 20 min at room temperature, then primary antibodies in blocker (overnight; 4 °C; Table 2-3). Cells were then washed three times with PBS (5 min; room temperature), blocked with blocking solution (30 min, room temperature), incubated with secondary antibodies (2 h; room temperature; Table 2-4), washed three times with PBS (5min; room temperature) and then mounted with DAPI (4',6-diamidino-2-phenylindole; nuclear stain) (Vector laboratories, UK).

Table 2-3: List of primary antibodies used in the immunostaining. Type of antigen, primary antibody with their source species and concentration used on microglia imaging.

Antigen/marker	Antibody (label, product code)	Specificity for secondary antibody	Concentration
Poly–N–acetyl lactosamine sugar residues	Lectin (Sigma-Aldrich, L0651)	Biotin-labelled	1:200
CD200	OX-102 (Abdserotec, MCA 1959GA)	Mouse IgG Anti-Rat	1:200
Fractalkine receptor	Cx3cr1 (Amsbio, TP501)	Rabbit IgG Anti-Rat	1:200
Iba1	Anti-Iba1 (Abcam, ab 5076)	Goat IgG Anti-Rat	1:500
Iba1	Anti-Iba1 (Wako, 019-19741)	Rabbit IgG Anti-Rat	1:2000
iNos	iNos (N-20) (Santa Cruz, sc-651)	Rabbit IgG Anti-Rat	1:100

Table 2-4: Secondary antibody dyes/fluorophores, with excitation and emission wavelengths.

Secondary antibody label	Excitation wavelength (nm)	Emission wavelength (nm)	Concentration
Cyanine 3 (Cy3)	550	570	1:200
Fluorescein isothiocyanate (FITC)	495	525	1:200

2.7 Microscopy and image analysis

2.7.1 Fluorescence microscopy

Immunostaining and phase contrast images for each sample were obtained using an Axio Scope A1 fluorescence microscope (Carl Zeiss MicroImaging, Germany), the images have been taken using 200 or 400 x magnification, similar exposure time was used to cross

the different condition / culture/ experiment. Photoshop CS3 (Adobe, USA) was used to merge counterpart images; three channels were merged to form 'triple merge' images. At least 100 cells from at least four microscopic fields were captured per condition for subsequent analysis using ImageJ software. Individual cells were delineated using phase contrast micrographs, and this outline transferred to the corresponding red or green channel micrographs for integrated density measurement, which is the sum of the pixel values in the selected area (with background intensity subtracted for each image; fluorescence intensity measured in multiple cell-free regions).

2.7.2 Morphology (shape parameters)

Several morphological parameters were also measured while the integrated density analysis was being performed. The morphology analysis has been done to test the hypothesis that microglia change their shapes in the activation state. These parameters are shown in Figure 2-2.

2.7.2.1 Area

Area was calculated automatically by ImageJ once individual objects were delineated and is expressed in square micrometres.

2.7.2.2 Perimeter

This parameter was calculated based on the outline length of a given object and is expressed in microns.

2.7.2.3 Feret's maximum and minimum diameters

Feret's maximum diameter is the distance between the two furthest points of an object. Feret's minimum diameter represents the perpendicular distance between the closest-possible two parallel lines, that touch the object edge while the entire object is between them.

Therefore, it can be stated as the shortest distance at which callipers could be set, while capturing the entire object. Feret's minimum is not necessarily perpendicular to Feret's maximum.

2.7.2.4 Aspect ratio

Aspect ratio is calculated as the ratio between the major and the minor axis of the best fitted ellipse to a given object.

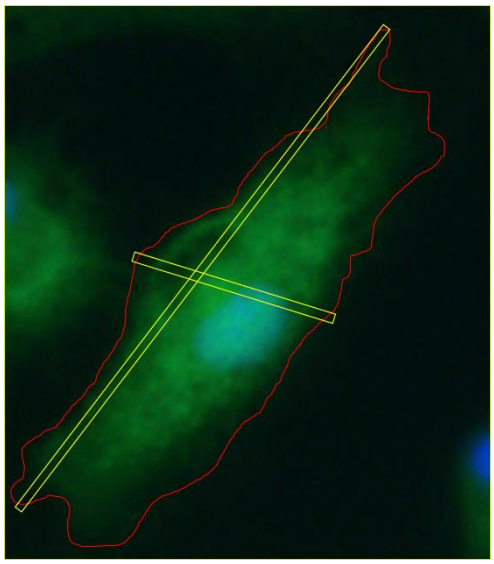

Figure 2-2: Morphological analysis involved multiple features. Outline of cell (red line) was drawn using ImageJ software, and computer analysis provided area, perimeter, longest axis (yellow) = Feret's diameter, shortest axis (yellow) = Feret's minimum diameter, and aspect ratio = Feret's diameter / Feret's minimum diameter.

2.8 Nitrite Quantification: Griess assay

Pro-inflammatory microglia produce ROS and RNS, including NO (Zielasek *et al.* 1992). To assess the production of NO in microglia, the extracellular release of nitrite (NO^{2-}), a stable metabolite of NO, was measured by Griess reagent (Promega) according to the instructions provided by the manufacturer. Supernatant samples (50 µl) were mixed with 50 µl of Griess reagent (sulfanilamide solution) in a 96-well plate and incubated at room temperature for 10 min in the dark then 50 µl of NED (N-(1-Naphthyl) ethylenediamine)

solution was added and incubated at room temperature for a further 10 min in the dark. The absorbance was measured with a 550 nm filter by a Promega microplate spectrophotometer (Promega Biosystems Sunnyvale, USA). A sodium nitrite standard curve was constructed with nitrite concentrations ranging from 0 to 100 μM. The concentration of nitrite was calculated with the linear equation derived from the standard curve.

2.9 Statistical analysis

Regarding the statistical analysis of qPCR results, advice was sought from a statistician. The advice was to perform the statistical analysis on the summary of the dose- response curve (half-maximal effective concentration (EC50) and maximum dose response) which is representative for the curve behaviour. Separate best-fit curves were produced for each dataset (GraphPad Prism software). EC50 and maximum dose response values were then derived from these curves and subjected to heteroscedasticity testing. The curves are generated from semilogarithmic plots, and the parameters derived from these curves were log normally distributed (Kenakin 2014). It was decided that Tukey's or Dunnett's post-hoc tests would be appropriate for datasets subjected to ANOVA.

The $2^{-\Delta\Delta Cq}$ method of qPCR analysis was used here (Livak & Schmittgen 2001). It has been suggested that the raw quantitation cycle (Cq) values generated by RT-PCR were unsuitable for statistical analyses unless been transformed to $2^{-\Delta\Delta Cq}$ (Schmittgen & Livak 2008). Changes in the gene of interest (GOI) expression are calculated relative to the average expression of three references genes, as recommended by MIQE guidelines (Bustin *et al.* 2009). The fold change was calculated by the following equation:

ΔCq = Cq (target gene) – Cq (average of three reference genes)

$\Delta\Delta Cq = \Delta Cq$ (treated) – ΔCq (untreated)

Fold change = $2^{-\Delta\Delta Cq}$

Individual dose-response curves have been fitted for each time point and medium in chapter 4 and 5 respectively, using GraphPad Prism software version 7 (GraphPad, USA), which allows the determination of dose-response curve summary statistics (EC50 and maximum dose response). A statistical comparison of dose response curves has not been carried out, only a comparison between summary statistics.

EC50 is concentration of an agonist that provokes a response halfway between the baseline (bottom) and maximum response (top). The EC50 values were derived using GraphPad Prism software, which can automatically generate these values by using the following equation:

$$Y=Bottom + (Top - Bottom) / (1+10^{((LogEC50-X) *Hillslope)})$$

The EC50 values have been expressed as p-values (−log of the value, pEC50) since EC50 values are log normally distributed, meaning that pEC50 will give a normal distribution. This approach is strongly recommended by Kenakin (2014). The baseline expression was calculated by comparing the controls (untreated) of serum free media to D10 media (in chapter 4).

Levene's test was used to determine the homogeneity of variance across the data. Non-homogenous data have been transformed (to become homogenous) by using log10. All statistical parametric tests were performed using normally distributed data (logarithmically expressed data) (Kenakin 2014), except the data discussed below which has been compared by the non-parametric Kruskal –Wallis test.

Statistical analyses including unpaired t-test, one-way ANOVA with Tukey's, one-way ANOVA with Dunnett's and Kruskal-Wallis with Dunn's were used throughout this thesis. Unpaired t-test was used to compare between two groups of data. One-way ANOVA with Tukey's was used for all-pairwise comparisons (Savillee, 1990), while, one-way ANOVA with Dunnett's was used for multiple-to-one comparisons (Shun et al., 2003).

Kruskal-Wallis with Dunn's was used for non-homogenous data (that could not be transformed with conventional transforming methods). This test has been used to compare nitrite concentration and immunostaining intensity, MNP-associated fluorescence intensity, and morphometrics with their controls. The chosen statistical test and level of significance were indicated in each figure legend. All data are presented as mean ± standard error of the mean (S.E.M.).

Chapter 3 : Validating the culture system and methods for microglial studies

3.1 Introduction

3.1.1 Microglial culture systems

Microglia cell culture systems were first described in the early twentieth century (Cammermeyer 1966). However, studying microglial behaviour has been delayed until methods to obtain and culture large number of microglial cells were developed and optimised. Although they are likely to behave differently from microglia *in vivo*, *in vitro* cultures provide large numbers of pure microglial cells which allows the detailed study of microglia phenotype, motility and other crucial mechanisms that characterise microglia, which cannot be sufficiently examined *in vivo*.

Nowadays there are many models to study the role of microglia n neurodegenerative diseases. These include primary microglia cultures, and microglia cell line cultures. These culture models share similarities but on the other hand they have critical differences that must be considered when choosing an appropriate model for neurodegenerative research.

3.1.1.1 Primary microglia cultures

The first description of a technique to isolate high-purity primary microglia was by Giulian and Baker (1986). Giulian and Baker used a neonatal rodent brain to produce sufficient numbers of microglia to perform microglia functional assessments. Warm-shake method was Giulian and Baker's principle which is still widely use today, although several modifications have been made to it, this technique could be performed on different species (mouse or rat). Most of early protocols to produce high purity microglial cultures were based on the use of neonatal rodent CNS tissue and few protocols have been designed to isolate adult microglia (Stansley *et al.* 2012). Although, adult microglia more mimic the *in vivo*

microglia in the mature brain (Ponomarev *et al.* 2005), however, cultured adult microglia do not survive for a long time, and are generated with low output and low purity (Nikodemova & Watters 2012). Therefore, it is difficult to use primary adult microglia to understand the biology of these cells (Frank *et al.* 2006) (as discussed in section 1.12).

Primary microglial cell culture has been used in many neuroinflammatory studies (Hunot *et al.* 1999; Parvathenani *et al.* 2003; Sondag *et al.* 2009; Gillardon *et al.* 2012), since they mimic *in vivo* microglia more closely than cell lines do. For example, in terms of secretory products and cell surface markers, it has been found that primary microglial cells' stimulation with LPS, that leads to activation of microglia *in vitro* in similar to *in vivo* activation (Colton 2009; Ransohoff & Perry 2009). The activated primary microglia has the ability to produce several pro-inflammatory cytokines such as: Il-1β, Il-6 and Tnf-α, also production of NO via upregulation of iNos and superoxide anions via activation of nicotinamide adenine dinucleotide phosphate (NADP) oxidase (Boje & Arora 1992).

The ability to measure microglia cellular function and morphology using this model makes it a useful first line research tool to screen the immunomodulatory potential of novel therapeutics.

3.1.1.2 Microglial cell lines

Microglial cell lines are typically easy to maintain in culture, which overcomes low yield and cost problems. However, apart from the genomic alterations that make them immortal, other differences in comparison to primary microglia include lack of production of some cytokines, nitrite free radical's production and different response to some stimuli (Table 3-1) (Stansley *et al.* 2012).

Table 3-1: Microglial cell lines often differ from primary and *in vivo* microglia. All of the cell lines listed here, fail to replicate a normal microglial response to these stimuli, whereas primary-derived microglia do mimic *in vivo* responses. Adapted from Stansley *et al.* (2012)

Stimulus	Normal *in vivo* response	Primary microglia	Cell lines		
			BV-2	HMO6	HAPI
LPS-treatment	IL-1β release	+	-	+	+
	NO production	+	+	-	+
Aβ-treatment	IL-1β release	+	+	-	-
LPS = lipopolysaccharide; Aβ= amyloid-beta, IL-1β= Interleukin-1 beta, NO= nitric oxide.					

3.1.1.2.1 Animal-derived microglial cell lines

Immortalised cell lines can be generated by infecting the cells with a retrovirus. Two commonly used mouse-derived cell lines are BV-2 and N9, and rat-derived lines include HAPI.

BV-2 cells were derived from murine neonatal microglia and are the most frequently used substitute for primary microglia. They have been used to study many neurodegenerative disease such as AD (Soccio *et al.* 2002; Simard *et al.* 2006; Lewis *et al.* 2010), PD (GAO *et al.* 2003) and stroke (Jin *et al.* 2014). Regarding neurodegeneration studies, it is important that BV-2, similar to primary microglia, express functional NADPH oxidase (key producers of ROS), an enzyme frequently implicated in microglia induction of neuronal damage (Wu *et al.* 2006). However, doubts have been raised that this cell line does not always model the reaction of primary or *in vivo* microglia. Horvath *et al.* (2008) compared BV-2 to primary rat microglia, demonstrating that primary microglia release the three pro-inflammatory cytokines Tnf-α, Il-1β and Il-6 in response to LPS stimulation.

However, BV-2 cells increased release of Tnf-α and Il-6 but not Il-1β, following LPS treatment. This lack of Il-1β production is a significant change from normal microglial behaviour. Another study also compared primary microglial and BV-2 cultures, this study found that LPS enhanced the release of Il-12 and keratinocyte derived chemokine in primary mouse microglia culture, however BV-2 displayed impaired capacity for the release of Il-12 and keratinocyte derived chemokine (Häusler *et al.* 2002).

N9 cells were also derived from murine neonatal microglia, but are less-frequently used in comparison to BV-2 cell line (Stansley *et al.* 2012). It has been suggested that this cell line shares many phenotypical characteristics with primary microglia (Hickman *et al.* 2008), for example unlike BV-2, N9 cells readily produce cytokines Il-6, Tnf-α and Il-1β upon stimulation with Aβ (Delgado *et al.* 1998). But in another study when both primary microglia and N9 cells were treated with a protein derived from the parasite Angiostrongylus cantonensis, a worm that causes a CNS infection, N9 expressed high mRNA level of *Il-6, Il-1β, Tnf-α, iNos, Il-5* and *Il-13* but primary microglia only expressed *Il-5* and *Il-13* mRNA (Wei *et al.* 2013). Such differences mean that data derived from cell lines should be validated using primary and *in vivo* testing.

HAPI were derived from rat neonatal microglia and are less frequently used in comparison to BV-2 and N9 (Stansley *et al.* 2012). There are two main studies that compare HAPI to the BV-2 cell line. The first one includes direct comparison of chemokine expression between BV-2 and HAPI cells following LPS treatment (Kremlev *et al.* 2004). This study found that LPS treatment of BV-2 enhanced the release of Ccl3, Ccl5, and Cxcl10, which are all upregulated in primary microglia; however, in HAPI, LPS induced release of Ccl3 and Ccl5, but not Cxcl10 (Kremlev *et al.* 2004). A second study directly compared the reactive and inflammatory profiles of the BV-2 and HAPI immortalised cell lines to primary rat microglia cell cultures across a broad range of assays including cell migration and

cytokine/chemokine production and release (Horvath *et al.* 2008). This study found that LPS enhanced the release of pro-inflammatory cytokines Tnf-α, Il-1β and Il-6 in primary microglia but different expression profiles were observed in both BV-2 and N9 which led the authors to suggest that BV-2 and HAPI cell cultures only partially model primary microglia and that their use should therefore be carefully considered (Horvath *et al.* 2008).

3.1.1.2.2 Human cell line: HMO6

Earlier studies on human microglia have been mostly in histological (i.e. dead) sections and less in primary cultures, as it is rare that human microglia become available in sufficient numbers to study their detailed cellular and molecular properties. One way to circumvent this problem was to produce a permanent (immortalised) human microglia cell line. Thus, Nagai and his group (2001) generated several stable clones of human microglia, including HMO6, by transduction of embryonic human microglia with a retroviral vector containing cDNA encoding for v-Myc oncogene. The HMO6 cells exhibited cell type-specific antigens for microglia-macrophages lineage cells including CD11b, CD68, CD86, HLA-ABC and actively phagocytosed latex beads. In addition, HMO6 cells showed ATP-induced responses like human primary microglia in Ca^{2+} influx spectroscopy. Both human primary microglia and HMO6 cells showed the similar cytokine gene expression in *IL-1β, IL-6, IL-8, IL-10, IL-12, IL-15* and *TNF-α*. Using HMO6 cells, Nagai and his group investigated whether both Aβ fragments and LPS could activate these cells. This study found that treatment of both human primary microglia and HMO6 immortalised human microglia cell line with Aβ and LPS upregulated gene expression and protein production of pro-inflammatory cytokines and chemokines in these cells in the same way (Nagai *et al.* 2001).

HMO6 are commercially-available, but relatively expensive since the cells were patented, which likely partly explains their limited usage. This may also be due to the fact

that these cells require biosafety level 2 procedures, due to risk to human health (American Type Culture Collection, ATCC). There are also few reports from non-affiliated groups about how representative these cells are of *in vivo* microglial behaviours.

3.1.2 LPS is a stereotypical pro-inflammatory stimulator

LPS is an important structural component of the outer membrane of gram-negative bacteria, it binds to Toll-like receptor (TLR)4 leading to the activation of microglia through a series of interactions with several proteins (Ulevitch & Tobias 1999). LPS enhances microglial activation and produces pro-inflammatory mediators such as Tnf-α, Il-1β and Il-6 both *in vitro* and *in vivo* (Nakamura *et al.* 1999; Possel *et al.* 2000).

LPS is one of the most widely studied immune-stimulatory components of bacteria and can induce systemic inflammation (Beutler & Rietschel 2003). Upon LPS recognition, TLR4 downstream leads to activation of NF-κB pathways in microglia (Kawai *et al.* 1999), Mitogen-activated protein kinases (MAPKs) pathways (Qin *et al.* 2005) and interferon regulatory factor 3 (IRF3) through the activation of several mediators (Figure 3-1).

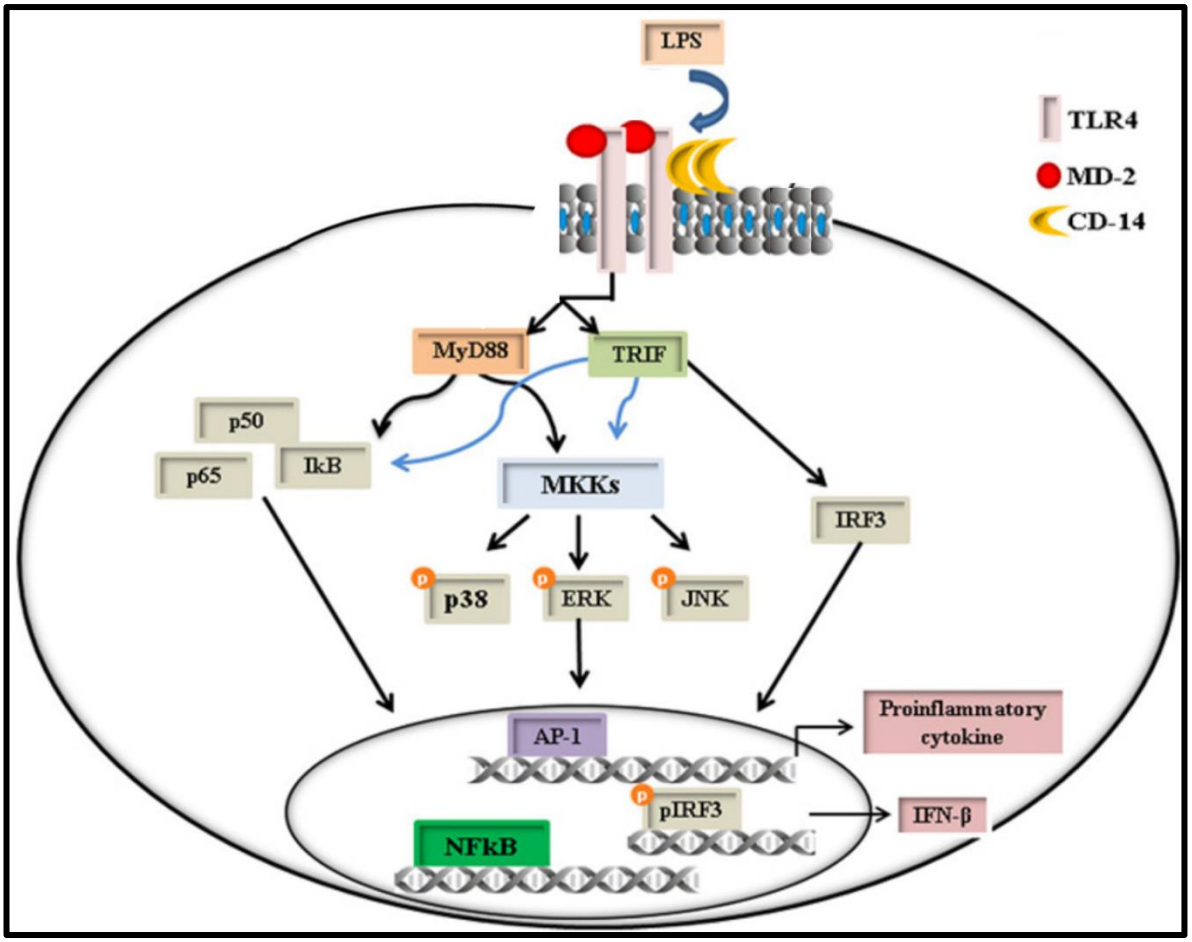

Figure 3-1: Illustration of the molecular events following LPS-TL4 interaction. Adapted from Murshid *et al.* (2015).

NF-κB, a major transcription factor, modulates inflammatory system through expressing pro-inflammatory genes (Ghosh *et al.* 1998). Under normal conditions, inhibitors of κB (IκB) form a complex with NF-κB, maintaining it in an inactivate form in the cytoplasm. Once stimulated by inflammatory signals such as LPS, IκB is phosphorylated and degraded releasing free NF-κB (Lappas *et al.* 2002). Afterward, NF-κB translocates into the nucleus and binds to the DNA binding site related to regulating the transcription of its target genes, triggering expression of pro-inflammatory enzymes and cytokines such as iNos, Tnf-α and Il-β.

MAPKs are one of the major kinase families associated with cellular processes such as differentiation, stress responses, apoptosis and immune defence (Bennett *et al.* 1997).

IRF3 translocation into the nucleus leads to regulation of the transcription and expression of type I interferons such Inf-β, Ccl5 and chemokine (C-X-C motif) ligand 10 (Cxcl10) (McCarthy *et al.* 2017). These three pathways are involved in regulating the inflammatory process.

LPS induction of Tnf-α leads to autocrine activation of TNFR, activation of JAK2/STAT1, and subsequent increase in Il-6 production; thus LPS-activation of Il-6 is a direct secondary effect, and this likely explains the delay in production of Il-6 reported in several studies (Minogue *et al.* 2012) (Figure 3-2).

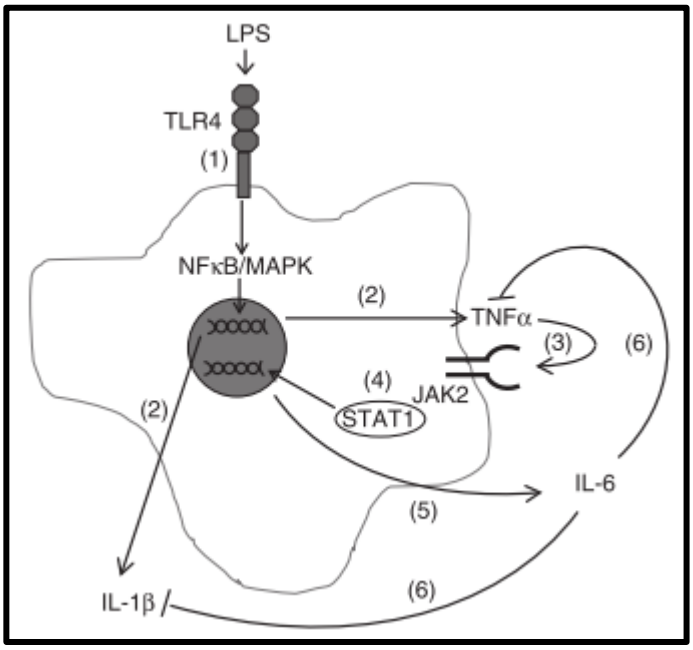

Figure 3-2: LPS-induced signalling and cytokine release. TLR4 is stimulated by LPS, (1) TLR4 leads to activation of NF-κB/MAPK pathways, (2) which leads to release of Tnf-α and Il-1β. (3) Released Tnf-α interacts with its receptor, (4) activating Janus kinase-2 (JAK2) and activators of transcription (STAT) (5) which up-regulate transcription and release of Il-6. (6) Il-6 feeds back to inhibit further release of Tnf-α and Il-1β. Adapted from Minogue *et al.* (2012).

3.1.3 Most microglial qPCR studies used insufficient and unvalidated reference genes

Reliable reference genes are vital for reliable qPCR data, and MIQE guidelines recommend multiple reference genes be employed (Bustin *et al.* 2009; Hellemans *et al.* 2007). It is increasingly recognised that some widely used reference genes (e.g., *Gapdh*) (Jimenez *et al.* 2008; Lisak *et al.* 2009; Fenn *et al.* 2012) may be unsuitable, with reports of experimental condition-induced changes in *Gapdh* expression (Everaert *et al.* 2011; Al-Sabah *et al.* 2015). For example Al-Sabah *et al.* (2015) reported that *in vivo* model of inflammatory joint pathology *Gapdh* transcript levels were significantly reduced compared to the control of this experiment. Another study suggested that the highly used *Gapdh* and *ACTB* have variable expression levels when they compared the mRNA levels directly in a cross sectional series of biopsy tissue from normal controls and subjects with asthma (Glare *et al.* 2002). This could be a problem since expression levels of reference genes should remain constant between the cells of different tissues and under different experimental conditions (Thellin *et al.* 1999). If these requirements are not fulfilled, then normalisation to varying references could cause misleading results (Bustin 2000). From this, a single reference gene cannot be used to accurately normalise RT-qPCR data and that the combination of multiple reference genes is preferred. Although increasing the number of reference genes for normalisation will improve the accuracy of the analysis, this is expensive and time consuming. Therefore, it has been suggested that the number of reference genes needed to be employed is dependent on the considerations of a researcher's purpose (Hu *et al.* 2009). Use of two to three stable reference genes is a valid normalisation strategy in most experimental conditions.

3.2 Aims and objectives

3.2.1 Aims

The aim of the study described in this Chapter is validation of primary microglial culture and qPCR methods.

3.2.2 Objectives

The objectives are:

- To determine the purity of microglial cultures derived from primary mixed glial culture.
- To confirm that primary microglia respond to LPS (e.g., concentrations and time points).
- To design and validate qPCR primers for multiple reference genes and genes of interest.
- To study sex-dependent differences in microglial gene expression.

3.3 Results

3.3.1 Microglial cultures were of high purity

Microglial markers were identified from the literature, and tested with microglial cultures. As described in section 2.6, cultures were maintained on coverslips, and immunostained to assess culture purity. All cultures were of high purity as judged by lectin-reactivity (>98 %). Cells also expressed Iba1 and lectin, confirming their microglial identity (Figure 3-3) (Shrivastava *et al.* 2012).

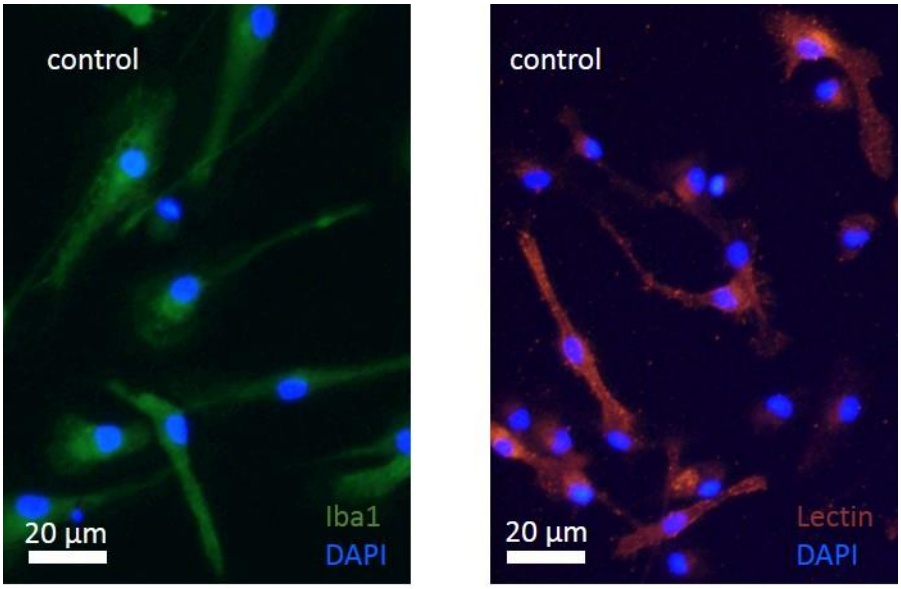

Figure 3-3: Iba1 and lectin labelling of microglia. Cells expressed Iba1 and lectin, confirming their microglial identity. Figure shows DAPI-stained nuclei as blue, Iba1 as green, and Lectin as red.

3.3.2 Confirmation of microglial response to LPS

A range of experimental LPS concentrations was chosen based on the literature search, but to confirm the biological efficacy of these doses in this experimental system, and to estimate response times, microglia were exposed to selected concentrations of LPS. As described in section 2.6, cultures were maintained on coverslips and immunostained to assess culture purity with and without LPS. All cultures were of high purity as judged by

lectin-reactivity (>98 %) treatment with LPS led to a significant increase in lectin integrated density (Figure 3-4). Time-lapse microscopy revealed clear cellular responses (e.g., morphological changes and cell death) (Jenkins *et al.* 2014) within 2 h at all concentrations (10, 50 and 1000 ng/ml; Figure 3-5; video 2 (video file submitted with thesis, Video 2; internet link: youtube.com/watch?v=JrN_OrGyQ2Q)), with no comparable changes evident in control cultures (same microscope/incubator setup, 6 h; without LPS; video 3 **(**video file submitted with thesis, Video 3; internet link: youtube.com/watch?v=LjcdbLhpm2s)).

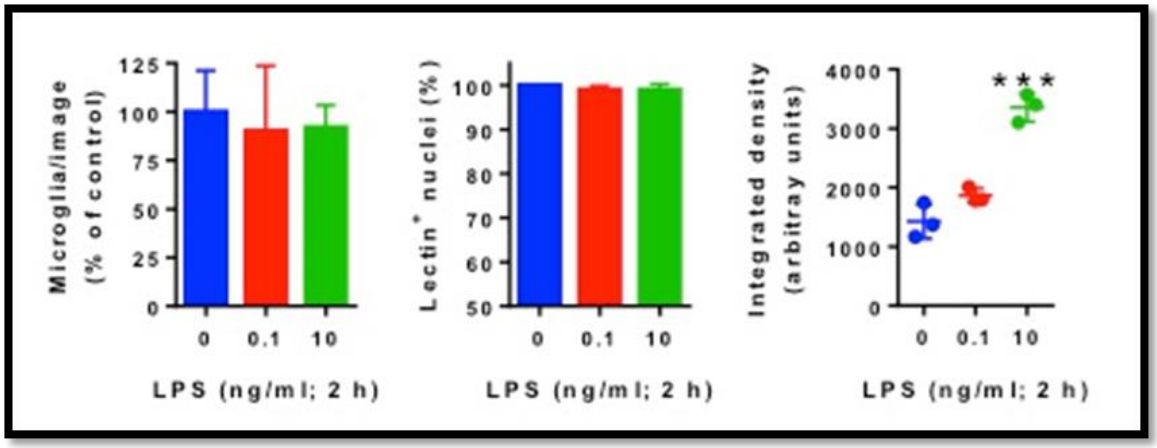

Figure 3-4: Microglial cultures were of high purity and intensity of lectin reactivity increased with LPS treatment. (A) Bar graph indicating cell count (microglia per image). (B) Bar graph indicating percentage of all nuclei showing lectin reactivity, confirming microglial identity. (C) Bar graph indicating intensity of lectin reactivity, which increased with the highest LPS concentration tested. These cultures were assessed after 2 h LPS treatment. ***p<0.001; One-way ANOVA with Dunnett's post-hoc test versus 0 LPS. All data are presented as mean ± S. E. M. of three independent experiments. .

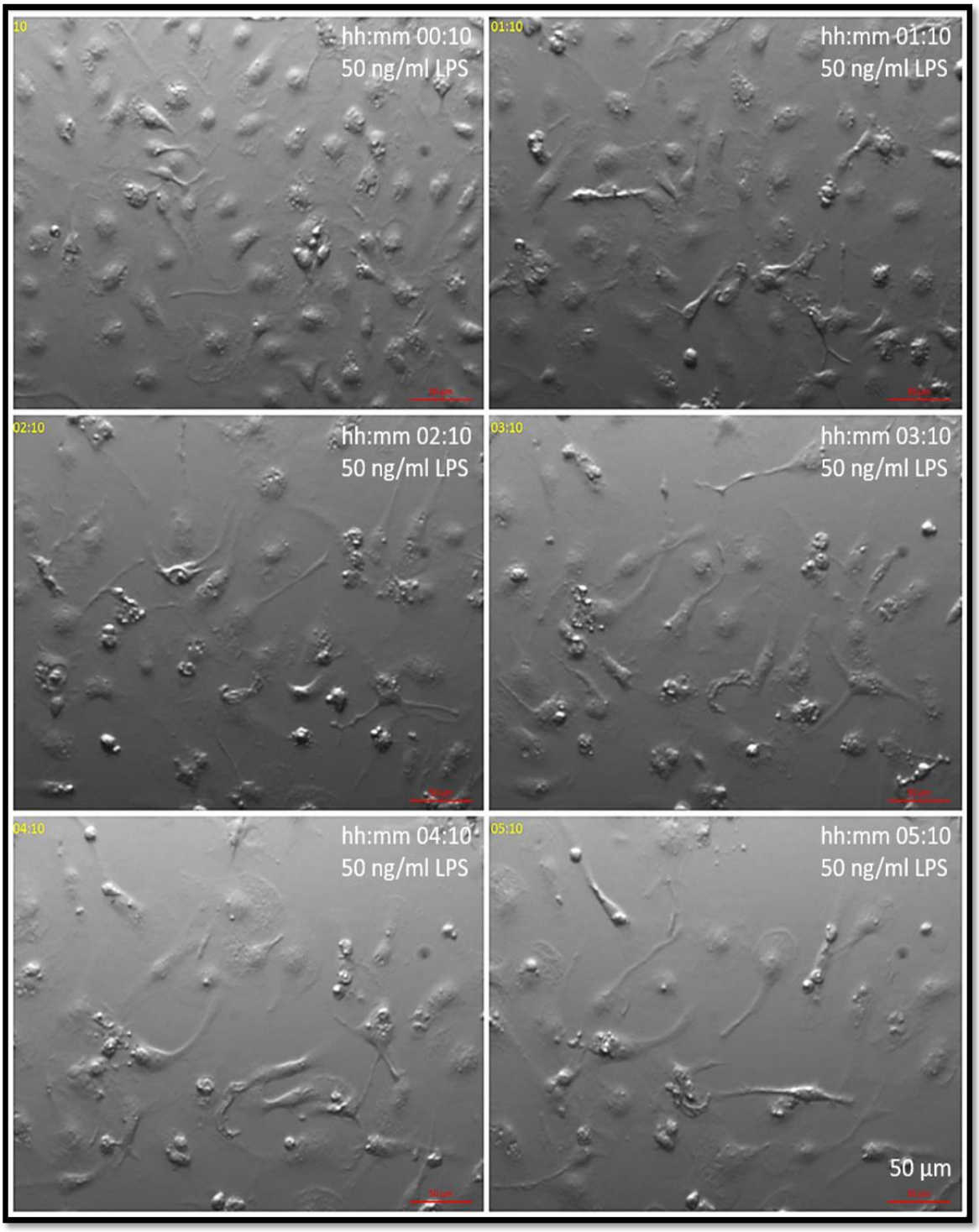

Figure 3-5: Microglia primary culture cells response to LPS *in vitro*. Transmitted light micrographs showing typical microglial morphologies immediately post-LPS (50 ng/ml). Many microglia exhibited short, thick processes after 5 h exposure at 50 ng/ml. Images are stills from time-lapse microscopy, 30 frames/hour. See supplementary video2; (video file submitted with thesis, Video2; internet link: youtube.com/watch?v=JrN_OrGyQ2Q).

3.3.3 qPCR

3.3.3.1 Multiple candidate reference genes were identified

It is a recommended practice to select multiple reference genes, rather than relying on a single reference gene (Bustin *et al.* 2009). But most researchers rely on a single reference gene, typically *Gapdh*. To the best of my knowledge, there are no reports attempting to validate *Gapdh* as a reference gene for microglia.

Microarray analyses of M1 activated microglia were identified in the literature and datasets obtained from repositories (Rock *et al.* 2005; Moran *et al.* 2007; Zawadzka *et al.* 2012). Only one study using LPS was identified (Zawadzka *et al.* 2012), but two further studies using the pro-M1 stimulus IFN-γ were found (Rock *et al.* 2005; Moran *et al.* 2007). Moran *et al.* (2007) study used primary new-born rat microglia. Rock *et al.* (2005) used primary human foetal microglia. Concentrations and timings of treatment varied between these studies (1 – 24 h), but all used pro-M1 stimuli. Datasets included fold-change in gene expression, following IFN-γ or LPS treatment (versus untreated controls), as well as copy numbers for each mRNA transcript. Genes present in high copy numbers were shortlisted, and fold-change averaged across all datasets. Then these transcripts with average fold-change less than 0.9 or greater than 1.1 were excluded, and candidate reference genes were selected from this list, and compared with *Gapdh* (Table 3-2) (Tarca et al. 2006). Notably, the widely-used reference gene *ACTB* showed a 16.5-fold increase with IFN-γ treatment (Moran *et al.*2007), raising questions about its validity. *Gapdh* data were not available for LPS treatment. IFN-γ showed varied *Gapdh* responses, with a 3.9-fold increase at 16 h (Moran *et al.* 2007), and 1.67-fold increase on average. However, Rock *et al.* (2005) showed 0.98-fold at 24 h. This variation meant that it was unclear whether *Gapdh* would likely serve

well as a reference gene. But due to its widespread use, it was included here for validation work.

Table 3-2: Candidate reference genes identified from microarray analyses. Number of fold change between treatment and control for the reference gene candidates. Note that most candidate reference genes were minimally affected, or unaffected by treatment with pro-M1 stimuli (average fold change 0.94 – 1.08), whereas *Gapdh* showed an average 1.67-fold increase in expression. However, no LPS-treated data were available for *Gapdh*, and most of this increase is represented by the 16 h data for IFN-γ (3.94-fold increase).

	Fold change in microglial mRNA expression					
	IFN-γ, human primary foetal cells (Rock *et al.* 2005)		**IFN-γ, primary newborn rat cells (Moran *et al.* 2007)**	**IFN-γ, human primary foetal cells (Rock *et al.* 2005)**	**LPS, primary newborn rat cells (Zawadzka *et al.* 2012)**	
Gene name	**1 h, 200 U/ml**	**6 h, 200 U/ml**	**16 h, 100 U/ml**	**24 h, 200 U/ml**	**24 h, 100 ng/ml**	**Average**
Atp6ap2	1.09	0.92		1.04	1.10	1.04
Gapdh	0.93	0.84	3.94	0.98		1.67
Gusb			0.90		1.11	1.01
Mtco2 (Cox-2)					0.97	0.97
Rpl22	1.14	0.87	0.99	0.76	0.97	0.95
Rpl32	1.27	0.87	0.84	0.70	1.01	0.94
St13	1.04	0.86	1.06	0.85	0.92	0.95
Usp14					1.08	1.08

INF-γ, interferon; LPS, Lipopolysaccharide; Atp6ap2, ATPase H (+)-transporting lysosomal accessory protein 2; Gapdh, Glyceraldehyde 3-phosphate dehydrogenase; Gusb, Beta-glucuronidases; Mtco2, Mitochondrially Encoded Cytochrome C Oxidase II; Rpl22, ribosomal protein L22; Rpl32, ribosomal protein L32; St13, suppression of tumorigenicity 13; Usp14, Ubiquitin Specific Peptidase 14.

3.3.3.2 Comparison of primers for candidate reference genes

qPCR primers were designed for *Gapdh* and the seven other candidate reference genes listed above. They generated clear amplicon bands, with several also producing faint bands, of sizes <100 bp, likely to indicate primer-dimers (Figure 3-6). The greatest size discrepancies were St13 and Gusb (>26% difference versus calculated amplicon size), which were then excluded as candidates. By assessing the predicted (software) and measured sizes (Table 3-3), microarray data and clarity/reproducibility of gel bands, *Rpl32* and *Usp14* were selected for further validation.

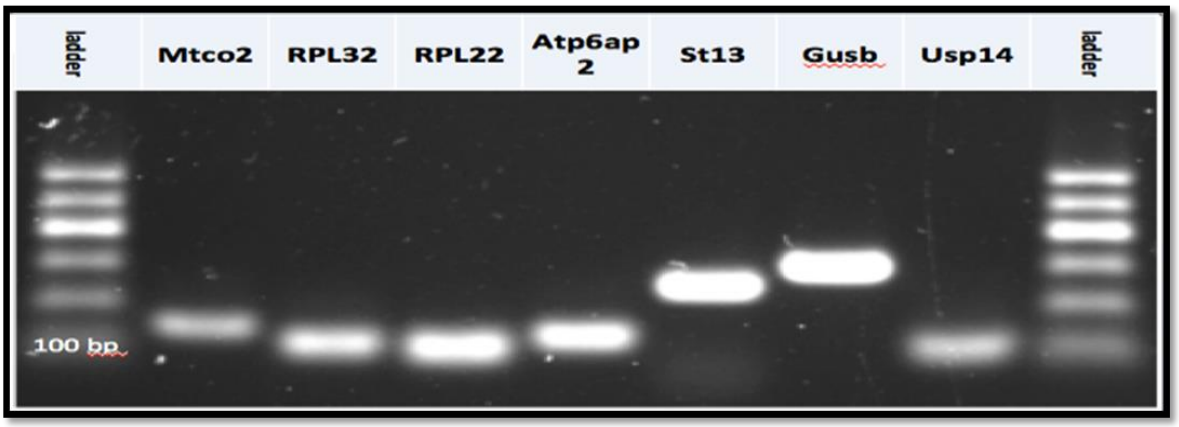

Figure 3-6: Gel image for reference gene candidate. Note that there is a single strong band present for each gene. Atp6ap2, ATPase H (+)-transporting lysosomal accessory protein 2; Gapdh, Glyceraldehyde 3-phosphate dehydrogenase; Gusb, Beta-glucuronidases; Mtco2, Mitochondrially Encoded Cytochrome C Oxidase II; Rpl22, ribosomal protein L22; Rpl32, ribosomal protein L32; St13, suppression of tumorigenicity 13; Usp14, Ubiquitin Specific Peptidase 14.

Table 3-3: List of primers amplicons size and melt curve (Tm) values.

	Amplicon size (bp; gels)				**Amplicon melting temperature Tm (melt curves)**	
Gene	**Predicted**	**Measured**	**Difference**	**Primer-dimers?**	**Lower**	**Upper**
Atp6ap2	138	120	-13 %	N		83.8
Gapdh	256	234	-9 %	Y	84.4	84.7
Gusb	306	226	-26 %	N	89.5	90
Mtco2	156	130	-17 %	N		80
Rpl22	117	105	-10 %	N		84
Rpl32	125	104	-17 %	Y	83.2	84
St13	138	192	39 %	Y		89
Usp14	117	107	-9 %	N		80.2

Atp6ap2, ATPase H (+)-transporting lysosomal accessory protein 2; Gapdh, Glyceraldehyde 3-phosphate dehydrogenase; Gusb, Beta-glucuronidases; Mtco2, Mitochondrially Encoded Cytochrome C Oxidase II; N, No; Rpl22, ribosomal protein L22; Rpl32, ribosomal protein L32; St13, suppression of tumorigenicity 13; Usp14, Ubiquitin Specific Peptidase 14; Y, Yes.

qPCR was performed using the three reference genes. The results show there was no LPS or Il-4 (M2 stimuli)-induced change in expression for the reference genes tested (*Gapdh*, *Usp14*, *Rpl32*), across a wide range of LPS and Il-4 (Figure 3-7, Figure 3-8), and there was no evidence of a dose-response effect. Therefore, the average of their Cq values should allow reliable evaluation of LPS-induced changes in GOI.

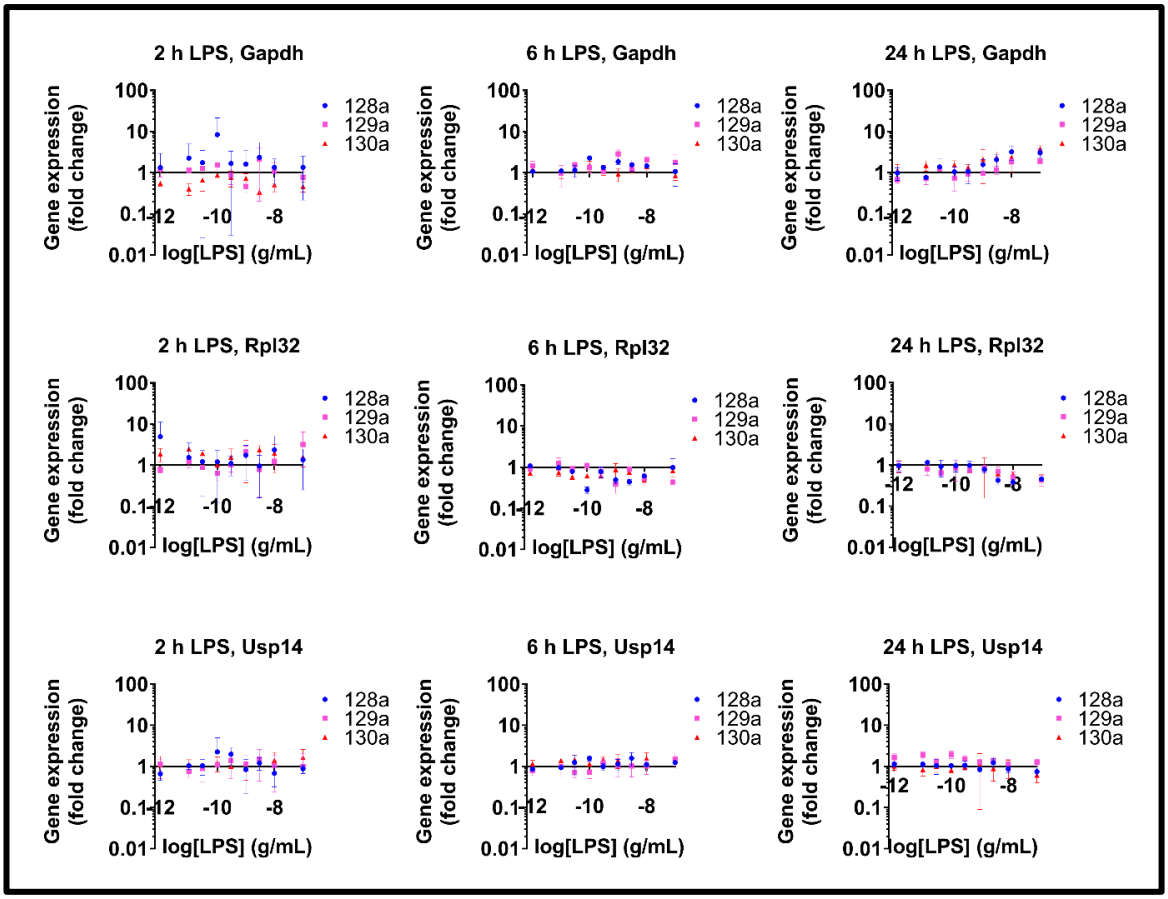

Figure 3-7: Candidate reference genes (*Usp14, Rpl32* and *Gapdh*) were unresponsive to LPS treatment. LPS was tested at a range of concentrations from 0.001- 100 ng/ml, and in the absence of LPS (signified on these graphs as the lowest LPS concentration 10^{-12}), for three different cultures at three-time points. For the 2, 6 and 24 h data, three technical replicates were performed for each culture (128, 129 and 130: biological replicates). Note that the error bars show that standard error of mean between technical replicates was limited. Also, note that the three biological replicates produced similar values, demonstrating high reproducibility.

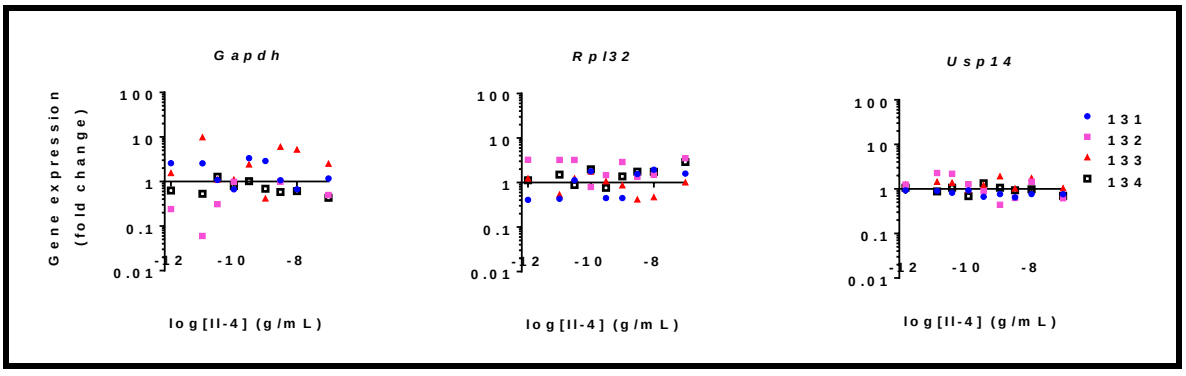

Figure 3-8: Candidate reference genes (*Usp14, Rpl32 and Gapdh*) were unresponsive to 24 h of Il-4. Note that the four biological replicates produced similar values, demonstrating high reproducibility, for four different cultures.

3.3.3.3 qPCR primers validation for GOIs

Samples were taken from pilot qPCR experiments and subjected to gel electrophoresis to determine whether each reaction/well generated a single amplicon of the expected size (Figure 3-9). Any amplified gDNA should appear as a larger than expected band, since primers were selected to bridge exon boundaries wherever possible. DNA ladders were used to generate a standard curve of migration distance versus nucleic acid size, which was in turn used to estimate amplicon size. (Figure 3-9 A) shows that single clear bands were generated for all genes, with migration distances close to expected size, with the exception of *Tgf-β*, which was investigated in more details, and new primers designed. These tests confirmed which qPCR signals were genuine, giving confidence in generated data.

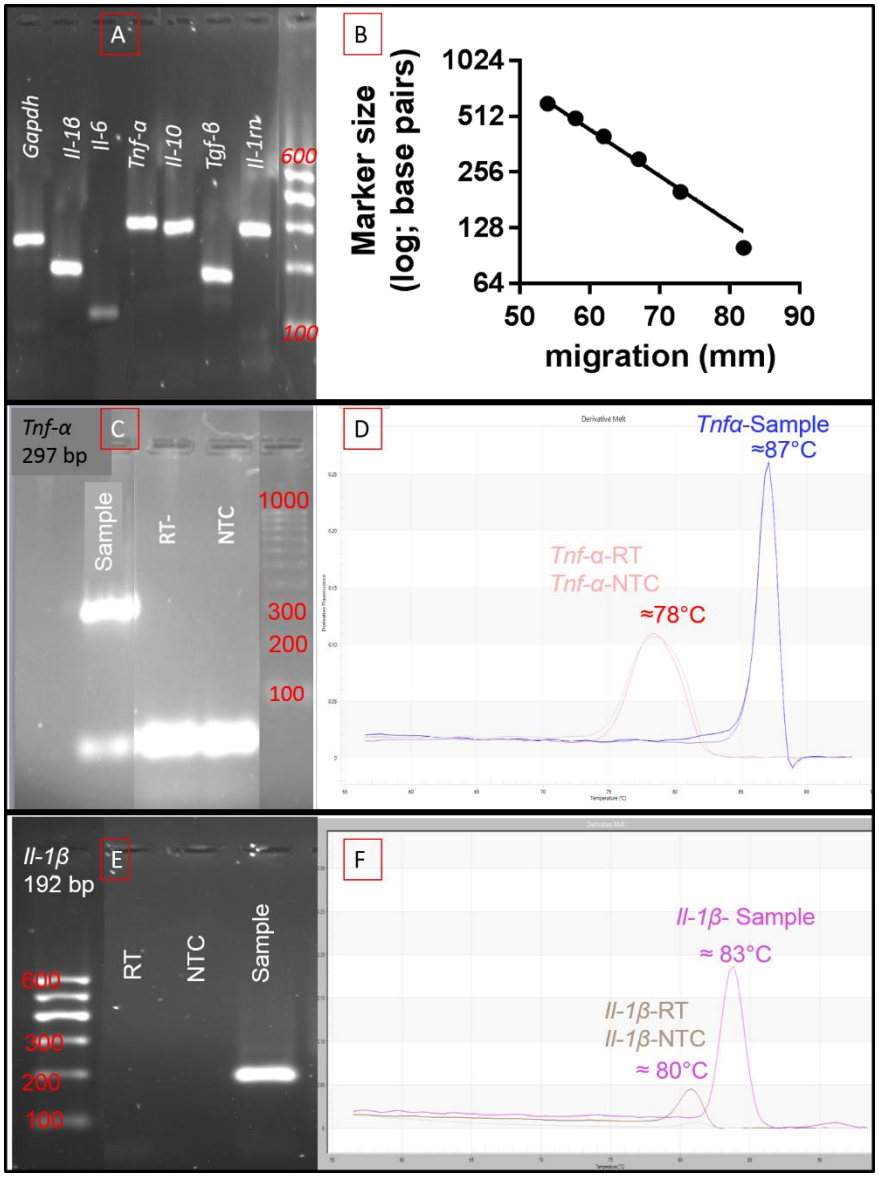

Figure 3-9: Example analysis to confirm amplicon identity and specificity. (A) gel images show that there is a single intense band present for each primer pair. (B) Standard curve of migration distance versus nucleic acid size for markers. (C, D) gel image and melt curve for *Tnf-α* (sample, RT- and NTC). Note that NTC and RT- do not show bands at the expected migration point for the *Tnf-α* amplicon (~297 bp), but sample does show bands near the 300 bp ladder marker. These samples generated melt curves at ~87 C, demonstrating that this Tm value is indicative of appropriate amplicon generation. In all lanes, bands have migrated beyond the 100 bp markers, indicative of non-specific signal, perhaps primer-dimers. These are possibly associated with the peak at 66.4 °C in the melt curve analysis. (E, F) gel and melt curve for *Il-1β*. Note that there is a single band present in *Il-1β*-Sample, with a migration distance suggesting a product size of 194 bp, compared to the expected size of 192 bp. Comparing this gel with the melt curve analysis demonstrates that the *Il-1β* amplicon has a Tm of ~83 °C. Both the NTC and RT- lanes show no clear signal, consistent with the lack of strong peaks in melt curve analysis. All samples generated faint bands smaller than 100 bp, suggesting some primer-dimer formation. NTC= no template control; RT= no reverse transcriptase control; Tm= primer melting temperature (the temperature at which one-half of the DNA duplex will dissociate to become single stranded).

3.3.3.4 Determining primer efficiency

The ΔΔCq method of qPCR analysis depends upon primer's efficiency being close to 100% (Kenneth J. Livak & Schmittgen 2001). In order to determine efficiency, qPCR was carried with a range of starting material concentrations. These were prepared as follow for each qPCR reaction:

- Microglial cDNA was used as the template for an endpoint PCR reaction, to provide cDNA enriched with the amplicon of interest.
- A second round of endpoint PCR was carried out using this amplicon-enriched source as the template, to generate DNA samples containing essentially only the amplicon of interest.
- The absorption at 260 nm was used to calculate the DNA concentration, and the Mw of the amplicon to calculate the amplicon concentration.
- Ranges of dilution were made with amplicon concentration from $1x10^7$ to $1x10^0$ amplicons/ 2 µl, and 2 µl aliquots of these were used as template for qPCR reactions.
- The Cq from qPCR reactions were plotted against amplicon concentration Figure 3-10 and the slope of the linear fit to these points used to calculate the efficiency of the qPCR since:

$$\text{PCR efficiency} = 10^{-1/\text{slope}} - 1$$

Table 3-4 summarises the slope for these standard curves and their related primer efficiency, which was close to 100 % efficiency for all primer pairs.

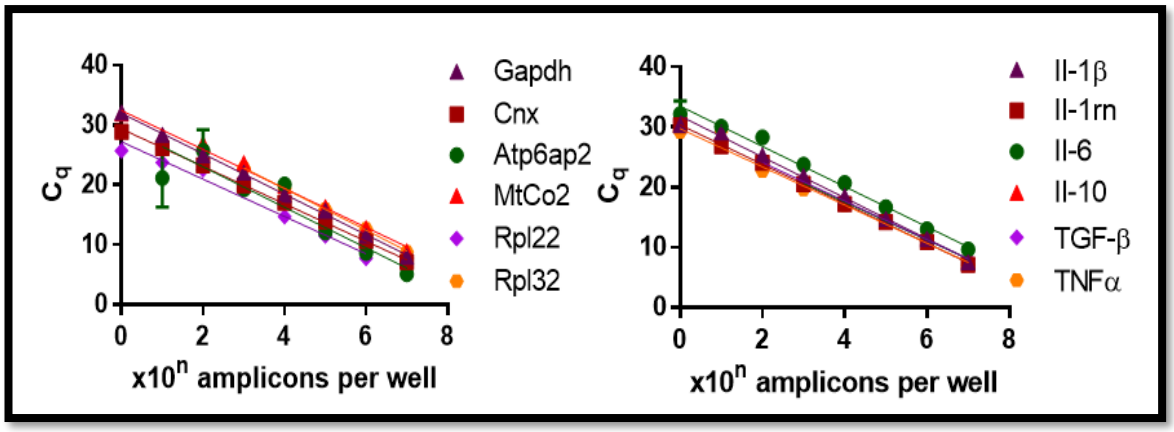

Figure 3-10: Calibration curves indicating qPCR amplification efficiency for primer pairs. X-axis represents increasing quantities of template (copy number, amplicons per well), which is associated with decreasing Cq values (y axis; threshold signal being reached at an earlier amplification cycle). As copy number (amount of template) increases, rate of amplification should increase proportionally (reducing Cq), if the reaction is 100 % efficient. The slope of each best-fit line is compared to the value predicted for 100 % efficiency. Note that the relationship between copy number and Cq is consistent except at the lowest copy number values for some primer pairs.

Table 3-4: List of primer standard curves slope, with their calculated primer efficiency.

Gene	n	Slope	R^2	$10^{-1/slope}$	Efficiency
Atp6ap2	3	-3.4	0.93	1.97	97 %
Cnx	3	-3.4	0.99	1.97	96 %
Gapdh	6	-3.4	0.99	1.98	98 %
Il-1β	6	-3.4	0.99	1.97	97 %
Il-1rn	3	-3.3	0.99	2.01	101 %
Il-6	3	-3.4	0.99	1.99	99 %
Il-10	6	-3.3	0.99	2.02	102 %
MtCo2	3	-3.3	0.99	2.03	103 %
Rpl22	3	-3.1	0.99	2.09	109 %
Rpl32	3	-3.5	0.99	1.94	94 %
Tgf-β	4	-3.2	0.99	2.05	105 %
Tnf-α	3	-3.2	0.99	2.06	106 %

3.3.3.5 Total RNA yield varied between cell types and affected mRNA purity

The amount of RNA extracted from microglia in the first few experiments was low. Therefore, a pilot study was performed to compare RNA yield of microglia with two other glia cell types (oligodendrocyte precursor cells [OPCs] and astrocytes) and a macrophages cell line (THP-1; human monocytic leukaemia) to determine whether the low yield was inherent to the microglial cells or to the RNA extraction techniques. Different cell numbers were used (36, 72, 144 and 720 x 10^4 cells per vessel) and two different flasks/plates (T25 flasks and 12 well plates) for the glia cells, but only one density for THP-1 (12 x 10^4 cell) since this cell line has markedly higher levels of proliferation. In each case, the cell number stated here was collected into a single RNeasy kit tube (i.e. increasing numbers of cells in the particular sample being processed for RNA extraction; so, volumes of all reagents are constant, while cell number varies). The data showed an increase in RNA yield with increasing concentration of cells in the extraction process, as expected, with microglia exhibiting a significant increase in RNA yields when extracted from a T25 flask (i.e. highest number of cells: 720 x 10^4; Figure 3-11; Figure 3-12). Therefore, by the time the experiments in chapter seven were performed, microglia were being routinely cultured in T25 flasks.

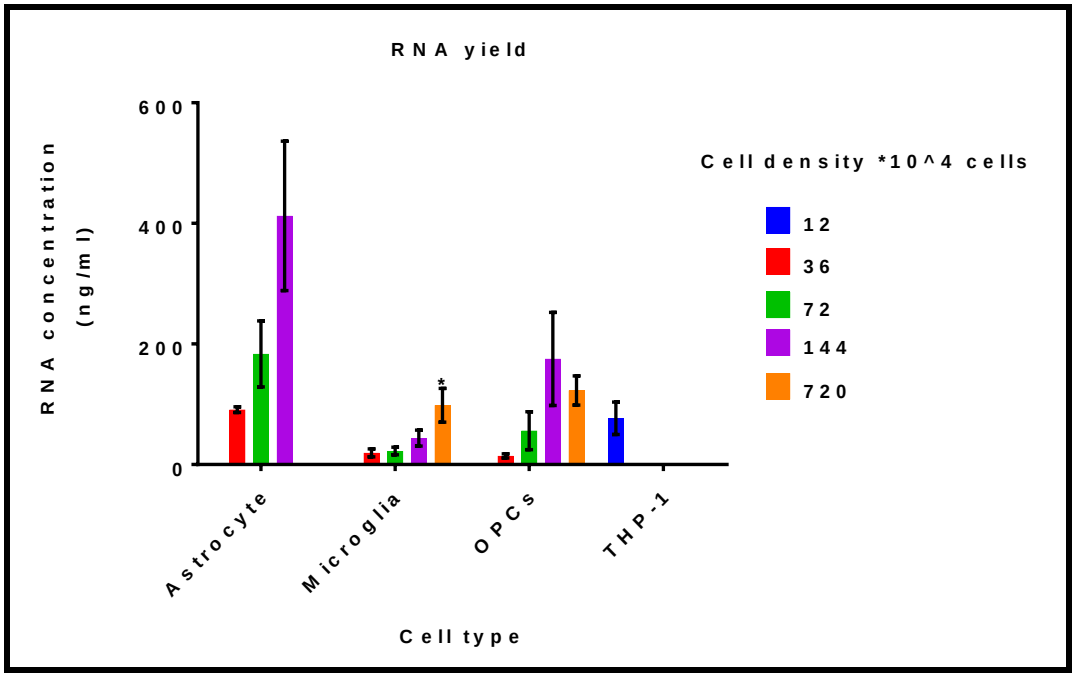

Figure 3-11: RNA extraction from microglia versus astrocyte versus OPCs versus macrophages from THP-1 cell line using RNeasy columns. Different plating density and wells effect on the RNA concentration. *p < 0. 05; One-way ANOVA with Tukey's post-hoc test for each cell type. All data are presented as mean ± S. E. M. of three independent experiments.

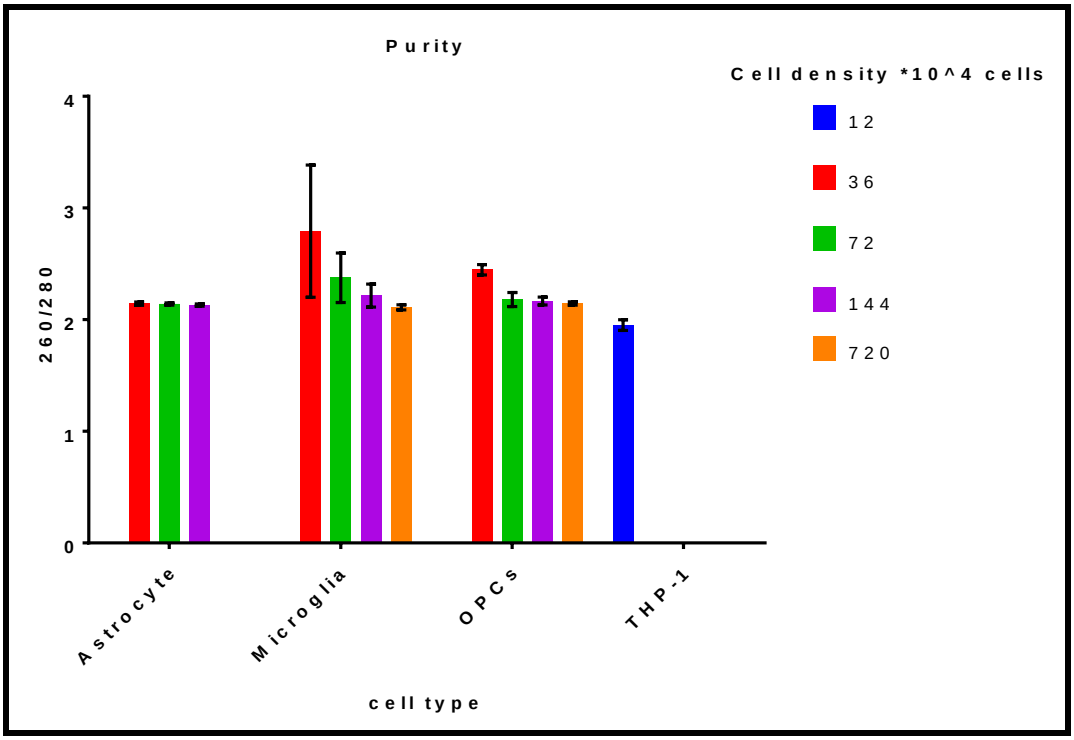

Figure 3-12: mRNA purity from RNA extraction from microglia versus astrocyte versus OPCs versus macrophages from THP-1 cell line using RNeasy columns. Different plating density and wells effect on the RNA purity. No significant difference; One-way ANOVA with Tukey's post-hoc test for each cell type. All data are presented as mean ± S. E. M. of three independent experiments.

3.3.4 No differences were detected between male and female microglia

A pilot study was performed to compare male and female microglial gene expression. All data are n = 1 or 2, which precludes any statistical evaluation, furthermore only one reference gene was used to normalise this data (*Gapdh*) since it was one of the first experiments and it was performed before the full validation of the three reference genes. Similar responses were observed for all genes (Figure 3-13). Although our data suggest limited (if any) gender differences, the literature indicated the presence of differences, at least later in development (Mouton *et al.* 2002; Schwarz & Bilbo 2012; Lenz *et al.* 2013; Hanamsagar *et al.* 2014; Sidor *et al.* 2014; Lenz & McCarthy 2015). Therefore, this thesis has limited the initial investigations to cultures derived exclusively from males, so that if any relevant gender differences were later discovered experimentally or in the literature, this would not be confounding for the data gathered here.

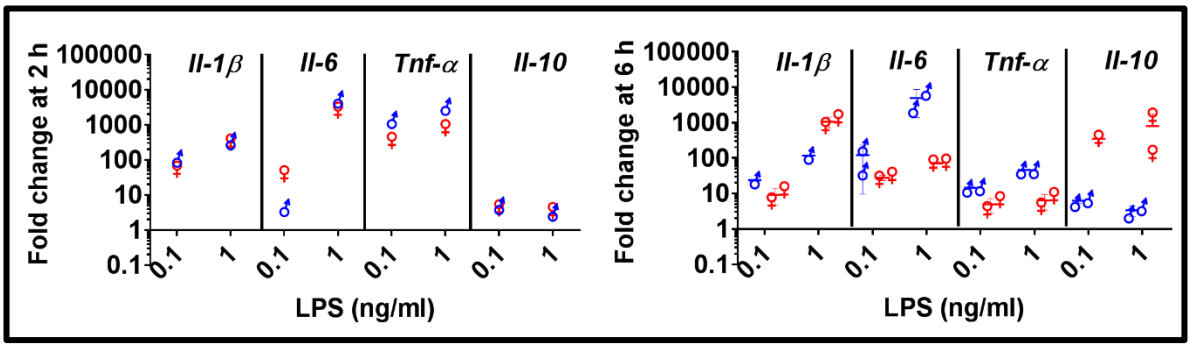

Figure 3-13: Male versus female microglial gene expression, following 2 and 6 h LPS treatment. LPS effect on different genes (*Il-1β, Il-6, Tnf-α* and *Il-10*) on 1-2 cultures at two times points (2 and 6 h). Note that for most genes and most concentrations/time points, changes in expression were similar for male and female samples. Males and females were compared from the same litters; *Gapdh* as reference gene; n =1 – 2 for all data presented here.

3.4 Discussion

Microglia are routinely cultured using the system described here, so data can be compared to the literature. The culture system described is robust and allowed consistent derivation of high purity microglial cultures, with large numbers of cells.

3.4.1 Microglial in cell culture

Lectin and Iba1 are widely used for the identification of microglia in brain tissue and in cell culture (Taylor *et al.* 2004). Lectin is a carbohydrate binding protein obtained from *Lycopersicon esculentum* (tomato), with affinity for poly-N-acetyl lactosamine sugar residues (Zhu & Laine 1989). It has been reported to label microglia through the recognition of glycoproteins containing terminal alpha-D-galactose residues in the rat nervous system (Ambalavanar and Morris, 1991). In another study, the authors reported that tomato lectin binding was found in relation to microglia cells (Acarin *et al.* 1994). Furthermore, Iba1 has been found to be highly and specifically expressed in microglia among the cultured brain cells (Ito *et al.* 1998). And that is why they have been used to detect the purity of microglia culture (Figure 3-3; Figure 3-4).

This study results suggested that LPS treatment leads to an increase in lectin staining intensity and microglial activation which go in parallel with what Acarin *et al.* (1994) have reported when they studied rat postnatal brain, that is amoeboid microglial cells always showed stronger binding of tomato lectin compared with ramified microglial.

The LPS concentration used in this study did not led to cell death (Figure 3-4), this result is in line with what Chao *et al.* (1994) have reported that treated microglia with 10 ng/ml LPS for 20 h had not induced a reduction in microglia cells number. Studies also reported that activated microglia display morphological changes from a highly branched resting state to a more amoeboid or rounded reactive state (Davis *et al.* 1994; Petersen &

Dailey 2004) which are in line with the results from time-lapse observations of this study. Furthermore, this time-lapse showed a range of microglial motility behaviours during and after activation, individual microglia cell extended a process to phagocytose another dead cell or migrate to the infection site. This indicates that a single microglial cell may take on different morphologies, and the morphological appearances in static images are not necessarily accurate predictors of cell motility behaviours. This supports the finding of Stence *et al.* (2001) that time-lapse analysis suggest not all microglia responded with the same time course, but there was a stereotypical sequence of dynamic morphological changes.

3.4.2 LPS as robust M1 stimulus; biological activity

LPS is one of the major outer surface membrane components present in almost all Gram-negative bacteria and acts as an extremely strong stimulator of innate or natural immunity in species ranging from insects to humans. For this reason, it has been used in many studies for investigation of cytokine induction in the brain (Ransohoff & Benveniste 1996). Many studies used only a single concentration of LPS (Mayer *et al.* 2001; Fan *et al.* 2005; Wang *et al.* 2005), and often few time points, or even a single time point. Therefore, I determined to carry out a more detailed characterisation of the dose- and time-responsiveness of the LPS response.

Data from this chapter are consistent with microglia being LPS-responsive and confirmed the biological activity of the LPS stocks used here. Early data also showed increased gene expression for pro-inflammatory genes (Il-1β, Il-6 and Tnf-α). Therefore, the cell system, LPS and qPCR primers used here seem suitable for characterising M1 microglial activation.

3.4.3 Multiple reference genes identified and validated

The MIQE guidelines suggested that more than one reference gene should be used to insure reliable qPCR result that could promote consistency between laboratories, and increase experimental transparency (Bustin *et al.* 2009). Using more than one reference gene increases the chances of detecting genuine changes in gene expression. Therefore, this study aimed to validate microglia reference gene that is lacking in microglia field.

This study results showed that three genes (*Rpl32*, *Usp14* and *Gapdh*) from the 7 candidates showed no dose-response changes across a wide range of concentration (0.00 – 100 ng/ml) of two different stimuli (LPS and Il-4). Over three different time points (2, 6 and 24 h) for LPS and one time point 24 h for Il-4. Therefore, this validatory data suggests that these genes can be recommended as standard reference genes, something currently lacking in rat microglial research.

3.4.4 Primers for genes of interest have been validated

The MIQE guidelines suggested that robust qPCR assays are correlated with high PCR efficiency (Bustin *et al.* 2009). If the PCR efficiencies vary that would be problematic during the interpretation of the results. Previous studies have reported that PCR efficiencies may vary from 80 % to 100 % (Kamphuis *et al.* 2001), or from 65 % to 90 % (Tichopad *et al.* 2003). However, this is not always included in calculations, with some researchers simply assuming 100% in their calculations.

When PCR efficiency is assumed to be 100%, but it is not 100%, then this leads to inaccurate $2^{-\Delta\Delta Cq}$ results. For example, when efficiencies vary over a range as small as 0.04, from 1.78 to 1.82, it results in a 4-fold error in relative expression (Ramakers *et al.* 2003). Therefore, it is necessary to evaluate specific PCR efficiencies before doing relative quantification (Rao *et al.* 2013).

PCR amplification efficiency has been established by means of calibration curves, because such calibration provides a simple, rapid and reproducible indication of the mean PCR efficiency. The results obtained here showed that the primer pairs selected for continuing study have efficiency close to 100%, with range from 94 % (*Rpl32*) to 106 % (*Tnf-α*), making these primer pairs suitable for quantification using $2^{-\Delta\Delta Cq}$ method.

3.4.5 Total RNA yield per cell/culture: microglia versus astrocyte versus OPCs versus THP1

The low total RNA yield and purity was a concern in the first few experiments on microglia. Several changes in the extraction protocol were made without improvement either in terms of yield or the purity. Therefore, a hypothesis that microglia has low quantities of total RNA per cell was generated.

To test this hypothesis, a comparison between different types of cells has been made. Also, different densities of cells per total RNA extraction procedure (e.g., standard volumes of reagent; 1 tube per sample) were compared. The results showed that microglia have low total RNA yield in comparison to other cell types. This is consistent with Dumbacher's report that RNA yields vary widely from different tissues and samples (Dumbacher 2013). Results generated here suggest that total RNA yield and purity increase with the number of cells being processed. Therefore, larger quantities of cells were used for qPCR studies, to improve yield and purity of total RNA.

3.4.6 Male versus female microglia

Various reports in the literature indicated differences between male and female microglia, especially in adult brain, although in neonatal brain reports are inconsistent (

Mouton *et al.* 2002; Schwarz & Bilbo 2012; Lenz *et al.* 2013; Hanamsagar *et al.* 2014; Sidor *et al.* 2014; Lenz & McCarthy 2015;).

In adult rodent CNS, there are differences in microglial morphology between male and female rodents (Schwarz *et al.* 2012). Significantly higher number of microglia are present in female rodents (rats and mice) hippocampus in comparison to male rodents hippocampus (Mouton *et al.* 2002; Schwarz *et al.* 2012). Female microglia have morphologies more closely resembling M1 microglia (Schwarz *et al.* 2012). Furthermore, female brains show higher immune activation as shown by higher level of Ccl20 and Ccl4, despite the presence of the great concentration of neuroprotective steroids estrogen and progesterone in compare to male microglia (Schwarz & Bilbo 2012).

In the neonatal rodent CNS, studies showed contradictory results. For example Crain *et al.* (2013) reported that in P3 mouse, female microglia has higher mRNA level of *Tnf-α, Il-1β, Il-10* and *Il-6* but no difference in *iNos* and *Arg1* expressions. On the other hand, Loram *et al.* (2012) reported no different between neonatal male and female microglia isolated from P (0-1) pups. However, the same study suggested an increased *Il-1β* gene expression of male microglia when treated with a high concentration of LPS (100 ng/ml).

The data presented in this chapter showed no difference between male and female rat microglia, in terms of pro-inflammatory gene expression, after treating them with low and medium doses of LPS (two time points). But it was decided to avoid possible sex differences by limiting initial investigations to cultures derived exclusively from males. Therefore, if any relevant gender differences were later discovered, experimentally or in the literature, this would not be confounding for the data gathered here.

3.5 Summary

This chapter has described validatory work on an *in vitro* microglial culture system, showing that this protocol generated a high purity microglia culture. Furthermore, this study showed (for the first time) validation of three reference genes: the widely used *Gapdh* and two other reference genes (*Rpl32* and *Usp14*) remained unaffected across a wide range of concentrations of different treatments, at different time points. Wide adoption of these reference genes could improve comparisons of qPCR results for microglial gene expression between different laboratories.

The preliminary results of this study suggested that there are no differences between male and female microglial pro-inflammatory gene expression, in response to LPS, at two time points. However, more biological replicate are required to be able to prove that statistically and further investigation of the possible effects of gender on microglial gene expression, which might become more obvious in juvenile or adult animals.

Chapter 4 : Characterising primary microglial culture in serum-free media

4.1 Introduction

4.1.1 *In vivo* data are important, but it is difficult to study microglia *in vivo*

In vivo experimentation is low throughput and difficult to both control and monitor. However, typical *in vitro* systems fail to mimic *in vivo* features that could be critical to microglial activation status. Differences between *in vitro* and *in vivo* include oxygen levels (Lennon *et al.* 2001), unrealistic 2D environment (Sun *et al.* 2006) and cellular environment (i.e. tissue-specific construction), mechanical and biochemical signals, with cell–cell communication also being altered under such simplified and highly biased conditions (Pampaloni *et al.* 2007).

The effects of the differences between the brain and the culture environment may confound the study of microglial activation for example, some studies showed that astrocytes (which are also cells of the CNS) were less activated in a 3D environment compared to a 2D environment (East *et al.* 2009; LaPlaca *et al.* 2010; Tickle 2017). Furthermore, the monocellular composition of the culture differs from the *in vivo* multicellular composition which may limit the ability to model diseases (Duell *et al.* 2011; Miki *et al.* 2012). In the case of this study, the inclusion of serum in culture media could be a confounding factor, as the presence of cytokines and other signalling molecules in serum might lead to low-level M1 activation or priming of microglia (priming microglia theory will be further discussed in Chapter Five). That is, although a strong (greater than physiologically-relevant) stimuli can increase pro-inflammatory responses *in vitro*, it is possible that the non-treated/ 'control' microglial cultures might be in a partially-M1 state, rather than the ideal M0 state (Figure 4-1).

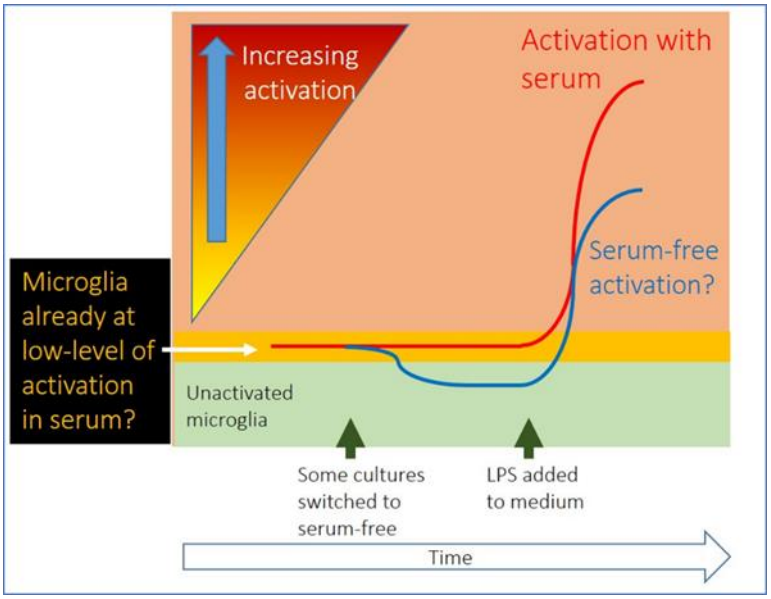

Figure 4-1: Hypotheses relating to microglial activation in serum versus non-serum media. LPS may produce a consistent increase in magnitude of activation, whether serum is present or not. But, if serum-exposed microglia are already activated to some extent, then I hypothesise that in serum-free media: 1. microglia will be in low level of activation (lower baseline in compare to serum contain media), 2. Higher EC50 and 3. Lower maximum dose response.

The BBB limits the access of most blood-borne molecules to the brain parenchyma, with the interstitial fluid here being of a more restricted composition than blood. Molecules are present at much lower levels in the brain than the blood, such as glucose (Mcnay *et al.* 2001), hormones (Amado *et al.* 1995) and immunoglobulins (Parsons & Webb 1982) (Table 4-1).

It would be of benefit to identify a serum-free media which can support microglia growth, as serum is an undefined mixture of growth factors and cytokines, many of which microglia would only encounter if the BBB becomes compromised. Microglia *in vivo* are surrounded by interstitial fluid, similar to the CSF, which is devoid of most serum-associated molecules. Here we propose that the use of serum is confounding, and culturing microglia without serum would more accurately mimic *in vivo* conditions, and possibly produce more clinically-predictive microglial behaviour.

Additionally, using serum-free medium would provide a defined culture environment, without confounding molecules which can induce immune-relevant responses, such as LPS, complement proteins and immunoglobulins, data relating to microglial activation could be more reliably generated. Finally, the investigations of the metabolic changes, namely; glucose, insulin and vitamins. can be more reliably performed, as serum would not introduce unknown quantities of these molecules, in addition to these introduced by the experimenter.

4.1.2 The differences between fetal bovine serum and cerebrospinal fluid

Fetal bovine serum (FBS) is a common supplement of cell culture media. It has been used for almost all human and animal cell culture (Brunner *et al.* 2010). FBS contains a mixture of factors that stimulate cell survival and regulate pH (van der Valk *et al.* 2004). There are concerted efforts to reduce and eliminate its use, since it its composition is an undefined mixture of nutrients, salts, hormones, growth factors and hundreds of different proteins and metabolites: proteomic studies showed over 1000 proteins (Anderson & Anderson 2002; Anderson *et al.* 2004), and another study found four thousand metabolites (Psychogios *et al.* 2011) present in serum. There are several further disadvantages of using FBS in cell culture media, including the increasing concerns about the global supply versus demand of FBS (Gstraunthaler *et al.* 2013), batch-to-batch variations and the different molecules present in serum that could cause different reactions, especially in immune cells. All those factors might affect culture health and confound immune studies, which could be classified as endogenous and exogenous substances.

4.1.2.1 Endogenous proteins

The major elements of serum, albumin and transferrin, are known, but serum also contains a wide range of minor components that may have a significant effect on microglia.

These components include nutrients (i.e. sugars), growth factors (i.e. cytokines), hormones, minerals and lipids. The different concentrations of these substances between microglia *in vivo* and *in vitro,* and their actions have not been fully studied (Freshney 2005).

Microglia in their natural brain environment get supplementary (nutritional) materials from the brain fluid, namely CSF. CSF composition and concentration are different from these of the serum present in the cell culture media (De Graaf *et al.* 2011). Despite the absence of serum in the CNS, current studies of CNS disease are performed in cultures containing serum. However, serum is thought to be a confounding factor, due to the presence of chemicals that may elicit an immune response, that might have a role in immune-mediated diseases within the CNS (Aizenman & de Vellis 1987). For example, in normal serum there is always an amount of cytokines (interleukins) (Kleiner *et al.* 2013), which is important for many functions such as regulating development and differentiation of the cells but normally their concentration is lower in the CNS than the blood circulation due to the selectivity of the BBB. Therefore, we hypothesise that culturing microglia in a serum-supplemented media may lead to activation of microglia or at least prime them.

Table 4-1: Variation of components contained within serum compared to the typical composition of CSF, which is like the interstitial fluid surrounding microglia *in vivo*.

	Typical composition of fetal bovine serum (contribution to media when supplemented at 10 %)		**Composition of cerebrospinal fluid (CSF)**	**Fold difference between 10 % FBS and CSF**
Components	**Range**	**Average concentrations**	**Average concentrations**	**10 % FBS / CSF**
Total protein (g/100 ml)	3.2 – 7.0	3.8	0.04 (Hong *et al.* 2010)	95
Albumin (g/100ml)	2.0 – 3.6	2.3	0.02 (Seyfert *et al.* 2004)	115
Endotoxin (ng/ml)	0.01 – 10.0	0.3	0.06 (Pentreath *et al.* 1996)	5
Haemoglobin (mg/100ml)	2.4 – 18.1	11.3	0.02 (Hong *et al.* 2010)	565
Cholesterol (mg/100ml)	12 – 63	31	0.2 (Mulder *et al.* 1998)	155
Glucose (mg/100ml)	85 – 247	125	60 (Tiraboschi *et al.* 2016)	2
Insulin (IU/ml)	6 – 14	10	0.92 (Molina *et al.* 2002)	11
The serum components value adapted from Price and Gregory (Price & Gregory, 1982).				

4.1.2.2 Exogenous substances

Serum can be a potential source of microbial contamination, such as fungi, bacteria or viruses (Dormont 1999; Wessman & Levings 1999). Furthermore, quality manufacturing testing allowances of endotoxin may reach 2.58 ng/ml which mean that 10 % FBS-supplemented media could have a total of 0.25 ng/ml of endotoxin. This is a concern for microglial studies as the endotoxin in the CSF does not typically exceed 0.012 ng/ml. Schaafsma *et al.* (2015) reported that 1 ng/ml LPS is the threshold concentration required to trigger mild and low-grade expression of pro-inflammatory mediators in primary microglia culture. The same study used a very low concentration of 0.005 ng/ml LPS which may be unrealistic since D10 media may contain 0.26 ng/ml endotoxin (LPS) (Table 4-2).

Table 4-2: Endotoxin in 10 % serum media versus CSF.

	FBS	**10 % serum**	**Contact with CSF**
EU	12.9	1.29	0.06
ng/ml	2.58	0.258	0.012

EU value is from Certificate of Analysis, Life Technologies, Lot number 41Q8641K, Brazilian FBS, catalogue number 10270.

EU = endotoxin units are used to describe lipopolysaccharide detection by Limulus amebocyte lysate (LAL) assay. One EU equals approximately 0.1 to 0.2 ng endotoxin/ml of solution. CSF = cerebrospinal fluid.

FBS = foetal bovine serum.

Consequently, many trials have been done to culture CNS cells in serum-free media. For example Saneto and de Vellis (1985) have cultured oligodendrocytes isolated from primary neonatal rat in chemically defined serum-free media. Brewer *et al.* (1993) optimised the survival of rat embryonic hippocampal neurons in serum-free media. However, there has been no systematic examination of the use of serum-free media for

microglial culture, with most researchers either withdrawing serum for several hours during an experimental treatment or continuing with serum throughout (Zielasek & Hartung 1996; Franciosi *et al.* 2005; Kobayashi *et al.* 2013).

4.1.3 Alternatives to fetal bovine serum in cell and tissue culture

Considering the mentioned disadvantages, many approaches for reducing the requirements for FBS in culture media and alternative animal serum replacements were defined (Jayme & Smith 2000). These authors have defined five classes of media: serum-containing media, reduced serum media, serum-free media, protein-free media and chemically defined media. While Brunner *et al.* (2010) have classified media into serum-free, animal-derived component-free or chemically defined media for cell culture applications.

- Chemically defined (CD): Chemically defined media do not contain proteins, hydrolysates or any other components of unknown composition. Highly purified hormones or growth factors added can be of either animal, plant or recombinant, but are added in known concentrations.
- Animal-derived component free (ADCF): These media contain no components of animal origin and are not necessarily chemically defined (e.g., may contain bacterial or yeast hydrolysates or plant extracts).
- Serum-free (SF): Serum-free media do not require supplementation with serum but may contain some protein fractions (e.g., animal tissue or plant extracts) and are thus regarded as chemically undefined (Yao *et al.* 2006; Chen *et al.* 2008). Thus, there is an urgent necessity to understand the effect of these media on the immune response of the immune cells and if serum has a real effect on stimulating the immune response.

4.1.4 Rationale for choices and design

A defined serum-free medium which supports microglial survival and phenotype-switching would be beneficial to researchers. This study described two commercially available serum-free media, developed for immune cell culture, were compared to a serum-supplemented medium typically used with primary microglia.

Macrophages-SFM (from here onwards, referred to as SFM) is a serum-free medium designed for the culture of human peripheral blood monocytes and macrophages. This medium has been used to study macrophages responses to LPS. For example in a study by Buechler *et al.*, (2000) 1 ng/ml of LPS has induced monocyte activation in a serum-supplemented medium while in macrophages-SFM media much higher doses of LPS (1000 ng/ml) are required to achieve identical responses. These media-dependent differences in cellular responses to LPS may be due to the activity of LPS-binding protein (LBP), which is known to be present in serum (Buechler *et al.* 2000). Similarly, Shapira *et al.* (1994) suggested that Tnf-α production in the presence of serum was higher than that in the absence of serum (1 ng/ml LPS in both cases). As microglia closely resemble macrophages, it has been suggested that this medium may support microglia too. Two studies have used this medium with microglia, in which Toescu *et al.* (1998) have studied the impact of depletion of intracellular Ca^{2+} stores in mouse brain microglia and its effect on plasma membrane Ca^{2+} pathway. Minelli *et al.* (2000) studied the effect of ammonium on cytoplasmic *p*H and Ca^{2+} concentration in cultured mouse microglial cells. However, none of these studies have measured the effect of serum on inflammatory profile.

Xvivo media are serum-free and chemically defined cell culture media. These media do not contain any artificial stimulators of cellular proliferation or undefined supplements. Although these media were specifically developed for hematopoietic cells,

many researchers used them to culture macrophages (Henriksen *et al.* 2004; Carter *et al.* 2011). Interestingly, Rey-Giraud *et al.* (2012) used Xvivo media to generate an *in vitro* model of monocyte-derived macrophages (MDM) under serum-free conditions. In which macrophages derived from monocytes were cultured in (I) serum-supplemented media with M-CSF for M2 macrophages, (II) GM-CSF for M1 macrophages, (III) Xvivo media supplemented with M-CSF and Il-4, Il-10 to induce activated M2 and (IV) GM-CSF and LPS together with IFN-γ to generate activated M1 phenotype. MDM differentiated under serum-free conditions displayed enhanced activity for M1 and tumour promoting property for M2 macrophages in contrast to MDM differentiated in the presence of serum (Rey-Giraud *et al.* 2012). Also, Lalive *et al.* (2005) have used these media to culture primary microglia, since the media support microglia survivor for a day before the experiment ended.

In the subsequent chapters in this thesis, I examined the concentration-response relationship between LPS and Il-4, and microglial activation towards M1 and M2 phenotypes, and the effect of repeat stimulation. For both of these types of investigation it is important that:

1. Basal activation of cells is minimal, as any underlying activation would alter the dose response relationship.
2. That cells can survive for the prolonged period (4 days) between bouts of stimulation.

In this Chapter, the hypothesis is that the presence of serum may alter basal activation; by using two serum free media to test this hypothesis; and to investigate whether these media support long-term culture.

4.2 Aims and objectives

4.2.1 Aims

The primary aim of this study is to assess whether microglia can be successfully cultured without serum supplementation. The secondary aim is to assess whether their behaviour is altered. To the best of my knowledge, there is no published work has directly compared of microglia behaviour, including LPS dose response using the normal serum containing media head to head with serum-free media, a question of significant importance for researchers, the reduction of animal protection usage, and potential clinical engineering of human microglia.

This Chapter aims to answer the following questions:

1. Do microglia survive in the absence of serum, in short and medium incubation times?
2. Does microglial activation differs when incubated in serum free media for acute (a day) and chronic (6 days) period of time?

4.2.2 Objectives

For a period of time that is sufficient for microglia to ‘recover’ from the first treatment, and then be challenged a second time, i.e. facilitating future experiments relating to priming:

- To confirm that qPCR reference genes are suitable for serum-free testing.
- To compare microglial viability and morphology between serum-free and serum-supplemented media.
- To compare dose-response curve summary statistics (EC50, baseline and maximum dose response) of pro-inflammatory genes, with or without serum-supplemented media.

4.3 Experimental procedures

4.3.1 Reagents and equipment

All reagents and equipment used are as described previously in Chapter Two. Two types of media (macrophages-SFM) were from Thermofisher Fisher Scientific (Loughborough, UK) and Xvivo were from Lonza (Cambridge, UK).

4.3.2 Preparation and treatment of microglia culture

Mixed glia culture preparation and high purity microglia culture isolation were described previously in Chapter Two. Microglia cultures were incubated in D10 media for 6 h, then media have been changed to serum-free media (Xvivo and SFM) and further incubated at 37 °C in 5 % CO2/95 % humidified air for 24 h (Figure 4-2), then cells have been treated with serial doses of LPS (0, 0.001, 0.01, 0.1, 1, 10 and 100 ng/ml). Later, cells were fixed and stained for morphological analysis, and RNA has been extracted for gene expression as described in Chapter Two.

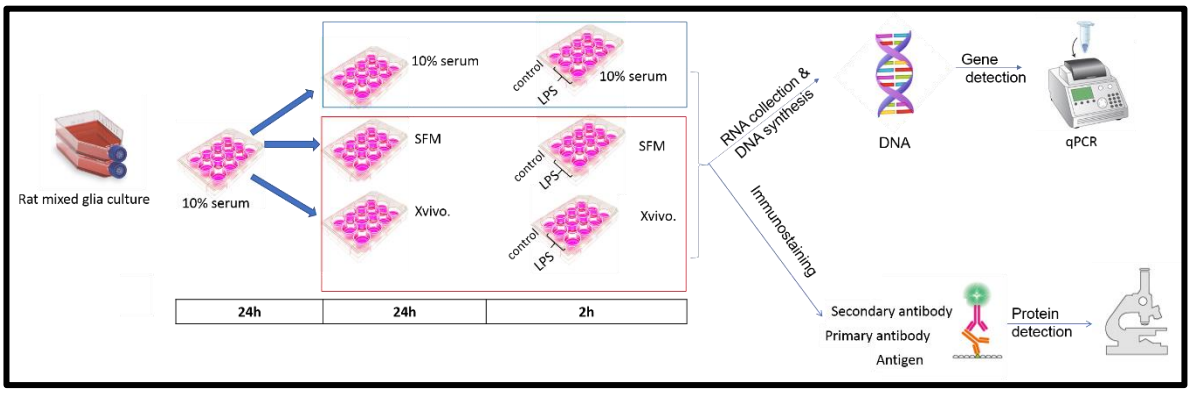

Figure 4-2: Schematic diagram illustrating the main procedure for serum-free media experiment. Microglia were isolated from rat mixed glia culture by mechanical shaking, and cultured at high purity culture. After microglia rested for 6 h, 10% FBS containing medium was removed, and replaced with serum-free medium . Then the cultures have been left in serum-free media for a day or 6 days. Then experimental treatment (e.g., LPS to induce M1 phenotype) has been added for 2 h; then cells were fixed and stained. In parallel, RNA can be extracted from cultures for qPCR analysis.

4.4 Results

4.4.1 The acute effects of serum-free conditions on microglia (24 h)

4.4.1.1 Microglial viability and morphology at 24 h serum-free media culture

All cultures were of high purity as judged by lectin-reactivity (>98 %; Figure 4-3A). No reduction in microglial numbers were observed in either serum-free media at 24 h (Figure 4-3B).

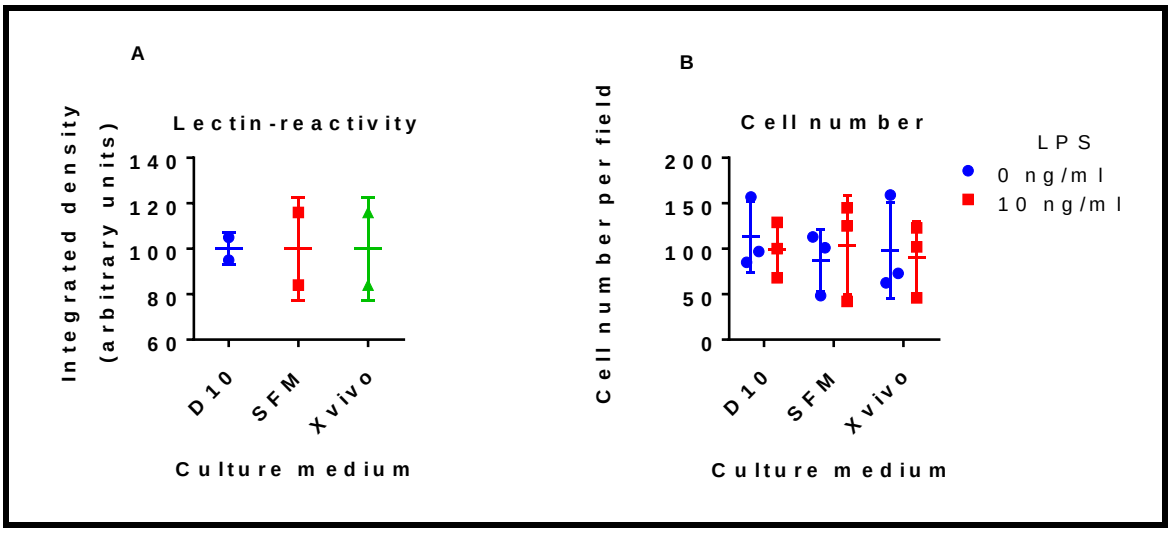

Figure 4-3: Intensity of microglial marker expression and cell number. (A) Intensity of lectin reactivity, in a pilot experiment (n = 2). Lectin-reactivity confirmed microglial identity. (B) Cell number. These cultures were assessed after 2 h LPS treatment (n = 3). No significant difference between D10 and the two serum free media was found; One-way ANOVA with Dunnett's post-hoc test versus D10, Also, unpaired t-tests for LPS versus control. All data are presented as the mean ± S. E. M. of two independent experiments in (A) and three independent experiments in (B). D10 = DMEM supplemented with 10 % FBS; SFM = serum-free media; Xvivo = hematopoietic media.

Cells were viable in D10 and the two serum free media, and expressed Cx3cr1 and CD200R, with the latter confirming their microglial identity, being exclusively expressed by microglia (Figure 4-4), there was no effect of serum or LPS on Cx3cr1 and CD200R expression (Figure 4-5). Furthermore, microglia were morphologically similar across all media (Figure 4-6).

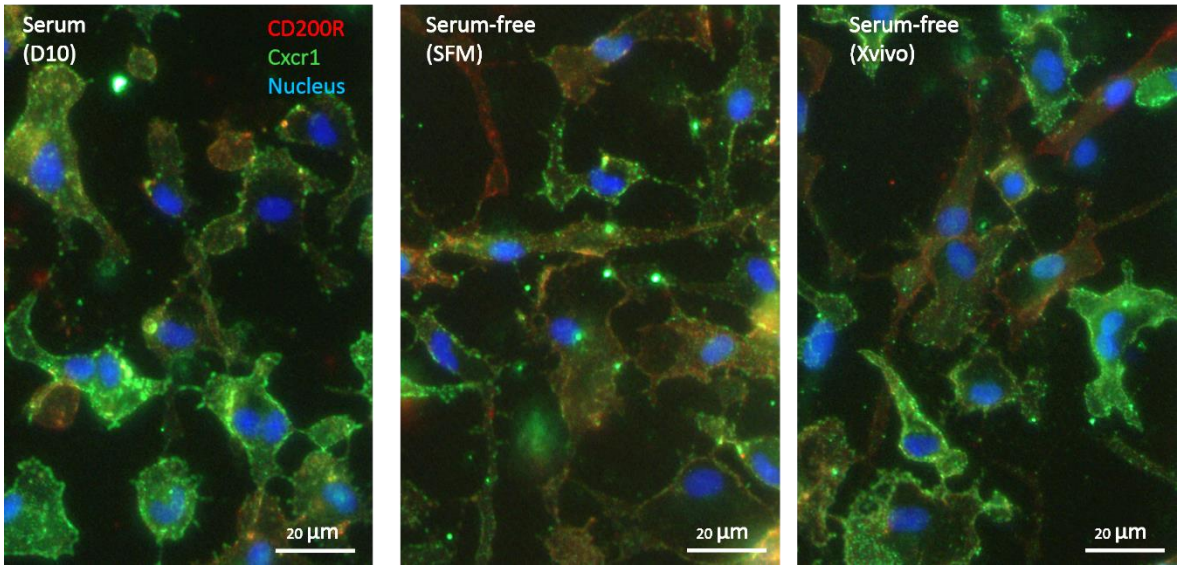

Figure 4-4: Fluorescence micrographs of immunostained microglia cultured in typical serum-supplementary media (D10) and two serum free media (SFM and Xvivo) . Cells expressed Cx3cr1 and CD200R, the latter confirming their microglial identity. The figure shows DAPI-stained nuclei as blue, Cx3cr1 as green and CD200R as red.

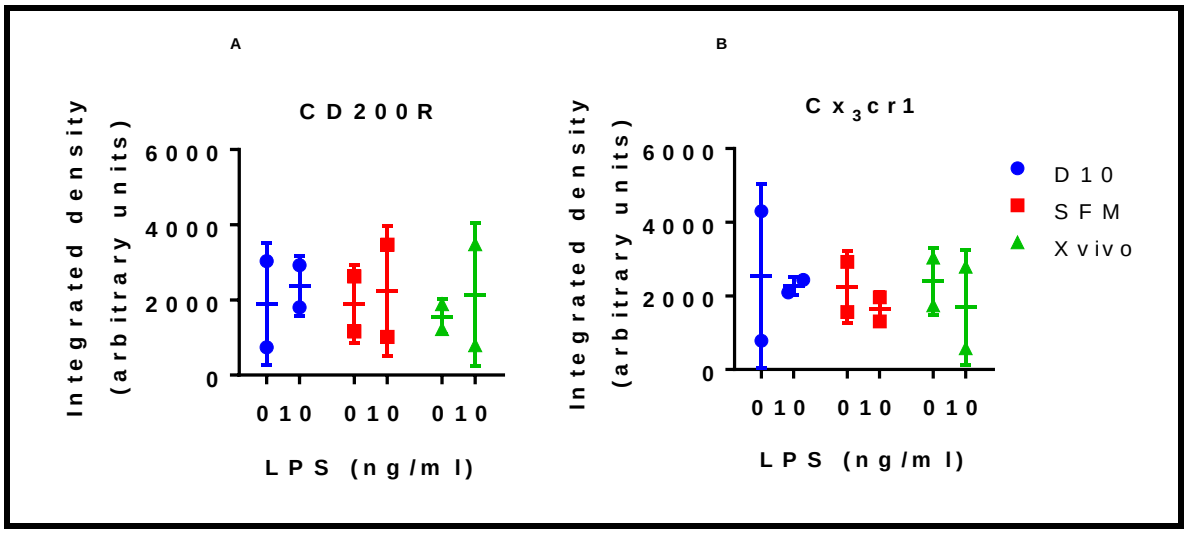

Figure 4-5: Intensity of microglial CD200R and Cx3cr1 markers expression in different media for one day. (A) Intensity of CD200R. (B) Intensity of Cx3cr1. These cultures were assessed after 2 h LPS treatment. All data are presented as mean ± S. E. M. of a pilot experiment (n = 2). D10 = DMEM supplemented with 10 % FBS; Xvivo = hematopoietic media.

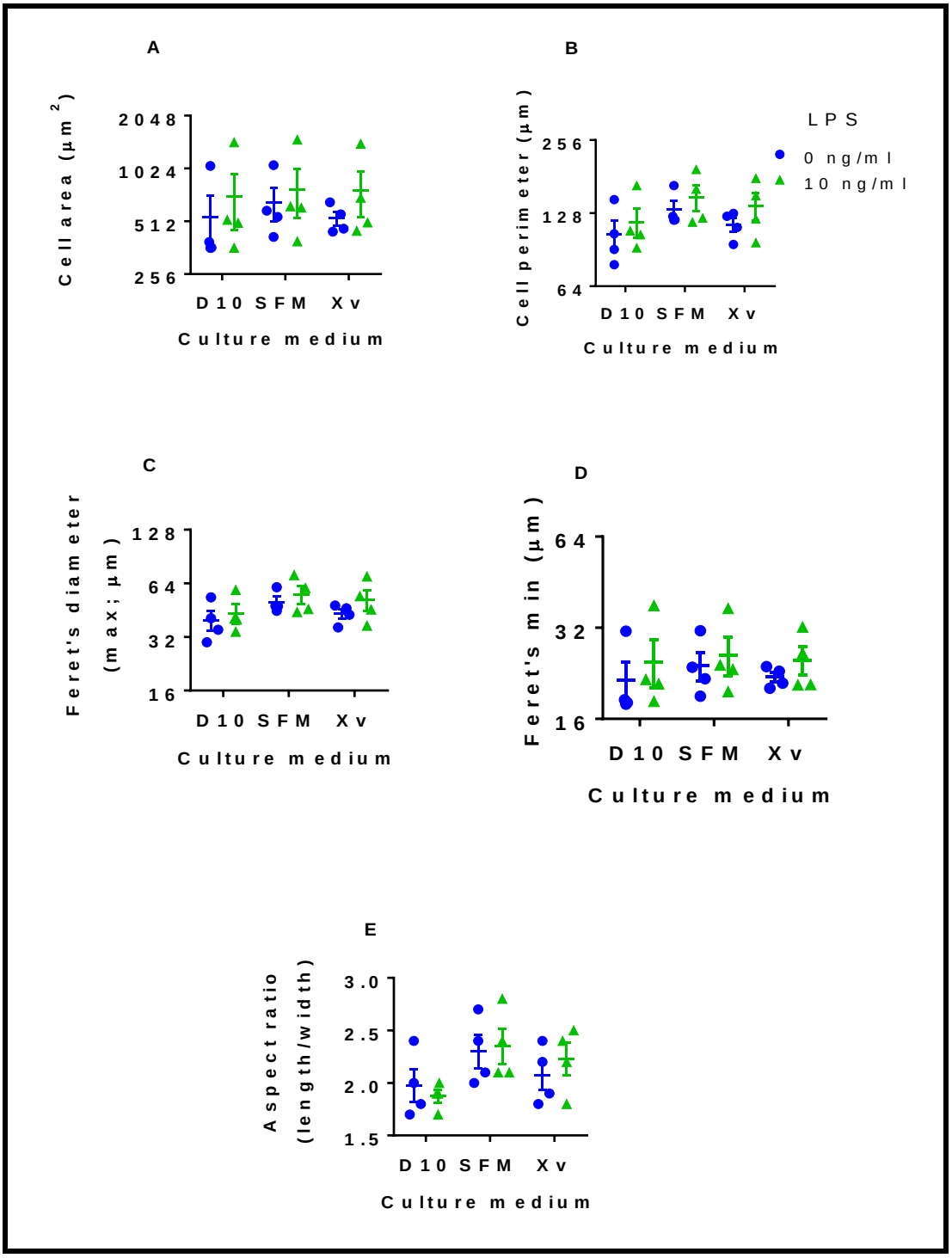

Figure 4-6: Morphological analyses of lectin-reactive microglia cells after treatment with 10 ng/ml LPS in different media for one day. (A) Area, (B) cell perimeter, (C) Feret's diameter, (D) minimum Feret's diameter, (E) aspect ratio. These cultures were assessed after 2 h LPS treatment. No significant differences were detected; one-way ANOVA with Dunnett's post-hoc test versus D10 without LPS. Also, unpaired t-tests for LPS versus control, within each medium. All data are presented as the mean ± S. E. M. of four independent experiments. D10 = DMEM supplemented with 10 % FBS; SFM = serum-free media; Xvivo = hematopoietic media. .

4.4.1.2 Validation of three reference genes: *Gapdh, Usp14 and Rpl32* on three different media

qPCR was performed using the three reference genes identified in Chapter Three. The results show there was no LPS-induced change in expression for the reference genes tested (*Gapdh*, *Usp14* and *Rpl32*), across a wide range of LPS concentrations and across different media (D10, SFM and Xvivo). No variations in relative expression (fold change) (Figure 4-7), and no evidence of a dose-response effect was observed. Therefore, the average of their Cq values should allow reliable evaluation of LPS-induced changes in GOI.

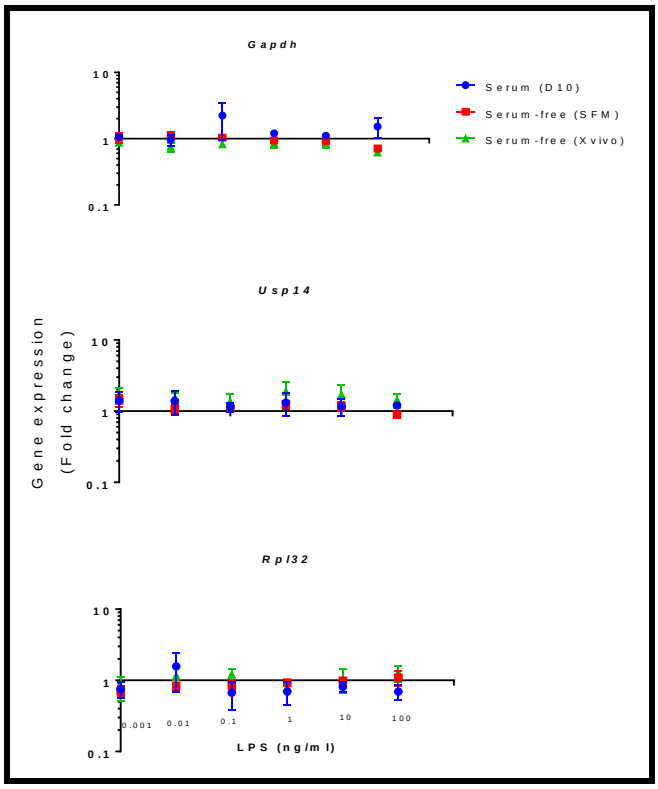

Figure 4-7: Reference genes (*Usp14, Rpl32* and *Gapdh*) were unresponsive to LPS treatment for 2 h, in three different media for one day. Y-axis represents log fold change versus average of reference genes (1 = no change) y= 1 showing average values for control within each media (i.e. D10 is compared to D10 control) and X-axis represents LPS concentration. The biological replicates produced similar values, demonstrating high reproducibility. All data are presented as the mean ± S. E. M. of three independent experiments. D10 = DMEM supplemented with 10 % FBS; SFM = serum-free media; Xvivo = hematopoietic media.

4.4.1.3 The acute effect of serum on *Il-1β* gene expression after 2 h of LPS treatment

There is a dose-responsive increase in *Il-1β* with LPS treatment in D10 and both serum-free media (SFM and Xvivo) (Figure 4-8).

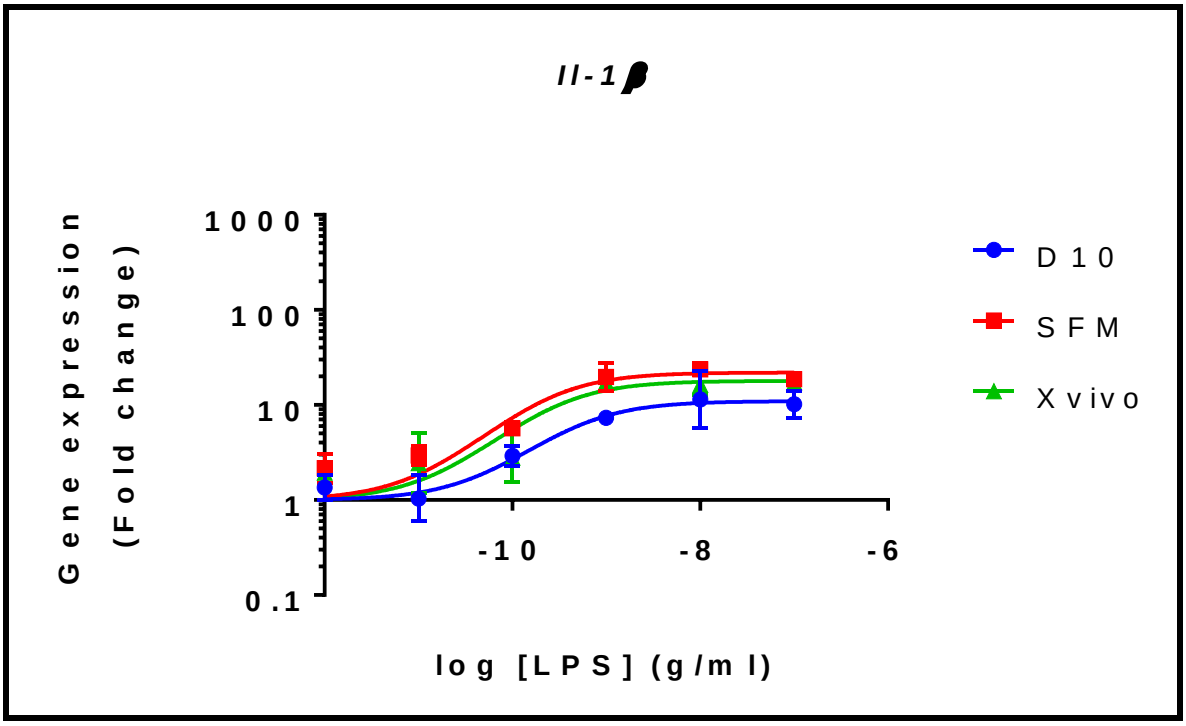

Figure 4-8: *Il-1β* dose response in different media for one day. Y-axis represents log fold change for each medium (1 = no change) and X-axis represents log LPS concentration. All data are presented as mean ± S. E. M. of three independent experiments. D10 = DMEM supply with 10 % FBS; SFM = serum-free media; Xvivo = hematopoietic media.

No significant difference in EC50, baseline expression and maximum gene response were detected between media (Figure 4-9).

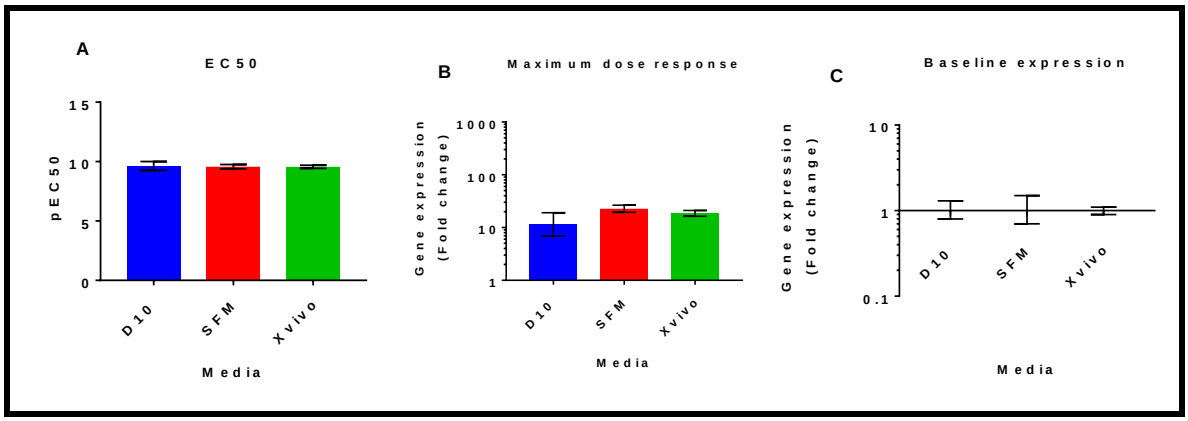

Figure 4-9: *Il-1β* dose response curves summary in different media for one day. (A) EC50 (B) Maximum dose response and (C) Baseline expression. In figure (A), Y-axis represents pEC50 in (g/ml), while in figures (B) and (C) the Y-axis represents log fold change and X-axis represents the different media. No significant difference between D10 and the two serum free media was found; One-way ANOVA with Dunnett's post-hoc test versus D10. All data are presented as mean ± S. E. M. of three independent experiments. D10 = DMEM supply with 10 % FBS; SFM = serum-free media; Xvivo = hematopoietic media.

4.4.1.4 The acute effect of serum on *Il-6* gene expression after 2 h of LPS treatment

There is a dose-responsive increase in *Il-6* with LPS treatment in D10 and both serum-free media (SFM and Xvivo) (Figure 4-10).

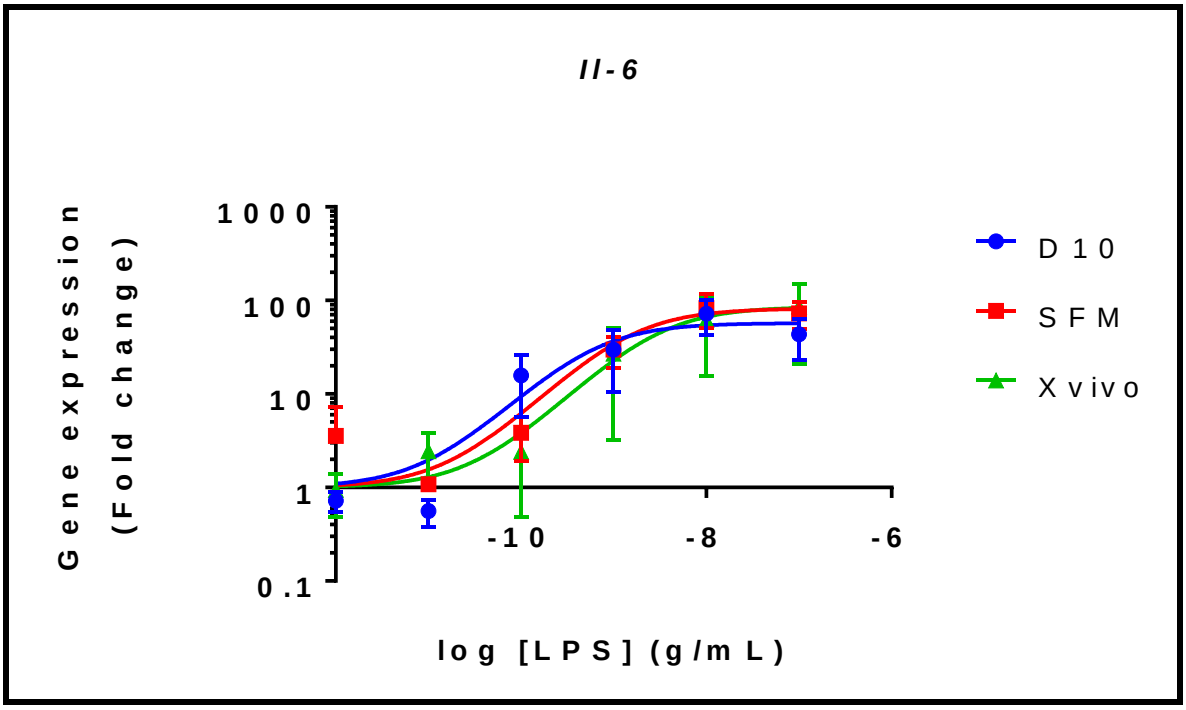

Figure 4-10 : *Il-6* dose response in different media for one day. Y-axis represents log fold change for each media (1 = no change) and X-axis represents log LPS concentration. All data are presented as mean ± S. E. M. of three independent experiments. D10 = DMEM supply with 10 % FBS; SFM = serum-free media; Xvivo = hematopoietic media.

No significant difference in EC50, baseline expression and maximum gene response were detected between media (Figure 4-11).

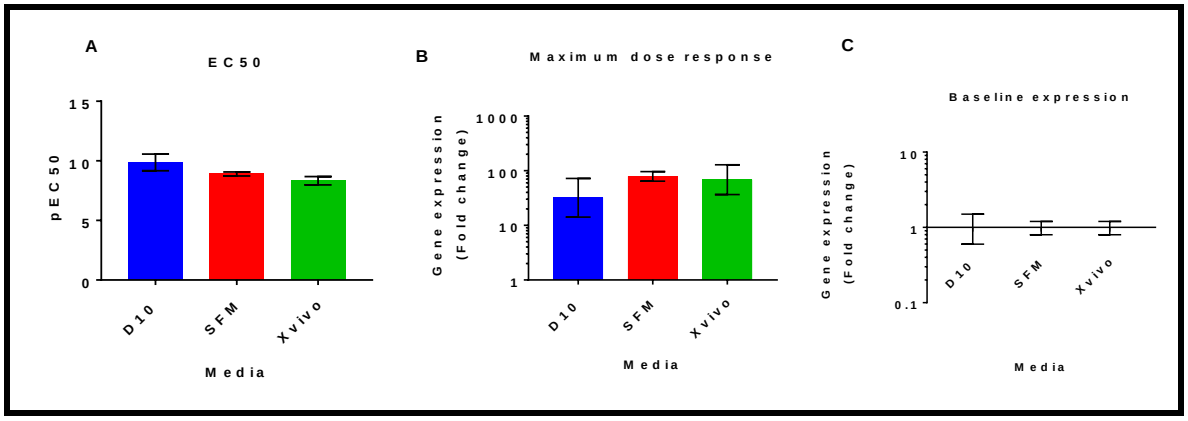

Figure 4-11: *Il-6* dose response curves summary in different media for one day. (A) EC50 (B) Maximum dose response and (C) Baseline expression. In figure (A), Y-axis represents pEC50 in (g/ml), while in figures (B) and (C) Y-axis represents log fold change and X-axis represents the different media. No significant difference between D10 and the two serum free media was found; One-way ANOVA with Dunnett's post-hoc test versus D10. All data are presented as the mean ± S. E. M. of three independent experiments. D10 = DMEM supply with 10 % FBS; SFM = serum-free media; Xvivo = hematopoietic media.

4.4.1.5 The acute effect of serum on *Tnf-α* gene expression after 2 h of LPS treatment

There is a dose-responsive increase in *Tnf-α* with LPS in D10 and both serum-free media (SFM and Xvivo) (Figure 4-12).

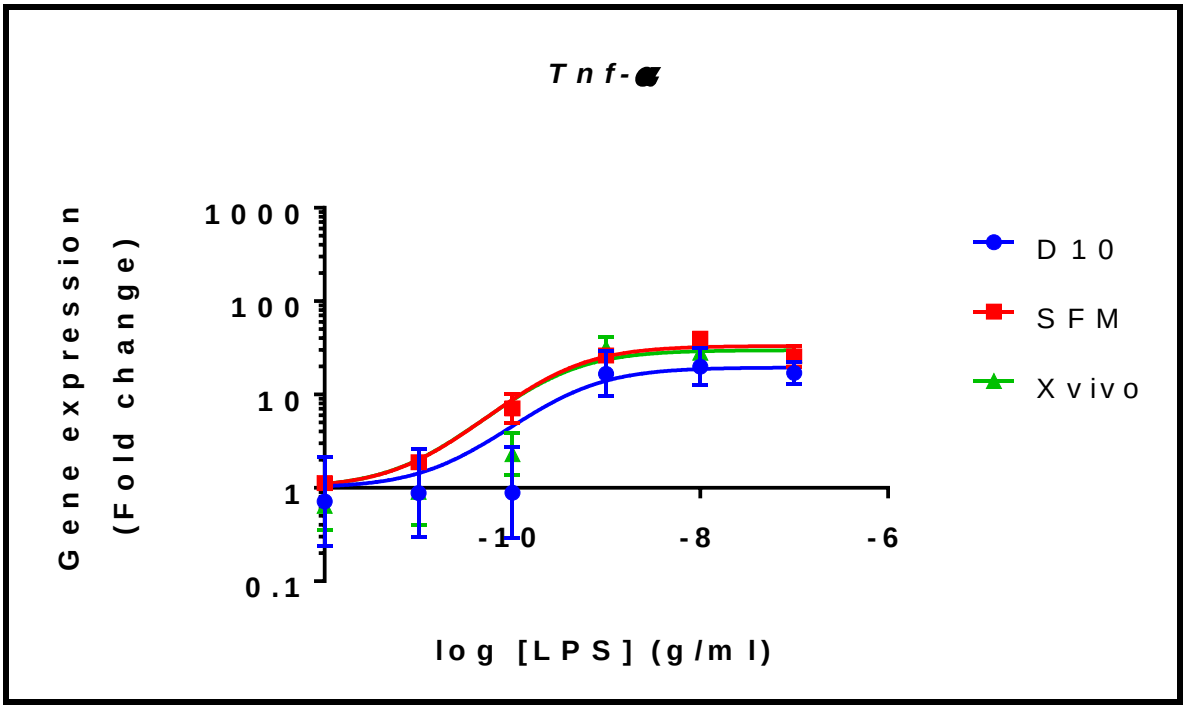

Figure 4-12: *Tnf-α* dose response in different media for one day. Y-axis represents log fold change for each medium (1 = no change) and X-axis represents log LPS concentration. All data are presented as mean ± S. E. M. of three independent experiments. D10 = DMEM supply with 10 % FBS; SFM = serum-free media; Xvivo = hematopoietic media.

No significant difference in EC50, baseline expression and maximum gene response were detected between media (Figure 4-13).

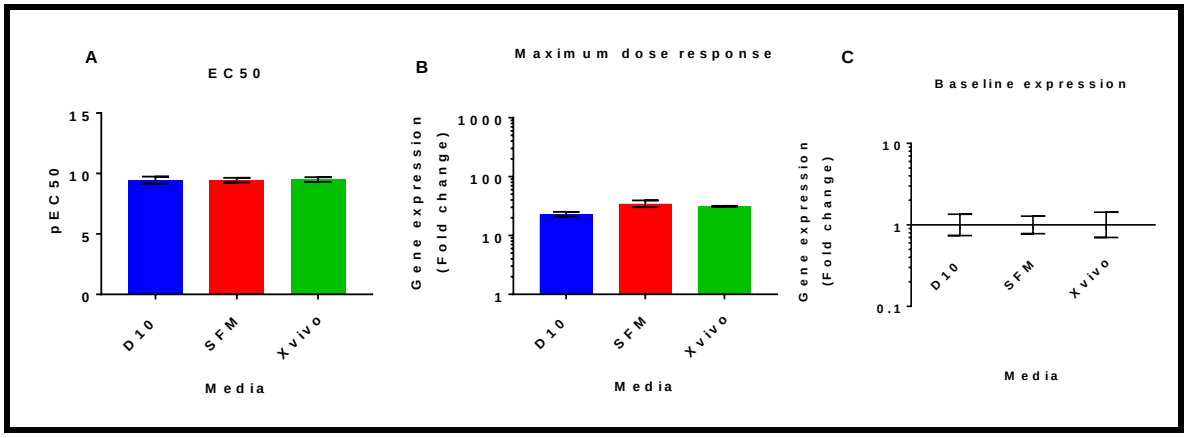

Figure 4-13: *Tnf-α* dose response curves summary in different media for one day. (A) EC50 (B) Maximum dose response and (C) Baseline expression. In figure (A), Y-axis represents pEC50 in (g/ml), while in figures (B) and (C) Y-axis represents log fold change and X-axis represents the different media. No significant difference between D10 and the two serum free media was found; One-way ANOVA with Dunnett's post-hoc test versus D10. All data are presented as mean ± S. E. M. of three independent experiments. D10 = DMEM supply with 10 % FBS; SFM = serum-free media; Xvivo = hematopoietic media.

4.4.2 The chronic effects of serum-free conditions on microglia (6 DIV)

4.4.2.1 Microglial viability at 6 DIV serum-free media culture

Cells expressed Iba1, confirming their viability in D10 and Xvivo. However, SFM did not support microglia survival. Although some fields show nuclei, no Iba1 is associated with these nuclei also there is a reduction in microglial numbers in serum-free media (SFM) when compared to both D10 and Xvivo, at 6 DIV (Figure 4-14).

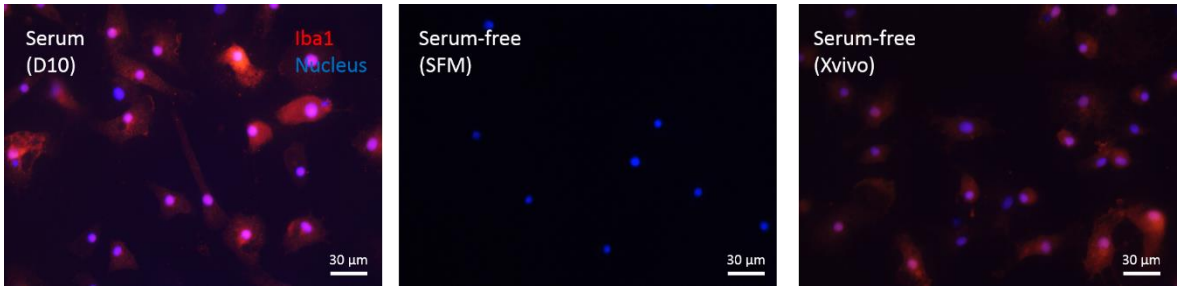

Figure 4-14: Iba1 labelling of microglia in different media for six days. Cells expressed Iba1, confirming their microglial identity. Figure show DAPI-stained nuclei as blue and Iba1 as red.

4.4.2.2 Validation of three reference genes: *Gapdh, Usp14 and Rpl32*.

qPCR was performed using three reference genes (identified in Chapter Three) for microglia cultured in D10 and Xvivo, the data for microglia cultured in SFM for 6 days has been excluded due to unhealthy culture. The results show there was no LPS-induced change in expression for the reference genes tested (*Gapdh, Usp14* and *Rpl32*), across a wide range of LPS concentrations and across two different media (D10 and Xvivo). With no evidence of a dose-response effect (Figure 4-15). Therefore, the average of their Cq values should allow reliable evaluation of LPS-induced changes in GOI.

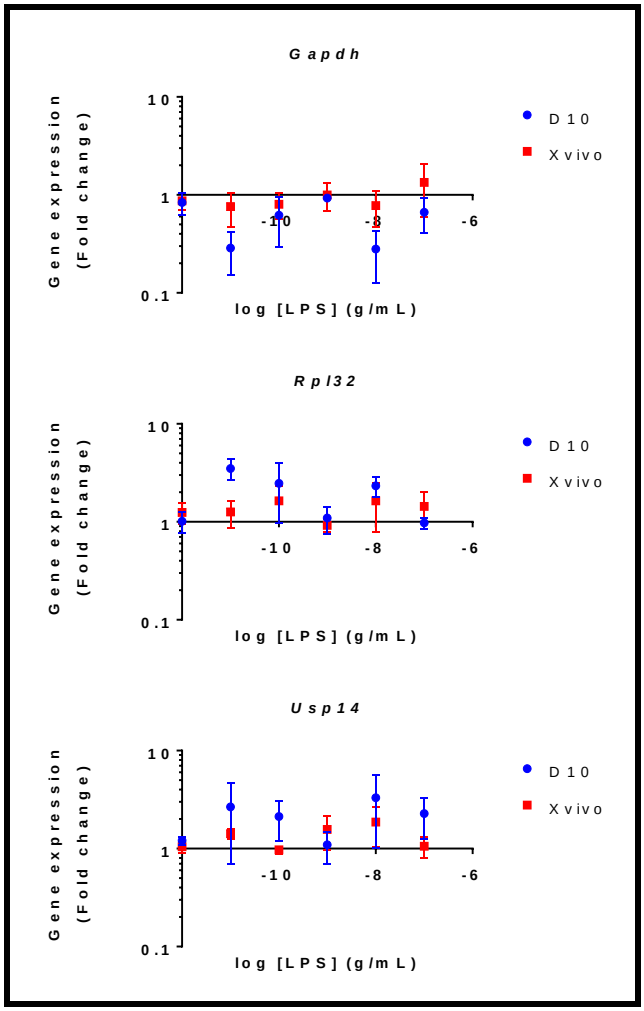

Figure 4-15: Reference genes (*Usp14, Rpl32* and *Gapdh*) were unresponsive to LPS treatment in different media for six days. Y-axis represents log fold change for each medium (1 = no change) and X-axis represents log LPS concentration. Best fit line produced by GraphPad Prism software, Line of best-fit calculated using (Y=Y intercept + slop * X) equation. All data are presented as mean ± S. E. M. of three independent experiments. D10 = DMEM supplemented with 10 % FBS; Xvivo = hematopoietic media.

4.4.2.3 The chronic effect of serum on *Il-1β* gene expression after 2 h of LPS treatment

There is a dose-responsive increase in *Il-1β* with LPS treatment both in D10 and Xvivo (Figure 4-16).

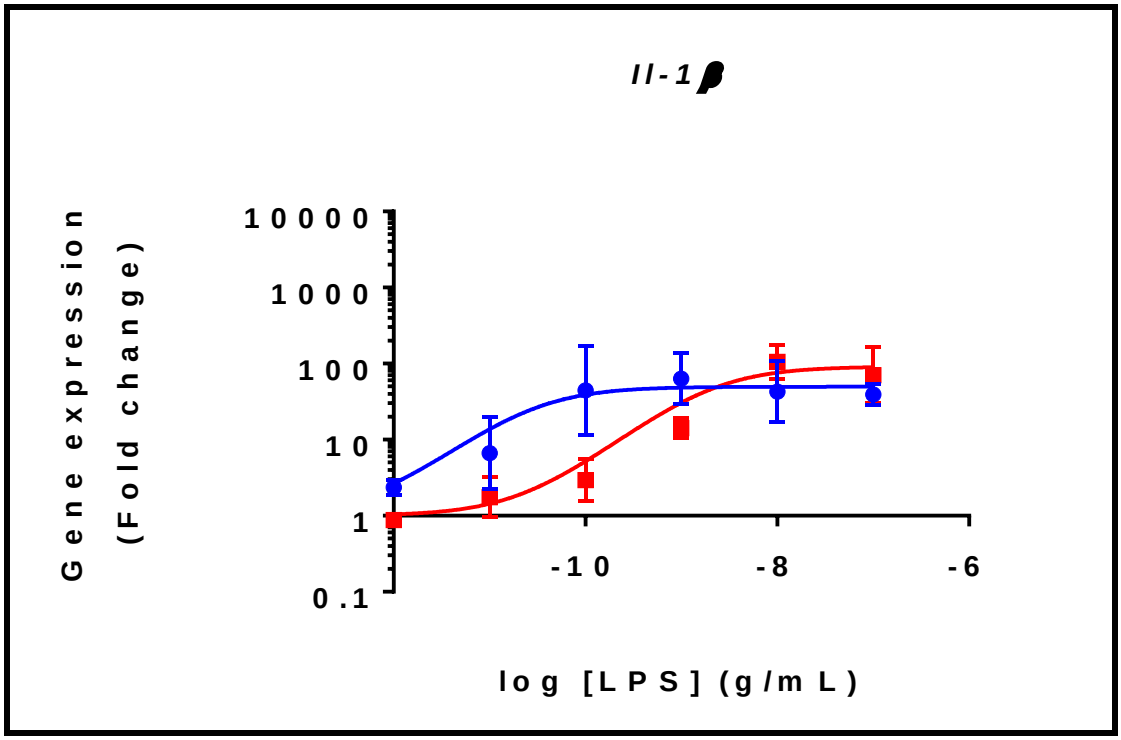

Figure 4-16: *Il-1β* dose response in different media for six days. Y-axis represents log fold change for each medium (1 = no change) and X-axis represents log LPS concentration. All data are presented as mean ± S. E. M. of three independent experiments. D10 = DMEM supply with 10 % FBS; Xvivo = hematopoietic media.

A significant difference was detected between D10 and Xvivo in EC50 (Figure 4-17 A), while no significant difference in baseline expression and maximum gene response was detected between media (Figure 4-17).

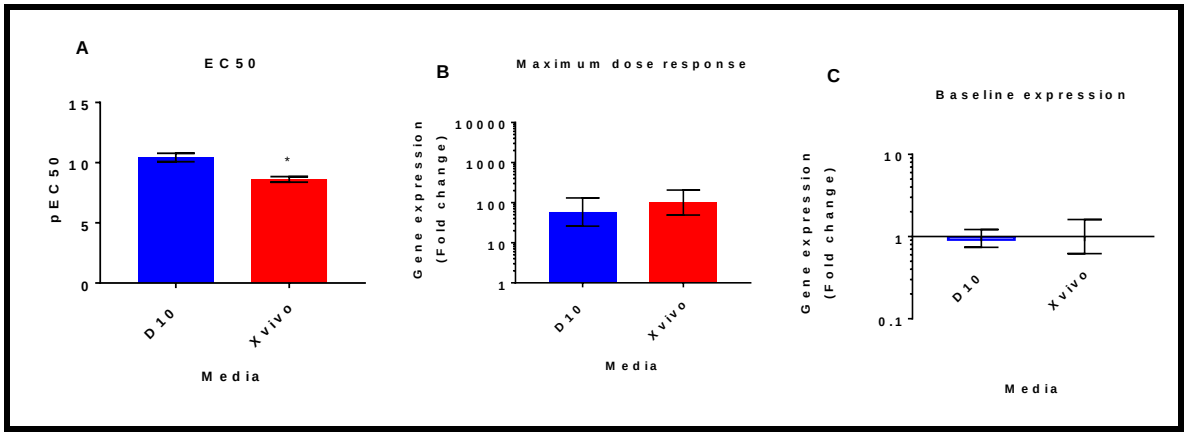

Figure 4-17: *Il-1β* dose response curves summary in different media for six days. (A) EC50, a significant difference between D10 and Xvivo was found. (B) Maximum dose response. (C) Baseline expression. In figure (A), Y-axis represents pEC50 in (g/ml), while in (B) and (C) Y-axis represents log fold change and X-axis represents the different media. *p < 0.05; unpaired t-test Xvivo versus D10. All data are presented as mean ± S. E. M. of three independent experiments. D10 = DMEM supply with 10 % FBS; Xvivo = hematopoietic media.

4.4.2.4 The chronic effect of serum on *Il-6* gene expression after 2 h of LPS treatment

There is a dose-responsive increase in *Il-6* with LPS treatment both in D10 and Xvivo (Figure 4-18).

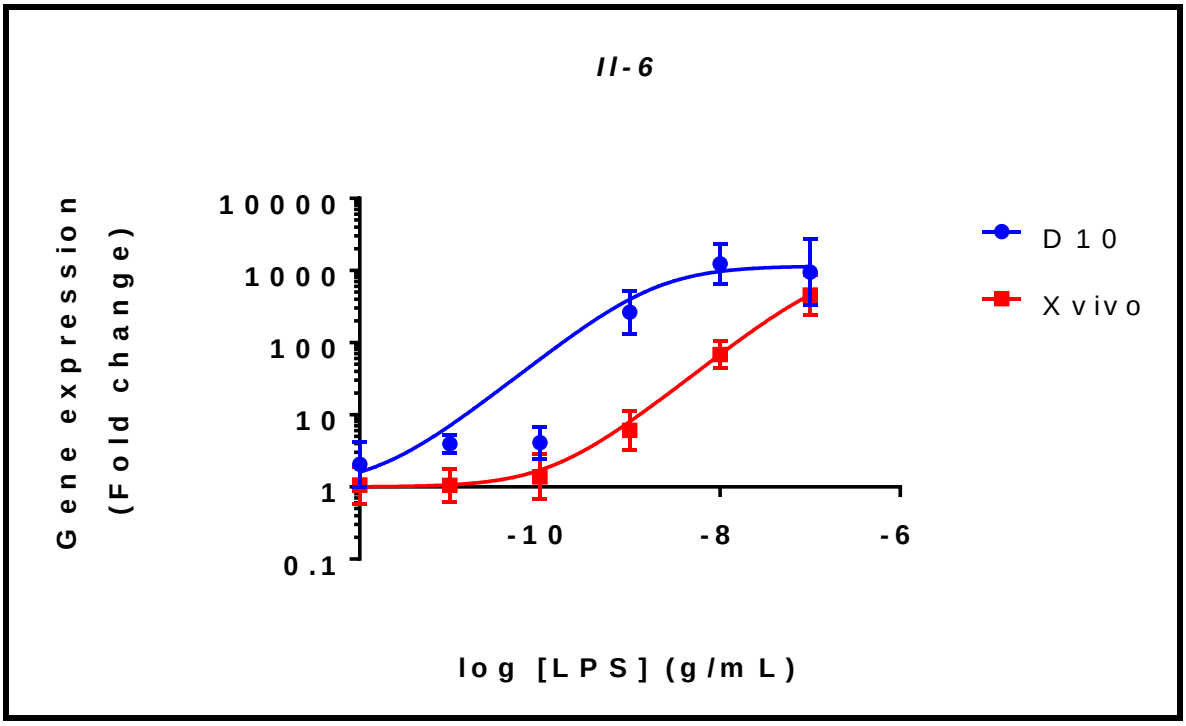

Figure 4-18: *Il-6* dose response in different media for six days. Y-axis represents log fold change for each medium (1 = no change) and X-axis represents log LPS concentration. All data are presented as mean ± S. E. M. of three independent experiments. D10 = DMEM supply with 10 % FBS; Xvivo = hematopoietic media.

No significant difference in EC50, baseline expression and maximum gene response was detected between D10 and Xvivo (Figure 4-19).

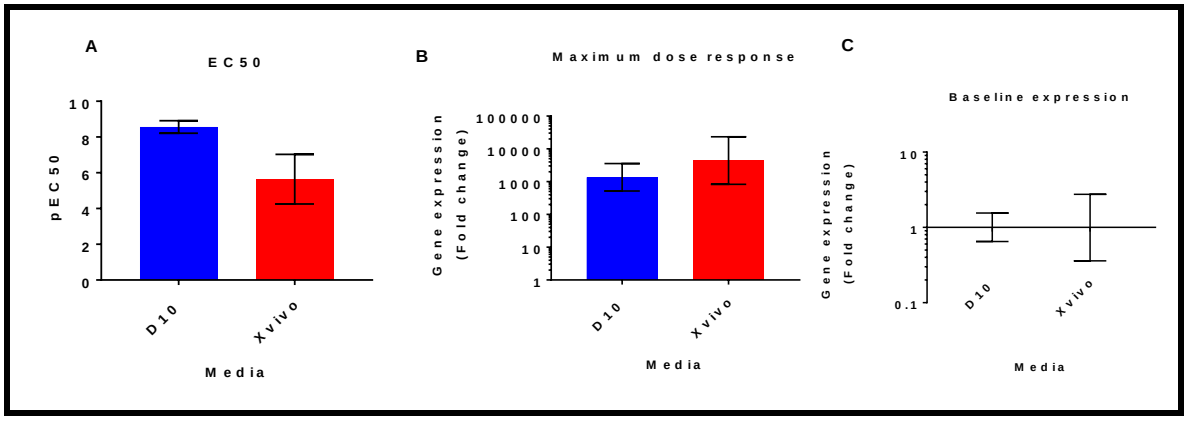

Figure 4-19: ***Il-6*** **dose response curves summary in different media for six days. (A) EC50 (B) Maximum dose response and (C) Baseline expression. In figure (A), Y-axis represents pEC50 in (g/ml), while in figures (B) and (C) Y-axis represents log fold change and X-axis represents the different media. No significant difference was found; unpaired t-test Xvivo versus D10. All data are presented as mean ± S. E. M. of three independent experiments. D10 = DMEM supply with 10 % FBS; Xvivo = hematopoietic media.**

4.4.2.5 The chronic effect of serum on *Tnf-α* gene expression after 2 h of LPS treatment

There is a dose-responsive increase in *Tnf-α* with LPS treatment both in in D10 and Xvivo (Figure 4-20).

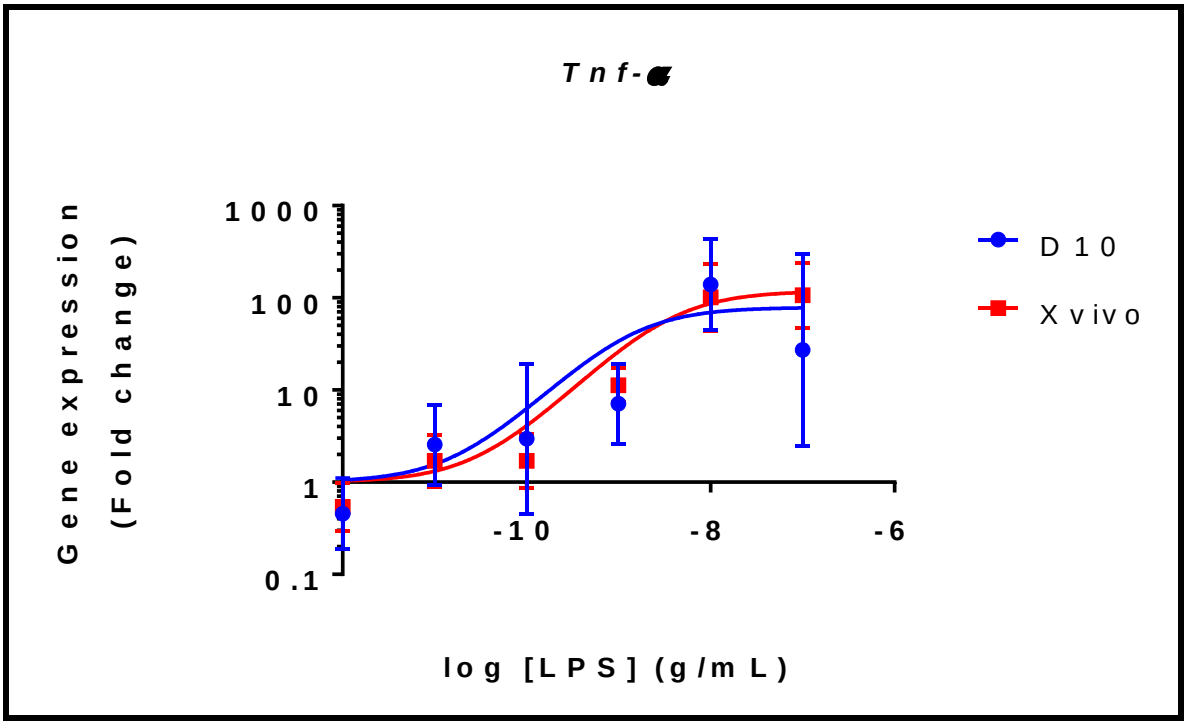

Figure 4-20: *Tnf-α* dose response in different media for six days. Y-axis represents log fold change for each medium (1 = no change) and X-axis represents log LPS concentration. All data are presented as mean ± S. E. M. of three independent experiments. D10 = DMEM supply with 10 % FBS; Xvivo = hematopoietic media.

No significant difference in EC50, baseline expression and maximum gene response detected between media (Figure 4-21).

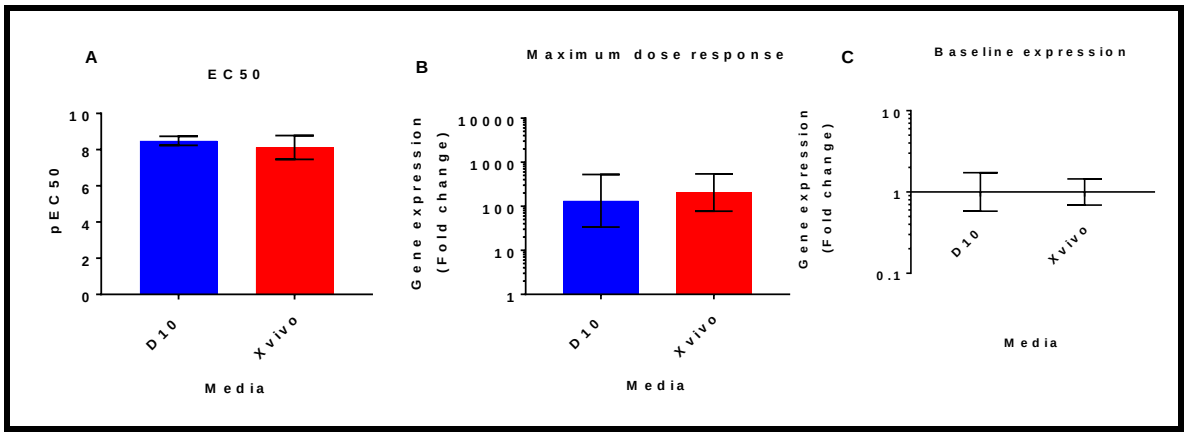

Figure 4-21: *Tnf-α* dose response curves summary in different media for six days. (A) EC50, (B) Maximum dose response and (C) Baseline expression. In figure (A), Y-axis represents pEC50 in (g/ml), while in figures (B) and (C) Y-axis represents log fold change and X-axis represents the different media. No significant difference was found; unpaired t-test Xvivo versus D10. All data are presented as mean ± S. E. M. of three independent experiments. D10 = DMEM supply with 10 % FBS; Xvivo = hematopoietic media.

4.5 Discussion

Understanding microglia-specific behaviours is critical to understanding neurological disease and developing therapeutic interventions.

Culture systems, which typically use serum-supplemented media, failed to replicate the serum-free environment of the brain. Although some studies temporarily omitted serum, basal media without supplemented serum are typically insufficient for microglial survival and possibly impair responsiveness (Zielasek & Hartung 1996; Franciosi *et al.* 2005; Kobayashi *et al.* 2013). Due to these problems, serum-supplementation remained a routine for microglial culture (Lian *et al.* 2016; Chi *et al.* 2018; Yousif *et al.* 2018). A defined serum-free media which supports microglial survival and phenotype-switching would be of scientific benefit for researchers. Here, two commercially available serum-free media, developed for immune cell culture, were compared to a serum-supplemented media typically used with primary microglia.

4.5.1 Microglial viability and morphology in serum-free media

No reduction in microglial cells numbers was observed in either serum-free media, at 24 h (Figure 4-3), suggesting that either of these media could be suitable for studying acute effects in microglia in short experiment length (one day in culture). Although, microglia survived when cultured in Xvivo media for 6 days, SFM did not support microglia survival (Figure 4-14). This suggests that SFM is not a good alternative media for long-term culturing of microglia.

Several *in vivo* studies have suggested that resting microglia adopt ramified shape characterised by small soma size and highly branched dynamic processes to scan their brain environment (Lawson *et al.* 1990; Thanos *et al.* 1993; Morrison & Filosa 2013). Changes in microglial morphology may be associated with alterations in their activation state; microglial

function may also change without a noticeable change in their morphology (Perry *et al.* 2010). Studies have described this morphological changes *in vivo* as a de-ramification in which the number of processes and process length are gradually reduced until the cell displays an amoeboid morphology characterised by increased cell bodies and irregular process shape (Orr *et al.* 2009; Qin *et al.* 2013; Hellwig *et al.* 2016). However, it has been reported that microglia in high purity culture adopt an amoeboid morphology with short and thick processes which become bipolar or tripolar when treated with activation stimuli such as LPS (Abd-El-Basset & Fedoroff 1995). It has been reported that culturing microglia in coculture with astrocytes leads to a morphology more like the ramified *in vivo* morphology (Kloss *et al.* 2001).

The hypothesis that 10 % serum leads to low level M1 activation could allow predictions that D10 microglia may be more rounded, with fewer processes. This study results showed that microglia were morphologically similar across all media which disagrees with Tanaka *et al.* (1998) study that reported that microglia adopt non- ramified morphology when cultured in serum-free media. My data do not support the hypothesis that serum free culture leads to less M1 activation. However, it is possible that, as my microglia were all derived from mixed glial cultures with 10 % serum, any alterations to activation status may have already occurred.

4.5.2 Pro-inflammatory response in D10

In serum-supplemented media, exposure of the microglial cells to LPS led to increased pro-inflammatory cytokine (*Il-6, Il-1β* and *Tnf-α*), indicative of M1 activation (Zhang *et al.* 2001; Liu *et al.* 2012; Pan *et al.* 2015; Orihuela *et al.* 2015). All three genes showed positive dose-response curves. The plateau suggests the highest dose of LPS chosen here (100 ng/ml) produces the maximal response for key M1-associated cytokines.

Results from D10 media are consistent with other researchers work. For example Puffenbarger *et al.* (2000) reported a similar expression for *Il-1β* and *Il-6* after incubating primary rat microglia with 10 ng/ml LPS for 24 h, and analogous expression was reported when using primary mouse microglia and a cell line (Puffenbarger *et al.* 2000; Liu *et al.* 2012; Kobayashi *et al.* 2013; Orihuela *et al.* 2015).

Few studies have fully investigated LPS dose responses, and most of them studied the effect of a small range of different LPS concentrations in terms of protein production, such as IL-1 (Lee *et al.* 1993) and Il-10 (Sheng *et al.* 1995). Although Loram *et al.*, (2012) described *Il-1β* gene dose response, they have used only three LPS concentrations. Therefore, determining a dose response curve allows EC50 to be calculated, which predicts the amount of LPS required to induce the half of maximum gene expression. Such information would be important when studying different drug effects on microglia.

4.5.3 Pro-inflammatory response in serum-free media

The hypothesis was that if the presence of serum led to primed microglia, then the amount of pro-inflammatory cytokine expression in serum-supplemented media will be higher than that of microglia plated in non-serum media when treating both of them with LPS.

If serum-free data were identical to the serum-supplemented response, this would imply that the presence of serum in microglia culture media does not cause microglial priming nor inhibition. But if serum-supplemented data showed a stronger pro-inflammatory response, this would imply that the presence of the serum in microglia culture media plays a role in priming microglia, which produces more pro-inflammatory cytokines in response to the next activation agent (LPS). A more limited pro-inflammatory response with serum, would imply that the serum had inhibitory agents which reduce microglial activation. For

example, anti-inflammatory stimuli such as Il-4, Il-10 or Tgf-β can be present in serum (Kleiner *et al.* 2013).

To test this hypothesis the effect of the presence of serum on microglial activation state was studied in the short term (only one-day on D10 in compare to other serum free media) and in longer term (6 days). Microglia in each medium were treated with LPS (0.01-100 ng/ml), and baseline response, maximum response and EC50 were compared between media.

In the short term, for both serum-free media tested, LPS-induced up-regulation of pro-inflammatory M1 genes (*Il-1β, Tnf-α* and *Il-6*) and was comparable with serum-supplemented media. EC50 values in D10 were similar to that of SFM and Xvivo. If microglial priming is caused by exposure to serum, it would be expected that D10 would have a high pEC50 value (more potent), as any given concentration of LPS would produce a greater response than seen in serum-free media. Furthermore, the baseline response and the maximum dose response of D10 was comparable to that of both serum-free media which indicate that serum containing media are not more harmful than the serum-free media in the short term.

Upon longer term exposure to serum (six days *in vitro*), this study data showed clear dose responses in the three pro-inflammatory genes (*Il-1β, Il-6* and *Tnf-α*) in D10 and Xvivo media only, as microglia did not survive in SFM and this prevented statistical comparison of SFM with D10 (and Xvivo). pEC50 in D10 was significantly higher in *Il-1β* in compared to Xvivo. *Il-6* pEC50 showed reduction in Xvivo, although it wasn't statistically different. The high potency in gene expression is consistent with the theory of serum might prime microglia.

This study results will be of value to the research community since they provide two alternative media that could be used to study microglia in short term culture, further validation to the three reference genes as being stable with and without serum, which will be a good tool to study microglia gene expression. Serum-supplementation media supports cell survival in even in longer incubation time (6 DIV), with no reduction in the number of cells, viability and morphology with increases in the incubation time. Therefore, D10 media have been chosen to perform the remaining experiments in this thesis.

4.6 Summary

In summary, this study has shown that primary microglial cells can be maintained in serum-free media. Importantly for neuropathological research and drug testing, microglia displayed typical pro-inflammatory responses in both these serum-free media. These findings showed that more realistic and tightly controlled experimental conditions (i.e. serum-free) could be used to assess microglial activation/phenotype-switching for short-term culture. In long-term culture this study showed that there is shift in the EC50 between D10 (serum supply media) and Xvivo (serum free media), however further study needed to confirm that.

Further experimental work should identify other media, including possibly developing chemically-defined media without proprietary (undeclared) concentrations of individual components, validate other assays in serum-free conditions, perform more detailed morphological assessments, test longer culture periods or gather *in vivo* data for comparison.

These advances offer substantial benefits to the microglial research community, including greater confidence in the clinical applicability of *in vitro* findings.

Chapter 5 : Characterising microglial responses to pro-inflammatory activation

5.1 Introduction

5.1.1 Neuroinflammation: activated microglia can exhibit various phenotypes and behaviours

Microglia exhibit a wide variety of behaviours largely intended to destroy foreign substance and remove debris, with additional roles in the development, brain remodelling, infections and trauma (see Chapter One). To achieve these effects, microglia can reversibly alter their phenotypes between the 'inactivated' state and various 'activated' states including a pro-inflammatory phenotype that induces neuroinflammation. Microglia are activated in response to different pathological states within the CNS including injury, ischemia and infection. The subsequent neuroinflammation produces pro-inflammatory cytokines such as Il-1β, Il-6, Tnf-α and enzymes, such as iNos, which might be toxic to other neural cells (Smith *et al.* 2012). Pro-inflammatory cytokines play important roles in neuroprotection but could also contribute to damage of neurons and other glia cells.

Each microglial cell responds to its immediate microenvironment, which can include signals from distant cells, either within or outside the CNS. In particular stages of disease/injury, most microglia at the lesion site adopt a specific phenotype, but this dominant phenotype often changes over time, until resolution of the disease state. For example, M1 microglia may dominate to combat infection, then M2 microglia become more numerous to stimulate tissue 'recovery', and finally, M0 microglia re-occupy the healthy tissue.

5.1.2 LPS induced responses

Microglia activated by LPS and/or IFN-γ are characterised as M1 classically activated microglia phenotype (Boche *et al.* 2013). LPS acts through the TLR4 receptor and induces a signal transduction cascade that modulates NF-κB-mediated gene expression and

leads to the production of pro-inflammatory cytokines, such as Il-1β, Il-6 and Tnf-α and free radicals such as RNS and ROS (Alexander & Rietschel 2001).

Tnf-α, a pro-inflammatory cytokine, interacts with one of two main receptors: TNFR1 or TNFR2. Their biological effects include cell proliferation, cell migration and apoptosis mediated through the activation of several downstream signal transduction cascades involving NF-κB, c-Jun N-terminal kinase (JNK) and p38 (Montgomery *et al.* 2013). Tnf-α has important neuroprotective effects, for example, Tarkowski *et al.* (1999) showed that Tnf-α expression is significantly and inversely correlated with intracerebral apoptosis and neuronal degradation. Furthermore, incubation of human neuronal cells with TNF-α led to production of B-cell lymphoma, a molecule known to down-regulate neuronal apoptosis.

Il-1β is a major pro-inflammatory cytokine in the brain, a member of the Il-1 cytokine family. The immune cells in the brain, microglia and astrocytes, both have the ability to synthesise and release the pro-Il-1β forms. Pro-Il-1β is cleaved by the protease caspase-1 to generate mature and bioactive Il-1β (Liu *et al.* 2013). The production of Il-1β depends on the activation of MAP kinases and NF-κB signalling pathways.

Il-6 is a pro-inflammatory cytokine mainly produced by activated microglia and astrocytes in different brain regions. Il-6 functions include regulation of neuronal processes, such as learning and memory (Donegan *et al.* 2014). The production of Il-6 relies on the activation of Toll-like receptor 2 (TLR2)-MyD88 signalling pathways in microglia (Jana *et al.* 2008; Vukic *et al.* 2009). Il-6 could stimulates microglia and astrocytes to release a cascade of pro-inflammatory cytokines and acute-phase proteins, such as C-reactive protein (CRP) (Querfurth & LaFerla 2010).

Other stimuli can induce a M1 phenotype in microglia. In an *in vitro* model to mimic myelin debris produced after injury, the exposure of microglia to myelin leads to the production of NO and Tnf-α with subsequent neuronal death (Pinteaux-Jones *et al.* 2008). Exposure of microglia to abnormal protein aggregates associated with neurodegenerative diseases, such as Aβ in AD and α-synuclein in PD, which drive microglia toward the M1 phenotype characterised by expression of pro-inflammatory markers such as NO and Tnf-α (Qin *et al.* 2002; Zhang *et al.* 2005). In an *in vitro* model, the exposure of microglia to dying neurons leads to microglial activation with cytokines production such as Tnf-α, Il-6 and RNS, as well as an increase in the expression of iNos enzyme (Pais *et al.* 2008). Notably, media from microglia exposed to dying neurons induced subsequent neuronal death.

5.1.3 The role of microglia in neurodegenerative processes

M1 microglia produce pro-inflammatory cytokines such as Il-1β, Tnf-α and Il-6, which are usually effective responses to infection or trauma. However, prolonged or excessive neuroinflammation can be toxic to neurons and other neural cells (Smith *et al.* 2012). This is proposed to contribute to the progression of some neurodegenerative diseases, although the precise role of microglia is still being investigated (McGeer *et al.* 1988; Rogers *et al.* 1988). Microglia can be neuroprotective by phagocytosing Aβ plaques as a reaction against Aβ accumulation (Takata *et al.* 2010). M2 microglia surround the plaques for Aβ phagocytosis as labelled by Ym1 (Jimenez *et al.* 2008). However, an age-dependent increase in both of the number and the size of Aβ plaques in AD might reflect a shift in microglia phenotype (Hardy & Selkoe 2002; Jimenez *et al.* 2008). The phagocytic activity of microglia is reduced by pro-inflammatory cytokines such as Ifn-γ, Il-1β and Tnf-α, which most likely shifts microglia into the pro-inflammatory M1 state (Jantzen *et al.* 2002) (Figure 5-1). The mechanism behind this inappropriate phenotype switching is unclear.

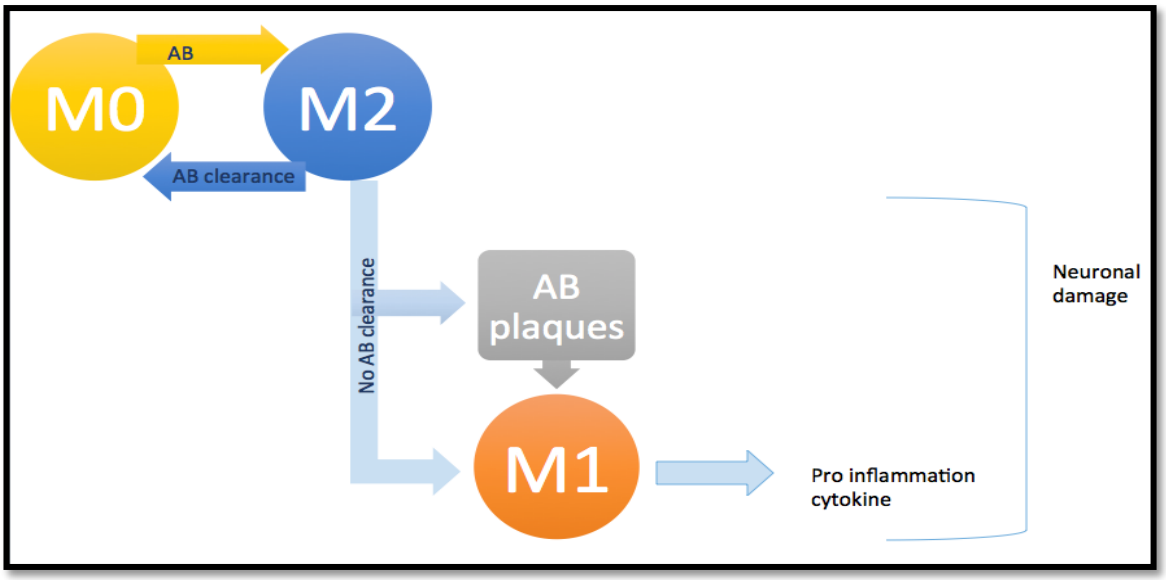

Figure 5-1: Schematic illustration of microglial phenotype proposed role in Alzheimer disease. The inappropriate microglia phenotype (M1) leads to AD progression and neuronal death.

5.1.4 Microglial 'priming' theory

Primed microglia may be defined as exhibiting an exaggerated inflammatory response to a second stimulus after an initial stimulus (hypersensitive pro-inflammatory phenotype), the initial stimulus could be a systemic illness or infection, and it leads to subsequent responses to disease, injury and affects disease outcome (Haley *et al.* 2017). Primed microglia may also be described as hyper-reactive cells, secreting large amounts of cytokines, chemokines and other reactive molecules associated with neurotoxicity (Holtman *et al.* 2015). However, the concept that microglia are primed remains poorly defined: no clear or unique descriptors (biomarkers) of primed microglia have been established to date. Lull and Block (2010) anticipated that primed microglia profile is defined by a lower threshold to be activated and 'switch' to a pro-inflammatory state, higher baseline expression of markers of inflammation and inflammatory mediators (Combrinck *et al.* 2002) and an exaggerated inflammatory response following immune activation (Norden *et al.* 2014).

Evidences suggested that microglial priming might be resulted from various causes, such as ageing (Niraula *et al.* 2017), systemic inflammation and/or neuroinflammation, for example TBI (Ziebell *et al.* 2016) or neurodegenerative disease (Hoeijmakers *et al.* 2016). As a result, primed microglia exhibit an exaggerated inflammatory response to secondary and sub-threshold challenges (Ouchi *et al.* 2005; Gao & Hong 2008; Wolf *et al.* 2017).

The microglial priming theory was first proposed in prion disease model, where Combrinck *et al.* (2002) hypothesised that microglia could be primed by chronic neurodegeneration. ME7-induced mouse has been used as a prion disease model associated with pro-inflammatory (M1) microglial activation, followed by further activation through LPS to mimic a peripheral infection. In prion disease model, application of LPS leads to increased microglial Il-1β and iNos expressions (Cunningham *et al.* 2005). Peripheral infection usually causes changes in behaviour (e.g., reduced appetite, depression, reduced motivation…, etc). These behavioural changes are mediated via the brain, suggesting that systemic inflammation can influence the CNS, often previously thought of as an 'immune-privileged' system, unaffected by systemic immune activity (Larson & Dunn 2001). Combrinck *et al.* (2002) showed that the sickness behaviour (temperature and activity responses) induced by LPS in animals with pre-clinical prion disease were exaggerated compared with controls and that this was associated with a significant increase in brain levels of Il-1β. This study found an interaction between peripheral and neuro-inflammation and suggested that further stimulation of an already primed microglial population by a peripheral infection may drive disease progression (Combrinck *et al.* 2002). After this study, other *in vivo* studies showed that the priming phenomena is not exclusive to prion disease (Cunningham *et al.* 2009; Fielda *et al.* 2010). Püntener *et al.* (2012) reported similar findings of microglial priming after systemic infection. In Püntener *et al.* (2012) study, a single LPS injection increased serum levels of Il-1β with no changes in brain Il-1β levels. However, a

second injection (24 h later) significantly increased brain Il-1β levels with a much smaller increase in serum Il-1β. Therefore, in several animal models of chronic neurodegenerative conditions, it seems that microglia become primed by the ongoing pathology. This result may indicates that sickness behaviour alters with repeated infection, suggesting priming phenotype.

Holtman *et al.* (2015) compared the gene expression networks in cell populations of primed microglia (isolated from mouse models for neurodegenerative disease and ageing) to M1 microglia (isolated from mouse models injected with LPS (10 mg/kg)), to study the difference in gene expression between M1 and M0' genes network. The acute LPS-activated microglia were most significantly enriched for the ribosome, TLR signalling and NOD-like receptor signalling pathways while the priming was significantly enriched: AD signalling, antigen presentation, lysosome and phagosome. Which according to Holtman *et al.* (2015) suggested a fundamental differences between the acute classical M1-profile and the priming profiles. Furthermore, Holtman *et al.* (2015) predicted that primed microglia are characterised by expression of cell surface markers like MHC II and Cxcr4. In addition, primed microglia enhanced response includes not only pro-inflammatory cytokines, such as *Tnf-α, Il-1β* and *Il-6* but also *Il-10* and *Tgf-β*.

To investigate whether microglia could be primed by systemic inflammation, Perry & Teeling (2013) microinjected a very small amount of LPS into the brain parenchyma, which, in normal animals, induced little or no inflammatory response. However, in animals previously challenged with *S. typhimurium*, there was a more robust inflammatory response at the site of the LPS injection.

Evidence from preclinical studies showed that microglia priming and the subsequent inflammatory response leads to tissue damage in animal models of prion disease

(Perry 2010), AD (Kitazawa *et al.* 2005), PD and MS (Pott Godoy *et al.* 2010; Moreno *et al.* 2011).

In summary, experimental and clinical evidences indicated that microglia do not return to homeostasis after injury but instead develop a primed and potentially hyper-reactive phenotype (Witcher *et al.* 2015). First infection may or may not trigger microglia to release cytokines; a secondary insult could induce primed microglia to release additional pro-inflammatory cytokines. Primed microglia are characterised by exaggerated responses to secondary insults such as repeated TBI (Witcher *et al.* 2015), immune challenge or stress (Niraula *et al.* 2017). This result in an amplified and prolonged neuroinflammation that negatively influences cognitive function (Figure 5-2). Studying microglial priming theory is important to provide a good understanding of how chronic systemic and/or neuroinflammation experienced throughout life may alter the responses of microglia potentially contributing to neurodegenerative disease progression.

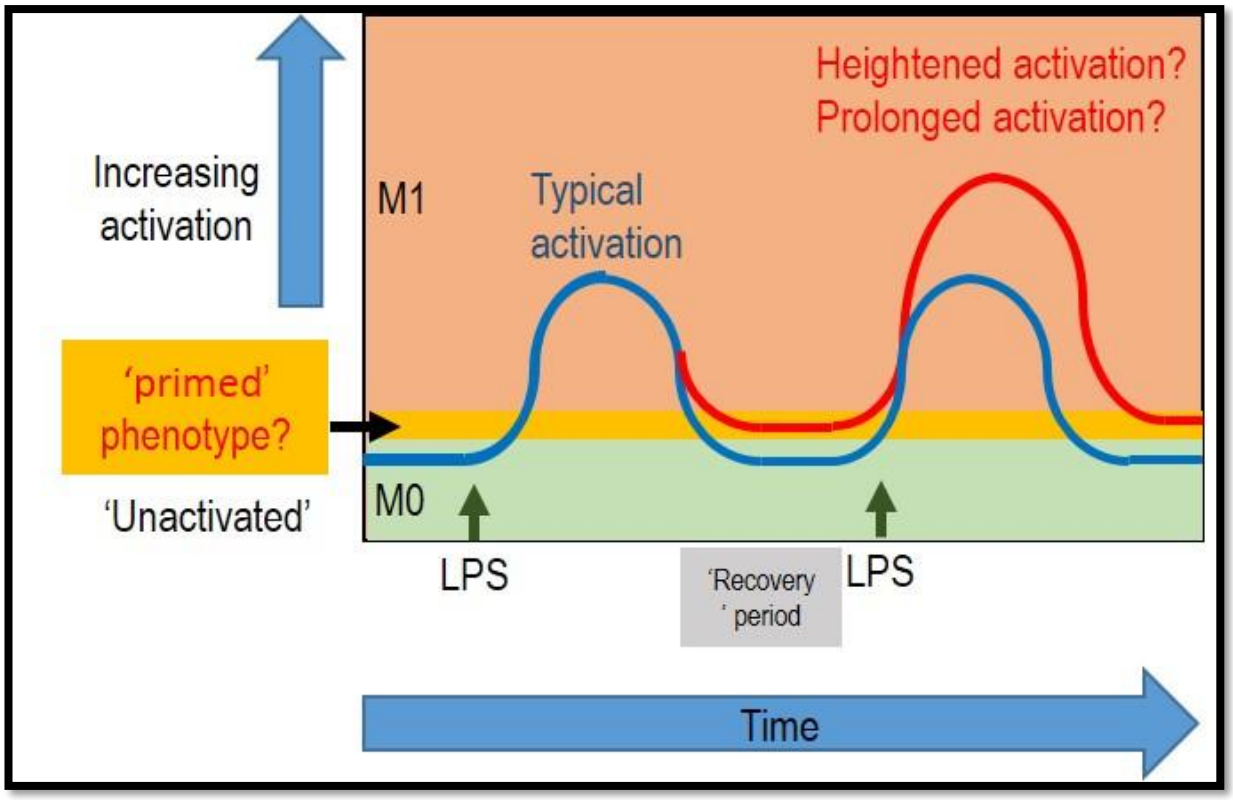

Figure 5-2: Schematic illustration explaining the output of testing the priming theory. The blue lines indicate the predicted microglial responses if microglia do not alter with 'priming' effects and return to standard M0 states after activation. Treating M0 microglia with LPS induces M1 activation, which dissipates over time. Repeating the LPS dose produces the same intensity of M1 response and the same dissipation to M0. However, if priming is simulated in our system, we can predict that the LPS will leave microglia 'primed' (neither M0 nor M1), and these primed microglia may show a greater M1 response on later LPS challenge (red line).

5.2 Aims and objectives

Although modulating microglial behaviour could provide a powerful technique to deliver therapy for previously untreatable diseases, it will require a thorough understanding of microglial phenotype switching in disease states, and the identification of drugs/interventions, which can bring about these changes. Therefore, an experimental system must be developed to study microglial behaviour, with a validation through exposure of microglia to well-established phenotype-inducing molecules, followed by assessment of markers' expression. Once validated, strategies to control phenotype switching can be evaluated using such model.

5.2.1 Aims

The first aim of the research described in this Chapter is to characterise phenotypic responses to the well-known microglial pro-inflammatory activator LPS, at a wide range of concentrations and multiple time points. To the best of my knowledge, no report covering such a wide range of concentrations, allowing the calculation of the EC50 for LPS with microglia has been found in the literature. Such comprehensive data would be of significant importance for the scientists and engineering of human microglia fields.

The second aim is to identify whether primary microglia are susceptible to 'priming'. If *in vitro* priming of microglia could be demonstrated, this would represent a useful model to study the mechanisms of priming, and to explore the interactions between different priming mechanisms.

5.2.2 Objectives

The objectives are:

- To generate qPCR dose-response data for LPS-treated microglia.
- To compare dose-response curve summary statistics (EC50 and maximum dose response) for each gene, and across different time points.
- To characterise NO expression across different LPS concentrations and time points.
- To determine whether microglial M1 responses are heightened after priming.

5.3 Experimental procedures

5.3.1 Reagents and equipment

All reagents and equipment used were described previously in Chapter Two.

5.3.2 Preparation and treatment of microglial culture

Mixed glia culture preparation and high purity microglia culture isolation were described previously in Chapter Two. Microglia cultures were incubated in D10 media for 24 h at 37 °C in 5 % CO2, 95 % humidified air. Cells have been treated with LPS (0, 0.001, 0.01, 0.03, 0.1, 0.3, 1, 3, 10 and 100 ng/ml) for 24 h, later RNA has been extracted for gene expression and media collected to run Griess assay as described in Chapter Two.

5.3.3 Repeated LPS treatment

To investigate priming (double dose) effect on microglia, an experiment was designed to determine the effect of second dose of LPS on pre-exposed microglia and if the second dose will lead to priming or tolerance status.

A pilot experiment was performed to determine how long the 'recovery' period should be, post-LPS treatment, for microglia to lose their M1 activation state. In this experiment, *Il-1β* was highly elevated after LPS treatment (6 h, 10 ng/ml). But when parallel cultures were allowed to recover (100 % media change without LPS, maintained for further 24, 48 or 96 h), *Il-1β* expression was indistinguishable from untreated microglia. This suggested that a 24 h 'recovery' period would be sufficient for M1 activation to expire. However, from the literature, 'recovery' periods for microglia were often chosen to be longer than 24 h. It was therefore decided to allow a 96 h 'recovery' period after removing LPS. There are 10 different conditions (Figure 5-3).

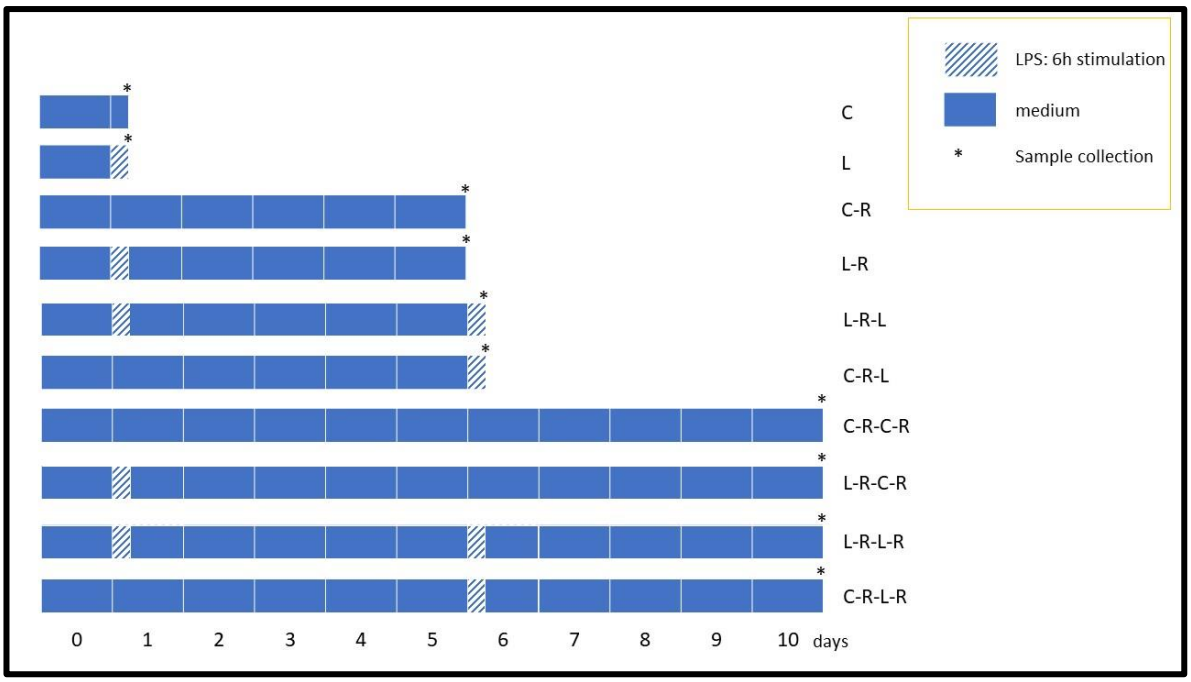

Figure 5-3: Illustration of repeated LPS experiment. There are 10 different conditions through 10 days where the blue boxes represent microglia in D10 media, striped boxes represent microglia facing 6 h of LPS then microglia have been washed and a fresh media added, then cells been left to recover or, media been collected for Griess assay and RNA been extracted for qPCR analysis. C: control; L: 6 h LPS; L-R: 6 h LPS followed by 96 h 'recovery' without LPS; C-R-C: microglia in D10 for 5 days; L-R-L: 6 h LPS followed by 96 h 'recovery' without LPS then 2nd dose LPS (6 h); C-R-L: microglia in D10 for 5 days then received LPS ('2nd' dose only); C-R-C-R: microglia in D10 for 10 days; L-R-L-R: 6 h LPS followed by 96 h 'recovery' without LPS then 2nd dose LPS (6 h) then another 96 h 'recovery'; C-R-L-R: microglia in D10 for 5 days then received LPS ('2nd' dose only) then 96 h 'recovery' without LPS; L-R-C-R: 6 h LPS followed by 96 h 'recovery' without LPS then D10 for 5 days.

5.4 Results

5.4.1 LPS dose-response effects

Gene expression analyses were performed, for a range of LPS concentrations and multiple time points. For each gene, dose-response curves were plotted, maximal responses determined and EC50 values calculated. Also, Griess assays were used to assess dose-response and time course in terms of nitrite production.

5.4.1.1 The effect of LPS on *Il-1β*

There is a dose-responsive increase in *Il-1β* with LPS treatment, at 2, 6 and 24 h (Figure 5-4).

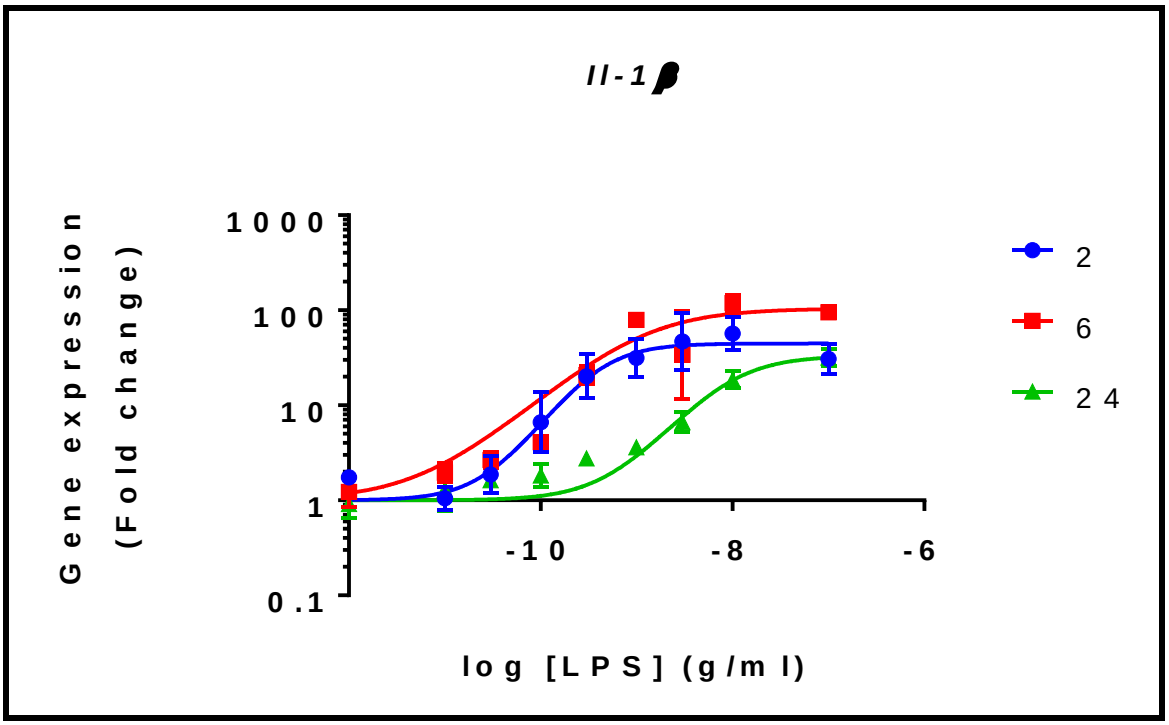

Figure 5-4: LPS effect on *Il-1β* gene expression at 2, 6 and 24 h. Y-axis represents log fold change versus average of reference genes (1 = no change) and X-axis represents log LPS concentration in (g/ml). All data are presented as the mean ± S. E. M of three independent experiments.

There is a significant decrease in LPS potency in 24h in comparison to both 2 and 6 h (Figure 5-5 A). There is a significant difference in maximum fold changes between 6 and 24 h (Figure 5-5 B).

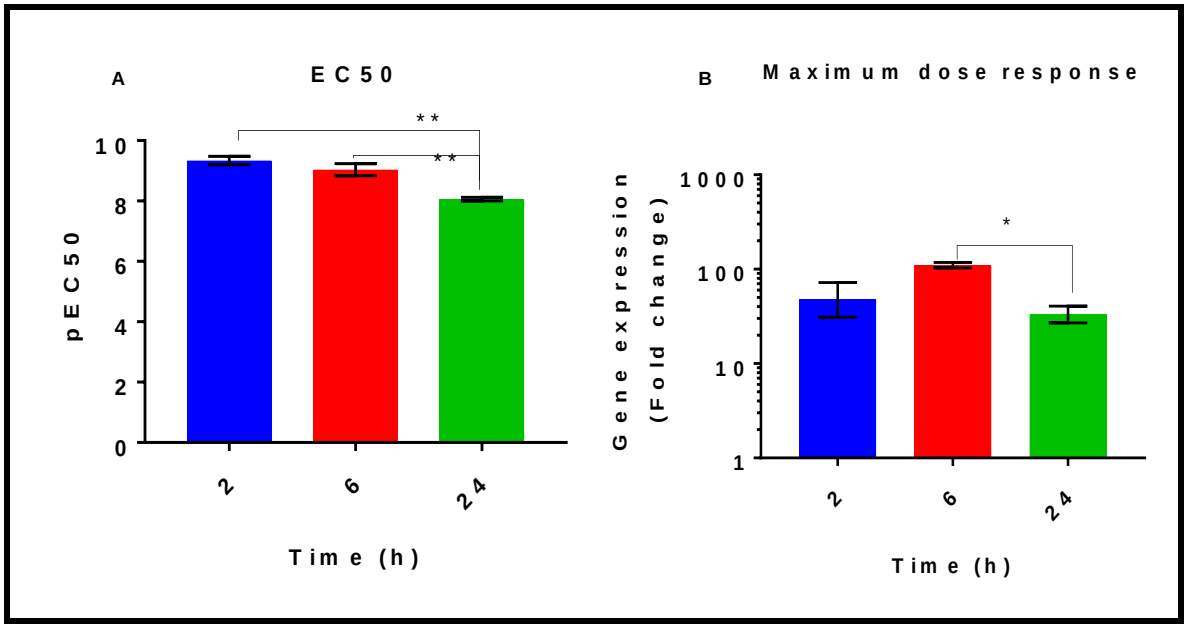

Figure 5-5: *Il-1β* dose response curves summary at different time points. (A) EC50, Y-axis represents pEC50 in (g/ml) and X-axis represents the different time points. EC50 concentration at 24 h is significantly less potency than 2 and 6 h. (B) Maximum fold change, Y-axis represents log fold change and X-axis represents the different time points, maximum dose response at 24 h is significantly lower than 6 h. *p < 0.05, **p < 0.01; One-way ANOVA with Tukey's post-hoc test for each time point versus the other two time points. All data are presented as mean ± S. E. M. of three independent experiments.

5.4.1.2 The effect of LPS on *Il-6*

There is a dose-responsive increase in *Il-6* with LPS treatment at 2, 6 and 24 h (Figure 5-6).

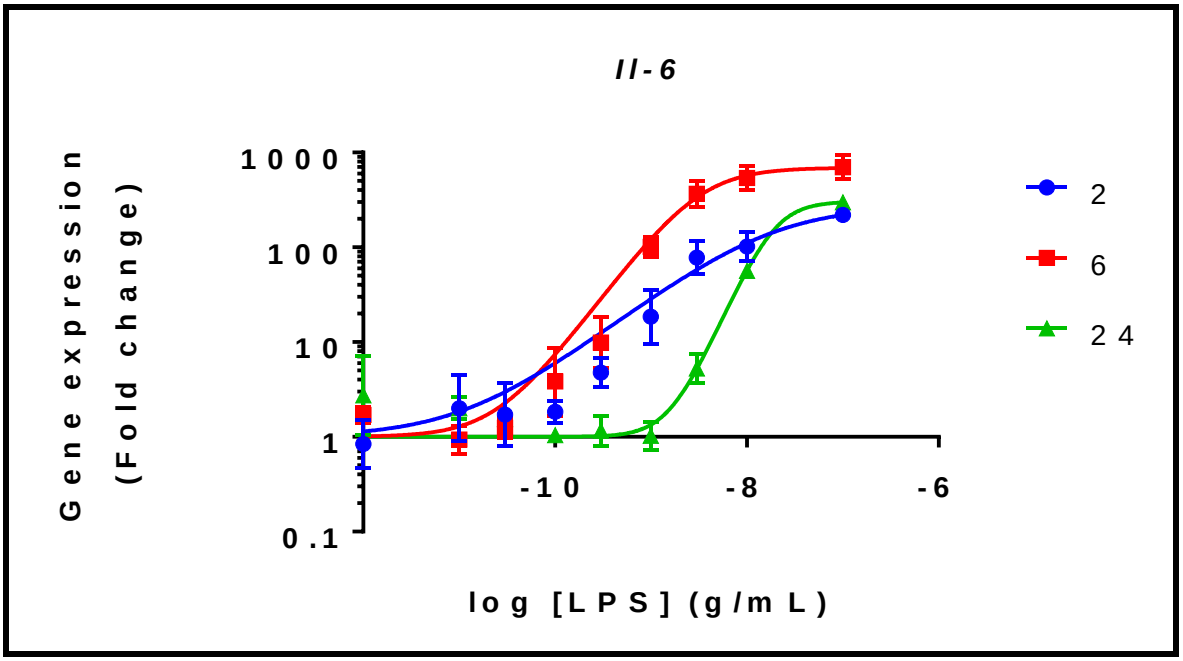

Figure 5-6: LPS effect on *Il-6* gene expression at 2, 6 and 24 h. Y-axis represents log fold change versus average of reference genes (1 = no change) and X-axis represents log LPS concentration in (g/ml). All data are presented as the mean ± S. E. M of three independent experiments.

There is no significant difference in EC50 and maximum fold changes between the different time points (Figure 5-7).

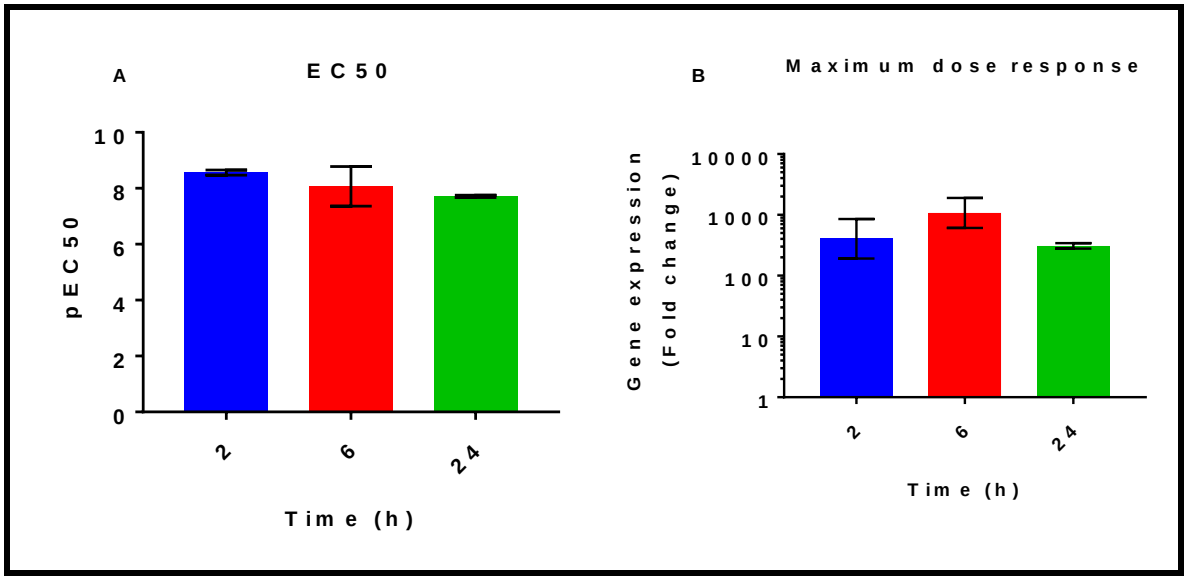

Figure 5-7: *Il-6* dose response curves summary at different time points. (A) EC50, Y-axis represents pEC50 in (g/ml) and X-axis represents the different time points. (B) Maximum fold change, Y-axis represents log fold change and X-axis represents the different time points. No significant difference; Kruskal-wallis with Dunn's post-hoc test for each time point versus the other two time points for pEC50;One-way ANOVA with Tukey's post-hoc test for each time point versus the other two time points for Maximum fold change. All data are presented as mean ± S. E. M. of three independent experiments.

5.4.1.3 The effect of LPS on *Tnf-α*

There is a dose-responsive increase in *Tnf-α* with LPS treatment at 2, 6 and 24 h (Figure 5-8).

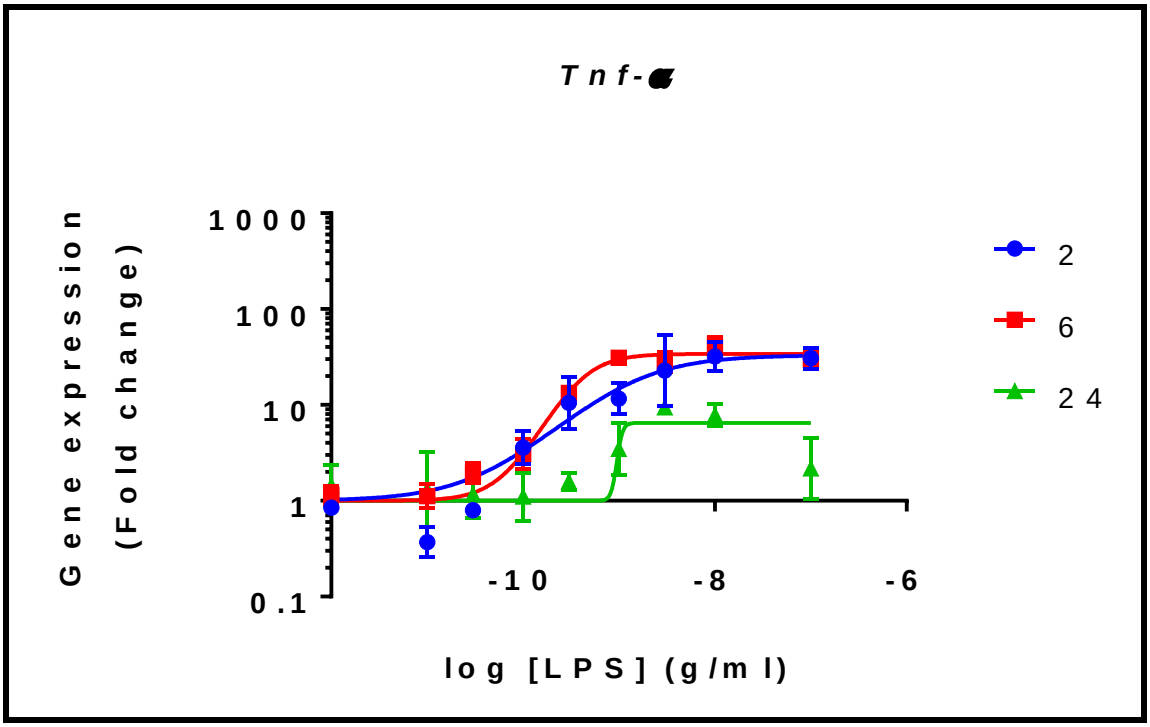

Figure 5-8: LPS effect on *Tnf-α* gene expression at 2, 6 and 24 h. Y-axis represents log fold change versus average of reference genes (1 = no change) and X-axis represents log LPS concentration in (g/ml). All data are presented as the mean ± S. E. M of three independent experiments.

There is no significant difference in EC50 between different time points (Figure 5-9A). There is a significant decrease in maximum dose response at 24 h in comparison to 2 and 6 h (Figure 5-9 B).

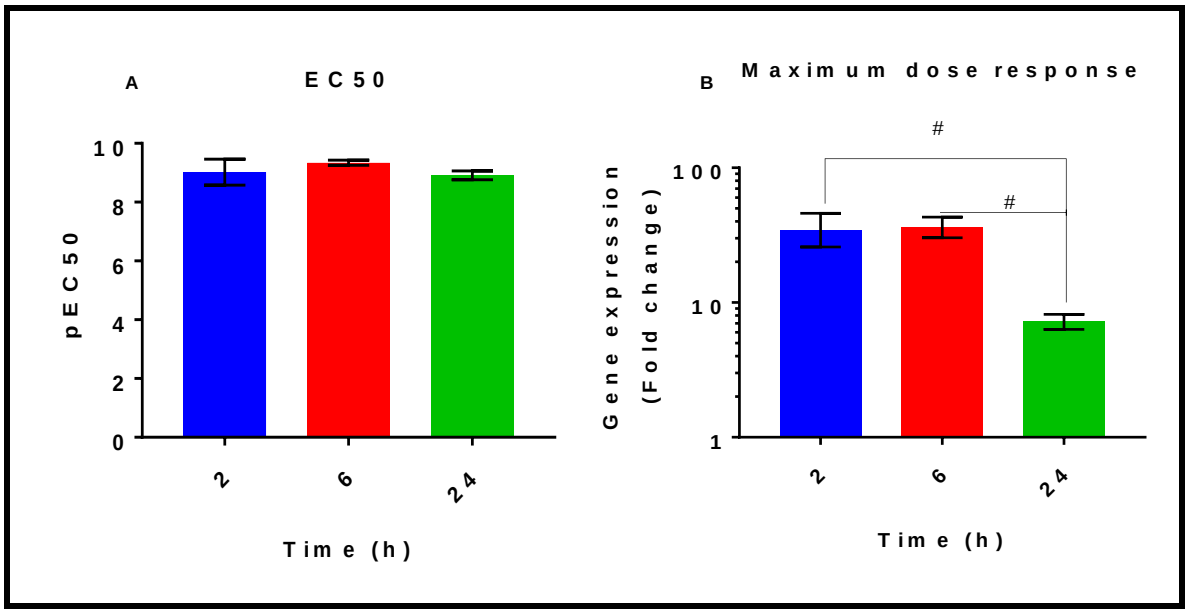

Figure 5-9: *Tnf-α* dose response curves summary at different time points. (A) EC50, Y-axis represents pEC50 in (g/ml) and X-axis represents the different time points. (B) Maximum fold change, Y-axis represents log fold change and X-axis represents the different time points. #p = 0.05; One-way ANOVA with Tukey's post-hoc test for each time point versus the other two time points. All data are presented as the mean ± S. E. M. of three independent experiments.

5.4.1.4 The effect of LPS on *Il-10*

There is a dose-responsive increase in *Il-10* with LPS treatment at 6 and 24 h only but not in 2 h (Figure 5-10).

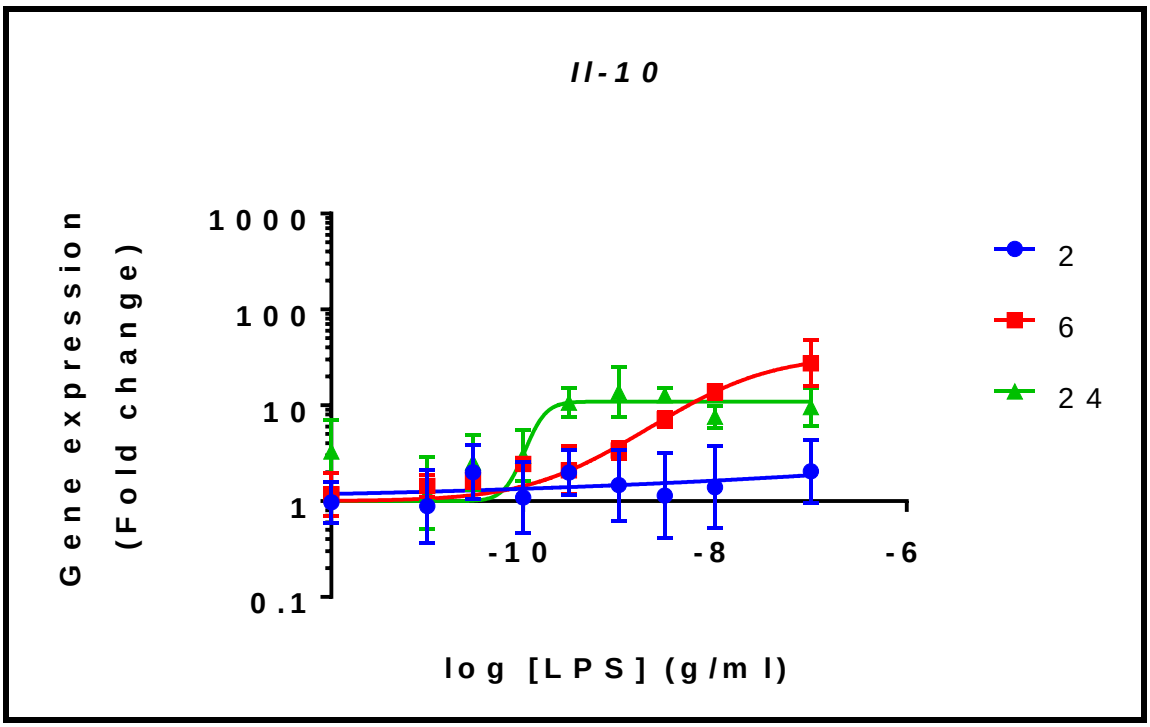

Figure 5-10: 2, 6 and 24 h LPS effect on *Il-10* gene expression. Y-axis represents log fold change versus average of reference genes (1 = no change) and X-axis represents log LPS concentration in (g/ml). All data are presented as the mean ± S. E. M of three independent experiments.

There is no meaningful curve fit was achieved for 2 h, and therefore no maximum fold changes and EC50 values that could be calculated for *Il-10* at 2 h. There is no significant difference in EC50 and maximum fold changes between 2 and 6 h (Figure 5-11).

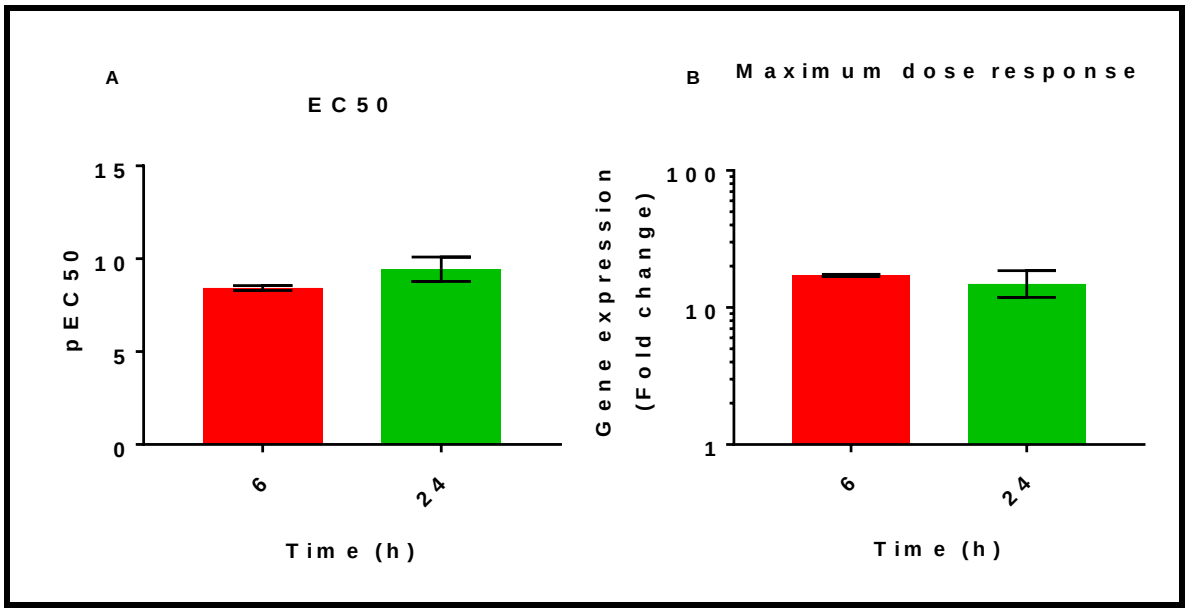

Figure 5-11: ***Il-10*** **dose response curves summary at different time points. (A) EC50, Y-axis represents pEC50 in (g/ml) and X-axis represents the different time points. (B) Maximum fold change. Y-axis represents log fold change and X-axis represents the different time points. No significant difference was found; unpaired t-test between 2 and 6 h. All data are presented as the mean ± S. E. M. of three independent experiments.**

5.4.1.5 The effect of LPS on *Tgf-β*

There is no LPS-induced change in expression of the M2 marker *Tgf-β*, since no consistent increase or decrease was detected in any time point (Figure 5-12). There is no meaningful curve fit for *Tgf-β*, and therefore no maximum fold changes and EC50 values could be calculated.

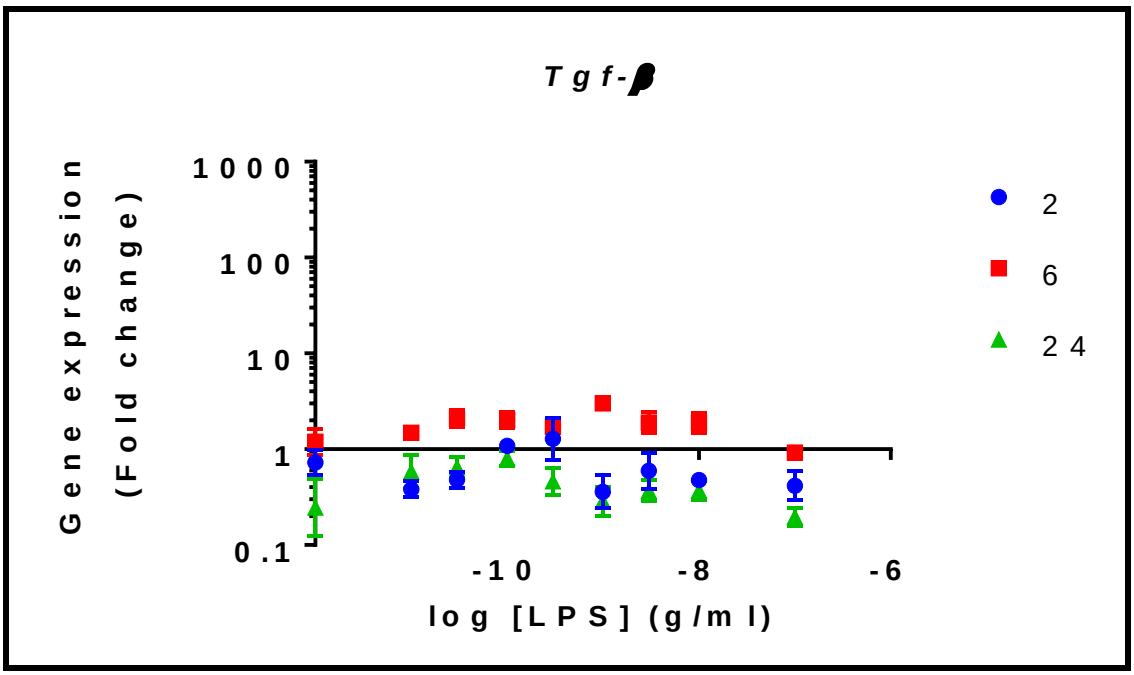

Figure 5-12: 2, 6 and 24 h LPS effect on *Tgf-β* gene expression. Y-axis represents log fold change versus average of reference genes (1 = no change) and X-axis represents log LPS concentration (g/ml). All data are presented as the mean ± S. E. M of three independent experiments.

5.4.1.6 Nitrite production

To investigate the effects of LPS-stimulated on nitrite production in primary microglia cells, cells were treated with a different LPS concentrations for 2, 6 and 24 h. The levels of nitrite in the culture media were determined with the Griess assay. LPS significantly increased nitrite production in primary microglia cells in a dose-dependent manner (Figure 5-13).

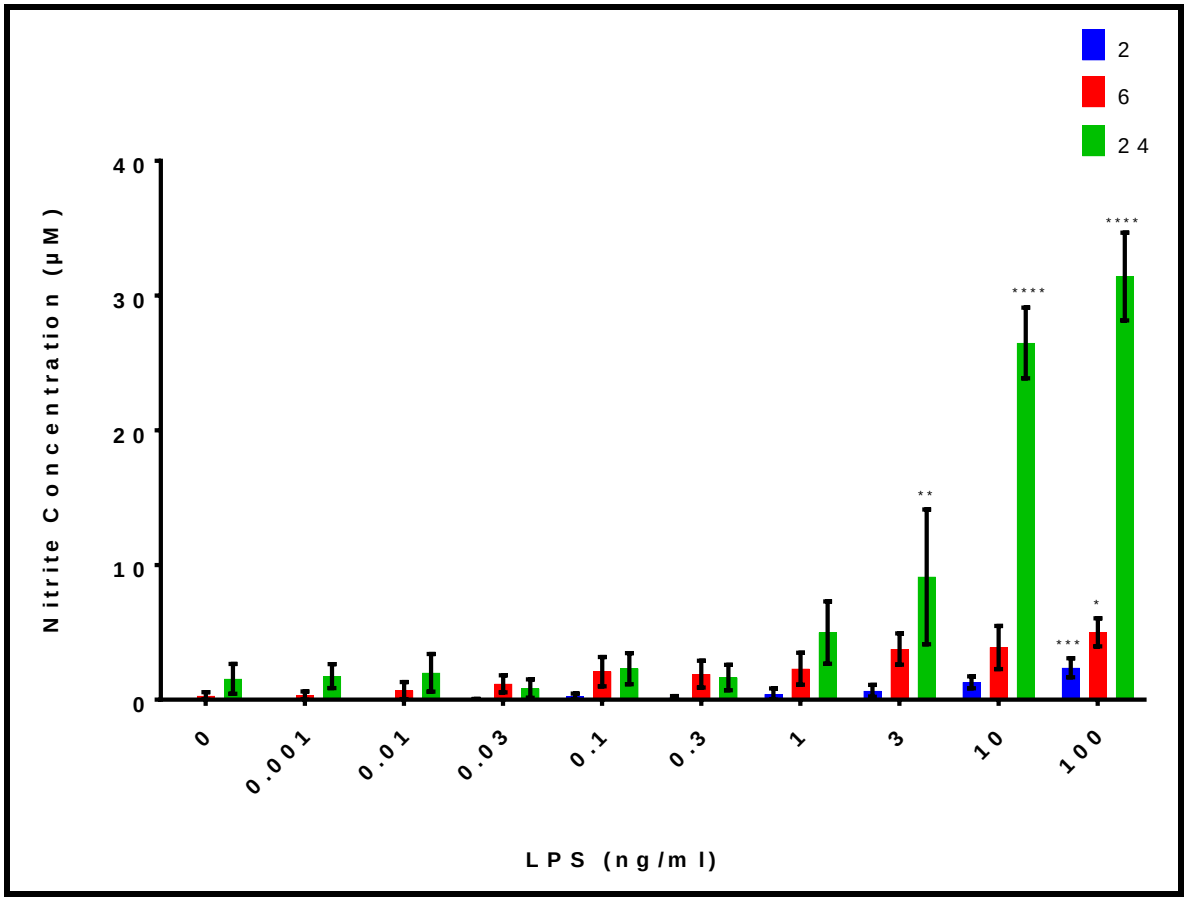

Figure 5-13: LPS-induced nitrite production. Nitrite production in microglia cells (6 × 10^5 cell/ml) after treatment with different LPS concentration (0-100 ng/ml) for 2, 6 or 24 h. LPS effect was assayed by measuring the levels of nitrite in the supernatant fluid using Griess reagent. *p < 0.05, **p < 0.01, ***p < 0.001, ****p < 0.0001; One-way ANOVA with Dunnett's post-tests for each time point in compare to its control (LPS=0). All data are presented as the mean ± S. E. M. of three independent experiments.

5.4.2 Repeated LPS treatment

After characterising the microglial response to single doses of LPS, it was important to investigate the priming effect of LPS on microglia. Therefore, an experiment was designed to investigate the effect of second dose of LPS on pre-exposed microglia.

As a routine through this work, qPCR was performed using the three reference genes identified in Chapter Three. The results show that there was no LPS-induced change in expression for the reference genes tested (*Gapdh, Usp14* and *Rpl32*), across the 10 different conditions. Variations in relative expression (fold change) was not statistically significant (Figure 5-14). Therefore, the average of their Cq values should allow a reliable evaluation of LPS-induced changes in GOI.

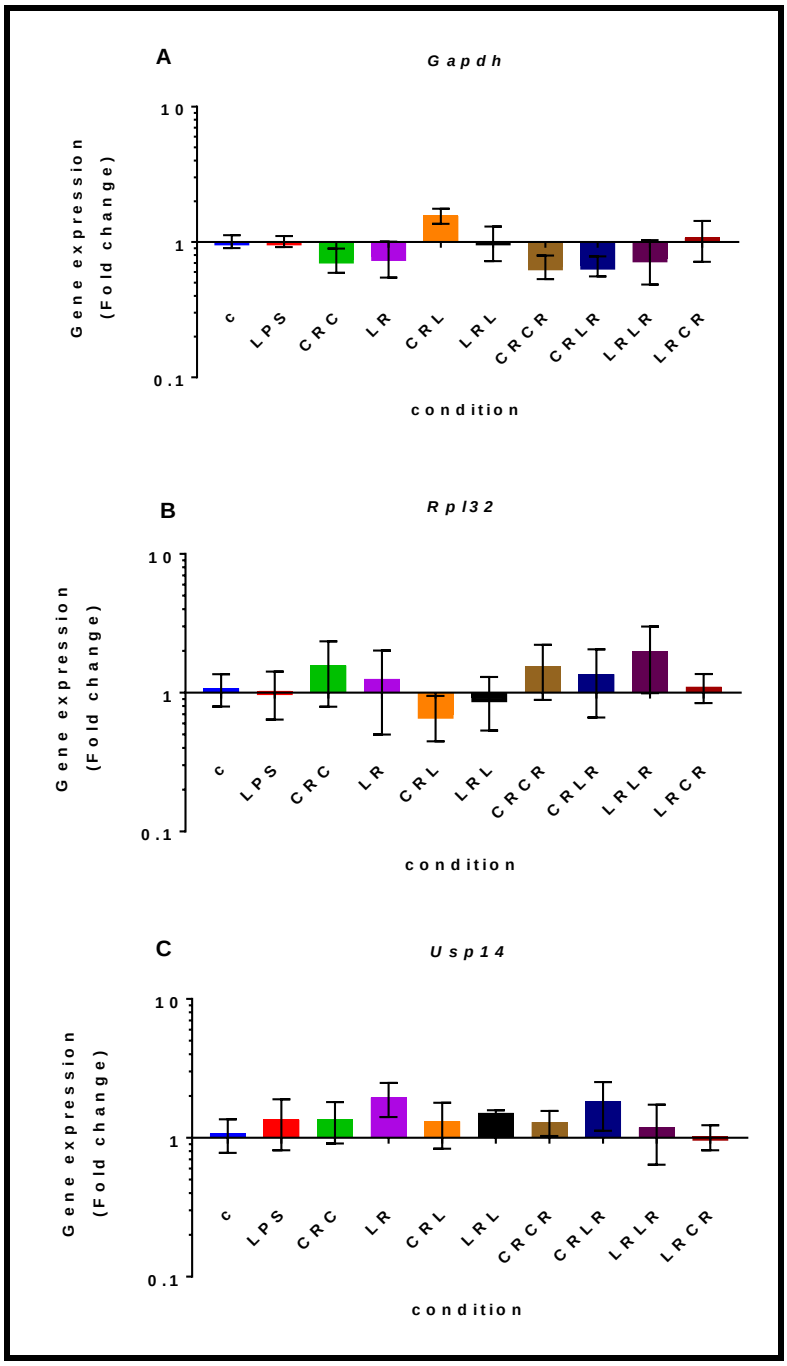

Figure 5-14: Reference genes were unresponsive to LPS treatment. (A) *Gapdh*, (B) *Rpl32*, (C) *Usp14*. The three biological replicates produced similar values, demonstrating high reproducibility. No significant difference, One-way ANOVA with Dunnett's post-hoc test versus C. All data are presented as mean ± S. E. M. of three independent experiments. C: control; L: 6 h LPS; L-R: 6 h LPS followed by 96 h 'recovery' without LPS; C-R-C: microglia in D10 for 5 days; L-R-L: 6 h LPS followed by 96 h 'recovery' without LPS then 2nd dose LPS (6 h); C-R-L: microglia in D10 for 5 days then received LPS ('2nd' dose only); C-R-C-R: microglia in D10 for 10 days; L-R-L-R: 6 h LPS followed by 96 h 'recovery' without LPS then 2nd dose LPS (6 h) then another 96 h 'recovery'; C-R-L-R: microglia in D10 for 5 days then received LPS ('2nd' dose only) then 96 h 'recovery' without LPS; L-R-C-R: 6 h LPS followed by 96 h 'recovery' without LPS then D10 for 5 days.

5.4.2.1 'Recovery' after first LPS

After 6 h LPS-treatment, microglia displayed a classical pro-inflammatory profile, with high levels of *Il-1β, Il-6, Tnf-α* and *iNos* expressions The expression of *Il-10*, a non classical M1-associated gene, was lower, at 7.2-fold. For cultures allowed to recover for 96 h, post-LPS exposure, M1-associated genes were all expressed at significantly lower levels (7.3-fold or lower), close to these in untreated microglia. In contrast, *Il-10* expression levels did not differ following the 'recovery' period (Figure 5-15).

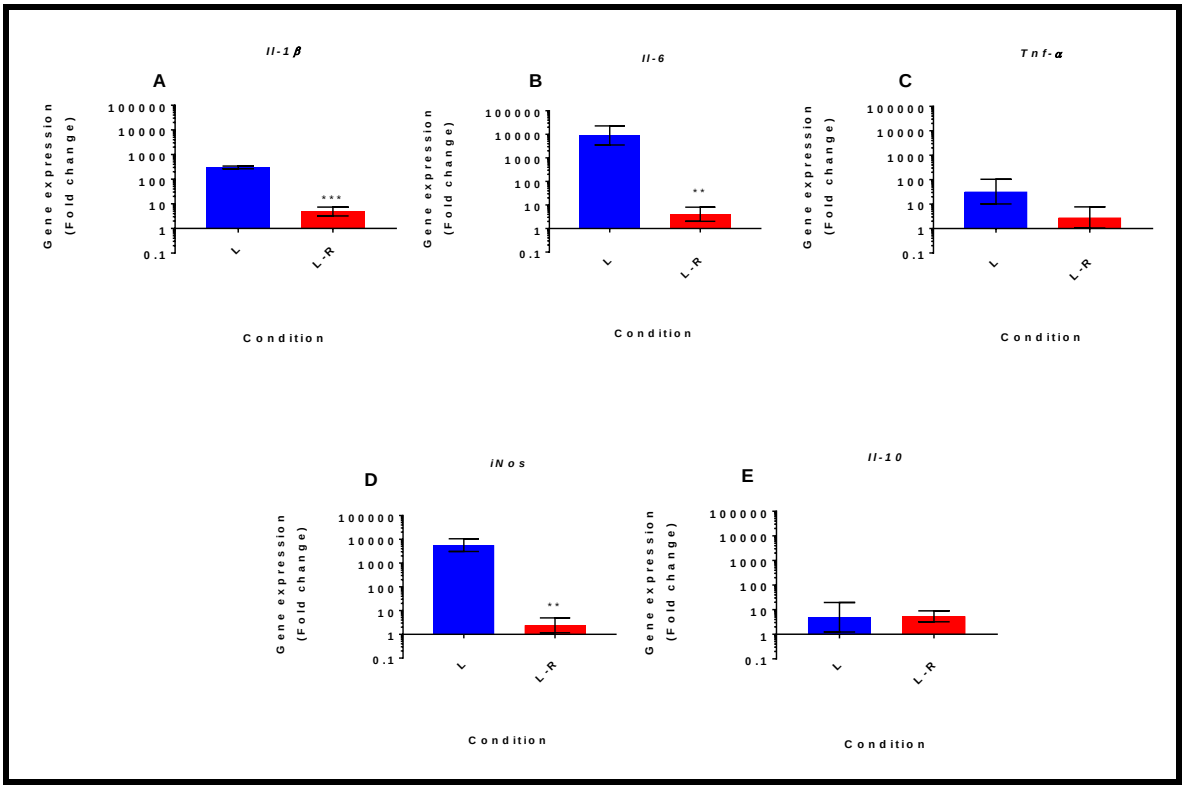

Figure 5-15: Microglia 'recovery' after first LPS treatment effect on gene expression. (A) *Il-1β*, (B) *Il-6*, (C) *Tnf-α*, (D) *iNos* and (E) *Il-10*. Y-axis represents log fold change versus average of reference genes (1 = no change) and X-axis represents difference conditions. **p<0.01, ***p<0.001; unpaired t-test L versus L-R. All data are presented as the mean ± S. E. M. of three independent experiments. (L) 6 h LPS. (L-R) 6 h LPS followed by 96 h 'recovery' without LPS.

5.4.2.2 Second dose of LPS after 'recovery' from the first dose.

After 6 h LPS-treatment, microglia displayed a classical pro-inflammatory profile, with high levels of *Il-1β, Il-6, Tnf-α* and *iNos* expressions. For cultures that received either one dose or two doses of LPS, there is no significant difference in any of M1-associated genes. In contrast, there is a significant increase in *Il-10* expression in these cultures that received only the second dose of LPS (Figure 5-16).

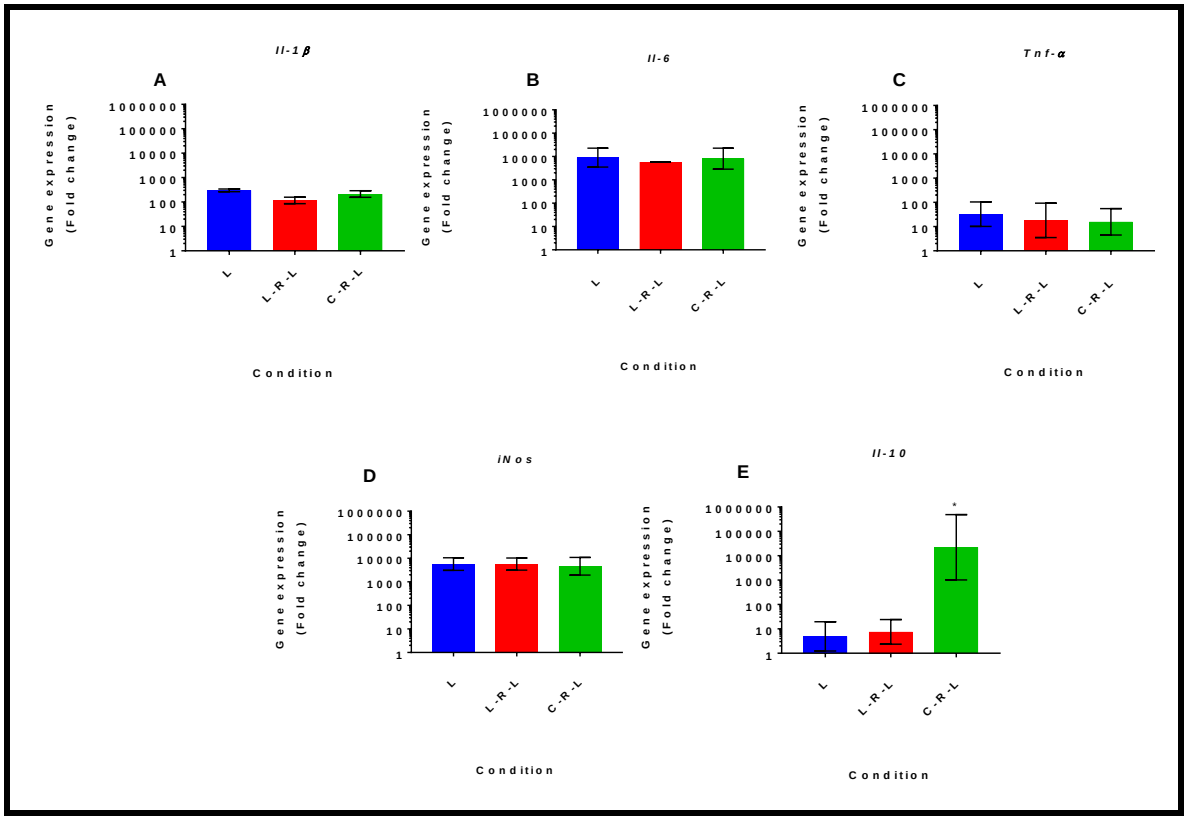

Figure 5-16: Microglia receiving 2nd dose of LPS after recovery from the first LPS treatment effects on gene expression. (A) *Il-1β,* (B) *Il-6,* (C) *Tnf-α,* (D) *iNos* and (E) *Il-10*. Y-axis represents log fold change versus average of reference genes (1 = no change) and X-axis represents difference conditions. *Il-10* gene expression in C-R-L is significantly higher than in L. *p < 0.05, One-way ANOVA with Dunnett's post-hoc test versus L. All data are presented as the mean ± S. E. M. of three independent experiments. (L) 6 h LPS; (L-R-L) 6 h LPS followed by 96 h 'recovery' without LPS then second 6 h LPS; (C-R-L) microglia in D10 for 5 days then received LPS ('2nd' dose only).

5.4.2.3 'Recovery' after second LPS treatment

Cultures allowed a 2nd recovery for 96 h, post-LPS exposure, M1-associated genes were all expressed, close to these in untreated microglia. In contrast, *Il-10* expression levels have shown a significant increase in these cultures that receive only the second dose of LPS and left to recover from it (Figure 5-17).

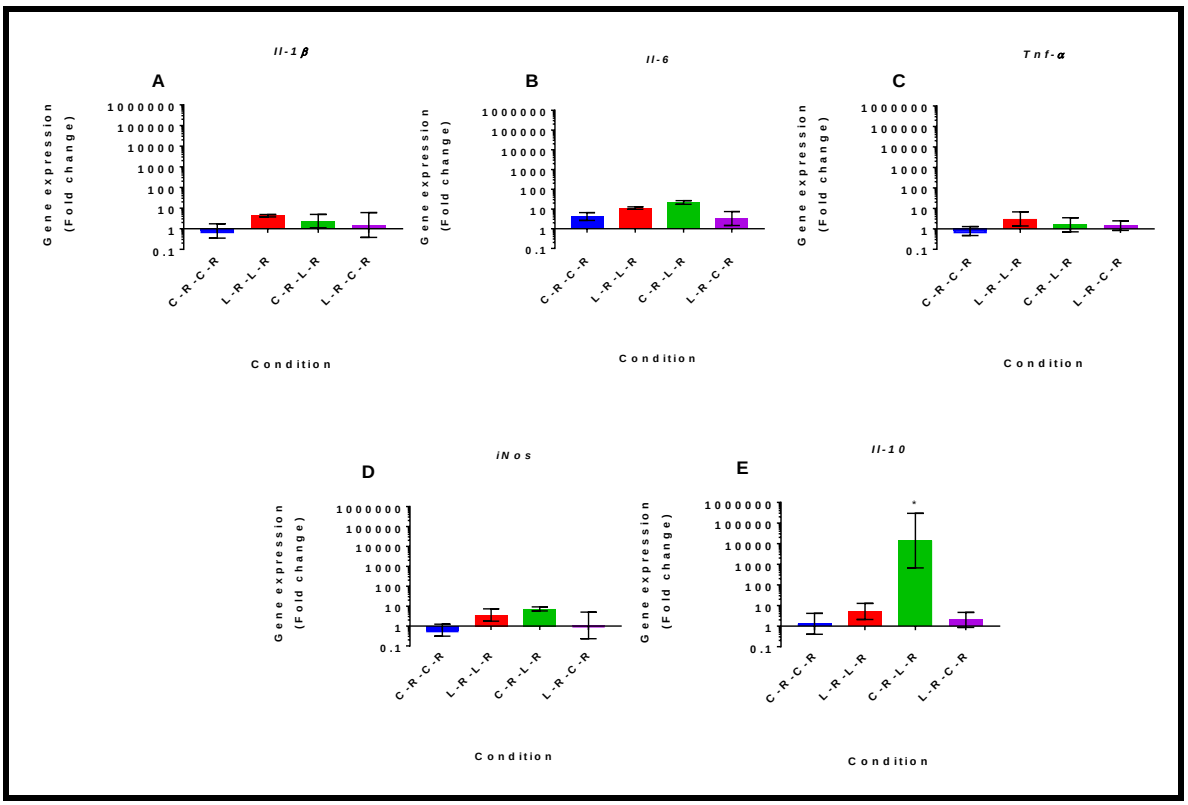

Figure 5-17: Microglia 'recovery' after 2nd dose of LPS treatment effect on gene expression. (A) *Il-1β*, (B) *Il-6*, (C) *Tnf-α*, (D) *iNos* and (E) *Il-10*. Y-axis represents log fold change versus average of reference genes (1 = no change) and X-axis represents difference conditions. Il-10 gene expression in C-R-L-R is significantly higher than in C-R-C-R. *p < 0.05, One-way ANOVA with Dunnett's post-hoc test versus C-R-C-R. All data are presented as the mean ± S. E. M. of three independent experiments. (C-R-C-R) microglia in D10 for 10 days; (L-R-C-R) 6 h LPS followed by 9 days in D10 (without LPS); (L-R-L-R) 6 h LPS followed by 96 h 'recovery' without LPS then second 6 h LPS followed by another 96 h 'recovery' without LPS; (C-R-L-R) microglia in D10 for 5 days then received LPS ('2nd' dose only) then 96 h 'recovery' without LPS.

5.4.2.4 Repeated LPS treatment effect on nitrite production

To investigate the effects of repeated LPS treatment on nitrite production in primary microglia cells, the levels of nitrite in the culture media were determined using Griess assay. Figure 5-18 shows that the nitrite concentration is significantly increased in these cultures that were treated two times with LPS and microglia recovered from two dose of LPS. However, there is no significant increase in any of other conditions.

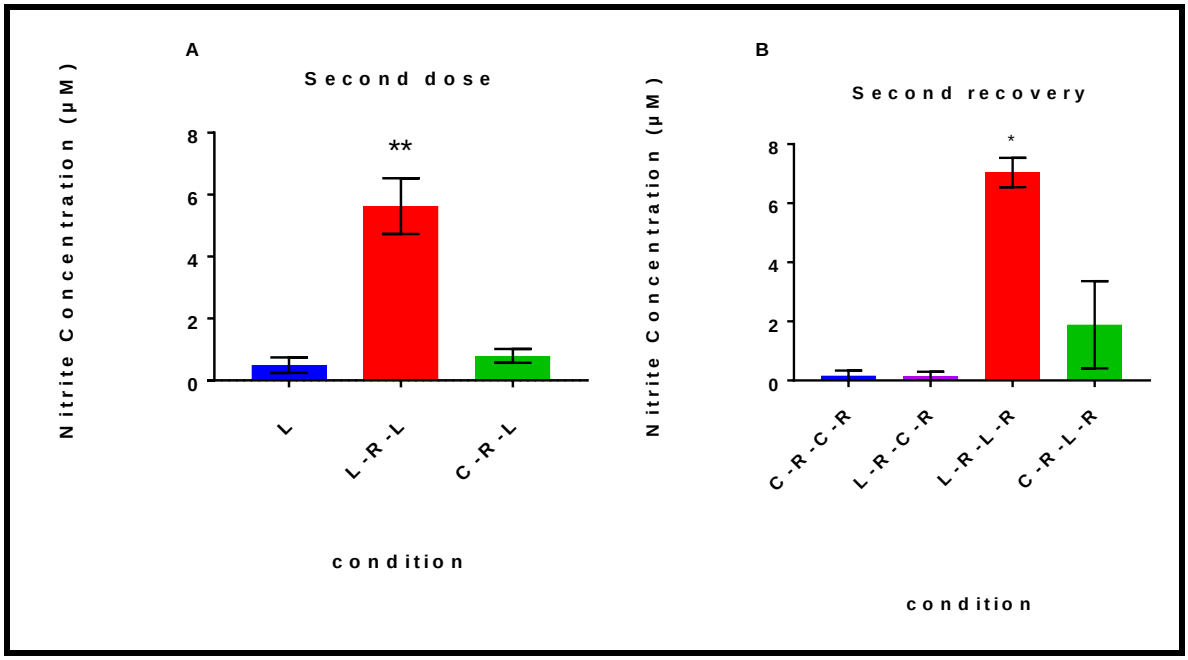

Figure 5-18: Nitrite concentration for the repeated LPS treatment. (A) nitrite production after 6h of LPS, two dose of LPS with 96 h recovery time between them (L-R-L) is significantly higher than only one first dose of LPS (L). (B) nitrite production after 96h recovery from LPS, microglia culture that recover from two dose of LPS (L-R-L-R) is significantly higher than control (C-R-C-R). *p < 0.05, **p < 0.01; One-way ANOVA with Dunnett's post-hoc test. All data are presented as the mean ± S. E. M of three independent experiments. L: 6 h LPS; L-R-L: 6 h LPS followed by 96 h 'recovery' without LPS then second 6 h LPS; C-R-L: microglia in D10 for 5 days then received LPS ('2nd' dose only). C-R-C-R: microglia in D10 for 10 days; L-R-C-R: 6 h LPS followed by 9 days in D10 (without LPS); L-R-L-R: 6 h LPS followed by 96 h 'recovery' without LPS then second 6 h LPS followed by another 96 h 'recovery' without LPS; C-R-L-R: microglia in D10 for 5 days then received LPS ('2nd' dose only) then 96 h 'recovery' without LPS.

5.5 Discussion

5.5.1 Microglial stimulation by LPS induces M1 phenotype

Exposure of the microglial cells to LPS led to an increased pro-inflammatory cytokine expression (*Il-6*, *Il-1β* and *Tnf-α*), suggestive of M1 activation (Zhang *et al.* 2001; Liu *et al.* 2012; Pan *et al.* 2015; Orihuela *et al.* 2016). All three genes showed positive dose-response curves as expected.

Il-1β showed a dose response curve at 2, 6 and 24 h. There is significance less potency at 24 h on compare to 2 and 6 h, it might be due the LPS-TLR4 pathways nature, as the production of *Il-6* feeds back to inhibit further release of *Tnf-α* and *Il-1β* (Minogue *et al.* 2012). The data also showed a significant reduction in maximal dose response at 24 h, it might be due to the potential impact of reduced potency (EC50 shifts to the right). Therefore, it is possible that, if a higher LPS concentrations has been tested, the maximum dose response would be more closely matches these seen at 2 and 6 h.

Il-6 showed a dose response curve at 2, 6 and 24 h. There are no significantly different in both EC50 and the maximum dose response at the different time points. However, the pEC50 was around 6 in Figure 5-7, while it was around 9 for the same gene and same condition media in Figure 4-11, which might be due to experimental artefact.

Tnf-α also showed a dose response curve at 2, 6 and 24 h. The high concentration at 24 h showed a significant reduction in *Tnf-α* expression. In agree with this results, Chao *et al.* (1992) reported that Tnf-α protein release decrease with increased LPS incubation time. Although there is no direct evidence of this, the cells might have gone over the maximum tolerated exposure to LPS. In line with this theory, Sawada *et al.* (1989) had showed increase in LPS cytotoxicity with increase the concentration. Furthermore, there is

evidences of bell-shaped dose response curve with two of the biological replicate showing fold change less than two fold change in 100 ng/ml.

As Table 5-1 indicates, many studies use a single (usually high) dose of LPS, or a small range of LPS concentrations. For example, Loram *et al.* (2012) used three LPS concentrations and measured the gene expressions of *Il-1β*, *Cd14* and *TLR4*. In agreement with the data presented here, they showed a dose response in *Il-1β* gene expression, when primary rat microglia cultures have been treated with 1, 10 and 100 ng/ml for 4 h. However, Loram *et al.* (2012) qPCR data analysis relied on using only one reference gene (*Gapdh*) and did not calculate EC50 values. Lee *et al.* (1993) study showed a dose dependent response of IL-1β with LPS up to a concentration of 10 µg/ml. The same study revealed that protein production of TNF-α in LPS stimulated microglia reached a peak at 4 h, the difference between their time point and ours might be related to the fact that they measured protein expression while this study measured gene expression (Lee *et al.* 1993). It should be noted that this study was carried out using human microglia, which adds translational value to their findings. Puffenbarger *et al.*, (2000) use the semi quantitative RNAse protection assay to investigate the effects of LPS on rat microglia. This report is one of the few microglial studies with a wide range of LPS concentrations: 1 – 1000 ng/ml. The authors did perform a time-course study (2 – 24 h) for *Il-1β, Il-6* and *Tnf-α. Il-1β* expression has been strong throughout, from 2 to 24 h. However, the LPS dose used (10 ng/ml) produced maximal gene expression in their dose-response study, and so it is possible that they may not have recognised a reduction in the potency of LPS at the 24hr time point. They also utilised two reference genes, *Gapdh* and *L32*.

The range of LPS doses used here provides EC50 values for each gene and reveals maximum fold-change for the major pro-inflammatory cytokines: *Il-1β, Il-6* and *Tnf-α*. Plateau suggests the highest dose of LPS chosen here (100 ng/ml) produces maximal

response for most genes and time points, and the potential bell-shaped dose response seen with Tnf-a suggests that higher concentrations may not be well tolerated (Gibbons & Dragunow 2006). These data validate the use of the model for studying the magnitude of M1 activation, enabling the comparisons between LPS and other stimuli.

Table 5-1: Comparison of the M1 microglia gene expretion in various time points and concentrations from various references.

Cells	Primary rat microglia culture			Primary mice microglia culture	Primary rat microglia culture			Primary mice microglia culture		Primary rat microglia culture	BV-2 Cell	Murine microglia cell line N9	Primary mice microglia culture		
Ref.	(Puffenbarger et al. 2000)			(Chhor et al. 2013)	(Puffenbarger et al. 2000)			(Chhor et al. 2013)	(Pan et al. 2015)	(Puffenbarger et al. 2000)	(Orihuela et al. 2015)	(Liu et al. 2012)	(Kobayashi et al. 2013)	(Chhor et al. 2013)	
Dose/ time point	Not stated	2 h	4 h		6 h	8 h	12 h		15 h	24 h				36 h	72 h
1 ng/ml	↑ *Il-1β, Tnf-α*														
10 ng/ml	↑ *Il-1β, Tnf-α, Il-6*	↑ *Il-1β, Tnf-α, Il-6*	↑ *Il-1β, Tnf-α, Il-6*		↑ *Il-1β, Tnf-α, Il-6*	↑ *Il-1β, Tnf-α, Il-6*	↑ *Il-1β*			↑ *Il-1β, Il-6*					
100 ng/ ml	↑ *Il-1β, Tnf-α, Il-6*										↑ *Il-1β, Tnf-α, Il-6*		↑ *Il-1β, Tnf-α,*		
1000 ng/ml	↑ *Il-1β, Tnf-α, Il-6*			↑ *Tnf-α, Il-6*				↑ *Il-1β, Tnf-α, Il-6*	↑ *Tnf-α, Il-6*					↑ *Il-1β, Tnf-α, Il-6, Il10*	↑ *Il-1β, Tnf-α, Il-6, Il10*
3 µg/ ml												↑*Il-6, Tnf-* α			

5.5.2 Other genes of interest

Tgf-β (an M2-associated gene) was unresponsive to LPS at any time point, consistent with *in vivo* data (Sierra *et al.* 2007), however Chhor *et al.* (2013) reported an increased expression at 36 h. Therefore, it may be useful to extend future experiments to include later time points. *Il-10* showed a dose response effect at 6 and 24 h . The literature contains some reports of *Il-10* upregulation following LPS treatment, including *in vivo* treatment (Sierra *et al.* 2007) but also reported of no effect (Silva *et al.* 2016). This possibly delayed response (compared to *Il-1β, Il-6* and *Tnf-α*) may indicate a secondary response to M1 activation (and so cytokine secretion) as LPS induces the production the pro-inflammatory cytokine Il-6, which induces the production of Il-10. The activation of Il-10 plays an important role in maintaining homeostasis. In CNS, microglia and astrocytes produce Il-10, which has been shown to inhibit LPS induced Il-6 secretion through negative feedback (Il-10 activates STAT3 which blocks TRAF6 downstream of LPS-TLR4 pathway) and stops the production of Il-6 (Lynch *et al.* 2004). However, there is no evidence of this in our study, since *Il-6* production remains high even at 24 h. This could be followed up by even longer experiments.

5.5.3 Nitrite production

Griess reaction is an indirect method for NO determination, by detecting its stable breakdown products NO_3^- and NO_2^-. This method involve NO_3^- reduction to NO_2^- and then NO_2^- determination by spectrophotometric measurement (Bryan & Grisham 2007). The production of nitrite is dependent on the dose of LPS; activated microglial cells can secrete nitrite. Stimulation of the NO pathway in microglial cells may be relevant to the pathogenesis of inflammatory and autoimmune demyelinating diseases of the brain (Zielasek *et al.* 1992).

NF-κB has been shown to be one of the most important upstream modulators for pro-inflammatory cytokines and iNos expression in microglia (Liu *et al.* 2011). iNos is the key enzyme for NO production and is quantitatively induced in activated glial cells after exposure to stimulus such as LPS and viral infections (McGeer *et al.*, 1993; Chew *et al.*, 2006). Therefore, it may be interesting to measure dose-responsive increase of iNos with LPS treatment at 2, 6 and 24 h similar to what have been done with the other M1 markers.

5.5.4 Repeated LPS treatment

In vivo evidence suggested that systemic infections lead to an increased inflammatory response in the CNS, and it has been proposed that this interaction might have an important influence on disease processes in the CNS (Perry *et al.* 2003). Infections and events such as trauma, injury or surgery trigger systemic inflammation. These signals will have an important impact on microglia state either by fully activating them or at least priming them (Norden *et al.* 2014). Therefore, if later a neurodegenerative disease occurs, it could be hypothesised that M0' microglia would generate a larger cytokine response than would unprimed microglia in the normal brain. Cytokines are typically not neurotoxic but imbalances and overproduction may lead to neuronal loss, and this may contribute to neurodegenerative diseases processes (Stroemer & Rothwell 1998). Even though studies suggested that M0' microglia have an important role in neurodegenerative disease, the mechanisms are not well understood. Therefore, to establish an *in vitro* model will be helpful to explore and generate hypotheses about M0 microglia.

The hypothesis was that if a microglial activation response was related to its previous experience, then the amount of pro-inflammatory cytokine produced by microglia treated with LPS and recovered from the first inflammation state will be higher than that of naïve microglia when treating both of them with LPS. We tested this hypothesis by

stimulating naïve microglia with LPS then leaving them to recover before stimulating them with a second dose of LPS and studying the differences in gene expression between naïve microglia and microglia with previous LPS experience.

The results showed that the recovery time that has been chosen here (4 days) is enough time for microglia to lose the M1 activation state, for example, when microglia were treated with 10 ng/ml for 6 h there was a significant increase in *Il-1β* (~ 300 fold increase) which was comparable to what was previously reported in section 5.4.1.1. The 4 days recovery time led to a significant decrease in M1 markers (*Il-1β, Il-6, Tnf-α* and *iNos*) while *Il-10* showed a non-significant change since it is a M2 marker which was not affected by LPS treatment. After the results confirmed the time point, a second dose of LPS was added. Although all the M1 markers were increased , the levels of these markers were almost similar across the different conditions (L, L-R-L and C-R-L). Furthermore, the effect of another recovery period tested here, to check if microglia have any memory for repeated infections. The results showed similar expression level in (C-R-C-R, L-R-L-R, C-R-LR and L-R-C-R) through all the M1 markers tested here, this result suggested that microglia M1 expression go back to the baseline expression when allowed them to recovered whether they received one or repeated dose of LPS.

In summary, the results generated in this chapter suggest that double dose (6h; 10 ng/ml LPS, recovery time and another 6h; 10 ng/ml LPS) does not exaggerate microglia inflammatory response. In line with this study, another study showed that when macrophages receive a similar LPS dose to what has been used here (10 ng/ml) no differences were recorded in *Il-6* and *Tnf-α* upon secondary challenge (Deng *et al.* 2013). On the other hand, results generated here showed that the anti-inflammatory *Il-10* marker has a higher expression in these cells that only received the 2nd dose of LPS (C-R-L) and these who recovered from the 2nd dose (C-R-L-R). Schaafsma *et al.*, (2015) have reported a similar

result, Il-10 protein expression was higher in (PBS-LPS) than in (LPS-PBS) and (LPS-LPS) *in vivo*. And this might be due to the neuroprotective nature of Il-10 and its important role in regulating CNS inflammation and infection. Furthermore, LPS induced Il-6 has been shown to activate Il-10 production by microglia (Ye & Johnson 2001). In contrast, Schaafsma *et al.* (2015) reported that in a similar neonatal mice microglia experiment, multiple dose of LPS led to a reduction in the pro-inflammatory gene expression as facing an infection might lead to acquisition of tolerance to the next infection.

In terms of Griess assay, it seems that microglia exposed to a double dose of LPS have a significantly higher nitric oxide production. Although, it is generally thought that NO production and pro-inflammatory mediators always increase in activated microglia/macrophages. Zhang and Morrison (1993) study showed that when macrophages are primed by pre-treatment with LPS NO production in response to second stimulation was increased, Tnf-α production is co-ordinately suppressed. Furthermore, this study result suggests that there is an increase in NO production even without high iNos gene expression (Figure 5-17). One explanation for this might be the disconnect between iNOS gene expression and iNOS protein, with significant enzyme activity present in the cell for a substantial length of time after gene expression is switched off. Counter to this argument, the half-life of iNOS protein is reported to be short (~1-2 hr) (Kolodziejski *et al.* 2004; Wang *et al.* 2009). These results support the concept that different mechanisms might be involved in priming and stimulating microglia to produce different genes and NO.

This study results also demonstrated that the first dose of LPS did not lead to either less or more response to second dose of LPS, as shown by cytokines gene expression. The results of the current study should be considered in the context of previously reported investigations. Endotoxin primed macrophages has been well described in various *in vitro* studies (Hirohashi & Morrison 1996; Bosisio *et al.* 2002; Sorgi *et al.* 2012). On the other

hand many other *in vitro* studies reported 'tolerance' (pre-activated cell reduces pro-inflammatory production) upon induction of systemic inflammation (Takasuka *et al.* 1991; Shinji *et al.* 1994).

In vitro studies showed that macrophages pre-treated with LPS have an increased superoxide anion production (León *et al.* 1992). Lehner *et al.* (2001) showed that despite a reduced cytokines response, acquired LPS tolerance was associated with enhanced resistance to infections by Gram-negative bacteria, mediated primarily through improved innate immune effector function. Pre-treatment with LPS enhanced survival of mice (Rayhane *et al.* 2000). In rats, endotoxin tolerance was associated with reduced cytokine expression within the lung and liver (Flohé *et al.* 1999). In prion disease model, Combrinck and his colleges (2002) demonstrated an exaggerated behavioural response and increased Il-1β synthesis in the CNS following a peripheral LPS challenge to animals with a pre-existing chronic inflammation. Using similar model, Cunningham and his co-worker (2002) showed an increase in Il-1β and Tnf-α in prion-diseased animals relative to control animals after injection of LPS (100 μg/kg).

As the goal of this experiment was to study the difference between naïve microglia and microglia with previous experience in term of gene expression using real time PCR. C-R and L-R-C conditions have not been included in this experiment. C-R-C and C-R were considered to be similar in term of gene expression. Furthermore L-R and L-R-C were also considered to be similar since changing the media and leaving the cells in D10 for extra 6 h will not affect gene expression. However, future work should include these condition as changing the media might have an effect on measured nitrite.

5.6 Summary

This Chapter has characterised the effects of a wide range of LPS concentration at three-time points (2, 6 and 24 h).

Establishing this model is important for future work, as knowing the EC50 and the maximum dose response for M1 microglia will help to provide a base line to study the effect of using different substance in the CNS, such as nanoparticles, which are considered as a new approach in the treatment of neurodegenerative diseases. Also, it helps in studying the effects of a second pro-inflammatory challenge, which will possibly allow the investigations of the effects of age and systemic inflammation on the onset and the progress of neurodegenerative diseases.

As part of future work, it will be helpful to study the effect of different challenges (e.g., ‘insulin’ dysregulation in diabetes and ‘leptin’ expression in obesity) on the second challenge. Also, the response to other materials in the presence of inflammation, for example is the nanoparticle effect on microglia different within a spinal cord injury site? Furthermore, the next step will focus more on the mediators that control the priming effect of microglia which will be of great benefit in terms of developing drugs designed to reduce the extreme microglia reaction in the neurodegenerative disease that leads to neuronal damage and death.

Chapter 6 : Characterising microglial responses to anti-inflammatory activation

6.1 Introduction

6.1.1 The role of M2 microglia in health and disease

Microglia play significant roles in the CNS. In normal healthy brain, microglia scan their environment for threats to homeostasis, and if an infection has been detected, microglia are activated and start to attack this infection by producing pro-inflammatory cytokines as described in Chapter Five. The pro-inflammatory state that followed by anti-inflammatory state, plays a role in tissue repair, wound healing and extracellular matrix composition (Colton & Wilcock 2010). Furthermore, the main M2 function is inhibiting inflammation and restoring homeostasis. Many of the characteristics of this anti-inflammatory state are reported to be recapitulated by *in vitro* stimulation by the anti-inflammatory cytokine Il-4 (Cherry *et al.* 2014).

Microglia can be driven toward M2 phenotype *in vitro* by stimulating them with Th2 cytokines, such as Il-4, Il-13, Il-10 and Tgf-β. Th2 is T helper cell type 2 that control other cells by releasing Th2 cytokines (Mills *et al.* 2000). As described in section 1.4.3, some researchers refer to M2 subtypes (a, b, c and sometimes others). This Chapter will use the broader M2 label, widely-used in the literature. These M2 microglia are characterised by the expression of anti-inflammatory markers: Arg1, Ym1 and Fizz1.

Several studies have demonstrated that microglia do not permanently adopt one phenotype but can alternate between different phenotypes as the environment changes (Cherry *et al.* 2014; Franco & Fernández-Suárez 2015). However, in many neurodegenerative diseases, the continued production of pro-inflammatory cytokines is reported, and it is hypothesised that this may form some part of the neurodegenerative process. The roles of M2 phenotype microglia in neurodegenerative diseases such as PD are not fully understood (Tang & Le 2015).

6.1.2 Il-4 induced responses

Il-4 is a multifunctional cytokine secreted mainly by Th 2 cells, mast cells, eosinophils and basophils (Gadani *et al.* 2012). Microglia can secrete Il-4 themselves, following M2 activation (Liu *et al.* 2017). Il-4 is well-known to control different immune responses, such as T-cell differentiation, and it is considered as an effective stimulus for the M2 phenotype in both microglia and macrophages (Fumagalli *et al.* 2015). Studies suggested that Il-4 has essential roles in brain function in both physiological and pathological conditions. For instance, T-cell derived Il-4 is critical in learning and memory in the healthy brain (Derecki *et al.* 2010). The brain level of Il-4 decreases with age, and it has been speculated that this may be associated with impaired memory function in aged populations, and the increased risk for development of neurodegenerative diseases such as AD (Nolan *et al.* 2005).

Il-4 interacts with Il-4R on microglia in the presence of JAK1/3 leading to phosphorylation of the transcription factor STAT6 (Gordon 2003). STAT6 phosphorylation promotes nuclear translocation and anti-inflammatory gene transcription such as Arg1, Fizz1, Ym1 and Il-10 (McCormick & Heller 2015a) (Figure 6-1).

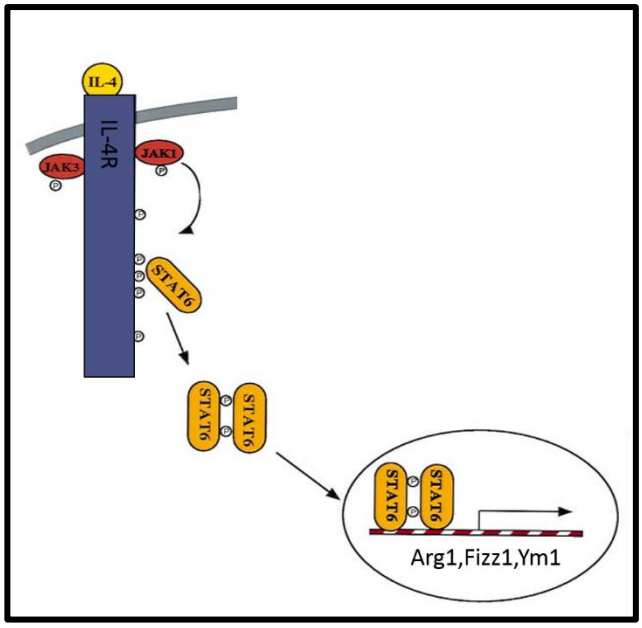

Figure 6-1: Il-4 pathway in microglia. Il-4 induced phosphorylation of JAK1/3, which in turn phosphorylates Il-4R and STAT6. This allows STAT6 to enter the nucleus and binds to a specific DNA sequences in IL-4–responsive genes. Adapted from Jiang *et al.* (2000)

Arg1 is an M2 macrophages/microglia marker that contributes to arginine metabolism (Morris 2004). On the one hand, arginine is catalysed by iNos to produce citrulline and NO. On the other, M2 microglia deprive iNos of its substrate through Arg1 activity, which metabolises arginine into urea and ornithine. NO production is controlled by the balance between expression of iNos and Arg1. This activity is upregulated with M1 activation. The enzymatic products in the Arg1 pathway such as hydroxyproline, proline and polyamine contribute to tissue repair (Busch & Silver 2007), collagen synthesis, cell proliferation and differentiation (Thomas & Thomas 2001), and help to protect neurons from injury caused by pro-inflammatory cytokines and NO (Williams 1997). In summary, the Arg1 pathway is important in maintaining a low level of NO, as well as promoting repair-related activities, which contributes to neuroprotection (Tang *et al.* 2014).

Fizz1 (also known as Relm-α) is an M2 marker that has an essential role in the control of collagen expression (Nair *et al.* 2009). Which suggest that Fizz1 plays a role in

the tissue repair since collagen remodelling or production are useful in repair following injury. Fizz1 is upregulated in infected and inflammatory locations (Holcomb *et al.* 2000) and contributes to insulin resistance (Munitz *et al.* 2009).

Ym1 (also known as Chi3l3) is an M2 marker induced by Il-4 or Il-13 stimulation by a STAT6-dependent mechanism (Welch *et al.* 2002). It dampens the inflammatory response and promotes tissue repair and healing response (Recklies *et al.* 2002). Furthermore, Ym1 positive microglia are always associated with increases in the phagocytic ability of microglia as in AD disease (Tang & Le 2015).

Il-10 is an anti-inflammatory cytokine produced by M2 microglia/ macrophages to inhibit pro-inflammatory cytokine synthesis (Tang & Le 2015). It has also been found to be released by M1 microglia, although only 24-36 h after the M1-stimulus (Chhor *et al.* 2013), an event also described here (Chapter Five). Furthermore, Il-10 has an essential role in the regulation of Il-6 in the brain through a negative feedback mechanism as discussed in section 3.3.2 (Orihuela *et al.* 2016). These markers are reported always to rise *in vitro* in response to Il-4. It would be useful, given that, to discuss how they change *in vivo* under different circumstances – in a way this is validation of the *in vitro* M2 state, rather than validation of these markers.

Beside Il-4, three major anti-inflammatory cytokines Il-13, Il-10 and Tgf-β stimulate microglia to adopt the M2 phenotype, and lead to a decreased pro-inflammatory responses (Zhou *et al.* 2012). Similar to Il-4, Il-13 can suppress the production of pro-inflammatory cytokines such as Il-1β, Il-6 and Tnf-α, and reduce NO release, which leads to protection against LPS induction of neuronal injury both *in vitro* and *in vivo* (Ledeboer *et al.* 2000; Zhao *et al.* 2006). Although these stimuli could drive microglia to M2 activation state, their pathways are different from that of Il-4 (Figure 6-2).

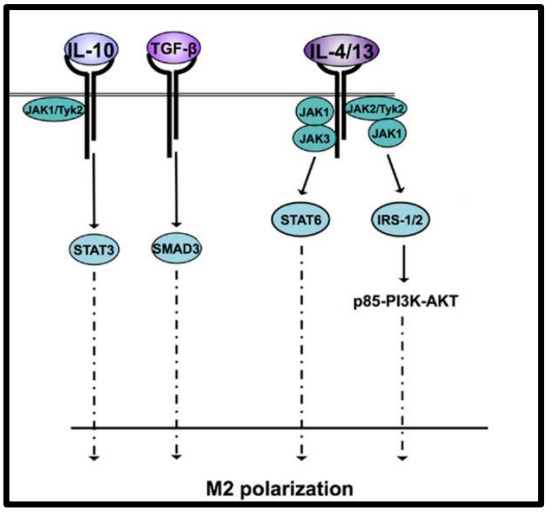

Figure 6-2: Different M2 stimuli induce M2 microglia phenotype through different pathways. IRS, insulin receptor substrate; JAK, Janus kinase; STAT, signal transducers and activators of transcription; TGF-β, transforming growth factor-β. Adapted from McCormick & Heller (2015b).

Tgf-β in general has an essential role in angiogenesis and ECM deposition, and contributes to suppressing pro-inflammatory microglial responses, all of which can be neuroprotective (Boche *et al.* 2003; Boche *et al.* 2006). Tgf-β enhances Il-4 stimulation of M2 microglia by increasing the expression of Arg1 and Ym1, suggesting that Tgf-β and Il-4 signals could be used together to increase the protective behaviours of this phenotype (Zhou *et al.* 2012). However, most published articles simply use Il-4 alone.

6.1.3 The importance of studying M2 microglia

After characterising M1 microglia in Chapter Five, the obvious next step was to validate *in vitro* culture model for the M2 phenotype. A thorough understanding of M1 and M2 activation will provide data (e.g., maximum gene expression responses) for comparison with microglia responses to different disease states or treatments. For example, these data could be compared with microglial responses to Aβ or a-synuclein aggregates, or to drugs. This would help researchers to understand how to control phenotype switching.

Several *in vivo* studies have been performed to understand the therapeutic value of driving microglia towards an M2 phenotype. An AD mouse model, which was injected with Il-4/Il-13, showed an upregulation of Arg1 and Ym1 positive (M2) microglia, with a reduction in Aβ plaque load and improved cognition (Kawahara *et al.* 2012). In an autoimmune encephalitis model, intraperitoneal injection of engineered adult neural stem cells expressing Il-10 resulted in reduced CNS inflammation and demyelination, with an increase in remyelination (Yang *et al.* 2009). In a third *in vivo* study, an adeno-associated virus (AAV) vector expressing the mouse Il-4 gene was injected into a 3-month-old AD mouse model. Five months later the result showed a reduction in Aβ plaques, improvement in the memory, and increase in neurogenesis (Kiyota *et al.* 2010). Despite the fact that inducing M2 polarisation to treat CNS injuries is a promising strategy, to the best of my knowledge, no studies have been carried out to fully investigate microglial responses across a range of doses and time points. In particular, Il-4 is widely-employed as an M2-promoter, but its influence on gene/protein expression in microglia has not been fully characterised.

By developing a better characterised model of M2 activation, we hope to have a model which can be used to study subtle changes in the sensitivity of the microglia to anti-inflammatory activation. So, for example, does prolonged treatment with high levels of insulin enhance the response to Il-4, or does the uptake of magnetic nanoparticles decrease the ability of these cells to respond to Il-4?

6.2 Aim and objectives

6.2.1 Aim

The aim of this Chapter is to characterise phenotypic responses to the well-known microglial anti-inflammatory activator Il-4, at a wide range of concentrations. Since microglial reactions across such a wide range of concentrations have not been reported. These data would allow the calculation of the EC50 for Il-4 – a finding of importance for scientists, and potentially of utility for therapeutic immunomodulation of human microglia.

6.2.2 Objectives

The objectives are:

- To identify M2 gene markers that respond to Il-4.
- To generate qPCR dose-response data for Il-4-treated microglia.

6.3 Experimental procedures

6.3.1 Reagents and equipment

All reagents and equipment used were described previously in Chapter Two. Il-4, Il-13 and Tgf-β were from PeproTech (USA). Two types of media were from ThermoFisher Scientific (Loughborough, UK; macrophages-SFM) and Lonza (Cambridge, UK; Xvivo).

6.3.2 Preparation and treatment of microglial cultures

Mixed glial culture preparation and pure microglia culture isolation were as described previously in Chapter Two. Microglia cultures were incubated in D10 media for 24 h at 37 °C in 5 % CO_2, 95 % humidified air, before being treated experimentally.

6.3.2.1 Dose response effect of Il-4

Cells were treated with Il-4 (0, 0.001, 0.01, 0.03, 0.1, 0.3, 1, 3, 10 and 100 ng/ml) for 24 h, and then mRNA was extracted for gene expression analysis as described in Chapter Two.

6.3.2.2 Effect of combined M2 stimuli combinations

Cells were treated with Il-4 (10 ng/ml), Il-13 (10 ng/ml), Tgf-β (1 ng/ml), Il-4/Il-13 or Il-4/Tgf-β for 24 h, then mRNA was extracted for gene expression as described in Chapter Two.

6.3.2.3 Effect of different serum concentrations and M2 stimuli combination

Microglia cultures were incubated in D10 media for 6 h, then media has been changed to normal 10 % FBS DMEM or (0 % FBS DMEM or HI 10 % FBS DMEM) and

further incubation at 37 °C in 5 % CO_2, 95 % humidified air for 24 h, then cells were treated with Il-4 (10 ng/ml), Il-13 (10 ng/ml), Tgf-β (1 ng/ml), Il-4/Il-13 or Il-4/Tgf-β for 24 h, later RNA was extracted for evaluation of gene expression as described in Chapter Two.

6.3.2.4 Effect of serum-free media on Il-4 treated microglia

Mixed glial culture preparation and pure microglia culture isolation were described previously in Chapter Two. Microglia cultures were incubated in D10 media for 6 h, then media was changed to serum-free media (Xvivo and SFM) and further incubated at 37 °C in 5 % CO_2, 95 % humidified air for 24 h, then cells were treated with Il-4 (10 ng/ml) for 24 h, then RNA was extracted for gene expression as described in Chapter Two.

6.4 Results

6.4.1 The effect of different time point of Il-4 on microglia gene expression

A pilot study has been performed with a serial concentration of Il-4 at three time points (2, 6, and 24 h) (Figure 6-3). Since none of these three-time points had shown a sign of M2 phenotype, the 24 h time point was chosen because it has been suggested by many researchers (Zhou *et al.* 2012; Chen *et al.* 2015).

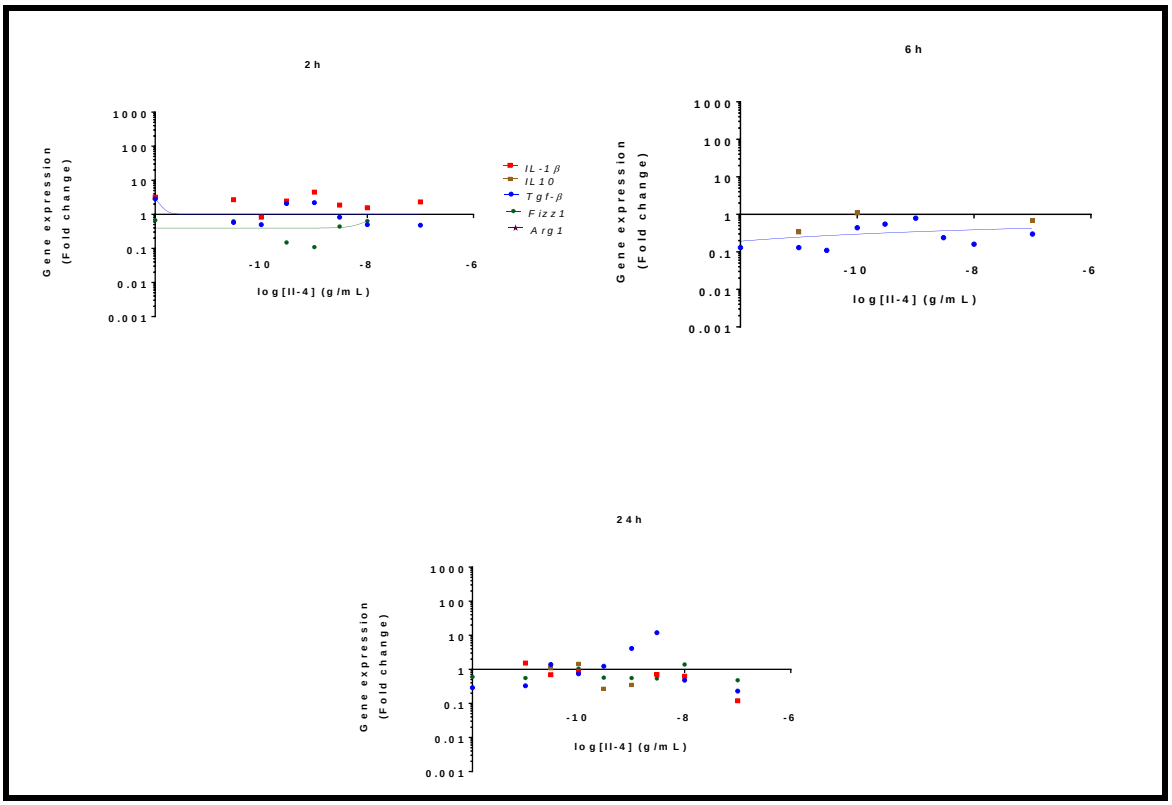

Figure 6-3: Effects of different time points of Il-4 on GOI gene expression. Y-axis represents log fold change versus average of reference genes (1 = no change) and X-axis represents Log Il-4 concentration in (g/ml). All data are of one experiment.

6.4.2 The effect of Il-4 on pro- and anti-inflammatory gene expression

qPCR was performed using the three reference genes, which were validated in section 3.3.3.2. No dose-dependent effects of Il-4 were detected either on the pro- or anti-inflammatory gene expression (Figure 6-4 and 6-5).

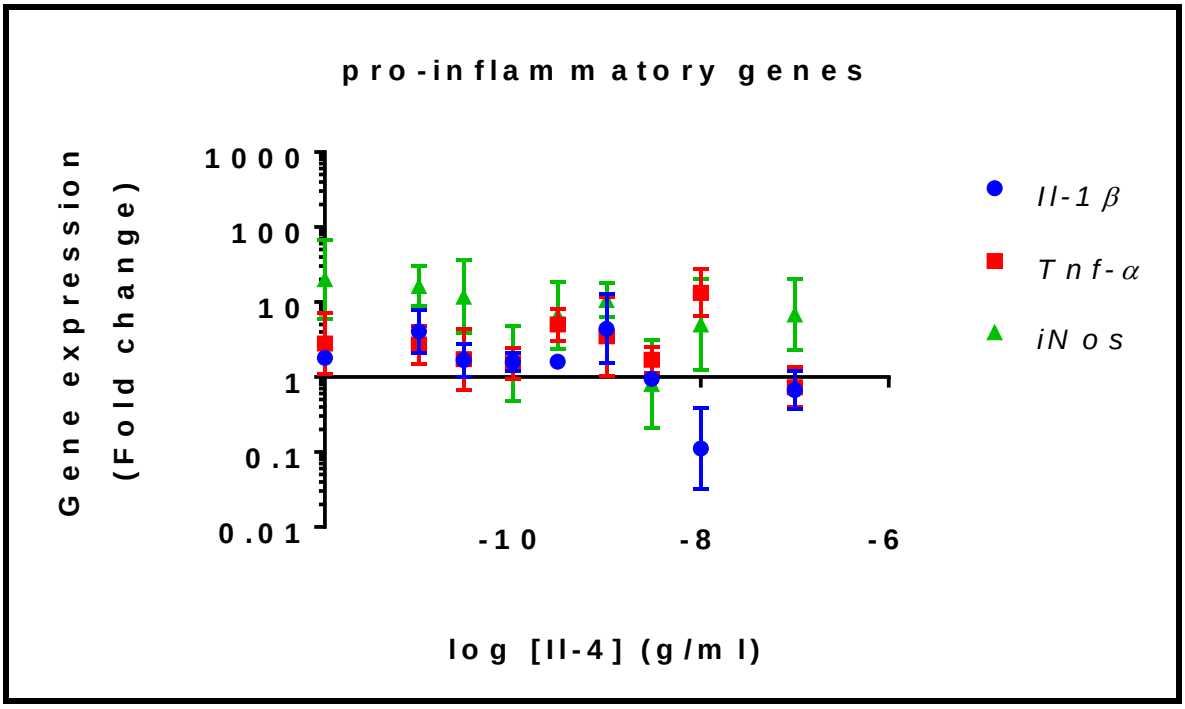

Figure 6-4: Il-4 effects on pro-inflammatory (*Il-1β, Tnf-α* and *iNos*) gene expression at 24 h. Y-axis represents log fold change versus average of reference genes (1 = no change) and X-axis represents log Il-4 concentration (g/ml). Dose response curves could not be fitted for any of the genes. All data are presented as the mean ± S. E. M. of three independent experiments.

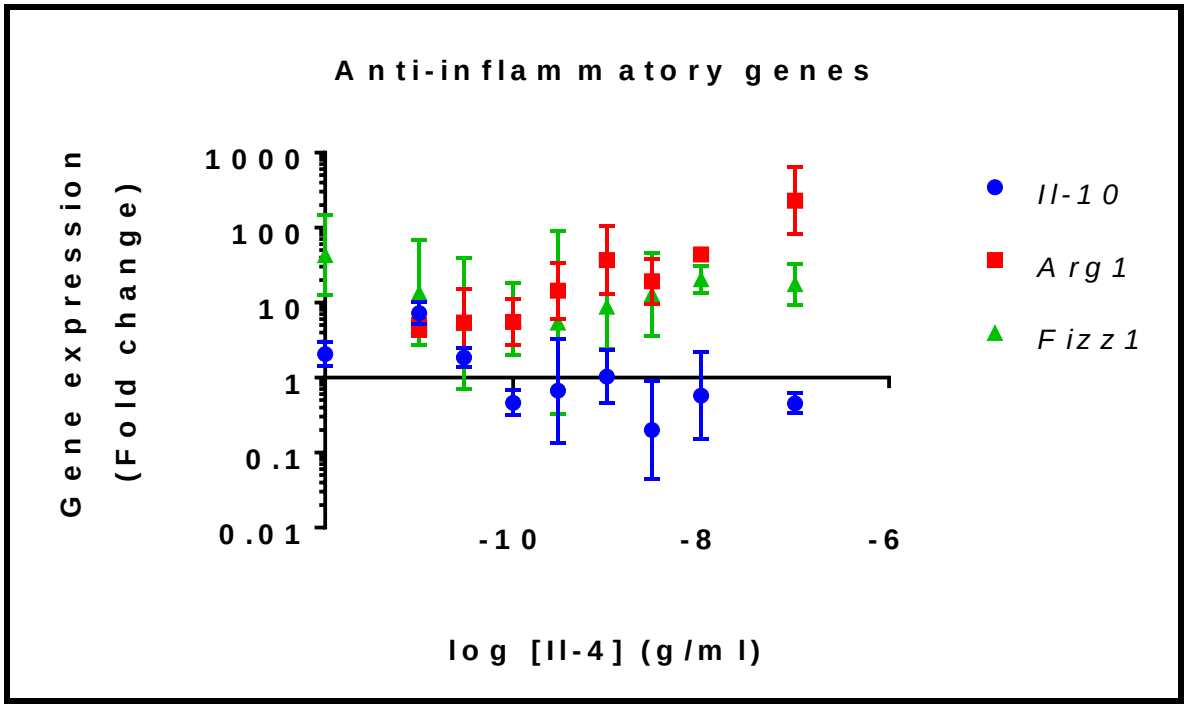

Figure 6-5: Il-4 effects on anti-inflammatory (*Il-10*, *Arg1* and *Fizz1*) gene expression at 24 h. Y-axis represents log fold change versus average of reference genes (1 = no change) and X-axis represents log Il-4 concentration. Dose response curves could not be fitted for any of the genes. All data are presented as the mean ± S. E. M. of three independent experiments.

6.4.3 The effect of Il-4 on *Il-4R* gene expression

No significant change in *Il-4R* gene expression with any of Il-4 concentration was detected (Figure 6-6).

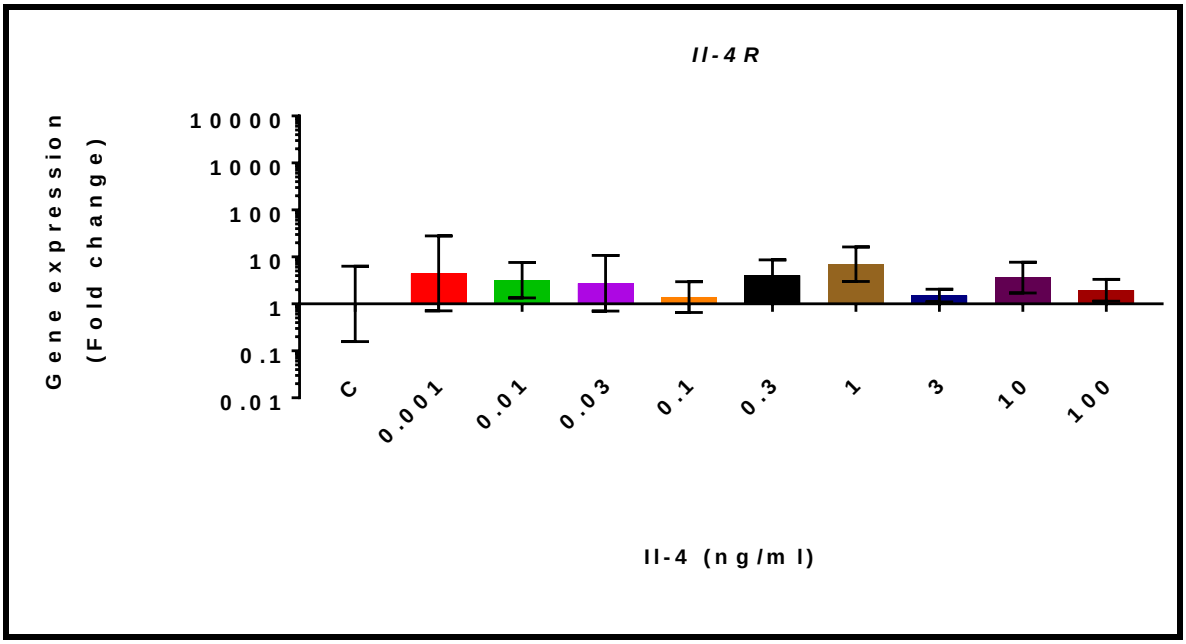

Figure 6-6: Il-4 effects on *Il-4R* gene expression at 24 h. Y-axis represents log fold change versus average of reference genes (1 = no change) and X-axis represents Il-4 concentration in (ng/ml). No significant difference was found; One-way ANOVA with Dunnett's post-hoc test versus C (control). All data are presented as the mean ± S. E. M. of three independent experiments.

6.4.4 The effect of different combinations of M2 stimuli on pro- and anti-inflammatory gene expression

Given that the previous experiments did not produce the expected responses from microglial cells, alternative methods to induce M2 activation were explored, including combinations of cytokines. There was a significant *Il-1β* downregulation with Il-4/Tgf-β stimuli (1/50th of control) (Figure 6-7A). There was no significant change in *Cd200R* expression (Figure 6-7 B).

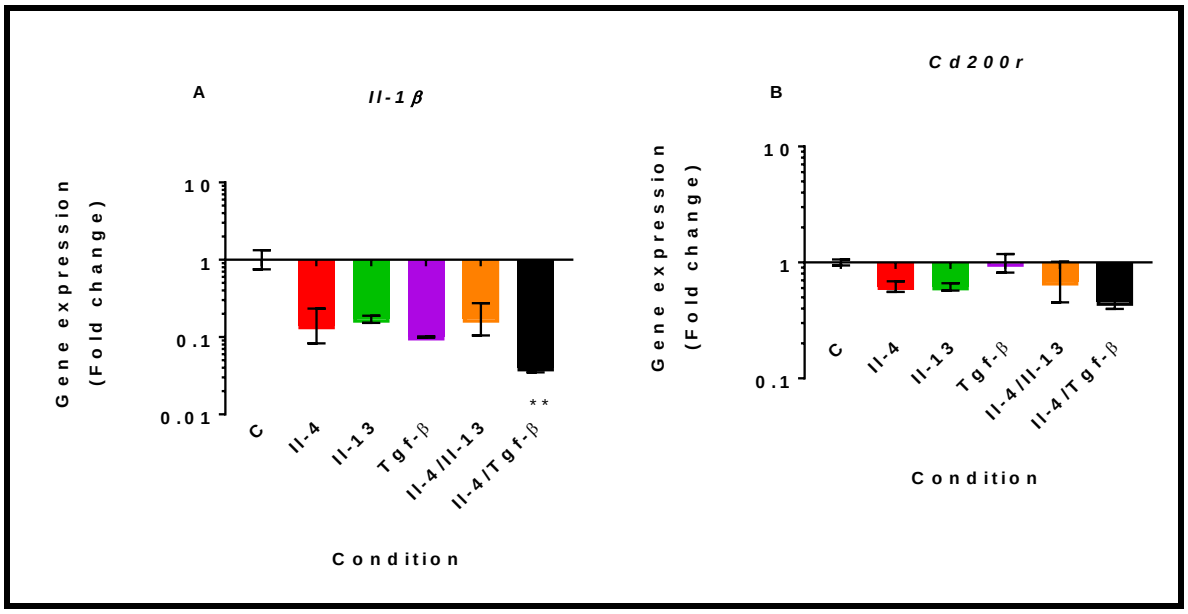

Figure 6-7: M2 stimuli effects on *Il-1β* and *Cd200r* gene expression at 24 h. (A) *Il-1β*, a significant difference between Il-4/Tgf-β treated microglia and control was found. (B) *Cd200r*, a significant decrease in Il-4/Tgf-β treated microglia versus control was found. Y-axis represents log fold change versus average of reference genes (1 = no change) and X-axis represents different M2 stimuli. **p < 0.01; One-way ANOVA with Dunnett's post-hoc test versus C (Control) for *Cd200r*; Kruskal-wallis with Dunn's post-hoc test versus control (C) for *Il-1β*. All data are presented as the mean ± S. E. M. of three independent experiments.

There is a significant increase in *Ym1* gene expression when treat microglia with Il-4/Il-13 (~ 7-fold from control) (Figure 6-8B). Although, all the other treatment shows gene expression over 1, none of the other treatments show a significant increase in any of the other M2 markers (Figure 6-8 A and C).

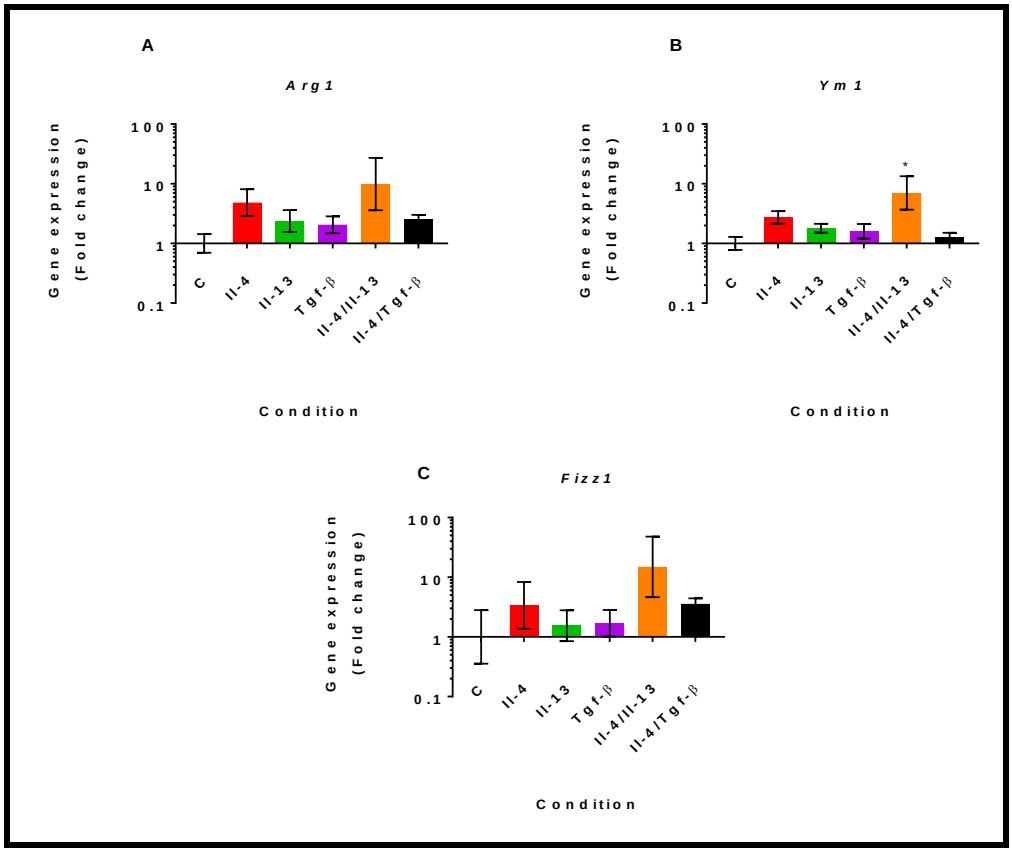

Figure 6-8: M2 stimuli effects on M2 markers gene expression at 24 h. (A) Arg1. (B) Ym1, a significant increase in Il-4/Il-13 treated microglia versus control was found. (C) Fizz1. Y-axis represents log fold change versus average of reference genes (1 = no change) and X-axis represents different M2 stimuli. *p < 0.05; One-way ANOVA with Dunnett's post-hoc test versus control (C) for Fizz1; Kruskal-Wallis with Dunn's post-hoc test versus C (control) for Arg1 and Ym1. All data are presented as the mean ± S. E. M. of three independent experiments.

6.4.5 The effect of different serum concentrations and M2 stimuli on gene expression

Due to the lack of robust changes in M2 markers, several experimental features were identified which could be masking or confounding the effects of pro-M2 stimuli. For example, molecules in serum may be binding/altering Il-4 and other M2 stimuli, reducing their effect on the cells. A pilot study was performed, using media without serum or with heat-inactivated serum (a process which is reported to denature immune-related proteins (Jungkind *et al.* 1986)), in combination with different M2 stimuli. Difference in serum conditions show no effect on microglial phenotypic markers (Figure 6-9).

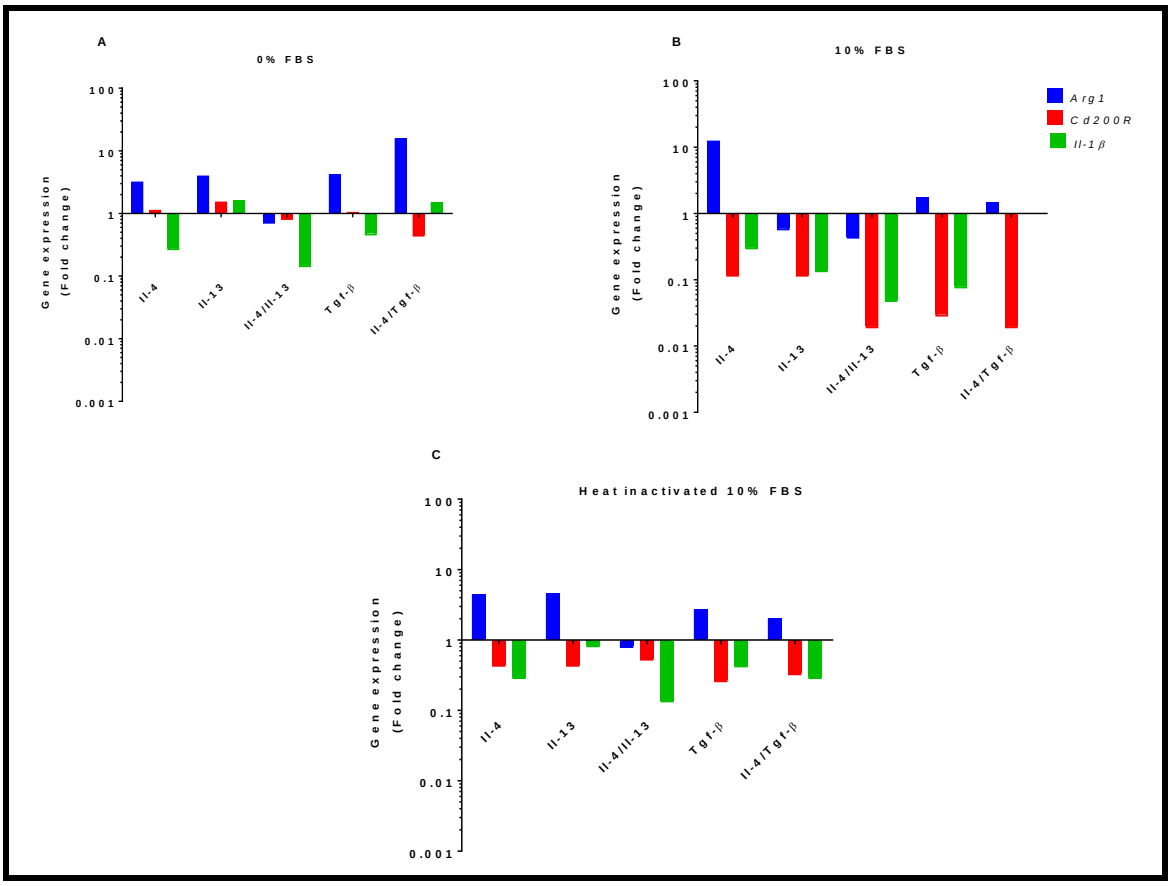

Figure 6-9: Serum conditions and M2 stimuli have no detected effect on gene expression. (A) 0 % FBS, (B) 10 % FBS and (C) 10 % HI FBS. Y-axis represents log fold change versus average of reference genes (1 = no change) and X-axis represents different M2 stimuli. All data presented are for pilot study (n = 1).

6.4.6 The effect of serum-free media on microglia stimulated by Il-4

There is no significant difference between D10 and the two serum-free media (Figure 6-10).

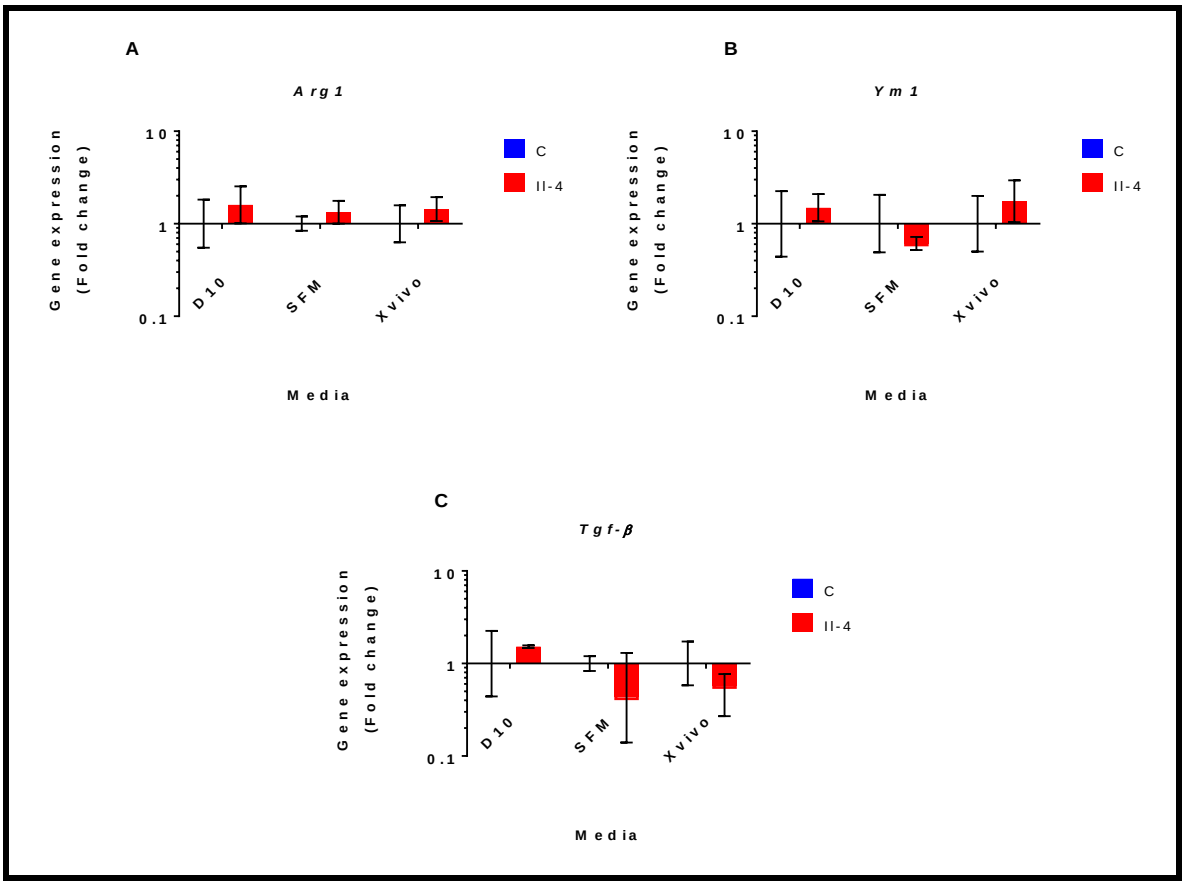

Figure 6-10: Effect of different media on M2 markers (*Arg1*, *Ym1* and *Tgf-β*) gene expression, after 24 h of Il-4 treatment. (A) *Arg1*, (B) *Ym1*, (C) *Tgf-β*. Y-axis represents log fold change versus average of reference genes (1 = no change) and X-axis represents different media. No significant differences were detected; one-way ANOVA with Dunnett's post-hoc test versus D10 without Il-4. Also, unpaired t-tests for Il-4 versus control, within each medium. All data are presented as the mean ± S. E. M. of three independent experiments.

6.5 Discussion

The main aim of this study was to generate a parallel data to Chapter Five (LPS and M1), but for M2 activation. Therefore, Il-4 was chosen as the stimulus, due to it being widely-used to drive both microglia and macrophage toward M2 phenotype. However, the data generated were not consistent with the gene expression changes that would be expected for M2 activation. Few significant changes in gene expression were detected. This was surprising, and a problem with the experimental setup was suspected. Various alterations were explored, but without success in resolving the issues.

6.5.1 Il-4 to drive microglia toward M2

Il-4 is well-known to induce microglia M2 polarisation *in vitro* and *in vivo* (Fenn *et al.* 2012; Chhor *et al.* 2013). Previous reports suggested that the main markers for M2 microglia are Arg1, Il-10 and Fizz1 (Chhor *et al.* 2013). Expression of these markers is consistent with a repair/reparatory phenotype, as Arg1 catalytic activity produces polyamines that support extracellular matrix repair and mitochondrial functions (Pesce *et al.* 2009). Within this model system, it was unexpected that many of M2 markers were not Il-4 responsive, at least at the concentrations and time points examined here. This suggests that we failed to drive microglia toward M2 phenotype.

The hypothesis was that if Il-4 led to anti-inflammatory microglia phenotype, then the amount of anti-inflammatory markers produced by treated microglia will be higher than that of non-treated (control) microglia. To test this hypothesis, a pilot study was performed with a serial concentration of Il-4 at 3-time points (Figure 6-3). Since none of these three-time points have shown a sign of an M2 phenotype, the 24 h time point was chosen because it has been suggested by many researchers (Zhou *et al.* 2012; Chen *et al.* 2015). Zhou *et al.* (2012) reported 25 fold change in mRNA expression on both *Ym1* and *Arg1*, when they

treated primary microglia culture with 10 ng/ml Il-4 for 24 h. While, Chen *et al.* (2015) reported even higher mRNA fold change with treated BV-2 cell line with 10 ng/ml Il-4 for 24 h. Furthermore, other researcher have reported an early detection of M2 marker even at 4, 6 and 12 h (Michelucci *et al.* 2009; Chhor *et al.* 2013). Which suggests that the lack of impact on M2 markers in this experiment is not due my choice of time point. It may be of interest to test other time points since Zhao *et al.* (2012) reported a late response at 48 h. Similarly, Chhor *et al.* (2013) reported M2 microglia at 36 h and 72 h (Table 6-1). In this study a range of concentrations were used from 0.001 to 100 ng/ml. All reported studies showed M2 activation by Il-4 concentrations within this range, and so it is unlikely that the lack of response in this study is due to the choice of Il-4 concentration.

Sawada *et al.* (1993) study found that mouse microglia expressed a basal level of *Il-4R*. Another study also reported that rat microglia expressed Il-4R, however, Zhao *et al.* (2006b) study suggested that treating primary microglia culture with 10 ng/ml Il-4 for 2 h did not induce an increase *Il-4R* gene expression. Although the results generated here were in line with Zhao *et al.* (2006b) report, we cannot be confident that *Il-4R* is unaffected by Il-4, especially with the lack of change detected in other M2 marker which make these data unreliable.

6.5.2 Why did we try different combinations?

As Il-4 did not produce the expected changes in expression for all M2 markers, other pro-M2 stimuli were tested, including Il-13 and Tgf-β. In this study, we tried to mimic Zhou *et al.* (2012) work in BV-2 cell line in order to drive microglia toward M2 phenotype. Zhou *et al.* (2012) suggested that Tgf-β treatment alone is not able to induce M2 microglia but treated together with Il-4, strongly enhances Il-4 induced M2 phenotype. *Arg1* and *Ym1*

expressions are significantly increased after co-treatment with Il-4 and Tgf-β. Unexpectedly, this observation was not seen in the primary microglia culture in term of M2 marker.

Furthermore, *Il-1β* showed a significant down regulation in the gene expression in the combination of Il-4/Tgf-β, which might be due to type II statistical error (failing to reject a false null hypothesis), and that could be investigated by increasing the sample size. Increasing the sample size usually leads to an increased probability of detection of a genuine difference, and rejection of false positives.

6.5.3 Why did we study the effect of serum?

Given the lack of obvious changes in M2 markers, it was hypothesised that the presence of serum might be confounding. Serum may contain pro-inflammatory stimuli, producing antagonistic pro-M1 microglial stimulation or Il-4 (or other pro-M2) stimuli may be present in serum. Therefore, we have tested medium without serum and with 10% heat inactivated serum, as well as the standard 10% FBS. This induced no significant changes, although there is a hint of increased M1 gene expression in the presence of serum. This suggests that the hypothesis that serum increases M1 gene expression, (which can be switched off by Il-4) and suppresses M2 gene expression. Therefore, further work has been done using the two serum-free media that have been tested in Chapter four, different serum-free formula SFM and Xvivo have been tested in comparison to normal D10 media; again, Il-4 induces no change in M2 marker gene expression.

Table 6-1: Comparison of M2 microglia gene expressions in various time points and concentrations from differant references.

Cells	**Primary mouse microglia culture**			**BV-2**	**Primary mouse microglia culture**	**Primary rat microglia culture**	**Primary mouse microglia culture**	
References	(Chhor *et al.* 2013)	(Michelucci *et al.* 2009)	(Chhor *et al.* 2013)	(Chen *et al.* 2015)	(Zhou *et al.* 2012)	(Zhao *et al.* 2006)	(Chhor *et al.* 2013)	
Dose/ time point	4 h	6 h	12 h	24 h		48 h	36 h	72 h
1 ng/ml		↓Il-1β, Ccr2, Tnf-α and ↑Arg1, Mmr, Ym (1/2), Fizz1						
10 ng/ml				↑Arg1, Fizz1, Ym1	↑Arg1, Ym1	↑Igf-1		
20 ng/ml	↑Cd206, Arg1, Il-12, Ifnγ, Il-13,		↑Cd32, Cd206, Arg1, Igf1, Gal-3, Il-12, Il-2, Ifnγ, Il-13 and ↓Cxcr1				↑ Il-12, Il-2, Ifnγ, Ccl2, Il-13 and ↓Cxcr1, Tgf-β, Cd32	↑Gal-3, Ccr2, Il-12, Il-2, Ifnγ, Ccl2, Il-13

6.6 Summary

Researchers assumed that microglia follow the same phenotypes M1 and M2 characteristic of macrophages. Microglial polarisation has not been fully established by research findings. Instead, the peripheral macrophages schema has been adopted in an attempt to simplify data interpretation.

In vitro microglial culture systems suitable for assessing M2 phenotype would be of value to understand the protective effect of microglia in neurodegenerative diseases and developing novel immunotherapies. In this Chapter, several suggested stimuli, namely; Il-4, Il-13 and Tgf-β failed to reliably alter gene expression for widely-used M2 markers, even after multiple changes were made to protocols, such as different time points, different concentrations, different combinations of stimuli and different media. Although it does not match the findings of many literatures, we have not got any clear understanding of the reasons behind that.

However, there is a potential value to be derived from a dataset covering gene expression changes over time and for a wide range of M2-stimulus concentrations. Future research should attempt to derive these data from an established culture system that reliably generates M2 microglia.

Chapter 7 : Microglial responses to different nanoparticle formulations, including ‘stealth’ coat

7.1 Introduction

Previous Chapters (five and six) have discussed characterising microglial phenotypes and understanding phenotypic switching. This was in the context of understanding microglial behaviour in disease states, and with the possibility of one day manipulating these phenotypes as a therapy. It should be recognised that drug delivery to the brain (and so to microglia) is often difficult to achieve, largely because of the BBB, which prevents many molecules from entering the CNS. Numerous methods are being explored to increase delivery to the brain, including physical disruption of the BBB (ideally temporarily and safely (Bellavance *et al.* 2008)), using viruses as vectors (Davidson & Breakefield 2003), and attaching various molecules to drugs to enhance crossing of the BBB (Gabathuler 2010).

Another alternative approach involves using nanoparticles (NPs) as non-viral drug delivery vectors. There are numerous reports of NPs formulations that can cross the BBB and enhance drug delivery to the CNS (Grabrucker *et al.* 2016; Saraiva *et al.* 2016; Belletti *et al.* 2018). Such techniques offer a better safety profile than the use of viruses or physical disruption of the BBB and allow relatively non-invasive systemic delivery (to the bloodstream), rather than direct, potentially dangerous, injection directly into the CNS.

Although there is an increasing body of evidence for NP formulations crossing the BBB, it cannot be assumed that this will result in efficacy of the treatment. Understanding the ultimate fate of the NPs and their cargo requires more detailed investigation of the interactions between neural cells and NPs. As the dominant immune cells in the CNS and given the evidence for greater NP uptake by microglia compared to other neural cell types, it is critical to assess how microglia respond to NPs. In particular, it will be valuable to

determine whether inflammatory responses to NPs are induced. Therefore, this Chapter addresses microglial interactions with NPs, in the context of possible future therapies.

7.1.1 Nanomedicines can cross blood brain barrier

Nanomedicine is defined as the application of nanobiotechnologies to medicine, which is making or using devices and materials with at least one dimension less than 1000 nanometres (Jain 2008). Nanomedicine represents a highly promising opportunity for the development of targeted drug delivery systems, non-invasive imaging, tissue regeneration methods, and with faster diagnostic treatments for various neurodegenerative disorders (Chen *et al.* 2016; Lee *et al.* 2016; Posadas *et al.* 2016; Poovaiah *et al.* 2018). The importance of NPs in particular are attributed to their ability to diffuse through biological membranes and interact closely with biomolecules to be functionalised in a wide variety of ways, e.g., drugs inside or attached to the surface, non-invasive tracking capabilities and remote manipulation, for example using magnetic fields (Tartaj *et al.* 2003).

NPs have arisen as a revolutionary solution for drug delivery to the CNS, due to the ability to tailor their physicochemical (such as size, shape and charge) properties to overcome the selective nature of the BBB, following minimally-invasive delivery into the peripheral bloodstream. Advances in this field could enable the diagnosis and treatment of many CNS diseases (Begley 2004). Therefore, NPs have become a highly suitable option for increasing drug delivery into the brain because their ability to cross the BBB (Nair *et al.* 2018). In the CNS, NPs can also be used as diagnostic tools, mainly in terms of contrast enhanced magnetic resonance imaging (MRI) of CNS malignancies (Weinstein *et al.* 2010). This may be particularly useful in tumour detection, delineation and maybe even treatment, as microglia (and invading macrophages) surround tumours and are prone to taking up NPs. Therefore, these NPs accumulations have been shown to reveal location and size of tumours.

Furthermore, the use of magnetic NPs is being investigated for hyperthermic ablation, where external magnetic fields are used to manipulate MNPs, delivering heat, thus thermally damaging tumour cells, which are less resistant to this effect. NPs could be targeted directly to the tumour cells, or this effect could be achieved through the neighbouring immune cells, including microglia (Zhu *et al.* 2016). NPs can also be designed to release their cargo in specific conditions, and so in specific locations, when given external signals. This can include magnetic stimulation. Research into these 'smart' NPs could provide valuable tools for CNS therapies.

Thus, NPs could play important roles in the diagnosis and treatment of neurodegenerative disorders. However, despite the wealth researches on crossing the BBB, little attention has been paid to the fate of these NPs once inside the brain. This is critical to design therapies, as drug delivery NPs may be intended to release their cargo extracellularly, for example to act on cell-surface receptors, or it may be intended for the NPs to be internalised by cells. In the latter case, it may be important to control which specific cell types take up the NPs. For example, in order to alter microglial phenotype, it is likely that the activation of cell surface receptors (e.g., Il-4R and Il-10R (Fenn *et al.* 2012; Orihuela *et al.* 2016)) will be required. This relies on requiring extracellular drug release, and so NPs will be more effective if there is limited cellular uptake. Whatever the intended outcome, it will be important to understand how microglia respond to NPs, as these cells are the most phagocytic in the brain parenchyma, and can be expected to clear foreign materials, including NPs (Ransohoff & Perry 2009; Lull & Block 2010).

7.1.2 Handling of nanoparticles by neural cells

The different neural cells types play different roles in the CNS (Table 7-1). Therefore, it is important to understand how all neural cell types handle different NPs, in

order to predict drug delivery. Microglia exhibit all forms of endocytosis: micropinocytosis, macropinocytosis and phagocytosis. Other neural cells types, including astroglia and oligodendroglia, have endocytotic activity (Noske *et al.* 1982; Triarhou *et al.* 1985; Tansey & Cammer 1998), although their endocytotic capacity is less than that of microglia. This has been observed when NPs uptake was studied in different neural cell types. *In vitro* studies found that microglial uptake of NPs were greater than in other CNS cells (Fleige *et al.* 2001; Pinkernelle *et al.* 2012; Jenkins *et al.* 2016). Fleige *et al.* (2001) experiment was one of the first studies that directly compared NP uptake by different neural cells, showing that NPs uptake by microglia is the highest compared to astrocytes and glioma cells. In Pinkernelle *et al.* (2012) study, an incubation of dissociated cerebellar cultures (multiple neural cell types) with NPs, showed that microglial uptake of NPs is 2, 4 and 8 times higher than astroglia, OPCs and neurons respectively. In Jenkins *et al.* (2013) study, an incubation of different glia cell types with NPs, showed that extent of uptake of NPs by microglia is far greater than in astroglia, OPCs and oligodendrocytes. Similarly, in an *in vivo* study of glioblastoma multiforme patients, NPs uptake by macrophages (either microglia or macrophages from the bloodstream) is higher than that of glioblastoma cells, although human glioblastoma cells have high ability to take up the particles *in vitro*, in the absence of macrophages (van Landeghem *et al.* 2009).

Table 7-1: Different CNS cell types and their function.

Cell type	Cell function
Astrocytes	Nutrient support, neurotransmitter reuptake, neurovascular coupling, gliotransmitter production
Microglia	Immune cells in the brain
Neurons	Information processing, sensory input integration, behaviour modulation
Oligodendrocytes	Myelination, trophic support for neurons

As discussed, microglia take up NPs more rapidly and to a greater extent than other neural cell types, outcompeting them. The study of this process has been referred to as 'competitive nanoparticle uptake dynamics' (Jenkins 2013). NPs taken up by microglia may inhibit nanoparticle uptake by other neural cell types, since it reduces the amount of available NPs to be taken up by other cells (Jenkins *et al.* 2016). Additionally, it has been proposed that the uptake of NPs by inactivated microglia may trigger an immune response, possibly affecting other nearby cells (Pickard & Chari 2010). This unintended inflammatory response could counteract the goal to use NPs in CNS pathological conditions. Also, NPs taken up by microglia are more likely to be degraded, possibly with destruction of the drug payload, without the intended effect. Effective delivery of drugs is likely to require that NPs escape uptake by microglia, and instead remain in the interstitial fluid, releasing drugs extracellularly.

So, employing NPs to manipulate microglia may be a valuable therapeutic strategy, but NPs design will be important, as this will influence the fate of the NPs, and whatever they may be delivering.

7.1.3 Designing nanoparticles for use in the brain

Nanoparticles are colloidal particles with all dimensions less than 1000 nm. For drug delivery purposes, an active ingredient (a drug or biologically active material) is attached, dissolved within or encapsulated (Singh & Lillard 2009). There are different classes of NPs, with diverse properties/applications related to their shapes, size and composition (Medina *et al.* 2007). To target the brain, it has been suggested that NPs with size of around 20 nm are small enough to cross the BBB and at the same time large enough to escape renal excretion (Tsou *et al.* 2017). Furthermore, different NP compositions are available such as liposomes, emulsions, polymers, ceramic NPs, metallic NPs, gold shell NPs, carbon NPs and quantum dots (Medina *et al.* 2007).

With respect to their applications in the CNS, liposomes, polymeric NPs and metallic particles have received particular attention to overcome crossing the BBB (Zeiadeh *et al.* 2018).

- Liposomes are NPs comprised of lipid bilayer membranes surrounding an aqueous interior. The amphiphilic molecules used for the preparation of these compounds have similarities with biological membranes (Hofheinz *et al.* 2005).
- Polymers such as polysaccharide chitosan NPs have been used as drug delivery systems (Agnihotri *et al.* 2004). Water-soluble polymer hybrids are polymer-protein conjugates or polymer-drug conjugates (Lee 2006).
- Metallic particles such as iron oxide NPs (e.g., maghemite Fe_2O_3 and magnetite Fe_3O_4) (López-Quintela *et al.* 2003).

Of these various formats, MNPs have been studied in recent years for their multifunctional biomedical capabilities, such as remotely controlled drug delivery (Adamiano *et al.* 2018), hyperthermic ablation of tumour cells (Cherukuri *et al.* 2010) and

non-invasive tracking through MRI (Daldrup-Link *et al.* 2011). These NPs are not composed purely of Fe_3O_4, as this will aggregate easily because of their large surface energy (Wu *et al.* 2016). Furthermore, it is not easy to transport such hydrophilic particles across a biological membrane system. Therefore, MNPs are routinely coated with different materials, mainly polymers, to prevent agglomeration and facilitate uptake by cells. Furthermore, these coatings can enhance biocompatibility, and provide functionality (i.e. via functional groups that can enable attachment of specific structures, such as fluorescent labels, antibodies, drugs, nucleic acids, …, etc.). MNPs can be coated with natural or synthetic polymers, with some of the most widely used coatings being albumin, dextran, PEG and polyethylene oxide (PEO) (Sattarahmady *et al.* 2016; Karimzadeh *et al.* 2017; Nosrati *et al.* 2017; Shaterabadi *et al.* 2017).

The choice of coating can dramatically influence particle fate and can be chosen to achieve particular therapeutic goals. In the case of prolonged extracellular drug delivery to microglia, following minimally-invasive delivery into the bloodstream, particle design should aim to avoid/limit clearance by the mononuclear phagocytise system (MPS; formerly the reticuloendothelial system, RES), enhance crossing of the BBB, and then also avoid/limit clearance by the microglia. To achieve such goals, material chemists have exploited so-called 'stealth' coatings.

Some of the stealth coatings that have been proposed include poly carboxybetaine, poly sulfobetaine, poly acrylic acid and PEG, due to their ability to escape clearance by the MPS, in comparison to non-stealth NPs (Li & Huang 2010). Some PEGylated NPs have been shown to cross the BBB and been found in the brain (Calvo *et al.* 2001; Hyun R Kim *et al.* 2007; Ensign *et al.* 2012). In the Calvo *et al.* (2001) study, PEGylated NPs have been compared to alternatively-coated and non-coated NPs, showing that the concentration of the PEGylated NPs is higher in the brain than the other non-coated and coated NPs. Importantly,

this high penetration of PEGylated NPs into the brain was achieved without any effect on permeability of the BBB. This is encouraging for clinical applications, as a disrupted BBB would be a serious side-effect.

Hutter *et al.* (2010) reported that Au NPs produced a low-level activation of microglia, using N9 cells (microglia cell line) incubated with PEGylated or non-coated Au NPs. Non-coated NPs led to activated microglia assessed by increase in IL-1α using enzyme-linked immunosorbent assay (ELISA), but that PEGylation of Au NPs prevented this activation. Furthermore, this study showed that PEGylated surface Au NPs were not take up by microglia at a significant level (Hutter *et al.* 2010).

7.1.4 Several nanoparticles have been tested with microglia

There are only a few reports in the literature studying microglial interactions with MNPs, and these will be summarised here.

Pickard *et al.* (2011) examined microglial uptake of Sphero Nile Red fluorescent magnetic particles (diameter 200 – 390 nm). These particles were comprised of a polystyrene core (stained with the fluorophore Nile Red) surrounded by a layer of polystyrene and magnetite, over which carboxyl groups were attached (Jenkins 2013). Although Sphero particles are relatively large, compared to many other nanoparticles, particles with diameter up to 1000 nm diameter have been used to track cells post-transplantation into the CNS, without adversely affecting biological functions, such as myelination (Dunning *et al.* 2004). Sphero particles have been used in MRI and cellular labelling, indicating their utility for biological applications (Pickard *et al.* 2011; Jenkins *et al.* 2013). These Sphero particles only exhibited toxicity at the highest concentration tested, and were reliably internalised by microglia, which accumulated huge numbers of particles per cell (Jenkins *et al.* 2013).

Electron microscopy suggested degradation of iron oxide particles within microglia, possibly releasing the iron into the cells (Pickard *et al.* 2011; Jenkins *et al.* 2013).

MNPs accumulation in microglia may lead to microglial activation and toxicity, this subsequently impairs the neuroprotective properties including the defence against pathogens and the repair function of microglia in brain (Petters *et al.* 2016). Petters *et al.* (2016) study, demonstrated that high concentrations of MNPs can induce toxicity in microglia, but that lower concentrations do not. Lysosome tracking indicated that MNPs taken up by microglia were likely to be degraded, supporting the idea that drug delivery MNPs should be designed to evade microglial uptake, or, possibly designed to escape intracellular trafficking into lysosomes. If MNPs escape this fate, and end up in the cytoplasm, cargo could be delivered to act inside microglia.

Furthermore, MNPs might affect microglia morphology (Neubert *et al.* 2015). Neubert *et al.* (2015) study, showed that the change in microglia morphology from the ramified (as in non-treated culture) to more amoeboid morphology and microglia uptake of MNPs highly depends on NP types, concentration and exposure time, as the microglia uptake of superparamagnetic iron oxide nanoparticle increases with increasing incubation time (24 h versus 6 h) and increasing MNPs concentration (0.5 versus 1.5 versus 3 mM). Furthermore, this study suggested that microglia exposure to MNPs leads to a change of microglia morphology such as thickened and enlarged cell bodies. However, the change in microglia morphology depends on MNP type since microglia showed more ramification when exposure to iron oxide nanoparticle and ferucarbotran but not ferumoxytol NPs (Neubert *et al.* 2015). To support the idea that the immune-effect of the MNPs on microglia, should be fully studied.

A recent study directly compared microglial interactions with PEGylated stealth MNPs, and a 'control' MNP, without a stealth coating (termed CMX-MNP particles) (Jenkins *et al.* 2016). Carboxymethyl dextran (CMX) coated Fe_3O_4 MNPs (termed CMX-MNPs) were prepared through a two-step method (Liu *et al.* 2011). Coating surface of Fe_3O_4 MNPs with dextran can reduce the aggregation of MNPs and help to form a stable colloid suspension in water. Dextran, a bacterially derived homopolysaccharide of glucose, is known for its biocompatibility, biodegradability, wide availability and ease of modification (Hermanson 2016). Carboxymethyl was chosen to modify dextran due to their well understood and stable pH-dependent hydrolysis rates (Park *et al.* 2011). CMX has been used in a range of biomedical applications because of its excellent aqueous solubility, biocompatibility and nonfouling properties (Hiemstra *et al.* 2007; Bachelder *et al.* 2008). Therefore, CMX represents a suitable coating for medical grade NPs.

PEG is a biocompatible, nontoxic and water-soluble polymer of much use in biomaterials, biotechnology and medicine (Harris 1997). Attaching PEG can increase solubility and limit immune clearance, so prolonging bioavailability times (Zhang *et al.* 2008; Wahajuddin & Arora 2012; Lehner *et al.* 2013). Two PEG-protein drugs, Adagen® and Oncaspar®, have been approved by the FDA (Zalipsky & Harris 1997). In fact, several PEGylated MNPs have been studied as depot devices for drug delivery, and they have been prepared in several fundamentally different ways (Zhao & Harris 1994; Brian *et al.* 2003). Researches about coating MNPs with a hydrophilic polymer such as PEG decreased particle recognition by macrophages cells and increased intracellular uptake by specific cancer cells, suggesting utility for cancer therapy and diagnosis (Zhang *et al.* 2002; Gupta & Curtis 2004; Gupta & Wells 2004). It has been widely used in drug/gene delivery, because of their 'stealth' coating, that could reduce immune clearance and increase circulatory times (Zhang *et al.* 2008; Wahajuddin & Arora 2012; Lehner *et al.* 2013).

From Jenkins *et al.* (2016) study, a reduction in the extent of stealth PEG-MNP uptake compared to CMX-MNPs has been reported, for multiple neural cell types. The idea that stealth MNPs are predicted to be 'invisible' to microglia, evading specific uptake, was investigated. PEG-MNPs were taken up by microglia, demonstrating that they are not 'invisible' to these cells, but the extent of uptake per cell was less than for the control NPs, showing some effect of PEG in terms of reducing clearance. Although this reduced uptake may only represent a modest benefit, it is not clear whether they also 'invisible' to cell surface or intracellular immune mechanisms?

In this Chapter, I will examine whether 'stealth' NPs cause alteration in microglial activation state.

7.2 Aims and objectives

7.2.1 Aims

This study primarly aims to assess whether ‘stealth’ NPs produce more limited pro-inflammatory microglial responses than other nanoparticles. To the best of my knowledge, a detailed study of microglial gene expression changes with ‘stealth’ NPs has never been done. The second aim is to examine whether microglia response to NPs will change if they are in the activation (M1) state – a question of significant importance for the scientists in the regenerative medicine fields.

7.2.2 Objectives

The objectives are:

- To identify the effect of NPs uptake on primary microglial activation status.
- To identify the effect of ‘stealth’ NPs on production of pro-inflammatory microglial responses, and if they more limited than for other nanoparticles.
- To identify the effect of prior M1 activation of microglia on how they respond to NPs.

7.3 Experimental procedures

7.3.1 Reagents and equipment

All reagents and equipment used were described previously in Chapter Two. CMX-MNPs and PEG-MNPs were supplied by Chemicell as aqueous suspensions. They were synthesised by the same manufacturer, having magnetite cores with a lipophilic dye (BODIPY) layer, overcoated with either carboxymethyl dextran (CMX-MNP) or 2 kDa diphosphate PEG (PEG-MNP) while Sphero were supplied by Spherotech Inc. (IL, USA).

7.3.2 Microglia culture

Mixed glia culture preparation and pure microglia culture isolation were as described previously in Chapter Two. Microglia cultures were maintained in D10-CM (D10-conditioned media), containing 10 % FBS and 20 % conditioned media from mixed glial culture flasks (a mixture of molecules released by astrocytes, OPCs and microglial cells) (Jenkins *et al.* 2015). All cultures were incubated at 37 °C in 5 % CO_2, 95 % humidified air. Cells were plated (6×10^5 cells/ml) on PDL-coated coverslips in 24-well plates for nanoparticle uptake and immunostaining or (24×10^5 cells/ml) on PDL-coated T25 flasks for gene expression.

7.3.3 nanoparticles uptake experiments

Based on previous work by Jenkins *et al.* (2016) a concentration of 2 µg/ml was chosen for both CMX-MNPs and PEG-MNPs and 20 µg/ml for Sphero. These concentrations did not produce toxic effects on microglia over 24 h, while allowing obvious identification of labelled cells (Pickard *et al.* 2011; Jenkins *et al.* 2016).

All the MNPs were heavily vortexed to dissociate them before being diluted in D10-CM, to 10 times the final concentration (i.e. 20 and 200 µg/ml, respectively).

7.3.3.1 Effect of nanoparticles on naïve microglia

At 24 h after microglia were plated, cultures received a 10 % medium change (to replace D10-CM with 10 times final concentration of the MNPs in D10-CM) and were incubated for a further 24 h. Control microglia cultures were treated with equal volumes of fresh D10-CM media, without MNPs. Samples were washed with PBS, then either fixed for immunostaining and NPs uptake, or processed for gene expression and Griess assay.

7.3.3.2 Effect of nanoparticles on M1 microglia

At 24 h after microglia were plated, cultures received a 10 % media change (replace D10-CM with 10x final concentration of the LPS in D10-CM) and incubated for 24 h. Then 100% of the media changes (MNPs in D10-CM). Control for this experiment first receive (LPS; 24 h) then cultures' media were replaced with fresh D10-CM media. Samples were washed with PBS, then either fixed for immunostaining and NPs uptake or processed for gene expression and Griess assay.

7.3.4 Nanoparticles uptake analysis

The extent of microglial uptake of MNPs was quantified using integrated density function (ImageJ, NIH, US). Individual MNP-labelled cells were outlined (using phase micrographs), then this outline was transferred to the corresponding red channel (MNP) micrograph and the integrated density measured (with background intensity subtracted for each image).

7.3.5 Viability assay

Cell viability was measured following MNP treatment using live/dead viability/cytotoxicity kit which contains calcein AM and ethidium homodimer-1. Cells were washed with PBS, incubated for 15 minutes with a PBS solution consisting of 4 μM calcein-

AM (produces green fluorescence in live cells) and 6 μM ethidium homodimer-1 (produces red fluorescence in dead cells). Cells were rewashed with PBS, fixed and then mounted for fluorescence microscopy. Cellular viability was measured by counting green (LIVE) and red (DEAD) cells using ImageJ software (NIH, US) then expressing the number of LIVE cells as a percentage of total cells (green + red) from a total of four images taken at 400 x magnification.

7.4 Results

7.4.1 The effect of nanoparticles on non-activated microglia

7.4.1.1 Nanoparticles toxicity

Live/dead staining and cell counts were used to assess the effects of MNPs on the viability of microglia. Microglia were treated with PEG-MNP, CMX-MNP, Sphero or LPS for 24 h, before viability assay. After live/dead staining, most cells with normal microglial morphologies appeared green (LIVE) with small numbers of rounded cells appearing red (DEAD) in all conditions. There were no significant differences between treatments in terms of percentage live, percentage dead or cell counts (Figure 7-1). Live/dead staining and cell counts reveal high cellular viability after MNPs or LPS treatment, comparable to control (untreated) cultures.

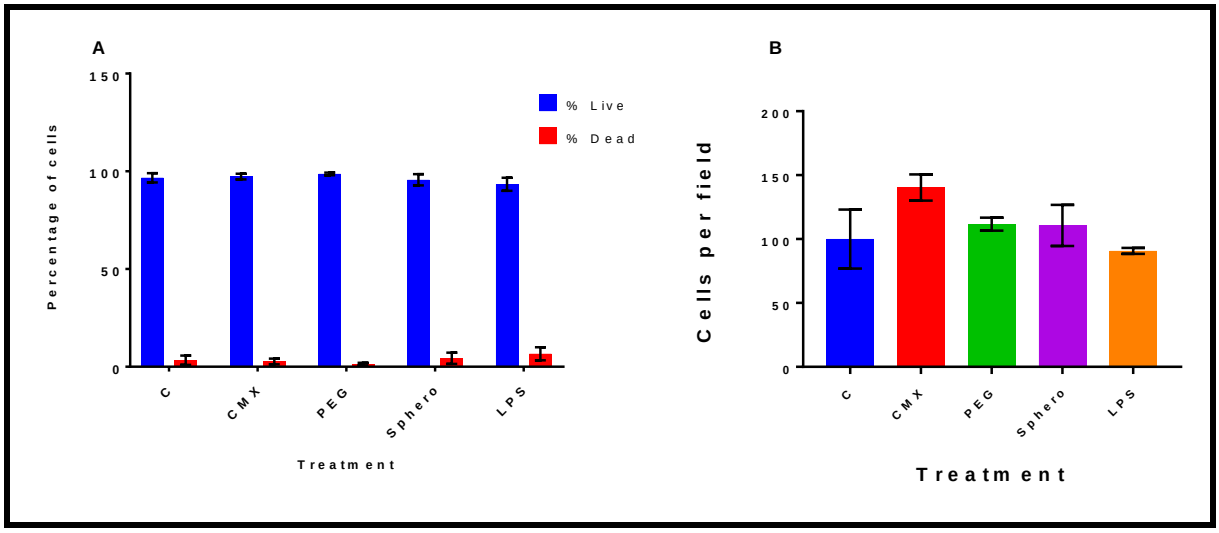

Figure 7-1: Microglial viability was unaffected by 24 h NPs exposure. (A) Bar chart showing the percentage of viable and dead cells. (B) Bar chart showing the total cells. 24 h PEG-MNP= 2 µg/ml, CMX-MNP= 2 µg/ml, Sphero= 20 µg/ml, LPS= 10 ng/ml. No significant differences; One-way ANOVA with Dunnett's post-hoc test versus C (control). All data are presented as mean ± S. E. M. of three independent experiments.

7.4.1.2 Nanoparticles uptake

Primary microglia were exposed to PEG-MNP and CMX-MNP (2 µg/ml) for 24 h. Fluorescence microscopy confirmed the internalisation of MNPs by microglia (Figure 7-2). Nearly every microglial cell showed some degree of uptake of MNPs. Using ImageJ software, the extent of MNPs uptake was assessed by measuring the integrated density value for each cell. The results showed that average cellular uptake of CMX-MNPs was significantly greater than uptake of PEGylated MNPs (Figure 7-3).

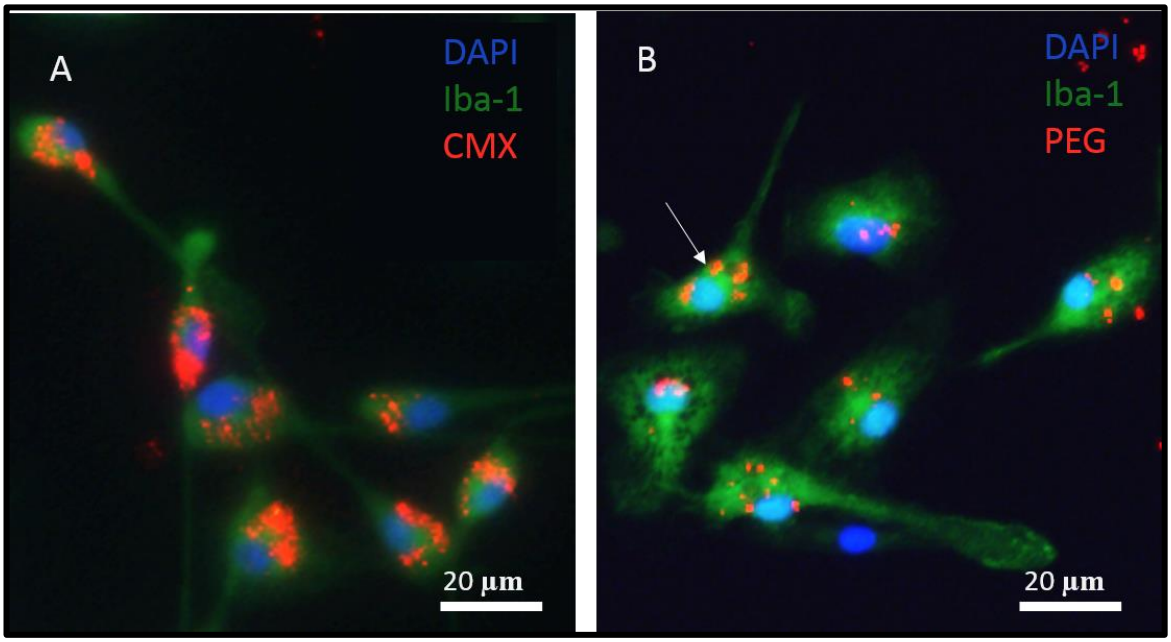

Figure 7-2: PEGylated MNPs are taken up by microglia less avidly than CMX-coated nanoparticles. Fluorescence micrographs of high purity microglial cultures following incubation with CMX- or PEG-coated fluorescent magnetic NPs (24 h). Micrographs show DAPI-stained nuclei as blue, cell bodies and processes as green (Iba1), and particles as red. Uptake of CMX-MNPs was extensive for almost all microglia, whereas uptake of PEG-MNPs was more heterogeneous, and often markedly lower, in extent (arrows indicate examples of uptake).

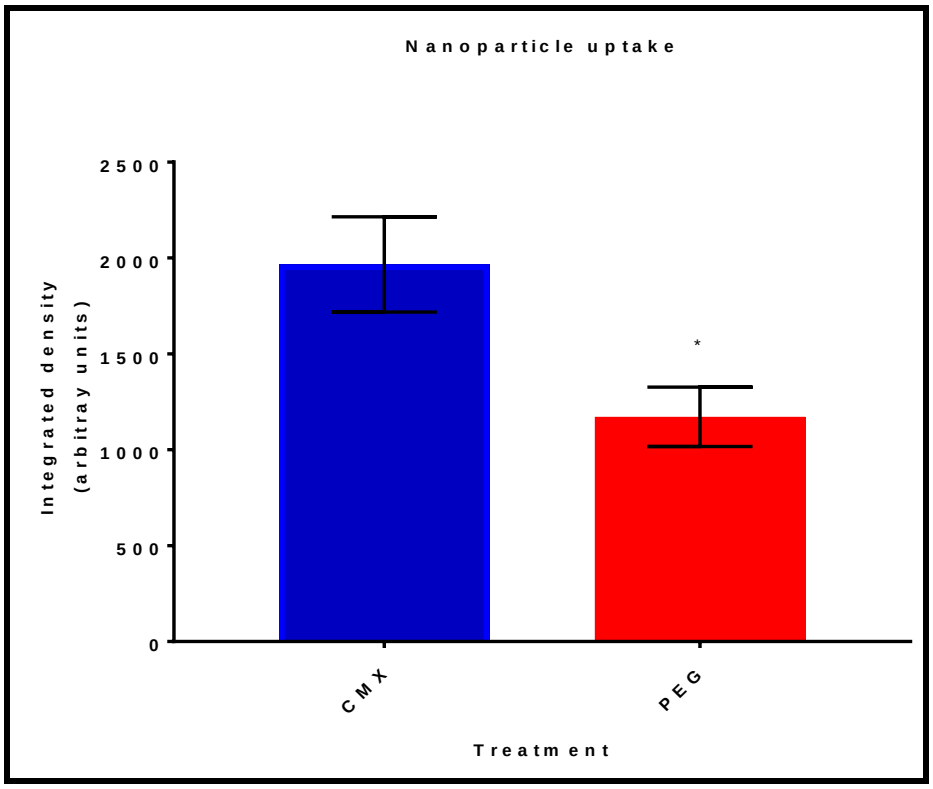

Figure 7-3: Uptake of PEGylated MNPs is significantly reduced compared to CMX-MNP (control nanoparticles) for microglia. Bar graph indicating the average extent of MNP-loading per cell, assessed by integrated density measurements, 24 h post-particle addition to high purity culture. *p < 0.05; unpaired t-test PEG versus CMX. All data are presented as mean ± S. E. M. of three independent experiments.

7.4.1.3 Nanoparticle effects on gene expression

7.4.1.3.1 Effect of nanoparticles on reference genes

qPCR was performed using the three reference genes identified in Chapter Three. The results show that there was no MNPs-induced change in expression for the reference genes tested (*Gapdh*, *Usp14* and *Rpl32*) (Figure 7-4). Therefore, the average of their Cq values should allow reliable evaluation of MNPs and LPS-induced changes in GOI.

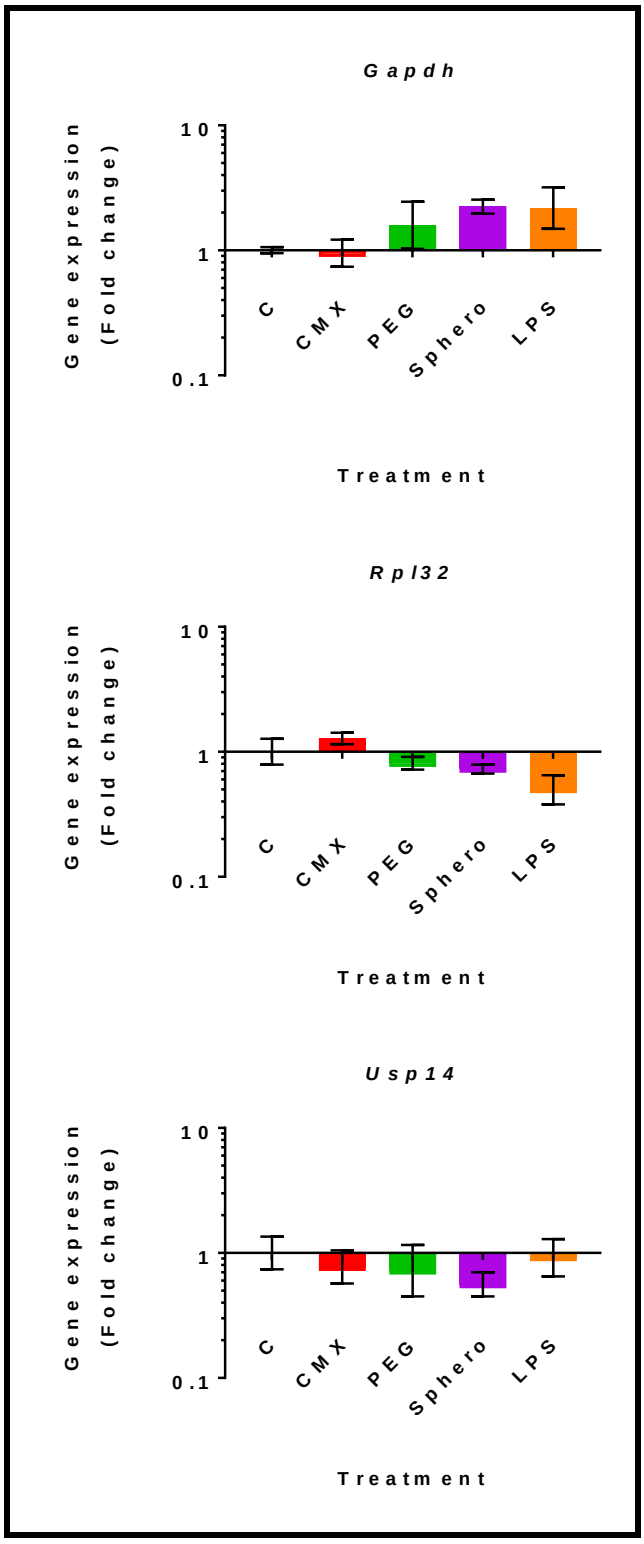

Figure 7-4: No changes in microglial reference gene expression following 24 h MNPs treatment. Bar graphs illustrating gene expression for (A) *Gapdh, (B) Rpl32, (C) Usp14*. Y-axis represents log fold change versus average of reference genes (1 = no change) and X-axis represents different treatment. There was no effect of any of the MNPs or LPS on the reference gene expression of microglia; One-way ANOVA with Dunnett's post-hoc test versus the control (C). All data are presented as the mean ± S. E. M. of three independent experiments.

7.4.1.3.2 Effect of nanoparticles on GOI

Microglia were treated with PEG-MNP, CMX-MNP, Sphero or LPS for 24 h, then qPCR was used to measure the relative changes in gene expression. No significant differences in gene expression were detected for any of MNPs. LPS was used as a positive control for M1 activation; results showed a significant increase in both *Il-1β* and *iNos* (M1 markers), as expected (Figure 7-5). No elevation in *Tnf-a* expression was detected, consistent with the values derived at 24 h in Chapter Five. The Chapter Five value for *Il-1β* (~18.5-fold increase) was comparable to the value here (~19.8-fold).

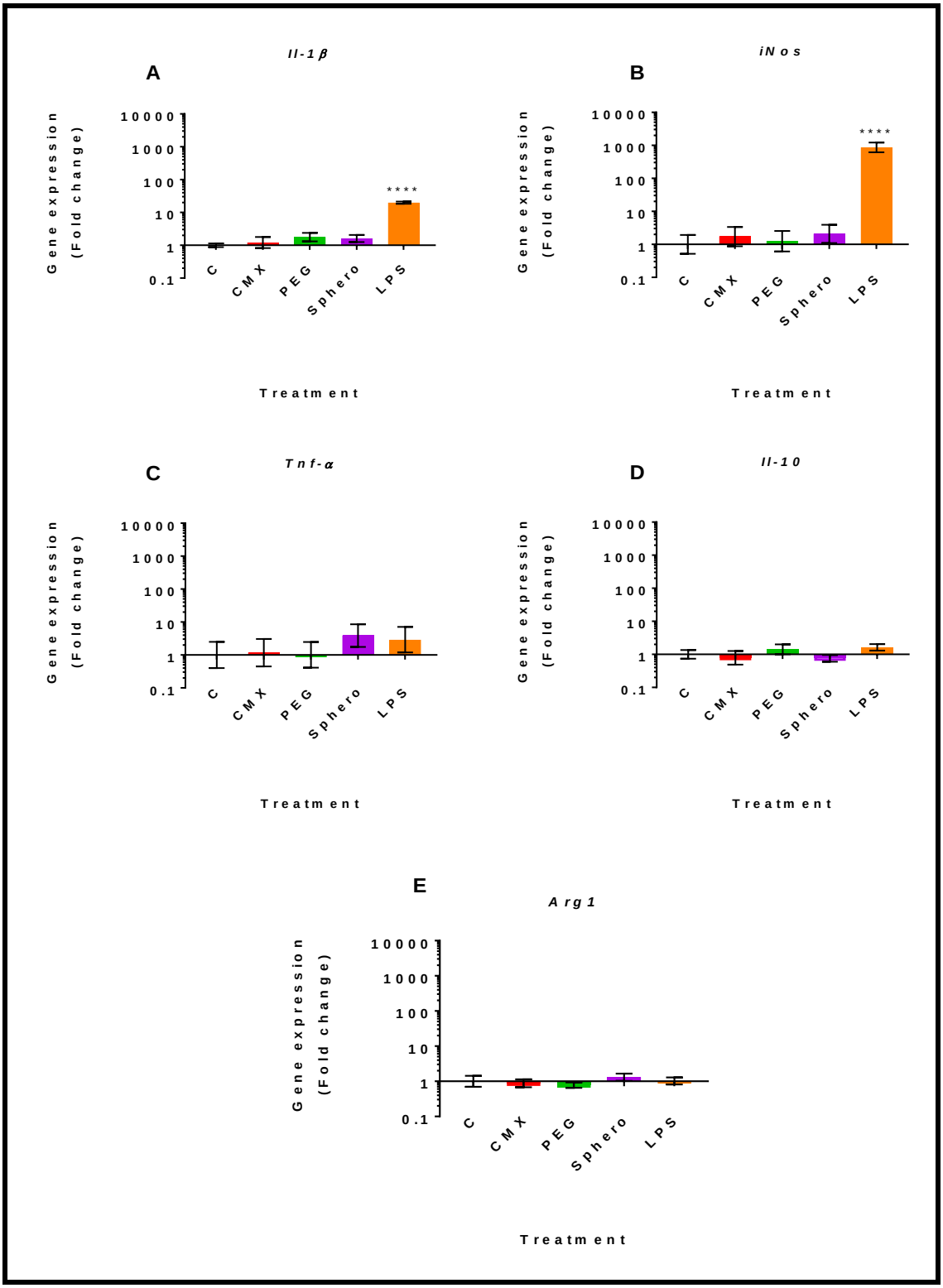

Figure 7-5: Microglia gene expression response to 24 h of MNPs. (A) *Il-1β*, (B) *iNos*, (C) *Tnf-α*, (D) *Arg1*, (E) *Il-10*. Y-axis represents log fold change versus average of reference genes (1 = no change) and X-axis represents different treatment. A significant increase in M1 markers (*Il-1β* and *iNos*) gene expression was found in LPS treated microglia. ****p < 0.0001, One-way ANOVA with Dunnett's post-hoc test versus the control (C). All data are presented as the mean ± S. E. M. of three independent experiments.

7.4.1.4 Nanoparticles effects on morphology

The effects of MNPs on microglial morphology were assessed using ImageJ after treatment with PEG-MNP, CMX-MNP, Sphero or LPS for 24 h. There was no significant difference between treated microglia and control (untreated cells) in any morphological measurements (Figure 7-6).

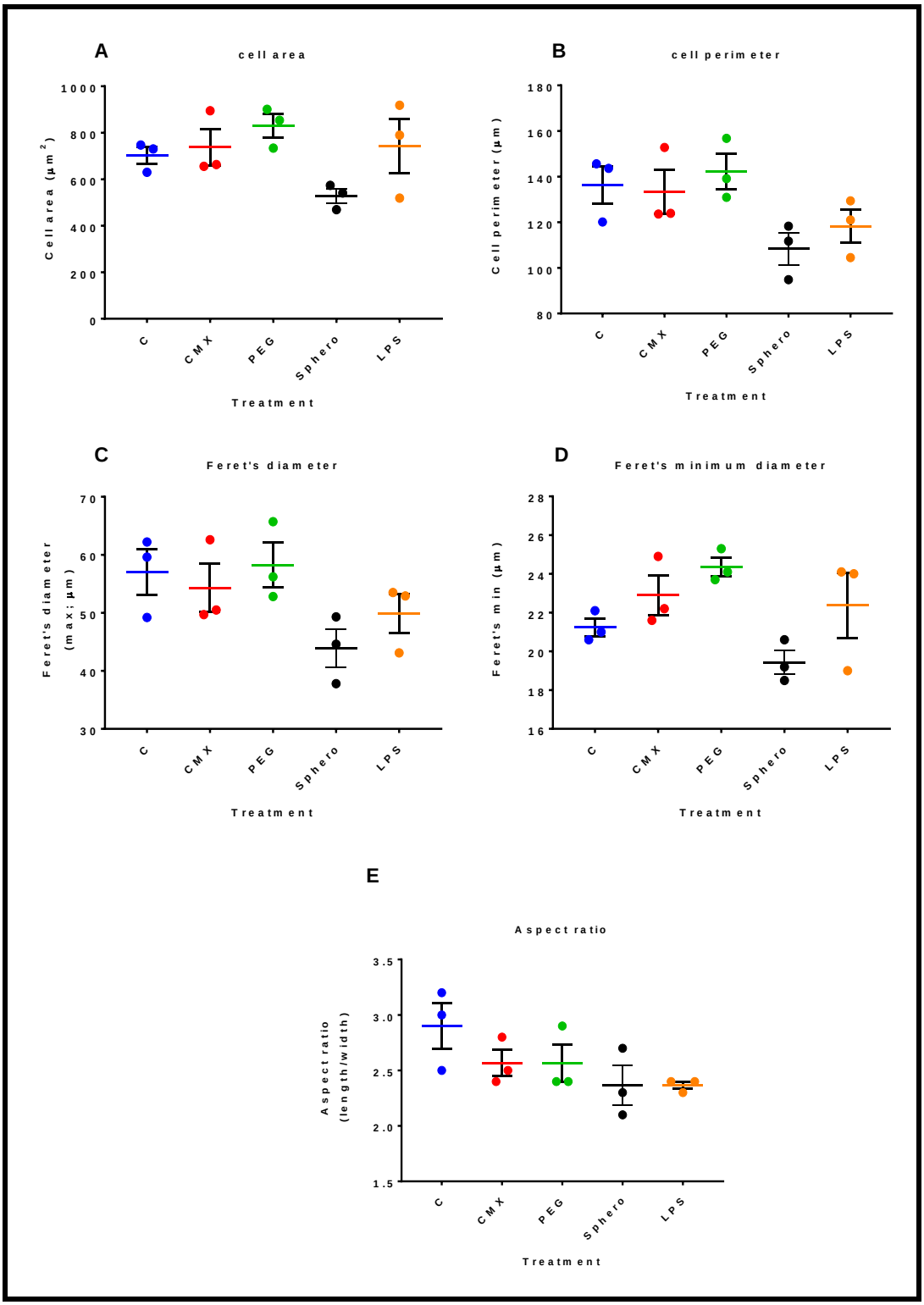

Figure 7-6: Morphological analyses of microglia cells treated with MNPs. Scatter plot showing average cellular (A) area, (B) perimeter, (C) Feret's diameter, (D) minimum Feret's diameter, and (E) aspect ratio. 24 h treatment with: PEG-MNP = 2 µg/ml, CMX-MNP = 2 µg/ml, Sphero = 20 µg/ml, LPS = 10 ng/ml. No significant difference; One-way ANOVA with Dunnett's post-hoc test versus C (control). All data are presented as mean ± S. E. M. of three independent experiments.

7.4.1.5 Nanoparticles effects on iNos protein expression

The effect of MNPs on iNos protein expression was assessed using immunocytochemistry and integrated density measurements after treating microglial cells with PEG-MNP, CMX-MNP, Sphero or LPS for 24 h. LPS induced significantly greater expression of iNos (Figure 7-7), consistent with pro-inflammatory activation. Neither CMX-MNPs nor PEG-MNPs altered iNos protein expression.

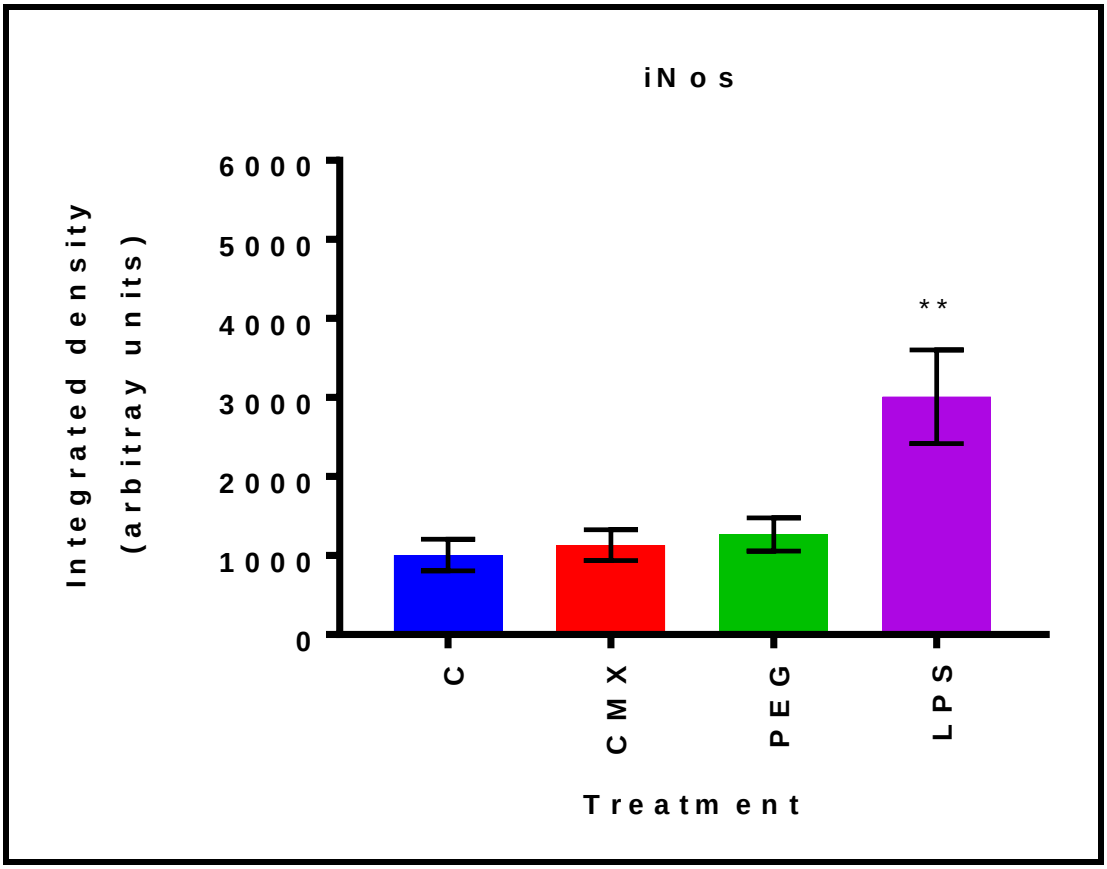

Figure 7-7: Microglial iNos protein expression was unaffected by MNP treatment. Bar graph indicating the extent of iNos expression per cell, assessed by integrated density measurements. After treatment with only media= C (control), PEG-MNP= 2 µg/ml, CMX-MNP= 2 µg/ml, , LPS= 10 ng/ml for 24 h. **p<0.01; One-way ANOVA with Dunnett's post-hoc test versus C. All data are presented as mean ± S. E. M. of three independent experiments.

7.4.1.6 Nanoparticles effects on nitrite

To investigate the effects of MNPs on iNos activity (production of RNS), cells were treated with PEG-MNP, CMX-MNP, Sphero, or LPS for 24 h. The levels of nitrite in the culture media were determined with the Griess assay, as a proxy for NO production. LPS significantly increased nitrite levels, while none of the MNPs had any effect on nitrite production (Figure 7-8).

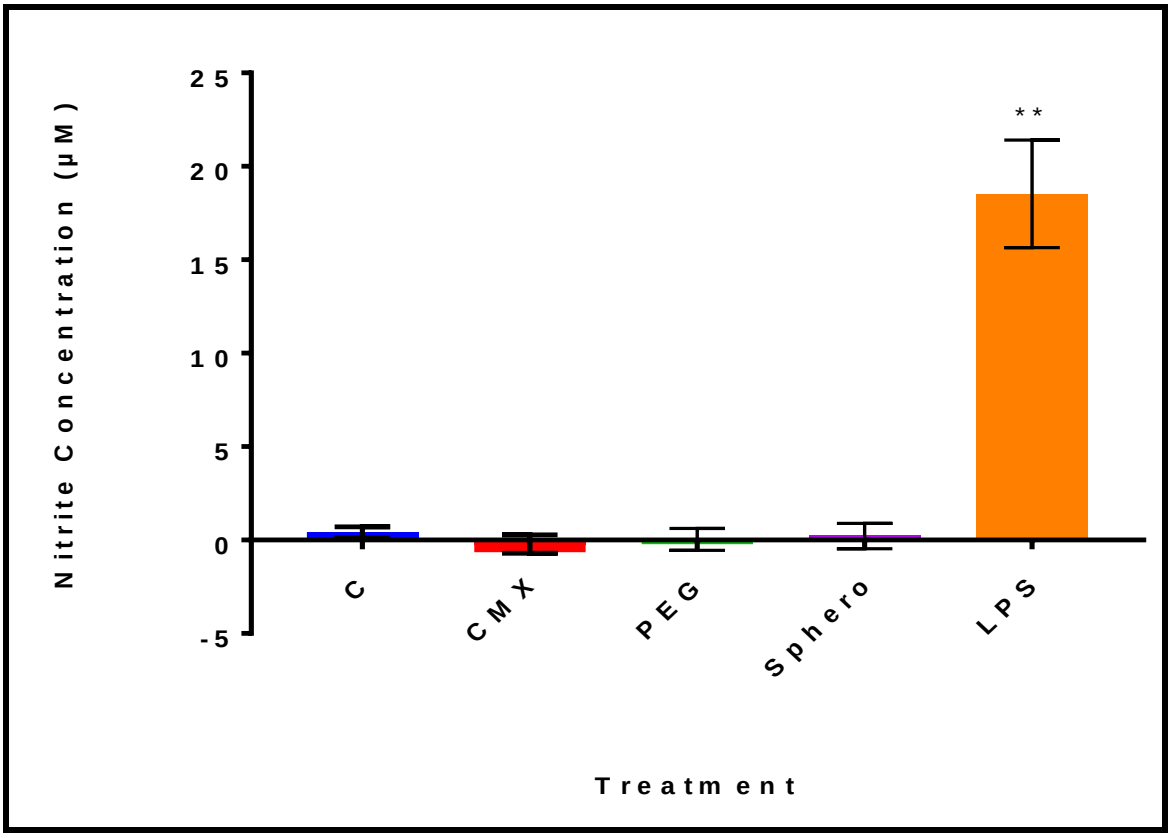

Figure 7-8: The effects of MNPs and LPS (as positive control) on nitrite production. Nitrite production was assayed by measuring the levels of nitrite in the supernatant fluid using Griess reagent after treating microglia with only media= C (control), PEG-MNP= 2 µg/ml, CMX-MNP= 2 µg/ml, Sphero= 20 µg/ml, LPS= 10 ng/ml for 24 h. There was no effect of any of the MNPs on nitrite production. There was a significant increase in nitrite production induced by LPS. **$p < 0.01$; One-way ANOVA with Dunnett's post-hoc test versus C. All data are presented as mean ± S. E. M. of three independent experiments.

7.4.2 The effect of nanoparticles on pro-inflammatory microglia (LPS pre-treatment)

7.4.2.1 Nanoparticles uptake by M1 microglia

Primary microglia were first exposed to LPS (10 ng/ml) for 24 h, to induce inflammatory activation, then exposed to PEG-MNP or CMX-MNP for 24 h (without LPS). Using ImageJ, the extent of MNP uptake per cell was assessed by measuring the integrated density. The result shows there is no difference in levels of MNPs uptake per cell with and without LPS pre-treatment (Figure 7-9).

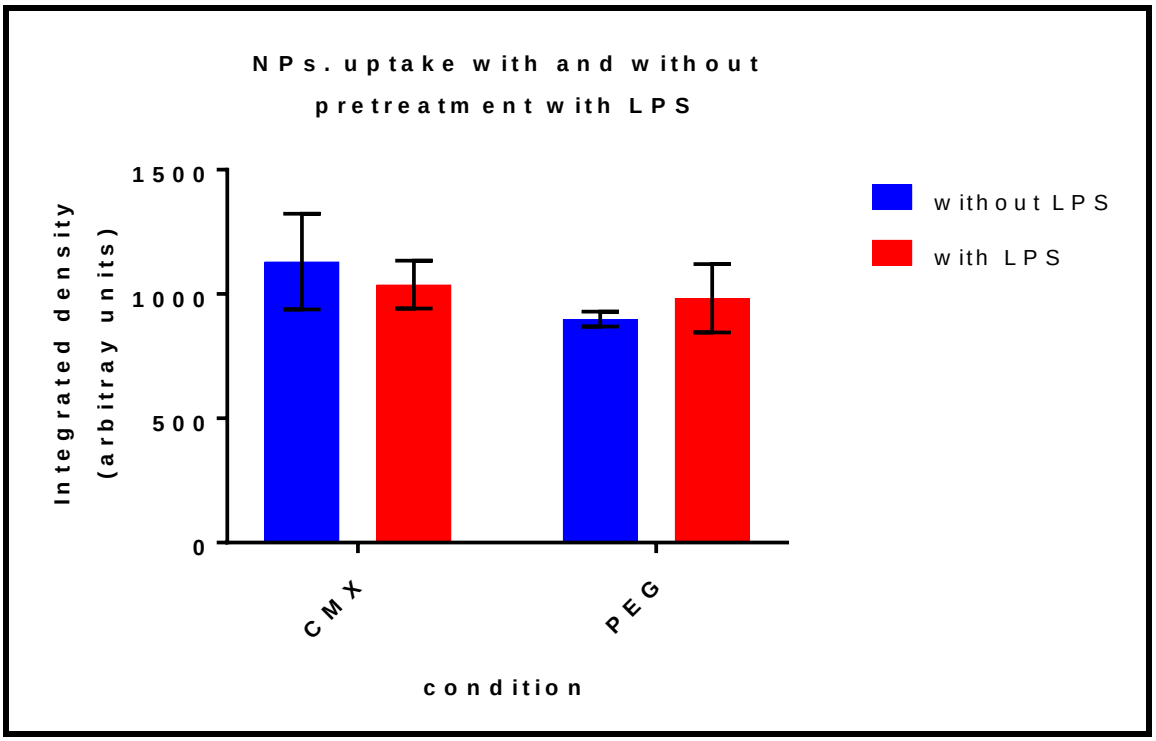

Figure 7-9: Microglial uptake of each MNP type is unaffected by prior pro-inflammatory activation. Bar graph indicating the average extent of MNP-loading per cell, assessed by integrated density measurements. 24 h after LPS treatment, microglia were exposed to MNPs. No significant difference; unpaired t-test; with LPS versus without LPS, for each MNP type. All data are presented as mean ± S. E. M. of three independent experiments.

7.4.2.2 Nanoparticles effects on M1 microglia morphology

The effect of MNPs on M1 microglia morphology was assessed using ImageJ. Microglia were first treated with LPS (10 ng/ml) for 24 h, then PEG-MNP, CMX-MNP, Sphero or LPS for a further 24 h. There was no significant difference in any morphological measurement between treated microglia and control (LPS-C) (Figure 7-10).

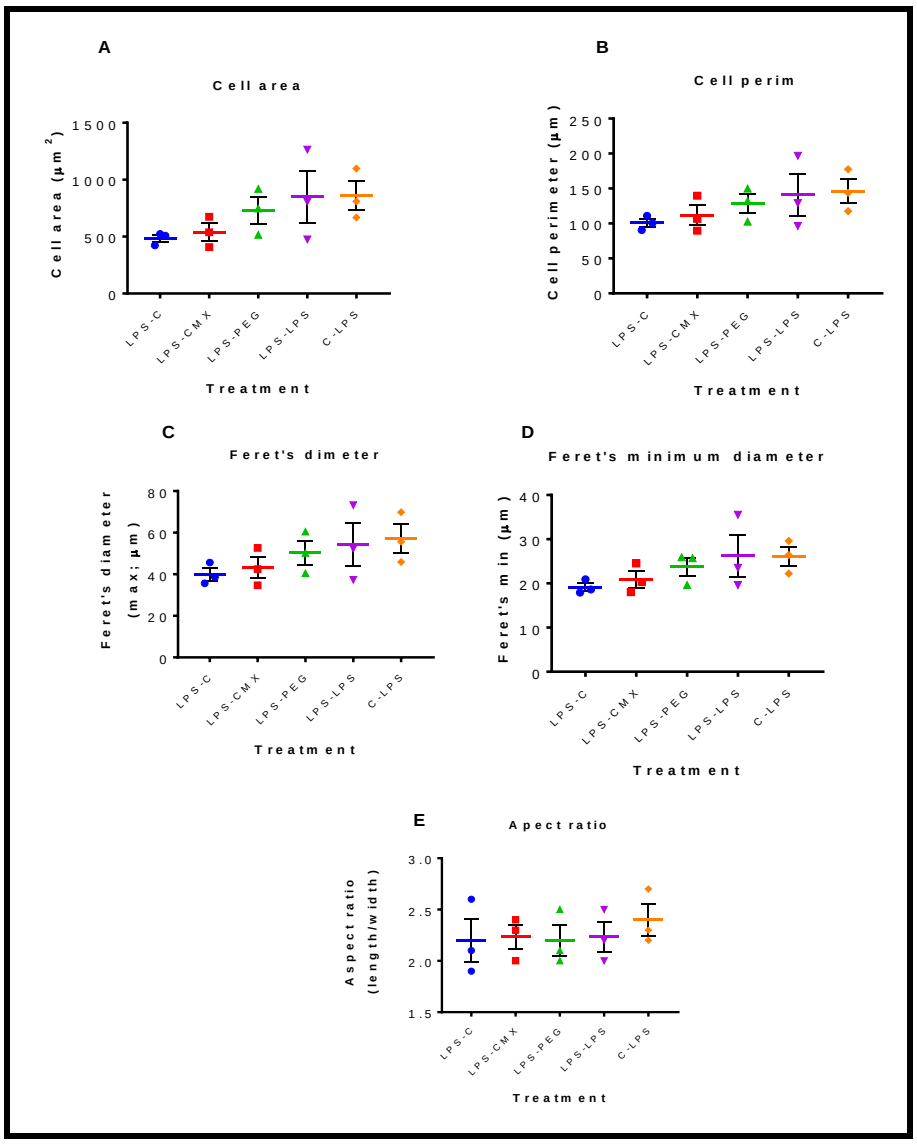

Figure 7-10: M1 microglial morphology was unaffected by MNP treatment. Scatter plot represent: (A) Area, (B) cell perimeter, (C) Feret's diameter, (D) minimum Feret's diameter, (E) aspect ratio. First cells were treated with LPS (10 ng/ml) for 24 h then treated with only media= C (control), PEG-MNP= 2 µg/ml, CMX-MNP= 2 µg/ml, Sphero= 20 µg/ml, LPS= 10 ng/ml for 24 h. No significant difference; One-way ANOVA with Dunnett's post-hoc test versus LPS-C. All data are presented as mean ± S. E. M. of three independent experiments. LPS-C: 24 h LPS followed by 24 h in D10 without LPS; LPS-CMX: 24 h LPS followed by 24 h CMX; LPS-PEG: 24 h LPS followed by 24 h PEG; LPS-LPS: 24 h LPS followed by another 24 h LPS; C-PEG: 24 h in D10 followed by 24 h LPS.

7.4.2.3 Nanoparticles effects on iNos protein expression on M1 microglia

The effect of MNPs on M1 microglia iNos protein expression was assessed using integrated density measurements. Microglia first treated with LPS (10 ng/ml) for 24 h then another 24 h exposure to PEG-MNP, CMX-MNP, Sphero, or LPS. No significant differences were detected between treatment groups (Figure 7-11).

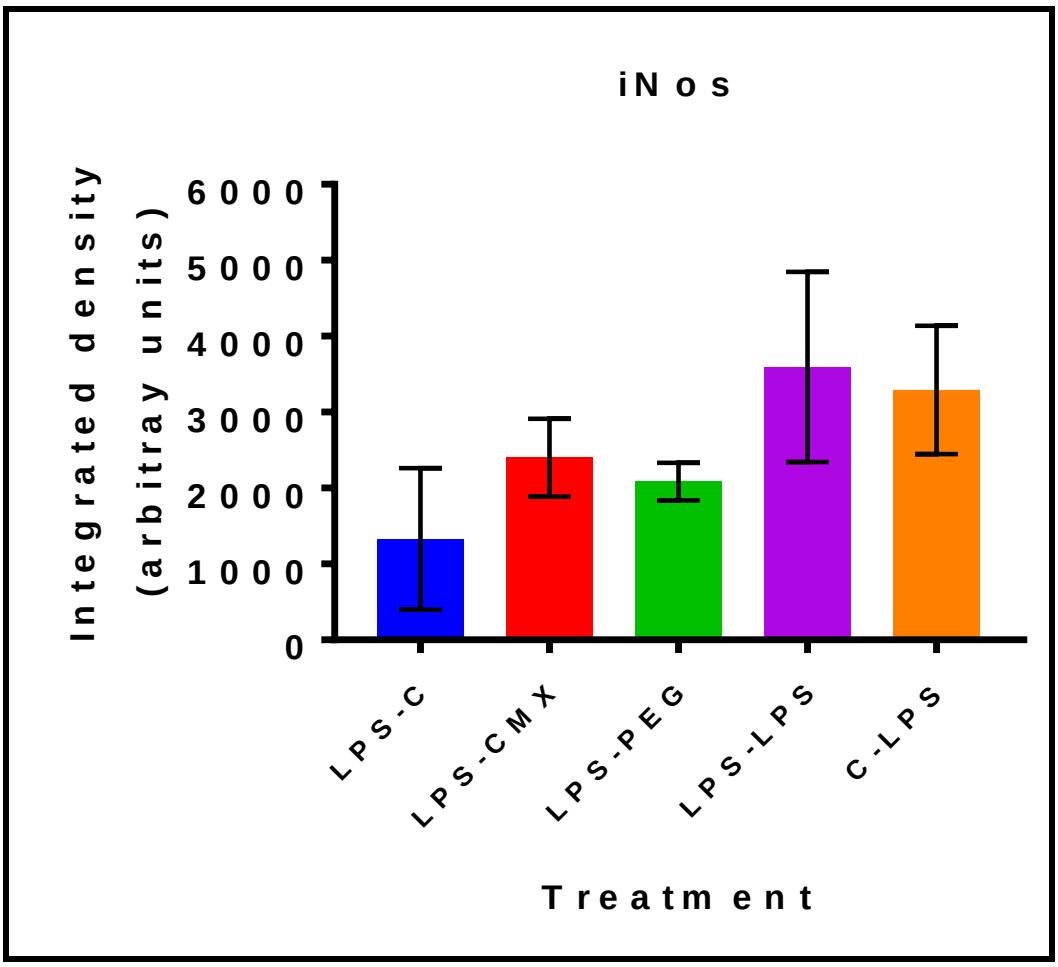

Figure 7-11: Nanoparticle effects on iNos protein expression on M1 microglia. First cells were treated with LPS (10 ng/ml) for 24 h then treated with only media= C (control), PEG-MNP= 2 µg/ml, CMX-MNP= 2 µg/ml, Sphero= 20 µg/ml, LPS= 10 ng/ml for 24 h. Bar graphs indicating the extent of iNos expression per cell, assessed by integrated density measurements. No significant difference; One-way ANOVA with Dunnett's post-hoc test versus LPS-C. All data are presented as mean ± S. E. M. of three independent experiments. LPS-C: 24 h LPS followed by 24 h in D10 without LPS; LPS-CMX: 24 h LPS followed by 24 h CMX; LPS-PEG: 24 h LPS followed by 24 h PEG; LPS-LPS: 24 h LPS followed by another 24 h LPS; C-PEG: 24 h in D10 followed by 24 h LPS.

7.4.2.4 Nanoparticles effects on nitrite in M1 microglia

To investigate the effects of MNPs on nitrite production in M1 microglia, cells were first treated with LPS (10 ng/ml) for 24 h then another 24 h exposure to PEG-MNP, CMX-MNP, Sphero or LPS. The levels of nitrite in the culture media were determined with the Griess assay, as a proxy for NO production. Pre-treatment of the cells with LPS, followed by 24 h without LPS (LPS-C) resulted in nitrite levels of ~2 µM (returned almost to baseline, compared to ~17 µM detected at 24 h LPS, Figure 7-8). Cultures treated identically, except for NP treatment during the latter 24 h period, exhibited comparable nitrite levels (no significant differences). In contrast, the cells that received a repeated dose of LPS (LPS-LPS), or only the second dose (C-LPS), showed nitrite levels significantly greater than cells received only the first dose of LPS (LPS-C) (Figure 7-12) again, comparable to (Figure 7-8).

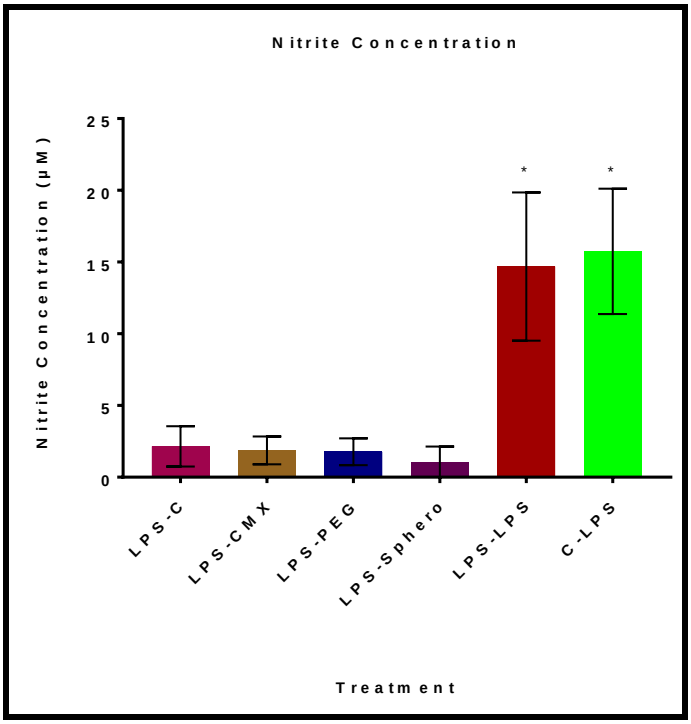

Figure 7-12: MNPs effect on nitrite production of M1 microglia. Nitrite production was assayed by measuring the levels of nitrite in the supernatant fluid using Griess reagent after treatment of microglia first with LPS (10 ng/ml) for 24 h then another 24 h exposure to only media= C (control), PEG-MNP= 2 µg/ml, CMX-MNP= 2 µg/ml, Sphero= 20 µg/ml, LPS= 10 ng/ml. There was no effect of any of the MNPs on nitrite production. There was a significant increase in nitrite production induced in C-LPS and LPS-LPS. *p<0.05; Kruskal-wallis with Dunn's post-hoc test versus LPS-C. All data are presented as mean ± S. E. M. of three independent experiments. LPS-C: 24 h LPS followed by 24 h in D10 without LPS; LPS-CMX: 24 h LPS followed by 24 h CMX; LPS-PEG: 24 h LPS followed by 24 h PEG; LPS-LPS: 24 h LPS followed by another 24 h LPS; C-PEG: 24 h in D10 followed by 24 h LPS.

7.5 Discussion

The main aim of this study was to understand whether microglia exhibit altered gene expression profiles in response to MNPs. Three different MNPs were chosen, which have previously been characterised in terms of size and chemistry; and shown to be broadly biocompatible with neural cells including microglia (Pickard *et al.* 2011; Jenkins *et al.* 2016). Consistent with previous reports, these NPs were internalised by microglia, and did not exhibit toxic effects. Also, PEGylated (stealth) MNPs were taken up to a lesser extent than control MNPs, consistent with the modest effects of a stealth coating reported previously (Jenkins *et al.* 2016).

The data generated here are consistent with the theory that PEGylated MNPs would not induce a strong pro-inflammatory microglial response. However, these data also showed that 'control' MNPs, without a stealth coating, did not cause inflammatory microglial responses. This conclusion is based on gene expression, protein expression and functional assays (Griess), as well as morphological analyses. Broadly, these results are promising for the future development of MNP-based therapies, as avoiding an inflammatory response would be desirable in most scenarios.

7.5.1 Nanoparticles toxicity

The hypothesis was that if the MNPs are non-toxic to microglia, then the total cells count, and percentage of live cells would be unaltered. To test whether there were any toxic effects of MNPs on microglia, cells were treated with three different types of MNPs (CMX-MNP, PEG-MNP and Sphero) or LPS. The results showed that none of the MNPs or LPS have a toxic effect on microglia either in these that received the previous dose of LPS or not. This study results are in line with Gupta & Wells (2004) report, that PEG-MNP is nontoxic to human dermal fibroblasts. The low toxicity of MNPs may be attributed to the fact that

these MNPs are hydrophilic, and their coating reduces the surface interactions with cells or proteins (Gupta & Wells 2004).

7.5.2 Nanoparticles uptake with and without LPS

It was previously hypothesised that PEG-MNPs may be 'invisible' to microglia, and so uptake of PEG-MNPs would be substantially lower than that of non-stealth MNPs (specifically, CMX-MNPs) (Jenkins *et al.* 2016). When tested, this effect was not as dramatic as predicted, although the levels of MNPs uptake per cell were lower for PEGylated MNPs. This study has attempted to build on this work. This study results showed that the uptake of CMX-MNPs was significantly higher than that of PEG-MNPs, which is in line with the previous report (Jenkins *et al.* 2016). This effect, now replicated here, may be due to PEGs ability to improve the biocompatibility of the MNPs by resisting protein adsorption (Zhang *et al.* 2002) (Figure 7-13), which may play a role in the recognition of MNPs by microglia cells (Zhang *et al.* 2002). Therefore, there may be clinical value in developing this strategy further, for example modifying the PEG coating (Jia *et al.* 2016; Pitek *et al.* 2016), or testing alternative stealth coatings such as derivatives of poly sulfobetaine, poly carboxybetaine and poly acrylic acid.

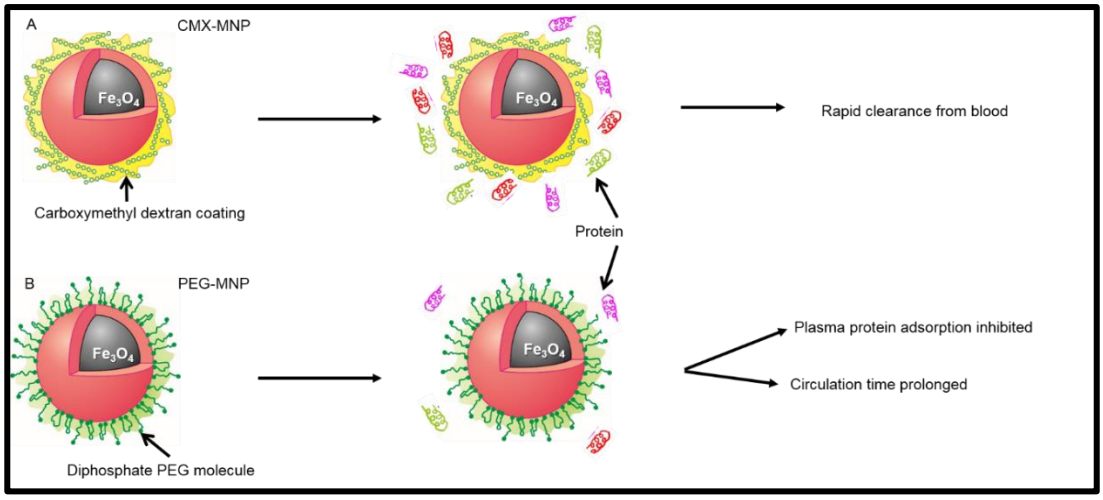

Figure 7-13: PEGylated coating inhibited protein adsorption. (A) CMX-PEG rapidly cleared by immune cell in the body. (B) PEG-MNP, PEGylating coating increase the circulation time by reducing the protein adsorption. Images created by Humphrey Yiu (Edinburgh University) (Jenkins *et al.* 2016).

This study showed that pre-treatment of microglial cells with LPS has no effect on MNPs uptake. That is, introducing these MNPs to pro-inflammatory microglia did not lead to altered uptake dynamics, compared to inactivated microglia. Therefore, predicted levels of MNP uptake by microglia may be unaffected by cellular activation status, in line with data generated here. Pickard and Chari (2010) have reported that LPS treated microglia in culture do not exhibit increased MNP uptake activity. In contrast, another study has reported that LPS treatment of microglial cell lines can induce increased uptake of ultra-small dextran-coated NPs both in 6 and 24 h (Cengelli *et al.* 2006). However, cell lines typically show greater levels of uptake than primary cells.

7.5.3 Nanoparticles effect on gene expression

The original study comparing PEG- and CMX-MNPs looked at levels of uptake, but failed to assess cellular responses. The central hypothesis underpinning this research, was that althogh both MNP types are taken up by microglia, internalisation of PEG-MNPs may generate lower inflammatory responses than other MNPs. LPS-treatment was used to

generate a clear M1-response, as a positive control. MNPs treated microglia were then compared to this, and an untreated control. This study showed that none of the different MNPs (PEG-coated, and two control MNPs) caused inflammatory responses in microglia.

In line with this study result, Wang *et al*. (2011) treated BV-2 cell lines with non coated iron oxide NPs for 6 h, the result showed no increase in Il-1β, Il-6 and Tnf-α protein production using ELISA. In contrast, a previous study using primary microglia to assess the effects of SiNPs, showed a significant increase in *Cox-2* (3 fold change) only at the highest concentration of NPs, and the same study reported a significant decrease in *Tnf-α* gene expression. However, SiNPs are chemically different from the NPs used in this study, therefore it is not surprising that the immune response to them differs from the results generated here. Furthermore, Choi *et al.* (2010) study did not state the amount of this decrease, and also their qPCR data depends completely on a single unvalidated reference gene (*ACTB*). Wu *et al.* (2013) study aimed to understand the effect of carboxydextran-coated iron oxide NPs on LPS-activated microglia by using ELISA assay to measure both Tnf-α and Il-1β protein production in BV-2 cell line. The results showed a decrease in Il-1β at higher NP concentrations (10 and 50 µg iron oxide NPs/ml) but not at the lowest concentration (1 µg). Wu *et al.* (2016) study showed no change in Tnf-α protein production at any concentration. Although the main aim of the Wu *et al.* study was to assess the effect of NPs on activated microglia, their experimental design involved treating the cells with different concentrations of NPs for 30 min, then with a high dose of LPS (100 ng/ml) for 24 h. Furthermore, Il-1β production in BV-2 cell line is known to be problematic issue as has been shown in Table 3-1.

In *in vivo* studies, chronic administration of aluminium oxide NPs to rats (1 mg/kg or 50 mg/kg) has been reported to cause microglial activation in cortex and hippocampus in the long exposure period (60 days) but not in the shorter exposure time (30 days) (Li *et al.*

2009). Aluminium oxide is unlikely to have clinical applications and this study was to assess the risk of exposure to these particles. Hutter *et al.* (2010) study found that intranasal administeration of sphero gold NPs for 24 h caused a small activation of microglia. However in the same study the results showed that PEGylated gold NPs did not lead to microglial activation.

As described above, various NPs formulations have been shown to induce neuroinflammation, or specifically to cause microglial pro-inflammatory responses. However, none of the three MNPs formulations tested here generated M1 microglial response. These results are promising in terms of iron oxide particles, with carboxyl, dextran or PEG surface chemistries, having possible clinical utility. Nonetheless, more work should be carried to test different incubation time effect and the response of other genes and proteins, for these, and other NP designs.

7.5.4 Nanoparticles effect on morphology with and without LPS

The hypothesis is that if MNPs activate microglia, then microglia morphology will be more amoeboid in shape. To test the MNPs effect on microglia morphology, microglia have been treated with three different types of MNPs (CMX-MNP, PEG-MNP and Sphero), LPS (as a positive control). This study results showed no difference between any of the treatments in comparison to the control and, perhaps surprisingly, even with the positive control (LPS). Incubation of microglia with CMX-MNP, PEG-MNP or Sphero MNPs did not alter the morphology of microglia; a similar observation has been made previously by Zhang *et al.* (2002) when they treat macrophages cells with a different PEGylated MNP to these used in this study. Although in Zhang *et al.* (2002) N-hydroxysuccinimide PEG has been used while in this study diphosphate PEG have been used but the lack of changes in the morphology in both studies prove the biocompatiblity of the PEG coating. And in line

with this study, Pickard & Chari (2010) suggested that short-term exposure to Sphero MNPs (similar to one type of the MNPs used in this study) did not lead to microglial activation, as judged by morphological criteria. The same study suggested the pretreated microglia with LPS lead to morphological changes. However, ImageJ has been used in this study to assess microglia morphology while the previous study was evaluated by non-quantitative visual inspection.

7.5.5 Nanoparticles effect on iNos protein expression and RNS with and without LPS

The hypothesis is that if MNPs activate microglia, then microglia expression of iNos protein and nitrite will be higher then that of the control. To test the MNPs effect on iNos protein and nitrite production, microglia were treated with three different types of MNPs (CMX-MNP, PEG-MNP and Sphero) and LPS (as a positive control) was used. The results showed that none of the MNPs lead to pro-inflammatory activation of microglia, in terms of expression of iNos or presence of nitrite, which is consistent with qPCR result generated here (unaltered *iNos* gene expression). LPS was used as a positive control to assess maximum microglial response, and to confirm that elevated levels would be expected at this time point. In contrast to this study, Wang *et al*. (2011) showed that exposure of the BV-2 microglial cell line to iron oxide NPs induced significant increase in nitrite (as assess by using similar technique to that used here: Griess assay). Similarly Choi *et al.* (2010) showed, that exposure of primary microglial culture to SiNPs induced the production of nitrite. Kim *et al.* (2009) study showed that treating microglia cells with methylprednisolone-NPs (24, 48 or 72 h) does induce significant increase in the production of nitrite (as assess by using similar technique to that used here: Griess assay). However, the same study showed that their control NP as they called it (saline-NP) did not induce any increase in nitrite at any time

point which could suggest the the nitrite production is in response to the methylprednisolone coating not to the NPs itself.

The result of iNos is consistent with that of nitrite production in the experiment where naïve microglia were treated with MNPs, and showed that MNPs have a comparable expression to that of untreated cells (control), while LPS treated cells (the positive control) show significant increase. At the same time, nitrite production from activated microglia treated with MNPs supports the hypothesis that MNPs do not induce activation respose in microglia, however, the result from iNos protein production was of high variablilty which unfortuntally could not support this hypothesis. Therefore, more replications are needed using the same assay to increase the strength of the data generated here.

7.6 Summary

Experiments in this study have provided data largely consistent with the hypothesis that microglial uptake of MNPs (CMX-MNP, PEG-MNP) does not cause inflammatory responses in microglia. Furthermore, the data generated here suggest that microglial activation state does not change the extent of NP uptake or alter microglia inflammatory response. Therefore, the results generated here considered as a promising findings for using MNPs in drug delivery or diagnoses.

Chapter 8 : General discussion

8.1 Summary of key research findings

An understanding of neurodegenerative diseases will be greatly enhanced by full recognition of microglial phenotype switching (as discussed in Chapter one). It has been widely speculated that events such as inappropriate M1 activation, loss of phagocytic function or microglial priming are key to disease onset or progression (Gao & Hong 2008). If this is true, then understanding microglia behaviour could offer a valuable insight into currently incurable and devastating diseases. Such insights could inform the development of effective therapies, based on neuroimmunomodulatory drugs, harnessing the protective/regenerative abilities of microglia.

To date, researches on microglia phenotypes often lack full characterisation of the phenotypes of the microglial model. Thus, researchers often depend on a single concentration of stimulus, a single time point or both. Such limitations in these studies make their models inappropriate to study microglial phenotypes switching in neurodegenerative diseases and for testing different treatments for these diseases. Therefore, more knowledge in these areas would need more suitable models to fully characterise microglial phenotypes.

This thesis has addressed the need to develop and characterise *in vitro* microglial culture systems suitable for assessing phenotypic changes. Such systems would be of high value for simulating diseases and developing novel immunotherapies. An attempt to characterise microglia phenotypes using gene expression is described in Chapter Five and Six. In this thesis, qPCR was used to measure the differences in microglial gene expressions in response to different stimuli.

qPCR is a robust, highly reproducible and sensitive method to quantitatively study gene changes across varying environmental or experimental conditions (Wong & Medrano 2005). Robust qPCR data analysis depends on using multiple reliable reference genes

(Bustin *et al.* 2013). However, a review of the literature shows that there is a notable lack of validation of microglial reference genes and a high reliance on using only a single reference gene (section 3.1.3). One of the aims of this study was to identify and validate rat microglia reference genes which could be used later by other researchers to study microglial gene expression (Chapter Three). In this study, three reference genes have been validated: *Gapdh*, *Rpl32* and *Usp14*, all of which were stable across different treatments, time points and compositions of culture media. *Gapdh* has been widely used as a reference gene, however, most researchers have routinely used it as a solo reference gene (Aires *et al.* 2019; Li *et al.* 2019; Stojiljkovic *et al.* 2019; Tröscher *et al.* 2019). Furthermore, Rpl32 has been also used as reference gene with or without microglia (Vecil *et al.* 2000; Sebastiani *et al.* 2006). These three validated reference genes were used in all subsequent experiments (in this thesis) to normalise the expression of "genes-of-interest".

In Chapter Four, there was an investigation into the possibility that supplementing the culture medium with serum could affect microglial behaviour, possibly confounding experimental conditions. Molecules in the serum might influence microglia, in ways that produce changes in gene expression. Also, it may be expected that small quantities of LPS or other TLR4 agonists in the serum would mean that for serum-supplemented medium, actual TLR4 activation could be greater than expected for the amount of LPS added (i.e. treatment group described as 1 ng/ml LPS, it could actually be ~1.2 ng/ml; see section 4.1.2.2 for discussion of LPS levels in FBS). If this was an influence, then an increase in pEC50 might be predicted in serum-supplemented media. Section 4.1.2 discussed the possibility that serum exposure does influence microglia.

It was demonstrated in this chapter that using serum-supplemented media had no effect on the baseline gene expression (i.e. without LPS), and no effect on pEC50 or maximum dose response (for LPS) for any of the M1 markers tested (*Il-1β, Il-6* and *Tnf-α*),

at least when used for a short period (24 h). In contrast, Colton *et al.* (1992) have reported that microglia cultures treated with 1-1000 U/ml Ifn-α/β for 24 or 48 h in serum free media produce 1l-1β protein level lower than that obtained of serum-supplemented media. The difference in the results between Colton *et al.* (1992) study and this study might be due to the slightly different activation mechanism between Ifn-α/β and LPS in microglia (Subramaniam & Federoff 2017). Furthermore, the non-effect of serum found in my study might be due to the prior exposure to serum during mixed glial culture (before isolation of microglia) which made changes that are not lost later, during the serum-free period. As there was no indication of any influence of serum on microglial activation, these data suggest that each of these two serum-free media could be used for short-term studies, providing more defined and reproducible experimental conditions. However, SFM failed to support microglia survival in longer-term culture (6 d) (Figure 4-14). Therefore, the conventional serum-supplemented medium was used for all subsequent experiments.

In Chapter Five, gene expression of M1 microglia markers (*Il-1β, Il-6* and *Tnf-α*) and some M2 microglia markers (*Tgf-β* and *Il-10*) have been characterised in detail. In Chapter Four, the LPS dose response effect was studied at one time point only (2 h) and across six LPS concentrations, while in Chapter Five, the dose response effect was studied in three time points (2, 6 and 24 h) and across nine LPS concentrations to increase the confidence in calculated pEC50.

It was demonstrated in this chapter that there is a dose response at 2, 6 and 24 h for all M1 markers. LPS showed less potency at 24 h for Il-β (Figure 5-5A) and the maximum dose response was lower at 24 h for both *Il-1β* and *Tnf-α* (Figure 5-5B; Figure 5-9B) but not *Il-6* (Figure 5-7B). The decrease in maximum response might be due to the shift in EC50 value. Or, LPS high concentration might lead to the risk of cytotoxicity, which could give a "bell shaped" dose response curve. There is a suggestion of this, for example, when we

examine the dose-responsive increase in *Tnf-a* expression after 24 h LPS exposure. Here, expression at the highest LPS concentrations is lower than the maximal effect seen with slightly lower concentration, suggestive of an interaction between the concentration and duration of LPS exposure, potentially leading to cell death. This could have been explored using direct measurements of cell number at the end of the experiment, or indirect measures of cell viability such as the MTT assay (Gerlier & Thomasset 1986) or the LDH assay (Korzeniewski & Callewaert 1983). In agreement with this assumption, Woodroofe *et al.* (1991) have reported that Il-1β protein production decreased by 21% when LPS concentration was increased from 1 to 5 µg/ml. *Tgf-β* showed no dose response at any time point, as expected. *Il-10* showed a dose response at 6 and 24 h but not at 2 h. This possibly delayed response (compared to *Il-1β, Il-6* and *Tnf-α*) may indicate a secondary response to M1 activation (and so cytokine secretion) as LPS induces the production the pro-inflammatory cytokine *Il-6*, which induces the (delayed) expression of the *Il-10* gene (Lynch *et al.* 2004).

The early steps in the development of an *in vitro* model to study M0' (primed microglia) gene expression was carried out in this study (Chapter Five). The first part of this chapter showed that 10 ng/ml LPS for 6 h induced a robust microglia response. Therefore, this concentration and time point were chosen to study the effect of a repeated dose of LPS. The recovery period (4 days between doses) was sufficient for microglia to lose M1 phenotype, with all M1 genes returning to baseline levels by this time point (Figure 5-15). In this study, a repeated dose of LPS had no effect on microglia behaviour (Figure 5-16). However, contradictory observations have been reported by other researchers (Deng *et al.* 2013; Schaafsma *et al.* 2015). In line with this study, Deng *et al.* (2013) have reported that stimulating macrophages with 10 ng/ml LPS resulted in comparable expression of *Il-6* and

Tnf-α upon secondary challenge. In contrast, Schaafsma *et al.* (2015) reported that multiple doses of LPS led to a decrease in the pro-inflammatory gene expression.

In Chapter Six, there was an attempt to fully characterise M2 microglia (in the same way as was used with M1 in Chapter Five) using Il-4 as a stimulus. However, none of the M2-associated genes that might be predicted to be up-regulated were found to be affected by Il-4. Several approaches at troubleshooting were performed to understand why this system did not replicate the literature, but without clear conclusions. Although, literature have not reported that M2 microglia responses were hard to evoke, M1 microglia response were more studied and described in literature than M2.

In Chapter Seven, the *in vitro* model of M1 activation developed earlier was challenged using NPs, a potential vector for drug delivery to the brain. NPs represent a promising tool to treat neurodegenerative disease with immunomodulatory drugs targeting microglia phenotype switching. Therefore, understanding the effects of drug delivery techniques such as NPs on microglial inflammatory responses would be relevant.

This study showed that NPs used here did not induced an immune-response from microglia *in vitro*, which is an important finding since they could provide a safe carrier for many neurodegenerative drugs. In line with this study's results, Wang *et al*. (2011) study showed that treating microglia with iron oxide NPs for 6 h resulted no increase in M1 marker (Il-1β, Il-6 and Tnf-α) protein production. In contrast, Choi *et al.* (2010) study showed that treated microglia with SiNPs (silica-based) resulted in an increase in *Cox-2* and a decrease in *Tnf-α* gene expression. However, SiNPs are chemically different from the NPs used in this study, and it is likely that the chemical composition of these particles will be more important than their size in terms of effects on the phenotype of the microglia, therefore it is

difficult to read too much into this particular observation in terms of the interpretation of our results.

In summary, an *in vitro* model of microglial switching has been refined and validated for M1 responses. Further refinement is necessary to study M2 switching. The NPs data suggested that NPs could be used without unintended inflammatory responses, and further testing is warranted in this regard.

8.2 Microglial phenotype model challenging

There are several challenges were associated with validation of *in vitro* microglia models using qPCR technique

8.2.1 Technical challenges

8.2.1.1 Aged versus neonatal microglia challenge

In this thesis, a model to study microglia was developed using neonatal microglia culture. There are some reports of developmental differences between neonatal and adult/aged microglia, including possible differences in inflammatory responses. Given these reports, studying aged microglia could be advantageous, especially since many neurodegenerative diseases develop with aging (Beal 1995). However, a model to study aged microglia would require large numbers of cells for qPCR (larger than typically yielded per animal). Adult microglia are not cultured as easily as early postnatal, and it was not considered viable to expand their numbers *in vitro* through growth factor drive. Therefore, it would require large number of adult animals to be euthanised and dissected to generate enough microglia for all of the time points and concentrations (treatments) necessary for the detailed studies described in this thesis. This would involve considerable expenditure of

resources, limited the throughput of the experiments, and would be more difficult to justify ethically.

Alternative methods were investigated to generate large numbers of adult microglia, including pilot studies involving seeding dissociated adult cortex on neonatal astrocyte cultures, a similar strategy was investigated by Masuch *et al.* (2016) using slice cultures. While this was successful in generating large numbers of microglia, it was not straightforward to demonstrate that these were of adult origin, rather than neonatal. Therefore, without a validated protocol for deriving large numbers of adult microglia, this particular research area was not pursued in this thesis. In future, a robust experimental strategy might be to use the neonatal model to generate experimental hypotheses, which could then be further tested in more "realistic", but technically challenging models, such as primary microglia derived from adult or diseased animals; organotypic culture; and/or in *in vivo* models including models of neurodegenerative diseases.

8.2.1.2 Pure microglia culture versus mixed glia or tissue culture challenge

One important purpose of studying microglial behaviour in a high purity *in vitro* system was to explore microglial phenotype/function without the presence of other CNS cells. However, such culture has limitations in comparison to the *in vivo* system, for example microglia responses can be influenced through communication with other cells. Microglia express receptors to communicate with neuronal cells, such as fractalkine–CX3CR1, CD200–CD200R and CD47–CD172 (Loane & Kumar 2016). Hence, it was expected that when microglia are cultured in the absence of such signals their phenotype profile might be different from that present *in vivo*, where cell-cell signalling occurs between cell types. To obtain high value microglial gene expression profiles for each phenotype, high purity microglial cultures are essential (for high confidence that changes are microglia-specific).

Co-culture work could be done in future, to assess whether similar changes are detected. Or, using high purity microglia culture with conditioned media from neuronal and mixed glia culture, could bring the effect of secreted factors of other brain cells on microglia, without cell-cell physical communication (Dai *et al.* 2015).

Using organotypic brain slice cultures to study microglia phenotype have advantages including providing all the CNS cell types and the 3D structure. Organotypic slices could be prepared from different CNS regions by slicing techniques with a usual thickness of 350 – 400 μm (Humpel 2015). Organotypic brain slice cultures can be maintained *in vitro* for several months; these slice cultures could bridge the gap between primary cell culture and pre-clinical animal experimentation (Jenkins 2013). Mertsch *et al.* (2001) reported that treated organotypic retina culture with LPS (100 ng/ml for 24h) have led to microglial activation, as authors assumed that higher levels of Tnf-α, Il-6 and MCP-1 were realised from activated microglia in the culture medium. Furthermore, studies that attempted to characterise microglial activation in organotypic slice culture have used immunohistochemistry (Hailer *et al.* 1996; Czapiga & Colton 1999; Lari & Kitchener 2014).

The slice 'wound' (tissue damaged during the procedure) might induce microgliosis due to the presence of cell debris. These activated microglia may confound investigations into inflammatory responses (Carson *et al.* 2008). Although using such system has many advantages over *in vitro* systems (realistic ECM, 3D) and the *in vivo* culture (the absence of infiltrating peripheral macrophages and blood-derived products leaking into the CNS), but the effects of slice 'wounding' on microglial activation state still need more characterisation.

8.2.1.3 Microglia low RNA yield challenge

One of the issues with studying microglia behaviours using qPCR technique was the small quantity of RNA extracted. This thesis showed that a high density of microglia

should be plated (compared to other cell types) in order to improve RNA yield and purity (Figure 3-11). The fact that microglia cells have low yield per cell limited the number of conditions/experiments that could be tested simultaneously. In line with these results, Mizee *et al.* (2017) reported a significant correlation between the number of human microglia cells used and the RNA yield obtained. The RNA yield was increased from 50 to 200 ng when the microglia cells numbers increased four times (Mizee *et al.* 2017).

8.2.1.4 Statistical analysis challenge

This study aimed to establish an *in vitro* model to study microglia phenotype, mainly using qPCR. In the early stages, several validatory procedures were carried out to ensure accurate qPCR results, such as validation of the reference genes, determining the specificity and efficiency of primers for genes of interest (Chapter three). There are no universally-agreed methods to statistically analyse qPCR results in the literature, which presented a challenge after the data were collected. Advice has been sought from statisticians, with respect to analytical methods.

8.2.2 The effect of different stimuli on M1 microglia challenge

In this thesis, the M1 microglia phenotype was well characterised in three different time points (2, 6 and 24 h) using LPS (Chapter Five). However, none of the other treatments investigated in this study had any obvious effect on M1 microglia behaviour. For example, using serum free media in Chapter four did not significantly change the baseline expression, pEC50 or maximum response of any of M1 markers (*Il-1β, Il-6* and *Tnf-α*). However, LPS was significantly more potent for inducing *Il-1β* expression when microglia were incubated for 6 days in D10 compared to Xvivo (Figure 4-17). None of the other M1 markers (*Il-6* and *Tnf-α*) showed a difference. In Chapter Five, microglia treated with repeated doses of LPS did not altered gene expression levels for M1 markers (Figure 5-16). Finally, in Chapter

Seven, microglia pre-treated with LPS (to induce M1), then challenged with different NPs, showed no difference in expression of iNos protein or nitric oxide, compared to LPS alone.

In line with the results of Chapter Seven, Papa *et al.* (2014) reported that LPS did not affect microglia response to NPs. Mouse microglia were cultured with 1000 ng/ml LPS for 18 h, inducing an M1 phenotype, then LPS was removed and replaced with poly (methyl methacrylate) NPs for 24 h. This resulted no change in Il-6 protein production (both LPS treated cells and LPS-NPs treated cells were significantly higher than non-treated cells; however, there was no difference between LPS and LPS-NPs) (Papa *et al.* 2014). Furthermore, in line with Chapter Five results, Nguyen *et al.* (2004) showed that repeated *in vivo* challenges with LPS (1 mg/kg every 2 weeks for a 3-month period) did not lead to microglial priming, although LPS clearly exacerbated the chronic inflammation associated with M1 microglia phenotype.

Although different stimuli (excepting LPS) used in this study did not produce obvious changes in microglia phenotype, the literature suggested that M1 activation status can be altered by similar treatments. For example, Markoutsa & Xu (2017) reported that pre-treating BV-2 (microglia cell line) with N-acetyl cysteine -NPs for 3 h, inhibited the subsequent activation by 100 ng/ml LPS, as detected by decreased production of ROS, RNS, Tnf-α, and Il-1β. Furthermore, several studies reported that pre-treated microglia with LPS strongly reduced pro-inflammatory cytokines Il-1β, Il-6 and Tnf-α, as compared with single stimulation (Ajmone-Cat *et al.* 2003; Cacci *et al.* 2008; Wuchert *et al.* 2008).

8.3 Future directions

The findings of this research have been discussed extensively within each relevant chapter, and therefore will not be elucidated further here. However, based on these findings, there are a number of areas in which these approaches could be developed.

1. Further validation could be performed using the shortlist of candidate qPCR reference genes, identified here (section 3.3.3.1). Validation should involve different stimuli (pro-M1, pro-M2 and pro-M0), to determine whether any of these genes may be truly universal reference genes, reliably unaltered by any stimuli. This would include Aβ, α-synuclein and any other disease-associated molecules. Genes that pass these tests could be recommended to the scientific community and would be of high value for cross-laboratory comparisons of qPCR data.
2. It is of great value to work towards serum-free microglial culture, to provide more tightly-controlled experimental conditions over longer time-periods, and possibly facilitate future clinical applications, requiring xeno-free (no animal-derived component) culture conditions. Further research will be required to determine whether serum is affecting microglial responses in other conditions (i.e. besides LPS treatment), or due to previous exposure to serum, before switching to serum-free conditions. That is, if microglia encounter serum during preparation, or earlier culture, the serum could affect the cells, in ways that are not reversed by then switching to serum-free media. This could be investigated by establishing mixed glial cultures in serum free media from the beginning, with one treatment group then being switched to serum, to study the effects. Also, serum may affect different genes to the ones being analysed here. Other techniques could also be used, such as microarray analysis, to evaluate a wide screen of different genes, possibly identifying serum-induced responses that were not identified here.
3. Future work to study M0' should consider/be aware of the 'sub-threshold' theory, that the first stimuli could be not strong enough to induce full M1 activation, but it could prime microglia that would be hyperactive in response to the second stimulus. This could be done by treating microglia with low LPS concentration (e.g., 0.01

ng/ml) known to be insufficient to activate microglia (no increase in M1 markers; as shown in Chapter Five), then after the (4 d) recovery period treat them with second dose of LPS (e.g., 10 ng/ml). Comparisons should focus on whether naïve microglia (no pre-treatment) respond differently to pre-treated (primed) microglia (Figure 8-1).

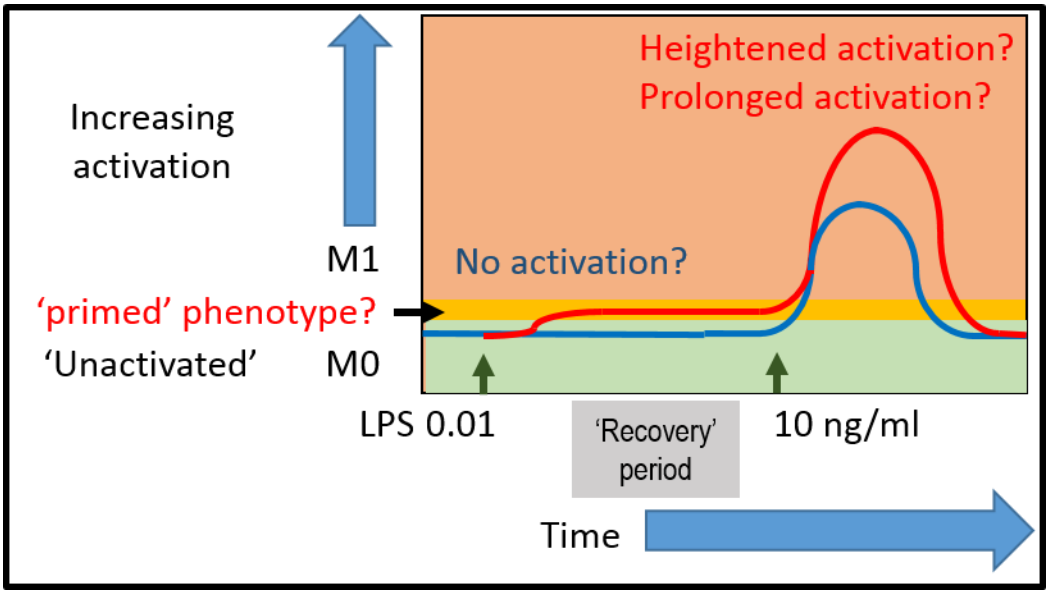

Figure 8-1: Scheme to explain the 'sub-threshold' priming theory. The blue lines indicate the predicted microglial responses if microglia do not alter with 'priming' effects and return to standard M0 states after activation. Treating M0 microglia with low dose of LPS does not induces M1 activation. Second high dose of LPS produces M1 response. However, if priming is simulated in this system, it could be predicted that the low dose of LPS will leave microglia 'primed' (neither M0 nor M1), and these primed microglia may show a greater M1 response on later LPS challenge (red line).

4. More detailed investigations could be performed to study the lack of clear M2 presentation in this system, such as studying the presence of Il-4R at rat microglia surface, and intracellular pathways related to Il-4R. This could be achieved using Western blotting to test the production of STAT6 (Il-4R downstream) (Nguyen & Benveniste 2000). It may be possible that these cells are reacting to Il-4 in this model, but somehow failing to produce the gene expression changes that were anticipated, and so the M2 phenotype is not being detected. Further assays could be done such as measuring the secretion of M2 markers by ELISA. Also, functional assay could be

performed to check if microglia change in ways that are neuroprotective (e.g., transferring microglia-conditioned medium to a neuronal culture, or co-culturing microglia with neurons).

5. Although there is no indication of M1 activation by nanoparticles at the level of gene expression or morphology, it is possible that other subtle changes may be occurring. Therefore, other assays could be used such as microarray which gives more general look at all the other genes. Furthermore, the bacterial endotoxin contamination of NPs should be fully studied before using these NPs in pre-clinical study. Traditional methods to study endotoxin contamination include Limulus amoebocyte lysate (LAL) assay which is a widely used test to quantify the endotoxin in pharmaceutical products and medical devices (Dobrovolskaia 2015). Demonstrating that biomaterials are endotoxin-free is a standard requirement prior to clinical approval. Also, assays should be conducted relating to toxicity outside the brain: e.g., clotting or accumulation of the NPs in other parts of the body such as liver or kidney. Long-term studies will be needed to assess NP fate, and whether NP breakdown products affect microglia, or other neural cells. Therefore, future work should include multiple CNS primary cell culture to estimate NPs cytotoxicity and its effect on the mixed glia culture.

8.4 Summary

This thesis has demonstrated the importance of refinement and validation of *in vitro* models to study microglia phenotype profile using gene expression. Three reference genes have been validated to study rat microglia for the first time which provide an important tool for other researchers for cross-laboratory comparisons of qPCR data. The present of serum in the culture media effect on microglia was studied both in short and long incubation periods (1 and 6 days, respectively), the results showed no evidence of serum influence the M1 activation state, at last over a short incubation period. An *in vitro* model of microglial switching has been refined and validated for M1 responses. Further refinement is necessary to study M2 switching. Additionally, the response of microglia to NPs has been tested, particularly their effect on inflammation state. This study showed that NPs did not induce inflammatory response in microglia, which is a promising finding when considering using these NPs in neuromodulatory therapies targeting microglia.

Appendix 1

Supplementary video files

Legends for supplementary videos

Video 1

Time-lapse phase contrast microscopy of mixed glial culture. Microglia are far more active than other cell types, with sweeping membrane all around the cell. Microglia, astrocytes and oligodendrocyte precursor cells (OPCs; generate oligodendrocytes, which myelinate nerve fibres) are all present. Examples of each are labelled. Culture has stratified, with astrocytes dominating the layer adherent to the culture plastic. Microglia and OPCs are largely on top of this layer. Note that a microglial cell to the right of the image appears to be moving within the astrocyte bed layer, and then emerges. The other microglial cells are highly active, but not travelling. They appear to remain within a 'territory', and extend membrane/processes in all directions, surveilling their immediate environment. A microglial cell in the upper-middle region extends a process down the image, and appears to identify a damaged cell, which it then phagocytoses.

Video 2

Microglia, brain immune cells (Macrophages), in culture. Filmed immediately post-treatment with lipopolysaccharide (LPS, 50 ng/ml; bacterial fragments, simulating infection). 2D, *in vitro*, glass coverslip, poly-D-lysine (PDL) coating / substrate. Note the

morphologies / shapes of the cells, and rates of membrane remodelling. Cells regularly leave a 'tail', a trailing membrane process. Sometimes cells return to the tail's anchorage point; sometimes the tail is retracted. Microglia are highly active, with sweeping membrane all around the cell. Often adopting a 'fried egg' morphology, with a prominent nucleus ('yolk') and surrounding membrane resembling the white of a fried egg. Some processes / branches form, but they are broader, flatter, not as fine, as processes *in vivo* (3D environment). Also note complex interior of microglia: many endosomes, lysosomes etc, containing acids, enzymes for degradation. Time-lapse microscopy; dynamic imaging. *In vitro* brain cells. Ref to filename: Micro TL 50ngml LPS 20fps labelled

Video 3

Microglia, brain immune cells (Macrophages), in culture. Prior to treatment with lipopolysaccharide (LPS; bacterial fragments, simulating infection). 2D, *in vitro*, glass coverslip, poly-D-lysine (PDL) coating / substrate. Note the morphologies / shapes of the cells, and rates of membrane remodelling. Cells regularly leave a 'tail', a trailing membrane process. Sometimes cells return to the tail's anchorage point; sometimes the tail is retracted. Microglia are highly active, with sweeping membrane all around the cell. Often adopting a 'fried egg' morphology, with a prominent nucleus ('yolk') and surrounding membrane resembling the white of a fried egg. Some processes / branches form, but they are broader,

flatter, not as fine, as processes *in vivo* (3D environment). Also note complex interior of microglia: many endosomes, lysosomes etc, containing acids, enzymes for degradation. Time-lapse microscopy; dynamic imaging. *In vitro* brain cells. Ref to filename: Micro TL preLPS 20fps labelled

References

Abbott, N.J. et al., 2010. Structure and function of the blood–brain barrier. *Neurobiology of Disease*, 37(1), pp.13–25.

Abbott, N.J. & Friedman, A., 2012. Overview and introduction: the blood-brain barrier in health and disease. *Epilepsia*, 53 Suppl 6(0 6), pp.1–6.

Abd-El-Basset, E. & Fedoroff, S., 1995. Effect of bacterial wall lipopolysaccharide (LPS) on morphology, motility, and cytoskeletal organization of microglia in cultures. *Journal of Neuroscience Research*, 41(2), pp.222–237.

Acarin, L. et al., 1994. Demonstration of poly-N-acetyl lactosamine residues in ameboid and ramified microglial cells in rat brain by tomato lectin binding. *The journal of histochemistry and cytochemistry : official journal of the Histochemistry Society*, 42(8), pp.1033–41.

Adamiano, A., Iafisco, M. & Tampieri, A., 2018. Magnetic core-shell nanoparticles. In *Core-Shell Nanostructures for Drug Delivery and Theranostics*. Elsevier, pp. 259–296.

Agnihotri, S.A., Mallikarjuna, N.N. & Aminabhavi, T.M., 2004. Recent advances on chitosan-based micro- and nanoparticles in drug delivery. *Journal of Controlled Release*, 100(1), pp.5–28.

Aires, I.D. et al., 2019. Blockade of microglial adenosine A $_{2A}$ receptor suppresses elevated pressure-induced inflammation, oxidative stress, and cell death in retinal cells. *Glia*.

Aizenman, Y. & de Vellis, J., 1987. Brain neurons develop in a serum and glial free environment: effects of transferrin, insulin- insulin-like growth factor-I and thyroid hormone on neuronal survival, growth and differentiation. *Brain Research*, 406(1–2), pp.32–42.

Ajmone-Cat, M.A., Nicolini, A. & Minghetti, L., 2003. Prolonged exposure of microglia to lipopolysaccharide modifies the intracellular signaling pathways and selectively promotes prostaglandin E2 synthesis. *Journal of Neurochemistry*, 87(5), pp.1193–1203.

Al-Sabah, A. et al., 2015. Importance of reference gene selection for articular cartilage mechanobiology studies. *Osteoarthritis and cartilage / OARS, Osteoarthritis Research Society*.

Alexander, C. & Rietschel, E.T., 2001. *Invited review: Bacterial lipopolysaccharides and innate immunity*,

Almolda, B., Gonzalez, B. & Castellano, B., 2011. Antigen presentation in EAE: role of microglia, macrophages and dendritic cells. *Frontiers in bioscience : a journal and virtual library*, 16, pp.1157–1171.

Aloisi, F., 2001. Immune function of microglia. *Glia*, 36(2), pp.165–79.

Aloisi, F. et al., 1998. Microglia are more efficient than astrocytes in antigen processing and in Th1 but not Th2 cell activation. *Journal of immunology (Baltimore, Md. : 1950)*, 160(10), pp.4671–4680.

Alzheimer's Association, 2018. *2018 Alzheimer's disease facts and figures*, Elsevier.

Amado, J. et al., 1995. Blood levels of cytokines in brain-dead patients: Relationship with circulating hormones and acute-phase reactants. *Metabolism*, 44(6), pp.812–816.

Anderson, N.L. et al., 2004. The human plasma proteome: a nonredundant list developed by combination of four separate sources. *Molecular & cellular proteomics : MCP*, 3(4), pp.311–26.

Anderson, N.L. & Anderson, N.G., 2002. The human plasma proteome: history, character, and diagnostic prospects. *Molecular & cellular proteomics : MCP*, 1(11), pp.845–67.

Andersson, U. & Tracey, K.J., 2012. Reflex Principles of Immunological Homeostasis. *Annual Review of Immunology*, 30(1), pp.313–335.

Appel, S.H., Beers, D.R. & Henkel, J.S., 2010. T cell-microglial dialogue in Parkinson's disease and amyotrophic lateral sclerosis: are we listening? *Trends in Immunology*, 31(1), pp.7–17.

Azizi, S.A. et al., 1998. Engraftment and migration of human bone marrow stromal cells implanted in the brains of albino rats--similarities to astrocyte grafts. *Proceedings of the National Academy of Sciences*, 95(7), pp.3908–3913.

Bae, Y.H. & Park, K., 2011. Targeted drug delivery to tumors: myths, reality and

possibility. *Journal of controlled release : official journal of the Controlled Release Society*, 153(3), pp.198–205.

Balakrishnan, K. et al., 2005. Plasma Aβ42 correlates positively with increased body fat in healthy individuals. *Journal of Alzheimer's Disease*, 8(3), pp.269–282.

Ballard, C. et al., 2011. Alzheimer's disease. *Lancet*, 377(9770), pp.1019–31.

Banks, W.A. et al., 2012. Pharmacokinetics and modeling of immune cell trafficking: quantifying differential influences of target tissues versus lymphocytes in SJL and lipopolysaccharide-treated mice. *Journal of Neuroinflammation*, 9(1), p.714.

Barbiero, J.K. et al., 2014. Neuroprotective effects of peroxisome proliferator-activated receptor alpha and gamma agonists in model of parkinsonism induced by intranigral 1-methyl-4-phenyl-1,2,3,6-tetrahyropyridine. *Behavioural Brain Research*, 274, pp.390–399.

Beal, M.F., 1995. Aging, energy, and oxidative stress in neurodegenerative diseases. *Annals of Neurology*, 38(3), pp.357–366.

Becher, B., Bechmann, I. & Greter, M., 2006. Antigen presentation in autoimmunity and CNS inflammation: how T lymphocytes recognize the brain. *Journal of Molecular Medicine*, 84(7), pp.532–543.

Bellavance, M.-A., Blanchette, M. & Fortin, D., 2008. Recent Advances in Blood–Brain Barrier Disruption as a CNS Delivery Strategy. *The AAPS Journal*, 10(1), pp.166–177.

Bennett, A.M., Tonks, N.K. & Bar-Sagi, D., 1997. Regulation of distinct stages of skeletal muscle differentiation by mitogen-activated protein kinases. *Science (New York, N.Y.)*, 278(5341), pp.1288–91.

Bennett, M.L. et al., 2016. New tools for studying microglia in the mouse and human CNS. *Proceedings of the National Academy of Sciences*, 113(12), pp.E1738–E1746.

Beutler, B. & Rietschel, E.T., 2003. Innate immune sensing and its roots: the story of endotoxin. *Nature Reviews Immunology*, 3(2), pp.169–176.

Blaylock, R., 2013. Immunology primer for neurosurgeons and neurologists part 2: Innate brain immunity. *Surgical Neurology International*, 4(1), p.118.

Blaylock, R.L. & Maroon, J., 2011. Immunoexcitotoxicity as a central mechanism in chronic traumatic encephalopathy-A unifying hypothesis. *Surgical neurology international*, 2, p.107.

Boche, D. et al., 2006. TGFβ1 regulates the inflammatory response during chronic neurodegeneration. *Neurobiology of Disease*, 22(3), pp.638–650.

Boche, D. et al., 2003. Transforming Growth Factor-β1-Mediated Neuroprotection against Excitotoxic Injury *in Vivo*. *Journal of Cerebral Blood Flow & Metabolism*, 23(10), pp.1174–1182.

Boche, D., Perry, V.H. & Nicoll, J.A.R., 2013. Review: activation patterns of microglia and their identification in the human brain. *Neuropathology and applied neurobiology*, 39(1), pp.3–18.

Boje, K.M. & Arora, P.K., 1992. Microglial-produced nitric oxide and reactive nitrogen oxides mediate neuronal cell death. *Brain Research*, 587(2), pp.250–256.

Boon, B.D.C. et al., 2018. Neuroinflammation is increased in the parietal cortex of atypical Alzheimer's disease. *Journal of Neuroinflammation*, 15(1), p.170.

Borlongan, C.V. & Emerich, D.F., 2003. Facilitation of drug entry into the CNS via transient permeation of blood brain barrier: laboratory and preliminary clinical evidence from bradykinin receptor agonist, Cereport. *Brain Research Bulletin*, 60(3), pp.297–306.

Bosisio, D. et al., 2002. Stimulation of toll-like receptor 4 expression in human mononuclear phagocytes by interferon-gamma: a molecular basis for priming and synergism with bacterial lipopolysaccharide. *Blood*, 99(9), pp.3427–31.

Brewer, G.J. et al., 1993. Optimized survival of hippocampal neurons in B27-supplemented neurobasal?, a new serum-free medium combination. *Journal of Neuroscience Research*, 35(5), pp.567–576.

Brites, D. & Vaz, A.R., 2014. Microglia centered pathogenesis in ALS: insights in cell interconnectivity. *Frontiers in cellular neuroscience*, 8, p.117.

Brochard, V. et al., 2009. Infiltration of CD4+ lymphocytes into the brain contributes to neurodegeneration in a mouse model of Parkinson disease. *The Journal of clinical investigation*, 119(1), pp.182–92.

Brunner, D. et al., 2010. Serum-free Cell Culture: The Serum-free Media Interactive Online Database. *ALTEX : Alternatives to animal experimentation*, 27(1).

Bruttger, J. et al., 2015. Genetic Cell Ablation Reveals Clusters of Local Self-Renewing Microglia in the Mammalian Central Nervous System. *Immunity*, 43(1), pp.92–106.

Bryan, N.S. & Grisham, M.B., 2007. Methods to detect nitric oxide and its metabolites in biological samples. *Free radical biology & medicine*, 43(5), pp.645–57.

Brydon, L. et al., 2008. Peripheral Inflammation is Associated with Altered Substantia Nigra Activity and Psychomotor Slowing in Humans. *Biological Psychiatry*, 63(11), pp.1022–1029.

Buckley, C.D. et al., 2001. Fibroblasts regulate the switch from acute resolving to chronic persistent inflammation. *Trends in Immunology*, 22(4), pp.199–204.

Buechler, C. et al., 2000. Regulation of scavenger receptor CD163 expression in human monocytes and macrophages by pro- and antiinflammatory stimuli. *Journal of Leukocyte Biology*, 67(1), pp.97–103.

Busch, S.A. & Silver, J., 2007. The role of extracellular matrix in CNS regeneration. *Current Opinion in Neurobiology*, 17(1), pp.120–127.

Bustin, S.A., 2000. Absolute quantification of mRNA using real-time reverse transcription polymerase chain reaction assays. *Journal of molecular endocrinology*, 25(2), pp.169–93.

Bustin, S.A. et al., 2009. The MIQE guidelines:Minimum Information for publication of quantitative real-time PCR experiments. *Clinical Chemistry*, 55(4), pp.611–622.

Butovsky, O. et al., 2014. Identification of a unique TGF-β-dependent molecular and functional signature in microglia. *Nature neuroscience*, 17(1), pp.131–43.

Butovsky, O. et al., 2015. Targeting miR-155 restores abnormal microglia and attenuates disease in SOD1 mice. *Annals of neurology*, 77(1), pp.75–99.

Cacci, E. et al., 2008. In vitro neuronal and glial differentiation from embryonic or adult neural precursor cells are differently affected by chronic or acute activation of microglia. *Glia*, 56(4), pp.412–425.

Calvo, P. et al., 2001. Long-Circulating PEGylated Polycyanoacrylate Nanoparticles as

New Drug Carrier for Brain Delivery. *Pharmaceutical Research*, 18(8), pp.1157–1166.

Calvo, P. et al., 2002. Quantification and localization of PEGylated polycyanoacrylate nanoparticles in brain and spinal cord during experimental allergic encephalomyelitis in the rat. *The European journal of neuroscience*, 15(8), pp.1317–26.

Cammermeyer, J., 1966. Morphologic distinctions between oligodendrocytes and microglia cells in the rabbit cerebral cortex. *American Journal of Anatomy*, 118(1), pp.227–247.

Carlson, N.G. et al., 1999. Inflammatory cytokines IL-1 alpha, IL-1 beta, IL-6, and TNF-alpha impart neuroprotection to an excitotoxin through distinct pathways. *Journal of immunology (Baltimore, Md. : 1950)*, 163(7), pp.3963–8.

Carson, M.J. et al., 2007. A rose by any other name? The potential consequences of microglial heterogeneity during CNS health and disease. *Neurotherapeutics : the journal of the American Society for Experimental NeuroTherapeutics*, 4(4), pp.571–9.

Carson, M.J., Crane, J. & Xie, A.X., 2008. Modeling CNS microglia: the quest to identify predictive models. *Drug discovery today. Disease models*, 5(1), pp.19–25.

Carter, G.C. et al., 2011. HIV-1 infects macrophages by exploiting an endocytic route dependent on dynamin, Rac1 and Pak1. *Virology*, 409(2), pp.234–250.

Carty, M. & Bowie, A.G., 2011. Evaluating the role of Toll-like receptors in diseases of the central nervous system. *Biochemical pharmacology*, 81(7), pp.825–37.

Cengelli, F. et al., 2006. Interaction of functionalized superparamagnetic iron oxide nanoparticles with brain structures. *The Journal of pharmacology and experimental therapeutics*, 318(1), pp.108–16.

Chabot, S. et al., 2002. Cytokine production in T lymphocyte–microglia interaction is attenuated by glatiramer acetate: a mechanism for therapeutic efficacy in multiple sclerosis. *Multiple Sclerosis*, 8(4), pp.299–306.

Chandra, S. et al., 2005. Alpha-synuclein cooperates with CSPalpha in preventing neurodegeneration. *Cell*, 123(3), pp.383–96.

Chao, C.C. et al., 1992. Cytokine Release from Microglia: Differential Inhibition by

Pentoxifylline and Dexamethasone. *Journal of Infectious Diseases*, 166(4), pp.847–853.

Chao, C.C. et al., 1994. Human microglial cell defense against Toxoplasma gondii. The role of cytokines. *Journal of immunology (Baltimore, Md. : 1950)*, 152(3), pp.1246–52.

Chao, C.C.C. et al., 1995. Interleukin-1 and tumor necrosis factor-alpha synergistically mediate neurotoxicity: involvement of nitric oxide and of N-methyl-D-aspartate receptors. *Brain, behavior, and immunity*, 9(4), pp.355–365.

Chen, G. et al., 2016. Nanochemistry and Nanomedicine for Nanoparticle-based Diagnostics and Therapy. *Chemical Reviews*, 116(5), pp.2826–2885.

Chen, Y. et al., 2008. NS21: Re-defined and modified supplement B27 for neuronal cultures. *Journal of Neuroscience Methods*, 171(2), pp.239–247.

Cherry, J.D.J.J.D. et al., 2014. Neuroinflammation and M2 microglia: the good, the bad, and the inflamed. *Journal of neuroinflammation*, 11(1), p.98.

Cherukuri, P., Glazer, E.S. & Curley, S.A., 2010. Targeted hyperthermia using metal nanoparticles. *Advanced Drug Delivery Reviews*, 62(3), pp.339–345.

Chhor, V. et al., 2013. Characterization of phenotype markers and neuronotoxic potential of polarised primary microglia in vitro. *Brain, behavior, and immunity*, 32, pp.70–85.

Chi, B. et al., 2018. *Experimental and therapeutic medicine.*, [Spandidos Pub.].

Choi, J. et al., 2010. Silica-based nanoparticle uptake and cellular response by primary microglia. *Environmental health perspectives*, 118(5), pp.589–95.

Colton, C.A., 2009. Heterogeneity of microglial activation in the innate immune response in the brain. *Journal of neuroimmune pharmacology : the official journal of the Society on NeuroImmune Pharmacology*, 4(4), pp.399–418.

Colton, C.A. et al., 1992. Regulation of microglial function by interferons. *Journal of Neuroimmunology*, 40(1), pp.89–98.

Combrinck, M.I., Perry, V.H. & Cunningham, C., 2002. Peripheral infection evokes exaggerated sickness behaviour in pre-clinical murine prion disease. *Neuroscience*, 112(1), pp.7–11.

Crain, J.M., Nikodemova, M. & Watters, J.J., 2013. Microglia express distinct M1 and M2 phenotypic markers in the postnatal and adult central nervous system in male and female mice. *Journal of neuroscience research*, 91(9), pp.1143–51.

Cunningham, C. et al., 2005. Central and systemic endotoxin challenges exacerbate the local inflammatory response and increase neuronal death during chronic neurodegeneration. *The Journal of neuroscience : the official journal of the Society for Neuroscience*, 25(40), pp.9275–84.

Cunningham, C. et al., 2009. Systemic Inflammation Induces Acute Behavioral and Cognitive Changes and Accelerates Neurodegenerative Disease. *BIOL PSYCHIATRY*, 65(4), pp.304–312.

Czapiga, M. & Colton, C.A., 1999. Function of microglia in organotypic slice cultures. *Journal of Neuroscience Research*, 56(6), pp.644–651.

Dai, X. et al., 2015. Activation of BV2 microglia by lipopolysaccharide triggers an inflammatory reaction in PC12 cell apoptosis through a toll-like receptor 4-dependent pathway. *Cell stress & chaperones*, 20(2), pp.321–31.

Daldrup-Link, H.E. et al., 2011. MRI of tumor-associated macrophages with clinically applicable iron oxide nanoparticles. *Clinical cancer research : an official journal of the American Association for Cancer Research*, 17(17), pp.5695–704.

van Dam, A.-M. et al., 1992. Appearance of interleukin-1 in macrophages and in ramified microglia in the brain of endotoxin-treated rats: a pathway for the induction of non-specific symptoms of sickness? *Brain Research*, 588(2), pp.291–296.

Dantzer, R. et al., 2008. From inflammation to sickness and depression: when the immune system subjugates the brain. *Nature Reviews Neuroscience*, 9(1), pp.46–56.

Davalos, D. et al., 2005. ATP mediates rapid microglial response to local brain injury in vivo. *Nature neuroscience*, 8(6), pp.752–8.

David, S. & Kroner, A., 2011. Repertoire of microglial and macrophage responses after spinal cord injury. *Nature reviews. Neuroscience*, 12(7), pp.388–99.

Davidson, B.L. & Breakefield, X.O., 2003. Viral vectors for gene delivery to the nervous system. *Nature Reviews Neuroscience*, 4(5), pp.353–364.

Davis, E.J., Foster, T.D. & Thomas, W.E., 1994. Cellular forms and functions of brain microglia. *Brain research bulletin*, 34(1), pp.73–8.

Delgado, R. et al., 1998. Melanocortin peptides inhibit production of proinflammatory cytokines and nitric oxide by activated microglia; Melanocortin peptides inhibit production of proinflammatory cytokines and nitric oxide by activated microglia. *Journal of Leukocyte Biology*, 63, pp.470–475.

Deng, H. et al., 2013. Molecular mechanism responsible for the priming of macrophage activation. *Journal of Biological Chemistry*, 288(6), pp.3897–3906.

Derecki, N.C. et al., 2010. Regulation of learning and memory by meningeal immunity: a key role for IL-4. *The Journal of experimental medicine*, 207(5), pp.1067–80.

Dobrovolskaia, M.A. et al., 2008. Preclinical Studies To Understand Nanoparticle Interaction with the Immune System and Its Potential Effects on Nanoparticle Biodistribution. *Molecular Pharmaceutics*, 5(4), pp.487–495.

Donath, M.Y. & Shoelson, S.E., 2011. Type 2 diabetes as an inflammatory disease. *Nature Reviews Immunology*, 11(2), pp.98–107.

Donegan, J.J. et al., 2014. A Novel Role for Brain Interleukin-6: Facilitation of Cognitive Flexibility in Rat Orbitofrontal Cortex. *The Journal of Neuroscience*, 34(3), pp.953–962.

Dong, X., 2018. Current Strategies for Brain Drug Delivery. *Theranostics*, 8(6), pp.1481–1493.

Doolittle, N.D. et al., 2000. Safety and efficacy of a multicenter study using intraarterial chemotherapy in conjunction with osmotic opening of the blood-brain barrier for the treatment of patients with malignant brain tumors. *Cancer*, 88(3), pp.637–647.

Dormont, D., 1999. Transmissible spongiform encephalopathy agents and animal sera. *Developments in biological standardization*, 99, pp.25–34.

Dorothée, G., 2018. Neuroinflammation in neurodegeneration: role in pathophysiology, therapeutic opportunities and clinical perspectives. *Journal of Neural Transmission*, 125, pp.749–750.

Duell, B.L. et al., 2011. Epithelial cell coculture models for studying infectious diseases:

benefits and limitations. *Journal of biomedicine & biotechnology*, 2011, p.852419.

Dumbacher, J., 2013. How to Increase the Quality and Quantity of your RNA Extractions | Biocompare Bench Tips. Available at: https://www.biocompare.com/Bench-Tips/128790-Four-Tips-for-Perfecting-RNA-Isolation/ [Accessed March 26, 2018].

East, E., Golding, J.P. & Phillips, J.B., 2009. A versatile 3D culture model facilitates monitoring of astrocytes undergoing reactive gliosis. *Journal of Tissue Engineering and Regenerative Medicine*, 3(8), pp.634–646.

ElAli, A., Thériault, P. & Rivest, S., 2014. The Role of Pericytes in Neurovascular Unit Remodeling in Brain Disorders. *International Journal of Molecular Sciences*, 15(4), pp.6453–6474.

English, C. & Aloi, J.J., 2015. New FDA-Approved Disease-Modifying Therapies for Multiple Sclerosis. *Clinical Therapeutics*, 37(4), pp.691–715.

Ensign, L.M. et al., 2012. Mucus-Penetrating Nanoparticles for Vaginal Drug Delivery Protect Against Herpes Simplex Virus. *Science Translational Medicine*, 4(138), p.138ra79-138ra79.

Everaert, B.R. et al., 2011. Importance of suitable reference gene selection for quantitative real-time PCR: special reference to mouse myocardial infarction studies. *PloS one*, 6(8), p.e23793.

Fan, L.-W. et al., 2005. Minocycline attenuates lipopolysaccharide-induced white matter injury in the neonatal rat brain. *Neuroscience*, 133(1), pp.159–168.

Fenn, A.M. et al., 2014. IL-4 Signaling Drives a Unique Arginase+/IL-1 + Microglia Phenotype and Recruits Macrophages to the Inflammatory CNS: Consequences of Age-Related Deficits in IL-4R after Traumatic Spinal Cord Injury. *Journal of Neuroscience*, 34(26), pp.8904–8917.

Fenn, A.M. et al., 2014. Immune activation promotes depression 1 month after diffuse brain injury: a role for primed microglia. *Biological psychiatry*, 76(7), pp.575–84.

Fenn, A.M. et al., 2012. Lipopolysaccharide-induced interleukin (IL)-4 receptor-α expression and corresponding sensitivity to the M2 promoting effects of IL-4 are impaired in microglia of aged mice. *Brain, behavior, and immunity*, 26(5), pp.766–77.

Ferreira, S.A. & Romero-Ramos, M., 2018. Microglia Response During Parkinson's Disease: Alpha-Synuclein Intervention. *Frontiers in Cellular Neuroscience*, 12(August), p.247.

Fetler, L. & Amigorena, S., 2005. Neuroscience. Brain under surveillance: the microglia patrol. *Science (New York, N.Y.)*, 309(5733), pp.392–3.

Fielda, R. et al., 2010. Systemic challenge with the TLR3 agonist poly I:C induces amplified IFNα/β and IL-1β responses in the diseased brain and exacerbates chronic neurodegeneration. *Brain, Behavior, and Immunity*, 24(6), pp.996–1007.

Fleige, G. et al., 2001. Magnetic Labeling of Activated Microglia in Experimental Gliomas 1. *Neoplasia*, 3, pp.489–499.

Flohé, S. et al., 1999. ENDOTOXIN TOLERANCE IN RATS: EXPRESSION OF TNF-α, IL-6, IL-10, VCAM-1 AND HSP 70 IN LUNG AND LIVER DURING ENDOTOXIN SHOCK. *Cytokine*, 11(10), pp.796–804.

Franciosi, S. et al., 2005. IL-8 enhancement of amyloid-beta (Aβ1-42)-induced expression and production of pro-inflammatory cytokines and COX-2 in cultured human microglia. *Journal of Neuroimmunology*, 159(1), pp.66–74.

Franco, R. & Fernández-Suárez, D., 2015. Alternatively activated microglia and macrophages in the central nervous system. *Progress in Neurobiology*, 131, pp.65–86.

Frank, M.G. et al., 2006. Rapid isolation of highly enriched and quiescent microglia from adult rat hippocampus: Immunophenotypic and functional characteristics. *Journal of Neuroscience Methods*, 151(2), pp.121–130.

Freilich, R.W., Woodbury, M.E. & Ikezu, T., 2013. Integrated expression profiles of mRNA and miRNA in polarized primary murine microglia. *PloS one*, 8(11), p.e79416.

Freshney, R.I., 2005. Serum-Free Media. In *Culture of Animal Cells*. Hoboken, NJ, USA: John Wiley & Sons, Inc.

Fu, R. et al., 2014. Phagocytosis of microglia in the central nervous system diseases. *Molecular neurobiology*, 49(3), pp.1422–34.

Fumagalli, S. et al., 2015. The Ischemic Environment Drives Microglia and Macrophage

Function. *Frontiers in Neurology*, 6, p.81.

Gabathuler, R., 2010. Approaches to transport therapeutic drugs across the blood–brain barrier to treat brain diseases. *Neurobiology of Disease*, 37(1), pp.48–57.

Gadani, S.P. et al., 2012. IL-4 in the brain: a cytokine to remember. *Journal of immunology (Baltimore, Md. : 1950)*, 189(9), pp.4213–9.

Galatro, T.F. et al., 2017. Transcriptomic analysis of purified human cortical microglia reveals age-associated changes. *Nature Neuroscience*, 20(8), pp.1162–1171.

Galea, I., Bechmann, I. & Perry, V.H., 2007. What is immune privilege (not)? *Trends in Immunology*, 28(1), pp.12–18.

GAO, H.-M. et al., 2003. Critical role of microglial NADPH oxidase-derived free radicals in the in vitro MPTP model of Parkinson's disease. *The FASEB Journal*, 17(13), pp.1954–1956.

Gao, H.-M. & Hong, J.-S., 2008. Why neurodegenerative diseases are progressive: uncontrolled inflammation drives disease progression. *Trends in Immunology*, 29(8), pp.357–365.

García, K.P. et al., 2014. Zwitterionic-Coated "Stealth" Nanoparticles for Biomedical Applications: Recent Advances in Countering Biomolecular Corona Formation and Uptake by the Mononuclear Phagocyte System. *Small*, 10(13), pp.2516–2529.

Gensel, J.C. & Zhang, B., 2015. Macrophage activation and its role in repair and pathology after spinal cord injury. *Brain research*, 1619, pp.1–11.

Gerlier, D. & Thomasset, N., 1986. Use of MTT colorimetric assay to measure cell activation. *Journal of Immunological Methods*, 94(1–2), pp.57–63.

Ghosh, S., May, M.J. & Kopp, E.B., 1998. NF-κB AND REL PROTEINS: Evolutionarily Conserved Mediators of Immune Responses. *Annual Review of Immunology*, 16(1), pp.225–260.

Gibbons, H.M. & Dragunow, M., 2006. Microglia induce neural cell death via a proximity-dependent mechanism involving nitric oxide. *Brain Research*, 1084(1), pp.1–15.

Gillardon, F., Schmid, R. & Draheim, H., 2012. Parkinson's disease-linked leucine-rich repeat kinase 2(R1441G) mutation increases proinflammatory cytokine release from

activated primary microglial cells and resultant neurotoxicity. *Neuroscience*, 208, pp.41–48.

Giri, S. et al., 2004. 5-aminoimidazole-4-carboxamide-1-beta-4-ribofuranoside inhibits proinflammatory response in glial cells: a possible role of AMP-activated protein kinase. *The Journal of neuroscience : the official journal of the Society for Neuroscience*, 24(2), pp.479–87.

Giulian, D. et al., 1986. Characterization of ameboid microglia isolated from developing mammalian brain. *The Journal of neuroscience : the official journal of the Society for Neuroscience*, 6(8), pp.2163–78.

Giunti, D. et al., 2014. Can we switch microglia's phenotype to foster neuroprotection? Focus on multiple sclerosis. *Immunology*, 141(3), pp.328–39.

Gjedde, A. & Crone, C., 1983. Biochemical Modulation of Blood-Brain Barrier Permeability. In Springer, Berlin, Heidelberg, pp. 59–74.

Glare, E.M. et al., 2002. β-Actin and GAPDH housekeeping gene expression in asthmatic airways is variable and not suitable for normalising mRNA levels. *Thorax*, 57, pp.765–770.

Glenn, J.A. et al., 1992. Characterisation of ramified microglial cells: detailed morphology, morphological plasticity and proliferative capability. *Journal of anatomy*, 180 (Pt 1, pp.109–18.

Godbout, J.P. et al., 2005. Exaggerated neuroinflammation and sickness behavior in aged mice following activation of the peripheral innate immune system. *FASEB journal : official publication of the Federation of American Societies for Experimental Biology*, 19(10), pp.1329–31.

Gorczynski, R. et al., 2004. CD200 Is a Ligand for All Members of the CD200R Family of Immunoregulatory Molecules. *The Journal of Immunology*, 172(12), pp.7744–7749.

Gordon, S., 2003. Alternative activation of macrophages. *Nature reviews. Immunology*, 3(1), pp.23–35.

Gordon, S. & Martinez, F.O., 2010. Alternative activation of macrophages: mechanism and functions. *Immunity*, 32(5), pp.593–604.

De Graaf, M.T. et al., 2011. Flow Cytometric Characterization of Cerebrospinal Fluid Cells. *Cytometry Part B (Clinical Cytometry)*, 80, pp.271–281.

Green, D.R. & Beere, H.M., 2000. Apoptosis. Gone but not forgotten. *Nature*, 405(6782), pp.28–9.

Gstraunthaler, G., Lindl, T. & van der Valk, J., 2013. A plea to reduce or replace fetal bovine serum in cell culture media. *Cytotechnology*, 65(5), pp.791–793.

Guerrero, J. & Reiter, R., 2002. Melatonin-Immune System Relationships. *Current Topics in Medicinal Chemistry*, 2(2), pp.167–179.

Gupta, A.K. & Wells, S., 2004. Surface-Modified Superparamagnetic Nanoparticles for Drug Delivery: Preparation, Characterization, and Cytotoxicity Studies. *IEEE Transactions on Nanobioscience*, 3(1), pp.66–73.

Gururaja, T.L. et al., 2007. Class of Small Molecules that Inhibit TNFa-Induced Survival and Death Pathways via Prevention of Interactions between TNFaRI, TRADD, and RIP1. *cell press*, 14, pp.1105–1118.

Hailer, N.P., Grampp, A. & Nitsch, R., 1999. Proliferation of microglia and astrocytes in the dentate gyrus following entorhinal cortex lesion: a quantitative bromodeoxyuridine-labelling study. *The European journal of neuroscience*, 11(9), pp.3359–64.

Hailer, N.P., J**?**rhult, J.D. & Nitsch, R., 1996. Resting microglial cells in vitro: Analysis of morphology and adhesion molecule expression in organotypic hippocampal slice cultures. *Glia*, 18(4), pp.319–331.

Haley, M.J. et al., 2017. Microglial Priming as Trained Immunity in the Brain. *Neuroscience*.

Hanamsagar, R. et al., 2014. 116. Sex differences in microglial morphology and number: Implications for function and behavior. *Brain, Behavior, and Immunity*, 40(2014), p.e34.

Hanisch, U.-K. & Kettenmann, H., 2007. Microglia: active sensor and versatile effector cells in the normal and pathologic brain. *Nature neuroscience*, 10(11), pp.1387–1394.

Hannestad, J. et al., 2012. Endotoxin-induced systemic inflammation activates microglia:

[11C]PBR28 positron emission tomography in nonhuman primates. *NeuroImage*, 63(1), pp.232–239.

Hardy, J. & Selkoe, D.J., 2002. The amyloid hypothesis of Alzheimer's disease: progress and problems on the road to therapeutics. *Science (New York, N.Y.)*, 297(5580), pp.353–6.

Harrison, N.A. et al., 2009. Inflammation Causes Mood Changes Through Alterations in Subgenual Cingulate Activity and Mesolimbic Connectivity. *Biological Psychiatry*, 66(5), pp.407–414.

Harry, G.J., 2013. Microglia during development and aging. *Pharmacology and Therapeutics*, 139(3), pp.313–326.

Häusler, K.G. et al., 2002. Interferon-γ differentially modulates the release of cytokines and chemokines in lipopolysaccharide- and pneumococcal cell wall-stimulated mouse microglia and macrophages. *European Journal of Neuroscience*, 16(11), pp.2113–2122.

Haynes, S.E. et al., 2006. The P2Y12 receptor regulates microglial activation by extracellular nucleotides. *Nature neuroscience*, 9(12), pp.1512–9.

Hefendehl, J.K. et al., 2014. Homeostatic and injury-induced microglia behavior in the aging brain. *Aging cell*, 13(1), pp.60–9.

Hellemans, J. et al., 2007. qBase relative quantification framework and software for management and automated analysis of real-time quantitative PCR data. *Genome biology*, 8(2), p.R19.

Hellwig, S. et al., 2016. Altered microglia morphology and higher resilience to stress-induced depression-like behavior in CX3CR1-deficient mice. *Brain, Behavior, and Immunity*, 55, pp.126–137.

Henriksen, P.A. et al., 2004. Gene delivery of the elastase inhibitor elafin protects macrophages from neutrophil elastase-mediated impairment of apoptotic cell recognition. *FEBS Letters*, 574(1–3), pp.80–84.

Hervé, F., Ghinea, N. & Scherrmann, J.-M., 2008. CNS Delivery Via Adsorptive Transcytosis. *The AAPS Journal*, 10(3), pp.455–472.

Hickman, S.E. et al., 2013. The microglial sensome revealed by direct RNA sequencing. *Nature Neuroscience*, 16(12), pp.1896–1905.

Hickman, S.E., Allison, E.K. & El Khoury, J., 2008. Microglial dysfunction and defective beta-amyloid clearance pathways in aging Alzheimer's disease mice. *The Journal of neuroscience : the official journal of the Society for Neuroscience*, 28(33), pp.8354–60.

Hirohashi, N. & Morrison, D.C., 1996. Low-dose lipopolysaccharide (LPS) pretreatment of mouse macrophages modulates LPS-dependent interleukin-6 production in vitro. *Infection and immunity*, 64(3), pp.1011–5.

Hoeijmakers, L. et al., 2016. Microglial Priming and Alzheimer's Disease: A Possible Role for (Early) Immune Challenges and Epigenetics? *Frontiers in Human Neuroscience*, 10, p.398.

Hofheinz, R.-D. et al., 2005. Liposomal encapsulated anti-cancer drugs. *Anti-Cancer Drugs*, 16(7), pp.691–707.

Holcomb, I.N. et al., 2000. FIZZ1, a novel cysteine-rich secreted protein associated with pulmonary inflammation, defines a new gene family. *The EMBO Journal*, 19(15), pp.4046–4055.

Holtman, I.R. et al., 2015. Induction of a common microglia gene expression signature by aging and neurodegenerative conditions: a co-expression meta-analysis. *Acta Neuropathologica Communications*, 3(1), p.31.

Hong, Z. et al., 2010. DJ-1 and α-synuclein in human cerebrospinal fluid as biomarkers of Parkinson's disease. *Brain*, 133(3), pp.713–726.

Horvath, R.J. et al., 2008. Differential migration, LPS-induced cytokine, chemokine, and NO expression in immortalized BV-2 and HAPI cell lines and primary microglial cultures. *Journal of neurochemistry*, 107(2), pp.557–69.

Hu, R. et al., 2009. Evaluation of putative reference genes for gene expression normalization in soybean by quantitative real-time RT-PCR. *BMC Molecular Biology*, 10(1), p.93.

Hu, X. et al., 2012. Microglia/Macrophage Polarization Dynamics Reveal Novel Mechanism of Injury Expansion After Focal Cerebral Ischemia. *Stroke*, 43(11),

pp.3063–3070.

Huh, S.H. et al., 2011. Ethyl pyruvate rescues nigrostriatal dopaminergic neurons by regulating glial activation in a mouse model of Parkinson's disease. *Journal of immunology (Baltimore, Md. : 1950)*, 187(2), pp.960–9.

Humpel, C., 2015. Organotypic brain slice cultures: A review. *Neuroscience*, 305, pp.86–98.

Hung, S. et al., 2002. Transient expression of Ym1, a heparin-binding lectin, during developmental hematopoiesis and inflammation. *Journal of Leukocyte Biology*, 72(1), pp.72–82.

Hunot, S. et al., 1999. FcepsilonRII/CD23 is expressed in Parkinson's disease and induces, in vitro, production of nitric oxide and tumor necrosis factor-alpha in glial cells. *The Journal of neuroscience : the official journal of the Society for Neuroscience*, 19(9), pp.3440–7.

Hutter, E. et al., 2010. Microglial Response to Gold Nanoparticles. *ACS Nano*, 4(5), pp.2595–2606.

Hyun R Kim, † et al., 2007. Translocation of Poly(ethylene glycol-co-hexadecyl)cyanoacrylate Nanoparticles into Rat Brain Endothelial Cells: Role of Apolipoproteins in Receptor-Mediated Endocytosis.

Italiani, P. & Boraschi, D., 2014. From Monocytes to M1/M2 Macrophages: Phenotypical vs. Functional Differentiation. *Frontiers in Immunology*, 5, p.514.

Ito, D. et al., 1998. Microglia-specific localisation of a novel calcium binding protein, Iba1. *Molecular Brain Research*, 57(1), pp.1–9.

Jana, M., Palencia, C.A. & Pahan, K., 2008. Fibrillar amyloid-beta peptides activate microglia via TLR2: implications for Alzheimer's disease. *Journal of immunology (Baltimore, Md. : 1950)*, 181(10), pp.7254–62.

Janelidze, S. et al., 2018. CSF biomarkers of neuroinflammation and cerebrovascular dysfunction in early Alzheimer disease. *Neurology*, p.10.1212/WNL.0000000000006082.

Jantzen, P.T. et al., 2002. Microglial activation and beta -amyloid deposit reduction caused

by a nitric oxide-releasing nonsteroidal anti-inflammatory drug in amyloid precursor protein plus presenilin-1 transgenic mice. *The Journal of neuroscience : the official journal of the Society for Neuroscience*, 22(6), pp.2246–54.

Jayme, D.W. & Smith, S.R., 2000. Media formulation options and manufacturing process controls to safeguard against introduction of animal origin contaminants in animal cell culture. *Cytotechnology*, 33(1/3), pp.27–36.

Jenkins, S.I., 2013. *Applications of magnetic particles for oligodendrocyte precursor cell transplantation strategies*.

Jenkins, S.I. et al., 2014. Magnetic nanoparticles for oligodendrocyte precursor cell transplantation therapies: progress and challenges. *Molecular and Cellular Therapies*, 2(1), p.23.

Jenkins, S.I. et al., 2016. "Stealth" nanoparticles evade neural immune cells but also evade all major brain cell populations: Implications for PEG-based neurotherapeutics. *Journal of controlled release : official journal of the Controlled Release Society*, 224, pp.136–145.

Jenkins, S.I., Roach, P. & Chari, D.M., 2015. Development of a nanomaterial bio-screening platform for neurological applications. *Nanomedicine: Nanotechnology, Biology, and Medicine*, 11(1), pp.77–87.

Jia, Z. et al., 2016. Active-target T1-weighted MR Imaging of Tiny Hepatic Tumor via RGD Modified Ultra-small Fe3O4 Nanoprobes. *Theranostics*, 6(11), pp.1780–91.

Jiang, H., Harris, M.B. & Rothman, P., 2000. IL-4/IL-13 signaling beyond JAK/STAT. *Journal of Allergy and Clinical Immunology*, 105(6 II), pp.1063–1070.

Jimenez, S. et al., 2008. Inflammatory response in the hippocampus of PS1M146L/APP751SL mouse model of Alzheimer's disease: age-dependent switch in the microglial phenotype from alternative to classic. *The Journal of neuroscience : the official journal of the Society for Neuroscience*, 28(45), pp.11650–61.

Jin, Q. et al., 2014. Improvement of functional recovery by chronic metformin treatment is associated with enhanced alternative activation of microglia/macrophages and increased angiogenesis and neurogenesis following experimental stroke. *Brain, Behavior, and Immunity*, 40, pp.131–142.

Jing Chen , Jessica B. Buchanan , Nathan L. Sparkman , Jonathan P. Godbout , Gregory G. Freund, R.W.J., 2008. Neuroinflammation and disruption in working memory in aged mice after acute stimulation of the peripheral innate immune system. *Brain, Behavior, and Immunity*, 22(3), pp.301–311.

Jungkind, D.L., DiRenzo, S.A. & Young, S.J., 1986. Effect of using heat-inactivated serum with the Abbott human T-cell lymphotropic virus type III antibody test. *Journal of clinical microbiology*, 23(2), pp.381–2.

Kamphuis, W. et al., 2001. Prostanoid receptor gene expression profile in human trabecular meshwork: a quantitative real-time PCR approach. *Investigative ophthalmology & visual science*, 42(13), pp.3209–15.

Kaneko, Y. et al., 1989. Ferritin immunohistochemistry as a marker for microglia. *Acta Neuropathologica*, 79(2), pp.129–136.

Kang, Z. et al., 2010. Astrocyte-Restricted Ablation of Interleukin-17-Induced Act1-Mediated Signaling Ameliorates Autoimmune Encephalomyelitis. *Immunity*, 32(3), pp.414–425.

Karimzadeh, I. et al., 2017. Superparamagnetic Iron Oxide (Fe_3O_4) Nanoparticles Coated with PEG/PEI for Biomedical Applications: A Facile and Scalable Preparation Route Based on the Cathodic Electrochemical Deposition Method. *Advances in Physical Chemistry*, 2017, pp.1–7.

Kawahara, K. et al., 2012. Intracerebral microinjection of interleukin-4/interleukin-13 reduces β-amyloid accumulation in the ipsilateral side and improves cognitive deficits in young amyloid precursor protein 23 mice. *Neuroscience*, 207, pp.243–260.

Kawai, T. et al., 1999. Unresponsiveness of MyD88-Deficient Mice to Endotoxin. *Immunity*, 11(1), pp.115–122.

Kempuraj, D. et al., 2016. Neuroinflammation Induces Neurodegeneration. *Journal of neurology, neurosurgery and spine*, 1(1).

Kenakin, T.P., 2014. *A pharmacology primer : techniques for more effective and strategic drug discovery* Fourth edi.,

Kierdorf, K. et al., 2013. Microglia emerge from erythromyeloid precursors via Pu.1- and Irf8-dependent pathways. *Nature neuroscience*, 16(3), pp.273–80.

Kigerl, K.A. et al., 2009. Identification of two distinct macrophage subsets with divergent effects causing either neurotoxicity or regeneration in the injured mouse spinal cord. *The Journal of neuroscience : the official journal of the Society for Neuroscience*, 29(43), pp.13435–44.

Kim, Y., Caldwell, J. & Bellamkonda, ravi v., 2009. Nanoparticle-mediated local delivery of methylprednisolone after spinal cord injury. *Biomaterials*, 30(13), pp.2582–2590.

Kim, Y.S. et al., 2007. A pivotal role of matrix metalloproteinase-3 activity in dopaminergic neuronal degeneration via microglial activation. *FASEB journal : official publication of the Federation of American Societies for Experimental Biology*, 21(1), pp.179–87.

Kitazawa, M. et al., 2005. Lipopolysaccharide-Induced Inflammation Exacerbates Tau Pathology by a Cyclin-Dependent Kinase 5-Mediated Pathway in a Transgenic Model of Alzheimer's Disease. *Journal of Neuroscience*, 25(39), pp.8843–8853.

Kiyota, T. et al., 2012. AAV serotype 2/1-mediated gene delivery of anti-inflammatory interleukin-10 enhances neurogenesis and cognitive function in APP+PS1 mice. *Gene therapy*, 19(7), pp.724–33.

Kiyota, T. et al., 2010. CNS expression of anti-inflammatory cytokine interleukin-4 attenuates Alzheimer's disease-like pathogenesis in APP+PS1 bigenic mice. *The FASEB Journal*, 24(8), pp.3093–3102.

Kleiner, G. et al., 2013. Cytokine levels in the serum of healthy subjects. *Mediators of inflammation*, 2013, p.434010.

Kloss, C.U.A. et al., 2001. Effect of Lipopolysaccharide on the Morphology and Integrin Immunoreactivity of Ramified Microglia in the Mouse Brain and in Cell Culture. *Experimental Neurology*, 168(1), pp.32–46.

Kobayashi, K. et al., 2013. Minocycline selectively inhibits M1 polarization of microglia. *Cell death & disease*, 4, p.e525.

Kolodziejski, P.J., Koo, J.-S. & Eissa, N.T., 2004. Regulation of inducible nitric oxide synthase by rapid cellular turnover and cotranslational down-regulation by dimerization inhibitors. *Proceedings of the National Academy of Sciences*, 101(52), pp.18141–18146.

Korzeniewski, C. & Callewaert, D.M., 1983. An enzyme-release assay for natural cytotoxicity. *Journal of Immunological Methods*, 64(3), pp.313–320.

Koso, H. et al., 2016. Conditional rod photoreceptor ablation reveals *Sall1* as a microglial marker and regulator of microglial morphology in the retina. *Glia*, 64(11), pp.2005–2024.

Kremlev, S.G., Roberts, R.L. & Palmer, C., 2004. Differential expression of chemokines and chemokine receptors during microglial activation and inhibition. *Journal of neuroimmunology*, 149(1–2), pp.1–9.

Kreutzberg, G.W., 1996. Microglia: a sensor for pathological events in the CNS. *Trends in Neurosciences*, 19(8), pp.312–318.

Lalatsa, A. & Butt, A.M., 2018. *Physiology of the Blood–Brain Barrier and Mechanisms of Transport Across the BBB*, Elsevier Inc.

van Landeghem, F.K.H. et al., 2009. Post-mortem studies in glioblastoma patients treated with thermotherapy using magnetic nanoparticles. *Biomaterials*, 30(1), pp.52–57.

De Lange, E., 2012. Understanding the influence of drug-target binding kinetics on drug effects to improve drug discovery View project Aging and the blood brain barrier, View project. *Current Pharmaceutical Biotechnology*, 13.

LaPlaca, M. et al., 2010. *Methods in Bioengineering: 3D Tissue Engineering*,

Lappas, M. et al., 2002. Nuclear Factor Kappa B Regulation of Proinflammatory Cytokines in Human Gestational Tissues In Vitro1. *Biology of Reproduction*, 67(2), pp.668–673.

Lari, R. & Kitchener, P.D., 2014. *The Application of Organotypic Brain Slice Culture to Study Microglial Differentiation by Lycopersicon esculentum and Sambucus nigra Lectin Histochemistry*,

Larson, S.J. & Dunn, A.J., 2001. Behavioral Effects of Cytokines. *Brain, Behavior, and Immunity*, 15(4), pp.371–387.

Lawson, L.J. et al., 1990. Heterogeneity in the distribution and morphology of microglia in the normal adult mouse brain. *Neuroscience*, 39(1), pp.151–70.

Ledeboer, A. et al., 2000. Interleukin-10, interleukin-4, and transforming growth factor-beta differentially regulate lipopolysaccharide-induced production of pro-

inflammatory cytokines and nitric oxide in co-cultures of rat astroglial and microglial cells. *Glia*, 30(2), pp.134–42.

Lee, C. et al., 2016. Biodegradable Nitrogen-Doped Carbon Nanodots for Non-Invasive Photoacoustic Imaging and Photothermal Therapy. *Theranostics*, 6(12), pp.2196–2208.

Lee, D.C. et al., 2013. Review: experimental manipulations of microglia in mouse models of Alzheimer's pathology: activation reduces amyloid but hastens tau pathology. *Neuropathology and applied neurobiology*, 39(1), pp.69–85.

Lee, L.J., 2006. Polymer Nanoengineering for Biomedical Applications. *Annals of Biomedical Engineering*, 34(1), pp.75–88.

Lee, S. et al., 2014. A small molecule binding HMGB1 and HMGB2 inhibits microglia-mediated neuroinflammation. *Nature Chemical Biology*, 10(12), pp.1055–1060.

Lee, S.C. et al., 1993. Cytokine production by human fetal microglia and astrocytes. Differential induction by lipopolysaccharide and IL-1 beta. *Journal of immunology (Baltimore, Md. : 1950)*, 150(7), pp.2659–67.

Lehnardt, S. et al., 2003. Activation of innate immunity in the CNS triggers neurodegeneration through a Toll-like receptor 4-dependent pathway. *Proceedings of the National Academy of Sciences of the United States of America*, 100(14), pp.8514–9.

Lennon, D.P., Edmison, J.M. & Caplan, A.I., 2001. Cultivation of rat marrow-derived mesenchymal stem cells in reduced oxygen tension: Effects on in vitro and in vivo osteochondrogenesis. *Journal of Cellular Physiology*, 187(3), pp.345–355.

Lenz, K.M. et al., 2013. Microglia are essential to masculinization of brain and behavior. *The Journal of neuroscience : the official journal of the Society for Neuroscience*, 33(7), pp.2761–72.

Lenz, K.M. & McCarthy, M.M., 2015. A Starring Role for Microglia in Brain Sex Differences. *The Neuroscientist*, 21(3), pp.306–321.

León, P. et al., 1992. Interleukin 1 and Its Relationship to Endotoxin Tolerance. *Archives of Surgery*, 127(2), p.146.

Letiembre, M. et al., 2009. Screening of innate immune receptors in neurodegenerative diseases: a similar pattern. *Neurobiology of aging*, 30(5), pp.759–68.

Lewis, T.L. et al., 2010. Overexpression of human apolipoprotein A-I preserves cognitive function and attenuates neuroinflammation and cerebral amyloid angiopathy in a mouse model of Alzheimer disease. *The Journal of biological chemistry*, 285(47), pp.36958–68.

Li, H., Cuzner, M.L. & Newcombe, J., 1996. Microglia-derived macrophages in early multiple sclerosis plaques. *Neuropathology and Applied Neurobiology*, 22(3), pp.207–215.

Li, J., Tang, Y. & Cai, D., 2012. IKKβ/NF-κB disrupts adult hypothalamic neural stem cells to mediate a neurodegenerative mechanism of dietary obesity and pre-diabetes. *Nature cell biology*, 14(10), pp.999–1012.

Li, M. et al., 2007. Glucocorticoids impair microglia ability to induce T cell proliferation and Th1 polarization. *Immunology Letters*, 109(2), pp.129–137.

Li, S.-D. & Huang, L., 2010. Stealth nanoparticles: high density but sheddable PEG is a key for tumor targeting. *Journal of controlled release : official journal of the Controlled Release Society*, 145(3), pp.178–81.

Li, X. et al., 2009. Glia activation induced by peripheral administration of aluminum oxide nanoparticles in rat brains. *Nanomedicine: Nanotechnology, Biology and Medicine*, 5(4), pp.473–479.

Li, Z. et al., 2019. Exosomes derived from mesenchymal stem cells attenuate inflammation and demyelination of the central nervous system in EAE rats by regulating the polarization of microglia. *International Immunopharmacology*, 67, pp.268–280.

Lian, H. et al., 2016. Astrocyte-Microglia Cross Talk through Complement Activation Modulates Amyloid Pathology in Mouse Models of Alzheimer's Disease. *The Journal of neuroscience : the official journal of the Society for Neuroscience*, 36(2), pp.577–89.

Liao, B. et al., 2012. Transformation from a neuroprotective to a neurotoxic microglial phenotype in a mouse model of ALS. *Experimental neurology*, 237(1), pp.147–52.

Liddelow, S.A. et al., 2017. Neurotoxic reactive astrocytes are induced by activated

microglia. *Nature*, 541(7638), pp.481–487.

Ling, E.A. & Wong, W.C., 1993. The origin and nature of ramified and amoeboid microglia: a historical review and current concepts. *Glia*, 7(1), pp.9–18.

Lipinski, C.A. et al., 2001. *Experimental and computational approaches to estimate solubility and permeability in drug discovery and development q settings*,

Lisak, R.P. et al., 2009. Differential effects of Th1, monocyte/macrophage and Th2 cytokine mixtures on early gene expression for molecules associated with metabolism, signaling and regulation in central nervous system mixed glial cell cultures. *Journal of neuroinflammation*, 6, p.4.

Lisi, L. et al., 2014. Proinflammatory-activated glioma cells induce a switch in microglial polarization and activation status, from a predominant M2b phenotype to a mixture of M1 and M2a/B polarized cells. *ASN neuro*, 6(3), pp.171–83.

Liu, B., 2006. Modulation of microglial pro-inflammatory and neurotoxic activity for the treatment of Parkinson's disease. *The AAPS journal*, 8(3), pp.E606-21.

Liu, D. et al., 2011. Anti-inflammatory effects of fluoxetine in lipopolysaccharide(LPS)-stimulated microglial cells. *Neuropharmacology*, 61(4), pp.592–599.

Liu, H.-C.C. et al., 2012. N9 microglial cells polarized by LPS and IL4 show differential responses to secondary environmental stimuli. *Cellular Immunology*, 278(1–2), pp.84–90.

Liu, L., Martin, R. & Chan, C., 2013. Palmitate-activated astrocytes via serine palmitoyltransferase increase BACE1 in primary neurons by sphingomyelinases. *Neurobiology of Aging*, 34(2), pp.540–550.

Liu, R. et al., 2017. Role of neuroinflammation in ischemic stroke. *Neuroimmunology and Neuroinflammation*, 4(8), p.158.

Liu, Y. et al., 2005. LPS receptor (CD14): a receptor for phagocytosis of Alzheimer's amyloid peptide. *Brain*, 128(8), pp.1778–1789.

Livak, K.J. & Schmittgen, T.D., 2001. Analysis of relative gene expression data using real-time quantitative PCR and the 2(-Delta Delta C(T)) Method. *Methods (San Diego, Calif.)*, 25(4), pp.402–408.

Livak, K.J. & Schmittgen, T.D., 2001. Analysis of Relative Gene Expression Data Using Real-Time Quantitative PCR and the 2−ΔΔCT Method. *Methods*, 25(4), pp.402–408.

Loane, D.J. et al., 2014. Progressive neurodegeneration after experimental brain trauma: association with chronic microglial activation. *Journal of neuropathology and experimental neurology*, 73(1), pp.14–29.

Loane, D.J. & Kumar, A., 2016. Microglia in the TBI brain: The good, the bad, and the dysregulated. *Experimental Neurology*, 275, pp.316–327.

Lobo-Silva, D. et al., 2016. Balancing the immune response in the brain: IL-10 and its regulation. *Journal of neuroinflammation*, 13(1), p.297.

Long, T.C. et al., 2007. Nanosize titanium dioxide stimulates reactive oxygen species in brain microglia and damages neurons in vitro. *Environmental health perspectives*, 115(11), pp.1631–7.

Long, T.C. et al., 2006. Titanium Dioxide (P25) Produces Reactive Oxygen Species in Immortalized Brain Microglia (BV2): Implications for Nanoparticle Neurotoxicity †. *ENVIRONMENTAL SCIENCE & TECHNOLOGY*, 40(14), pp.4346–4352.

López-Quintela, M. et al., 2003. *SYNTHESIS OF NANOPARTICLES IN MICROEMULSIONS*,

Lorenzo, A. et al., 1994. Pancreatic islet cell toxicity of amylin associated with type-2 diabetes mellitus. *Nature*, 368(6473), pp.756–760.

Löscher, W. & Potschka, H., 2005. Role of drug efflux transporters in the brain for drug disposition and treatment of brain diseases. *Progress in Neurobiology*, 76(1), pp.22–76.

Louveau, A. et al., 2015. Targeting the CD80/CD86 costimulatory pathway with CTLA4-Ig directs microglia toward a repair phenotype and promotes axonal outgrowth. *Glia*, 63(12), pp.2298–312.

Lucin, K.M. & Wyss-Coray, T., 2009. Immune Activation in Brain Aging and Neurodegeneration: Too Much or Too Little? *Neuron*, 64(1), pp.110–122.

Lue, L.F. et al., 2001. Inflammatory repertoire of Alzheimer's disease and nondemented elderly microglia in vitro. *Glia*, 35(1), pp.72–9.

Lynch, A.M. et al., 2004. Lipopolysaccharide-induced increase in signalling in hippocampus is abrogated by IL-10 - a role for IL-1β? *Journal of Neurochemistry*, 88(3), pp.635–646.

Lynch, M.A., 2014. The impact of neuroimmune changes on development of amyloid pathology; relevance to Alzheimer's disease. *Immunology*, 141(3), pp.292–301.

Lyons, A. et al., 2007. CD200 ligand receptor interaction modulates microglial activation in vivo and in vitro: a role for IL-4. *The Journal of neuroscience : the official journal of the Society for Neuroscience*, 27(31), pp.8309–13.

Lysle, D.T. et al., 1999. Endogenous opioids regulate the expression of inducible nitric oxide synthase by splenocytes. *The Journal of pharmacology and experimental therapeutics*, 288(2), pp.502–8.

Ma, L. & Chung, W.K., 2014. Quantitative analysis of copy number variants based on real-time LightCycler PCR. *Current protocols in human genetics / editorial board, Jonathan L. Haines ... [et al.]*, 80, p.Unit 7.21.

Malam, Y., Loizidou, M. & Seifalian, A.M., 2009. Liposomes and nanoparticles: nanosized vehicles for drug delivery in cancer. *Trends in Pharmacological Sciences*, 30(11), pp.592–599.

Mandrekar-Colucci, S. & Landreth, G.E., 2010. Microglia and inflammation in Alzheimer's disease. *CNS & neurological disorders drug targets*, 9(2), pp.156–67.

Manocha, G.D. et al., 2017. Defining the contribution of neuroinflammation to Parkinson's disease in humanized immune system mice. *Molecular Neurodegeneration*, 12(1), p.17.

Mantovani, A. et al., 2002. Macrophage polarization: tumor-associated macrophages as a paradigm for polarized M2 mononuclear phagocytes. *Trends in Immunology*, 23(11), pp.549–555.

Mantovani, A. et al., 2004. The chemokine system in diverse forms of macrophage activation and polarization. *Trends in immunology*, 25(12), pp.677–86.

Markoutsa, E. & Xu, P., 2017. Redox Potential-Sensitive *N* -Acetyl Cysteine-Prodrug Nanoparticles Inhibit the Activation of Microglia and Improve Neuronal Survival. *Molecular Pharmaceutics*, 14(5), pp.1591–1600.

Martinez, F.O. et al., 2006. Transcriptional Profiling of the Human Monocyte-to-Macrophage Differentiation and Polarization: New Molecules and Patterns of Gene Expression. *The Journal of Immunology*, 177(10), pp.7303–7311.

Masciopinto, F. et al., 2012. Effects of long-term treatment with pioglitazone on cognition and glucose metabolism of PS1-KI, 3xTg-AD and wild-type mice. *Cell Death & Disease*, 3(12), pp.e448–e448.

Masliah, E. et al., 1991. Immunoreactivity of CD45, a protein phosphotyrosine phosphatase, in Alzheimer's disease. *Acta Neuropathologica*, 83(1), pp.12–20.

Masuch, A. et al., 2016. Microglia replenished OHSC: A culture system to study *in vivo* like adult microglia. *Glia*, 64(8), pp.1285–1297.

Mayer, A.M. et al., 2001. Effect of a short-term in vitro exposure to the marine toxin domoic acid on viability, tumor necrosis factor-alpha, matrix metalloproteinase-9 and superoxide anion release by rat neonatal microglia. *BMC Pharmacology*, 1(1), p.7.

McCarthy, G.M. et al., 2017. CNS cell-type localization and LPS response of TLR signaling pathways. *F1000Research*, 6, p.1144.

McCarthy, K.D. & de Vellis, J., 1980. Preparation of separate astroglial and oligodendroglial cell cultures from rat cerebral tissue. *J. Cell Biol.*, 85(3), pp.890–902.

McColl, B.W., Rothwell, N.J. & Allan, S.M., 2007. Systemic inflammatory stimulus potentiates the acute phase and CXC chemokine responses to experimental stroke and exacerbates brain damage via interleukin-1- and neutrophil-dependent mechanisms. *The Journal of neuroscience : the official journal of the Society for Neuroscience*, 27(16), pp.4403–4412.

McCormick, S.M. & Heller, N.M., 2015a. Commentary: IL-4 and IL-13 receptors and signaling. *Cytokine*, 75(1), pp.38–50.

McCormick, S.M. & Heller, N.M., 2015b. Regulation of Macrophage, Dendritic Cell, and Microglial Phenotype and Function by the SOCS Proteins. *Frontiers in Immunology*, 6, p.549.

McGeer, P.L. et al., 1988. Reactive microglia are positive for HLA-DR in the substantia nigra of Parkinson's and Alzheimer's disease brains. *Neurology*, 38(8), pp.1285–

1285.

Mcnay, E.C., Mccarty, R.C. & Gold, P.E., 2001. Fluctuations in Brain Glucose Concentration during Behavioral Testing: Dissociations between Brain Areas and between Brain and Blood. *Neurobiology of Learning and Memory*, 75, pp.325–337.

Mecha, M. et al., 2015. Endocannabinoids drive the acquisition of an alternative phenotype in microglia. *Brain, behavior, and immunity*, 49, pp.233–45.

Medina, C. et al., 2007. Nanoparticles: pharmacological and toxicological significance. *British Journal of Pharmacology*, 150, pp.552–558.

Medzhitov, R., 2008. Origin and physiological roles of inflammation. *Nature*, 454(7203), pp.428–435.

Mertsch, K. et al., 2001. Characterization of microglial cells and their response to stimulation in an organotypic retinal culture system. *The Journal of Comparative Neurology*, 431(2), pp.217–227.

Michelucci, A. et al., 2009. Characterization of the microglial phenotype under specific pro-inflammatory and anti-inflammatory conditions: Effects of oligomeric and fibrillar amyloid-beta. *Journal of neuroimmunology*, 210(1–2), pp.3–12.

Miki, Y. et al., 2012. The advantages of co-culture over mono cell culture in simulating in vivo environment. *The Journal of Steroid Biochemistry and Molecular Biology*, 131(3–5), pp.68–75.

Mills, C.D. et al., 2000. Paradigm M-1/M-2 Macrophages and the Th1/Th2. *J Immunol*, 164, pp.6166–6173.

Minelli, A. et al., 2000. Ammonium triggers calcium elevation in cultured mouse microglial cells by initiating Ca2+ release from thapsigargin-sensitive intracellular stores. *Pflügers Archiv - European Journal of Physiology*, 439(3), pp.370–377.

Minogue, A.M., Barrett, J.P. & Lynch, M.A., 2012. LPS-induced release of IL-6 from glia modulates production of IL-1β in a JAK2-dependent manner. *Journal of neuroinflammation*, 9, p.126.

Mizee, M.R. et al., 2017. Isolation of primary microglia from the human post-mortem brain: effects of ante- and post-mortem variables. *Acta Neuropathologica*

Communications, 5(1), p.16.

Modi, G., Pillay, V. & Choonara, Y.E., 2010. Advances in the treatment of neurodegenerative disorders employing nanotechnology. *Annals of the New York Academy of Sciences*, 1184(1), pp.154–172.

Moehle, M.S. et al., 2012. LRRK2 inhibition attenuates microglial inflammatory responses. *The Journal of neuroscience : the official journal of the Society for Neuroscience*, 32(5), pp.1602–11.

Molina, J.A. et al., 2002. Cerebrospinal fluid levels of insulin in patients with Alzheimer's disease. *Acta neurologica Scandinavica*, 106(6), pp.347–50.

Montgomery, S.L. et al., 2013. Chronic Neuron- and Age-Selective Down-Regulation of TNF Receptor Expression in Triple-Transgenic Alzheimer Disease Mice Leads to Significant Modulation of Amyloid- and Tau-Related Pathologies. *The American Journal of Pathology*, 182(6), pp.2285–2297.

Moran, L.B., Duke, D.C. & Graeber, M.B., 2007. The microglial gene regulatory network activated by interferon-gamma. *Journal of neuroimmunology*, 183(1–2), pp.1–6.

Moreno, B. et al., 2011. Systemic inflammation induces axon injury during brain inflammation. *Annals of Neurology*, 70(6), pp.932–942.

Morris, S.M., 2004. Recent advances in arginine metabolism. *Current Opinion in Clinical Nutrition and Metabolic Care*, 7(1), pp.45–51.

Morrison, H.W. & Filosa, J.A., 2013. A quantitative spatiotemporal analysis of microglia morphology during ischemic stroke and reperfusion. *Journal of Neuroinflammation*, 10(1), p.782.

Mosser, D.M., 2003. The many faces of macrophage activation. *Journal of Leukocyte Biology*, 73(2), pp.209–212.

Mosser, D.M. & Edwards, J.P., 2008. Exploring the full spectrum of macrophage activation. *Nature reviews. Immunology*, 8(12), pp.958–69.

Mount, M.P. et al., 2007. Involvement of interferon-gamma in microglial-mediated loss of dopaminergic neurons. *The Journal of neuroscience : the official journal of the Society for Neuroscience*, 27(12), pp.3328–37.

Mouton, P.R. et al., 2002. Age and gender effects on microglia and astrocyte numbers in brains of mice. *Brain Research*, 956(1), pp.30–35.

Mukherjee, S., Ghosh, R.N. & Maxfield, F.R., 1997. Endocytosis. *Physiological reviews*, 77(3), pp.759–803.

Mulder, M. et al., 1998. Reduced Levels of Cholesterol, Phospholipids, and Fatty Acids in Cerebrospinal Fluid of Alzheimer Disease Patients Are Not Related to Apolipoprotein E4. *Alzheimer Disease &amp*, 12(3), pp.198–203.

Munitz, A. et al., 2009. Resistin-Like Molecule Decreases Glucose Tolerance during Intestinal Inflammation. *The Journal of Immunology*, 182(4), pp.2357–2363.

Nagai, A. et al., 2001. Generation and Characterization of Immortalized Human Microglial Cell Lines: Expression of Cytokines and Chemokines. *Neurobiology of disease*, 8(6), pp.1057–68.

Nagamoto-Combs, K. et al., 2007. Prolonged Microgliosis in the Rhesus Monkey Central Nervous System after Traumatic Brain Injury. *Journal of Neurotrauma*, 24(11), pp.1719–1742.

Nair, K.G.S., Ramaiyan, V. & Sukumaran, S.K., 2018. Enhancement of drug permeability across blood brain barrier using nanoparticles in meningitis. *Inflammopharmacology*, 26(3), pp.675–684.

Nair, M.G. et al., 2009. Alternatively activated macrophage-derived RELM-{alpha} is a negative regulator of type 2 inflammation in the lung. *The Journal of experimental medicine*, 206(4), pp.937–52.

Nakamura, Y., Si, Q.S. & Kataoka, K., 1999. Lipopolysaccharide-induced microglial activation in culture: temporal profiles of morphological change and release of cytokines and nitric oxide. *Neuroscience Research*, 35(2), pp.95–100.

Nayak, D., Roth, T.L. & McGavern, D.B., 2014. Microglia development and function. *Annual review of immunology*, 32, pp.367–402.

Neubert, J. et al., 2015. New findings about iron oxide nanoparticles and their different effects on murine primary brain cells. *International journal of nanomedicine*, 10(March 2016), pp.2033–49.

Neumann, H., Kotter, M.R. & Franklin, R.J.M., 2009. Debris clearance by microglia: An essential link between degeneration and regeneration. *Brain*, 132(2), pp.288–295.

Nikodemova, M. & Watters, J.J., 2012. Efficient isolation of live microglia with preserved phenotypes from adult mouse brain. *Journal of Neuroinflammation*, 9(1), p.635.

Nimmerjahn, A., Kirchhoff, F. & Helmchen, F., 2005. Resting microglial cells are highly dynamic surveillants of brain parenchyma in vivo. *Science (New York, N.Y.)*, 308(5726), pp.1314–8.

Niraula, A., Sheridan, J.F. & Godbout, J.P., 2017. Microglia Priming with Aging and Stress. *Neuropsychopharmacology*, 42(1), pp.318–333.

Noda, H. et al., 2013. Fingolimod phosphate promotes the neuroprotective effects of microglia. *Journal of Neuroimmunology*, 256(1–2), pp.13–18.

Nolan, Y. et al., 2005. Role of interleukin-4 in regulation of age-related inflammatory changes in the hippocampus. *The Journal of biological chemistry*, 280(10), pp.9354–62.

Norden, D.M., Muccigrosso, M.M. & Godbout, J.P., 2014. Microglial Priming and Enhanced Reactivity to Secondary Insult in Aging, and Traumatic CNS injury, and Neurodegenerative Disease. *Neuropharmacology*, 96(Pt A), pp.29–41.

Noske, W. et al., 1982. Phagocytotic activity of glial cells in culture. *Experimental Cell Research*, 142(2), pp.437–445.

Nosrati, H. et al., 2017. New advances strategies for surface functionalization of iron oxide magnetic nano particles (IONPs). *Research on Chemical Intermediates*, 43(12), pp.7423–7442.

Novak, M.L. & Koh, T.J., 2013. Phenotypic transitions of macrophages orchestrate tissue repair. *The American journal of pathology*, 183(5), pp.1352–63.

O'Keefe, G.M., Nguyen, V.T. & Benveniste, E.N., 1999. Class II transactivator and class II MHC gene expression in microglia: modulation by the cytokines TGF-β, IL-4, IL-13 and IL-10. *European Journal of Immunology*, 29(4), pp.1275–1285.

Obeso, J.A. et al., 2010. Missing pieces in the Parkinson's disease puzzle. *Nature medicine*, 16(6), pp.653–61.

Ohtsuki, S. & Terasaki, T., 2007. Contribution of Carrier-Mediated Transport Systems to the Blood–Brain Barrier as a Supporting and Protecting Interface for the Brain; Importance for CNS Drug Discovery and Development. *Pharmaceutical Research*, 24(9), pp.1745–1758.

Orihuela, R., McPherson, C. a. & Harry, G.J., 2016. Microglial M1/M2 polarization and metabolic states. *British Journal of Pharmacology*, 173(4), pp.649–665.

Orr, A.G. et al., 2009. Adenosine A2A receptor mediates microglial process retraction. *Nature Neuroscience*, 12(7), pp.872–878.

Ouchi, Y. et al., 2005. Microglial activation and dopamine terminal loss in early Parkinson's disease. *Annals of Neurology*, 57(2), pp.168–175.

Padrós, F., Knudsen, R. & Blasco-Costa, I., 2018. Histopathological characterisation of retinal lesions associated to Diplostomum species (Platyhelminthes: Trematoda) infection in polymorphic Arctic charr Salvelinus alpinus. *International Journal for Parasitology: Parasites and Wildlife*, 7(1), pp.68–74.

Pais, T.F. et al., 2008. Necrotic neurons enhance microglial neurotoxicity through induction of glutaminase by a MyD88-dependent pathway. *Journal of Neuroinflammation*, 5(1), p.43.

Pampaloni, F., Reynaud, E.G. & Stelzer, E.H.K., 2007. The third dimension bridges the gap between cell culture and live tissue. *Nature Reviews Molecular Cell Biology*, 8(10), pp.839–845.

Pan, J. et al., 2015. Malibatol A regulates microglia M1/M2 polarization in experimental stroke in a PPARγ-dependent manner. *Journal of neuroinflammation*, 12(1), p.51.

Pandey, P.K., Kumar Sharma, A. & Gupta, U., 2016. Blood brain barrier: An overview on strategies in drug delivery, realistic in vitro modeling and in vivo live tracking. *Tissue Barriers*.

Papadopoulos, V.E. et al., 2018. Modulation of β-glucocerebrosidase increases α-synuclein secretion and exosome release in mouse models of Parkinson's disease. *Human Molecular Genetics*, 27(10), pp.1696–1710.

Parsons, L.M. & Webb, H.E., 1982. Blood brain barrier disturbance and immunoglobulin G levels in the cerebrospinal fluid of the mouse following peripheral infection with

the demyelinating strain of Semliki Forest virus. *Journal of the neurological sciences*, 57(2–3), pp.307–18.

Parvathenani, L.K. et al., 2003. P2X7 mediates superoxide production in primary microglia and is up-regulated in a transgenic mouse model of Alzheimer's disease. *The Journal of biological chemistry*, 278(15), pp.13309–17.

Pawate, S. & Bagnato, F., 2015. Newer Agents in the Treatment of Multiple Sclerosis. *The Neurologist*, 19(4), pp.104–117.

Peferoen, L.A.N. et al., 2015. Activation status of human microglia is dependent on lesion formation stage and remyelination in multiple sclerosis. *Journal of neuropathology and experimental neurology*, 74(1), pp.48–63.

Peña-Altamira, E. et al., 2016. Changing paradigm to target microglia in neurodegenerative diseases: from anti-inflammatory strategy to active immunomodulation. *Expert Opinion on Therapeutic Targets*, 20(5), pp.627–640.

Pentreath, V.W. et al., 1996. Endotoxins in the blood and cerebrospinal fluid of patients with African sleeping sickness. *Parasitology*, 112(01), p.67.

Perry, V.H., 2010. Contribution of systemic inflammation to chronic neurodegeneration. *Acta Neuropathologica*, 120(3), pp.277–286.

Perry, V.H., Newman, T.A. & Cunningham, C., 2003. The impact of systemic infection on the progression of neurodegenerative disease. *Nature Reviews Neuroscience*, 4(2), pp.103–112.

Perry, V.H., Nicoll, J.A.R. & Holmes, C., 2010. Microglia in neurodegenerative disease. *Nature reviews. Neurology*, 6(4), pp.193–201.

Pesce, J.T. et al., 2009. Arginase-1-expressing macrophages suppress Th2 cytokine-driven inflammation and fibrosis. *PLoS pathogens*, 5(4), p.e1000371.

Petersen, M.A. & Dailey, M.E., 2004. Diverse microglial motility behaviors during clearance of dead cells in hippocampal slices. *Glia*, 46(2), pp.195–206.

Pey, P. et al., 2014. Phenotypic profile of alternative activation marker CD163 is different in Alzheimer's and Parkinson's disease. *Acta neuropathologica communications*, 2, p.21.

Pickard, M.R. et al., 2011. Magnetic Nanoparticle Labeling of Astrocytes Derived for Neural Transplantation. *Tissue Engineering Part C: Methods*, 17(1), pp.89–99.

Pickard, M.R. & Chari, D.M., 2010. Robust uptake of magnetic nanoparticles (MNPs) by central nervous system (CNS) microglia: Implications for particle uptake in mixed neural cell populations. *International Journal of Molecular Sciences*, 11(3), pp.967–981.

Pinkernelle, J. et al., 2012. Magnetic nanoparticles in primary neural cell cultures are mainly taken up by microglia. *BMC Neuroscience*, 13(1), p.32.

Pinteaux-Jones, F. et al., 2008. Myelin-induced microglial neurotoxicity can be controlled by microglial metabotropic glutamate receptors. *Journal of Neurochemistry*, 106(1), pp.442–454.

Pitek, A. S. et al., 2016. Serum albumin 'camouflage' of plant virus based nanoparticles prevents their antibody recognition and enhances pharmacokinetics. *Biomaterials*, 89, pp.89–97.

Plastira, I. et al., 2016. 1-Oleyl-lysophosphatidic acid (LPA) promotes polarization of BV-2 and primary murine microglia towards an M1-like phenotype. *Journal of Neuroinflammation*, 13(1), p.205.

Polazzi, E. & Monti, B., 2010. Microglia and neuroprotection: From in vitro studies to therapeutic applications. *Progress in Neurobiology*, 92(3), pp.293–315.

Ponomarev, E.D. et al., 2005. Development of a culture system that supports adult microglial cell proliferation and maintenance in the resting state. *Journal of Immunological Methods*, 300(1–2), pp.32–46.

Poovaiah, N. et al., 2018. Treatment of neurodegenerative disorders through the blood–brain barrier using nanocarriers. *Nanoscale*, 10(36), pp.16962–16983.

Posadas, I., Monteagudo, S. & Ceña, V., 2016. Nanoparticles for brain-specific drug and genetic material delivery, imaging and diagnosis. *Nanomedicine*, 11(7), pp.833–849.

Possel, H. et al., 2000. Selective upregulation of inducible nitric oxide synthase (iNOS) by lipopolysaccharide (LPS) and cytokines in microglia: In vitro and in vivo studies. *Glia*, 32(1), pp.51–59.

Pott Godoy, M.C., Ferrari, C.C. & Pitossi, F.J., 2010. Nigral neurodegeneration triggered by striatal AdIL-1 administration can be exacerbated by systemic IL-1 expression. *Journal of Neuroimmunology*, 222(1–2), pp.29–39.

Prati, F., De Simone, A., et al., 2015. 3,4-Dihydro-1,3,5-triazin-2(1 *H*)-ones as the First Dual BACE-1/GSK-3β Fragment Hits against Alzheimer's Disease. *ACS Chemical Neuroscience*, 6(10), pp.1665–1682.

Prati, F., De Simone, A., et al., 2015. Multitarget Drug Discovery for Alzheimer's Disease: Triazinones as BACE-1 and GSK-3β Inhibitors. *Angewandte Chemie*, 127(5), pp.1598–1602.

Prince, M. et al., 2013. The global prevalence of dementia: a systematic review and metaanalysis. *Alzheimer's & dementia : the journal of the Alzheimer's Association*, 9(1), p.63–75.e2.

Prinz, M. et al., 2011. Heterogeneity of CNS myeloid cells and their roles in neurodegeneration. *Nature Neuroscience*, 14(10), pp.1227–1235.

Prinz, M. & Priller, J., 2014. Microglia and brain macrophages in the molecular age: from origin to neuropsychiatric disease. *Nature reviews. Neuroscience*, 15(5), pp.300–12.

Psychogios, N. et al., 2011. The Human Serum Metabolome D. Flower, ed. *PLoS ONE*, 6(2), p.e16957.

Puffenbarger, R.A., Boothe, A.C. & Cabral, G.A., 2000. Cannabinoids inhibit LPS-inducible cytokine mRNA expression in rat microglial cells. *Glia*, 29(1), pp.58–69.

Pul, R. et al., 2011. Glatiramer Acetate Modulates TNF-α and IL-10 Secretion in Microglia and Promotes Their Phagocytic Activity. *Journal of Neuroimmune Pharmacology*, 6(3), pp.381–388.

Qiao, X., Cummins, D.J. & Paul, S.M., 2001. Neuroinflammation-induced acceleration of amyloid deposition in the APP ^{V717F} transgenic mouse. *European Journal of Neuroscience*, 14(3), pp.474–482.

Qin, H. et al., 2005. LPS induces CD40 gene expression through the activation of NF- B and STAT-1 in macrophages and microglia. *Blood*, 106(9), pp.3114–3122.

Qin, L. et al., 2002. Microglia enhance β-amyloid peptide-induced toxicity in cortical and

mesencephalic neurons by producing reactive oxygen species. *Journal of Neurochemistry*, 83(4), pp.973–983.

Qin, L. et al., 2013. NADPH oxidase and aging drive microglial activation, oxidative stress, and dopaminergic neurodegeneration following systemic LPS administration. *Glia*, 61(6), pp.855–868.

Querfurth, H.W. & LaFerla, F.M., 2010. Alzheimer's Disease. *New England Journal of Medicine*, 362(4), pp.329–344.

Ramakers, C. et al., 2003. Assumption-free analysis of quantitative real-time polymerase chain reaction (PCR) data. *Neuroscience Letters*, 339(1), pp.62–66.

Ramesh, G., MacLean, A.G. & Philipp, M.T., 2013. Cytokines and Chemokines at the Crossroads of Neuroinflammation, Neurodegeneration, and Neuropathic Pain. *Mediators of Inflammation*, 2013, pp.1–20.

Ramos Robles, B. et al., 2018. Immunoendocrine abnormalities in the male reproductive system during experimental pulmonary tuberculosis. *Tuberculosis*, 109, pp.109–116.

Ransohoff, R.M., 2016. How neuroinflammation contributes to neurodegeneration. *NEUROIMMUNOLOGY*, 353(6301), pp.777–783.

Ransohoff, R.M. & Benveniste, E.N., 1996. *Cytokines and the CNS*, CRC Press.

Ransohoff, R.M. & Perry, V.H., 2009. Microglial Physiology: Unique Stimuli, Specialized Responses. *Annual Review of Immunology*, 27(1), pp.119–145.

Rao, X. et al., 2013. An improvement of the 2ˆ(-delta delta CT) method for quantitative real-time polymerase chain reaction data analysis. *Biostatistics, bioinformatics and biomathematics*, 3(3), pp.71–85.

Rath, M. et al., 2014. Metabolism via Arginase or Nitric Oxide Synthase: Two Competing Arginine Pathways in Macrophages. *Frontiers in immunology*, 5, p.532.

Rayhane, N. et al., 2000. Administration of endotoxin associated with lipopolysaccharide tolerance protects mice against fungal infection. *Infection and immunity*, 68(6), pp.3748–53.

Recklies, A.D., White, C. & Ling, H., 2002. The chitinase 3-like protein human cartilage glycoprotein 39 (HC-gp39) stimulates proliferation of human connective-tissue cells

and activates both extracellular signal-regulated kinase- and protein kinase B-mediated signalling pathways. *The Biochemical journal*, 365(Pt 1), pp.119–26.

Rey-Giraud, F., Hafner, M. & Ries, C.H., 2012. In Vitro Generation of Monocyte-Derived Macrophages under Serum-Free Conditions Improves Their Tumor Promoting Functions M. Rojas, ed. *PLoS ONE*, 7(8), p.e42656.

Rey, C. et al., 2016. Resolvin D1 and E1 promote resolution of inflammation in microglial cells in vitro. *Brain, Behavior, and Immunity*, 55, pp.249–259.

Ridolfi, E. et al., 2013. The Role of the Innate Immune System in Alzheimer's Disease and Frontotemporal Lobar Degeneration: An Eye on Microglia. *Clinical and Developmental Immunology*, 2013, pp.1–11.

Rock, R.B. et al., 2005. Transcriptional response of human microglial cells to interferon-gamma. *Genes and immunity*, 6(8), pp.712–9.

Rogers, J. et al., 1988. Expression of immune system-associated antigens by cells of the human central nervous system: Relationship to the pathology of Alzheimer's disease. *Neurobiology of Aging*, 9, pp.339–349.

Rojo, A.I. et al., 2010. Nrf2 regulates microglial dynamics and neuroinflammation in experimental Parkinson's disease. *Glia*, 58(5), pp.588–598.

Ruth M. Barrientos , Emily A. Higgins, Joseph C. Biedenkapp, David B. Sprunger, Karli J. Wright-Hardesty, Linda R.Watkins, JerryW. Rudy, S.F.M., 2006. Peripheral infection and aging interact to impair hippocampal memory consolidation. *Neurobiology of Aging*, 27(5), pp.723–732.

Saijo, K. & Glass, C.K., 2011. Microglial cell origin and phenotypes in health and disease. *Nature reviews. Immunology*, 11(11), pp.775–87.

Sambrano, G.R. & Steinberg, D., 1995. Recognition of oxidatively damaged and apoptotic cells by an oxidized low density lipoprotein receptor on mouse peritoneal macrophages: role of membrane phosphatidylserine. *Proceedings of the National Academy of Sciences*, 92(5), pp.1396–1400.

SantaLucia, J., 2007. Physical principles and visual-OMP software for optimal PCR design. *Methods in molecular biology (Clifton, N.J.)*, 402, pp.3–34.

Saraiva, C. et al., 2016. Nanoparticle-mediated brain drug delivery: Overcoming blood–brain barrier to treat neurodegenerative diseases. *Journal of Controlled Release*, 235, pp.34–47.

Sarlus, H. & Heneka, M.T., 2017. Microglia in Alzheimer's disease. *Journal of Clinical Investigation*, 127(9), pp.3240–3249.

Sastre, M., Klockgether, T. & Heneka, M.T., 2006. Contribution of inflammatory processes to Alzheimer's disease: molecular mechanisms. *International journal of developmental neuroscience : the official journal of the International Society for Developmental Neuroscience*, 24(2–3), pp.167–76.

Satoh, J.-I., 2017. Gene expression profiles of M1 and M2 microglia characterized by comparative analysis of public datasets. *Clinical & Experimental Neuroimmunology*, 9, pp.124–138.

Sattarahmady, N. et al., 2016. Albumin coated arginine-capped magnetite nanoparticles as a paclitaxel vehicle: Physicochemical characterizations and in vitro evaluation. *Journal of Drug Delivery Science and Technology*, 36, pp.68–74.

Sawada, M. et al., 1993. Expression of cytokine receptors in cultured neuronal and glial cells. *Neuroscience Letters*, 160(2), pp.131–134.

Sawada, M. et al., 1989. Production of tumor necrosis factor-alpha by microglia and astrocytes in culture. *Brain Research*, 491(2), pp.394–397.

Schaafsma, W. et al., 2015. Long-lasting pro-inflammatory suppression of microglia by LPS-preconditioning is mediated by RelB-dependent epigenetic silencing. *Brain, Behavior, and Immunity*, 48, pp.205–21.

Scherrmann, J.-M., 2005. Expression and function of multidrug resistance transporters at the blood–brain barriers. *Expert Opinion on Drug Metabolism & Toxicology*, 1(2), pp.233–246.

Schmid, C.D. et al., 2009. Differential gene expression in LPS/IFNgamma activated microglia and macrophages: in vitro versus in vivo. *Journal of neurochemistry*, 109 Suppl, pp.117–25.

Schmittgen, T.D. & Livak, K.J., 2008. Analyzing real-time PCR data by the comparative CT method. *Nature Protocols*, 3(6), pp.1101–1108.

Schooten, E. et al., 2018. MAGE-A antigens as targets for cancer immunotherapy. *Cancer Treatment Reviews*, 67, pp.54–62.

Schwarz, J.M. & Bilbo, S.D., 2012. Sex, glia, and development: Interactions in health and disease. *Hormones and Behavior*, 62(3), pp.243–253.

Schwarz, J.M., Sholar, P.W. & Bilbo, S.D., 2012. Sex differences in microglial colonization of the developing rat brain. *Journal of Neurochemistry*, 120(6), p.no-no.

Sebastiani, G. et al., 2006. The cAMP-specific phosphodiesterase 4B mediates Aβ-induced microglial activation. *Neurobiology of Aging*, 27(5), pp.691–701.

Seyfert, S., Faulstich, A. & Marx, P., 2004. What determines the CSF concentrations of albumin and plasma-derived IgG? *neurological sciences*, pp.31–33.

Shapira, L. et al., 1994. Porphyromonas gingivalis lipopolysaccharide stimulation of human monocytes: dependence on serum and CD14 receptor. *Oral Microbiology and Immunology*, 9(2), pp.112–117.

Shaterabadi, Z., Nabiyouni, G. & Soleymani, M., 2017. High impact of in situ dextran coating on biocompatibility, stability and magnetic properties of iron oxide nanoparticles. *Materials Science and Engineering: C*, 75, pp.947–956.

Shen, Z. et al., 2018. PEGylated "stealth" nanoparticles and liposomes. *Engineering of Biomaterials for Drug Delivery Systems*, pp.1–26.

Sheng, W.S. et al., 1995. Tumor necrosis factor alpha upregulates human microglial cell production of interleukin-10 in vitro. *Clinical and diagnostic laboratory immunology*, 2(5), pp.604–8.

Shinji, H., Akagawa, K.S. & Yoshida, T., 1994. LPS induces selective translocation of protein kinase C-beta in LPS-responsive mouse macrophages, but not in LPS-nonresponsive mouse macrophages. *Journal of immunology (Baltimore, Md. : 1950)*, 153(12), pp.5760–71.

Shrivastava, K., Gonzalez, P. & Acarin, L., 2012. The immune inhibitory complex CD200/CD200R is developmentally regulated in the mouse brain. *Journal of Comparative Neurology*, 520(12), pp.2657–2675.

Sidor, M.M., Halgren, C.R. & Foster, J. a, 2014. The impact of early life immune

challenge on behavior and microglia during postnatal development. *Inflammation and Cell Signaling*, pp.1–9.

Sierra, A. et al., 2013. Janus-faced microglia: beneficial and detrimental consequences of microglial phagocytosis. *Frontiers in Cellular Neuroscience*, 7.

Sierra, A. et al., 2007. Microglia derived from aging mice exhibit an altered inflammatory profile. *Glia*, 55(4), pp.412–424.

Simard, A.R. et al., 2006. Bone Marrow-Derived Microglia Play a Critical Role in Restricting Senile Plaque Formation in Alzheimer's Disease. *Neuron*, 49(4), pp.489–502.

Singh, R. & Lillard, J.W., 2009. Nanoparticle-based targeted drug delivery. *Experimental and Molecular Pathology*, 86(3), pp.215–223.

Skelly, D.T. et al., 2013. A Systematic Analysis of the Peripheral and CNS Effects of Systemic LPS, IL-1B, TNF-α and IL-6 Challenges in C57BL/6 Mice M. L. Block, ed. *PLoS ONE*, 8(7), p.e69123.

Smith, C. et al., 2013. The neuroinflammatory response in humans after traumatic brain injury. *Neuropathology and Applied Neurobiology*, 39(6), pp.654–666.

Smith, J.A. et al., 2012. Role of pro-inflammatory cytokines released from microglia in neurodegenerative diseases. *Brain research bulletin*, 87(1), pp.10–20.

Smith, M.E., 1999. Phagocytosis of myelin in demyelinative disease: a review. *Neurochemical research*, 24(2), pp.261–8.

Soccio, R.E. et al., 2002. The cholesterol-regulated StarD4 gene encodes a StAR-related lipid transfer protein with two closely related homologues, StarD5 and StarD6. *Proceedings of the National Academy of Sciences*, 99(10), pp.6943–6948.

Söderstjerna, E. et al., 2014. Silver and Gold Nanoparticles Exposure to In Vitro Cultured Retina – Studies on Nanoparticle Internalization, Apoptosis, Oxidative Stress, Glial- and Microglial Activity E. A. Rozhkova, ed. *PLoS ONE*, 9(8), p.e105359.

Sondag, C.M.C. et al., 2009. Beta amyloid oligomers and fibrils stimulate differential activation of primary microglia. *Journal of neuroinflammation*, 6(1), p.1.

Sorgi, C.A. et al., 2012. GM-CSF priming drives bone marrow-derived macrophages to a

pro-inflammatory pattern and downmodulates PGE2 in response to TLR2 ligands. *PloS one*, 7(7), p.e40523.

Spittau, B. et al., 2015. TGFβ1 increases microglia-mediated engulfment of apoptotic cells via upregulation of the milk fat globule-EGF factor 8. *Glia*, 63(1), pp.142–53.

Stansley, B., Post, J. & Hensley, K., 2012. A comparative review of cell culture systems for the study of microglial biology in Alzheimer's disease. *Journal of neuroinflammation*, 9(1), p.115.

Stence, N., Waite, M. & Dailey, M.E., 2001. Dynamics of microglial activation: a confocal time-lapse analysis in hippocampal slices. *Glia*, 33(3), pp.256–66.

Stojiljkovic, M.R. et al., 2019. Phenotypic and functional differences between senescent and aged murine microglia. *Neurobiology of Aging*, 74, pp.56–69.

Stollg, G. & Jander, S., 1999. The role of microglia and macrophages in the pathophysiology of the CNS. *Progress in Neurobiology*, 58(3), pp.233–247.

Stroemer, R.P. & Rothwell, N.J., 1998. Exacerbation of Ischemic Brain Damage by Localized Striatal Injection of Interleukin-1β in the Rat. *Journal of Cerebral Blood Flow & Metabolism*, 18(8), pp.833–839.

Subramaniam, S.R. & Federoff, H.J., 2017. Targeting Microglial Activation States as a Therapeutic Avenue in Parkinson's Disease. *Frontiers in Aging Neuroscience*, 9, p.176.

Sudduth, T.L. et al., 2013. Neuroinflammatory phenotype in early Alzheimer's disease. *Neurobiology of Aging*, 34(4), pp.1051–1059.

Sulzer, D., 2007. Multiple hit hypotheses for dopamine neuron loss in Parkinson's disease. *Trends in neurosciences*, 30(5), pp.244–50.

Sulzer, D. et al., 2017. T cells from patients with Parkinson's disease recognize α-synuclein peptides. *Nature*, 546(7660), pp.656–661.

Sun, T. et al., 2006. Culture of skin cells in 3D rather than 2D improves their ability to survive exposure to cytotoxic agents. *Journal of Biotechnology*, 122(3), pp.372–381.

Suuronen, T. et al., 2006. Characterization of the pro-inflammatory signaling induced by protein acetylation in microglia. *Neurochemistry International*, 49(6), pp.610–618.

Suuronen, T. et al., 2003. Regulation of microglial inflammatory response by histone deacetylase inhibitors. *Journal of Neurochemistry*, 87(2), pp.407–416.

Svec, D. et al., 2015. How good is a PCR efficiency estimate: Recommendations for precise and robust qPCR efficiency assessments. *Biomolecular detection and quantification*, 3, pp.9–16.

Szulzewsky, F. et al., 2015. Glioma-Associated Microglia/Macrophages Display an Expression Profile Different from M1 and M2 Polarization and Highly Express Gpnmb and Spp1. *Plos One*, 10(2), p.e0116644.

Takasuka, N., Tokunaga, T. & Akagawa, K.S., 1991. Preexposure of macrophages to low doses of lipopolysaccharide inhibits the expression of tumor necrosis factor-alpha mRNA but not of IL-1 beta mRNA. *Journal of immunology (Baltimore, Md. : 1950)*, 146(11), pp.3824–30.

Takata, K. et al., 2010. Galantamine-induced amyloid-{beta} clearance mediated via stimulation of microglial nicotinic acetylcholine receptors. *The Journal of biological chemistry*, 285(51), pp.40180–91.

Takata, K. et al., 2012. Microglial Amyloid-β1-40 Phagocytosis Dysfunction Is Caused by High-Mobility Group Box Protein-1: Implications for the Pathological Progression of Alzheimer's Disease. *International journal of Alzheimer's disease*, 2012, p.685739.

Tang, Y. et al., 2014. Jmjd3 is essential for the epigenetic modulation of microglia phenotypes in the immune pathogenesis of Parkinson's disease. *Cell Death & Differentiation*, 21(3), pp.369–380.

Tang, Y. & Le, W., 2015. Differential Roles of M1 and M2 Microglia in Neurodegenerative Diseases. *Molecular neurobiology*, 53(2), pp.1181–1194.

Tansey, F.A. & Cammer, W., 1998. Differential uptake of dextran beads by astrocytes, macrophages and oligodendrocytes in mixed glial-cell cultures from brains of neonatal rats. *Neuroscience Letters*, 248(3), pp.159–162.

Tarca, A.L., Romero, R. & Draghici, S., 2006. Analysis of microarray experiments of gene expression profiling. *American journal of obstetrics and gynecology*, 195(2), pp.373–88.

Taylor, D.L. et al., 2004. Activation of group II metabotropic glutamate receptors underlies

microglial reactivity and neurotoxicity following stimulation with chromogranin A, a peptide up-regulated in Alzheimer's disease. *Journal of Neurochemistry*, 82(5), pp.1179–1191.

Taylor, R. a. & Sansing, L.H., 2013. Microglial responses after ischemic stroke and intracerebral hemorrhage. *Clinical and Developmental Immunology*, 2013(Figure 1).

Temsamani, J. & Vidal, P., 2004. The use of cell-penetrating peptides for drug delivery. *Drug Discovery Today*, 9(23), pp.1012–1019.

Thaler, J.P. et al., 2012. Obesity is associated with hypothalamic injury in rodents and humans. *The Journal of clinical investigation*, 122(1), pp.153–62.

Thanos, S., Mey, J. & Wild, M., 1993. Treatment of the Adult Retina with Microglia-suppressing Factors Retards Axotomy-induced Neuronal Degradation and Enhances Axonal Regeneration in viva and in vitro. *The Journal of Neuroscience*, 13(2), pp.455–466.

Thellin, O. et al., 1999. Housekeeping genes as internal standards: use and limits. *Journal of Biotechnology*, 75(2–3), pp.291–295.

Thomas, T. & Thomas, T.J., 2001. Polyamines in cell growth and cell death: molecular mechanisms and therapeutic applications. *Cellular and Molecular Life Sciences*, 58(2), pp.244–258.

Thurgur, H. & Pinteaux, E., 2018. Microglia in the Neurovascular Unit: Blood–Brain Barrier–microglia Interactions After Central Nervous System Disorders. *Neuroscience*.

Tichopad, A. et al., 2003. Standardized determination of real-time PCR ef®ciency from a single reaction set-up. *Nucleic Acids Research*, 31(20), p.122.

Tickle, J.A., 2017. *Engineering neural cells in implantable materials SUBMISSION OF THESIS FOR A RESEARCH DEGREE*. keele.

Tiraboschi, J. et al., 2016. Cerebrospinal luid viral escape and acute encephalitis in a patient on boosted protease inhibitor monotherapy. *Antiviral Therapy*, 21(5), pp.461–464.

Toescu, E.. et al., 1998. Long-term activation of capacitative Ca2+ entry in mouse

microglial cells. *Neuroscience*, 86(3), pp.925–935.

Torres-Platas, S.G. et al., 2014. Evidence for increased microglial priming and macrophage recruitment in the dorsal anterior cingulate white matter of depressed suicides. *Brain, behavior, and immunity*, 42, pp.50–9.

Tremblay, M.-È., Lowery, R.L. & Majewska, A.K., 2010. Microglial interactions with synapses are modulated by visual experience. *PLoS biology*, 8(11), p.e1000527.

Triarhou, L.C., Del Cerro, M. & Herndon, R.M., 1985. Ultrastructural evidence for phagocytosis by oligodendroglia. *Neuroscience Letters*, 53(2), pp.185–189.

Tröscher, A.R. et al., 2019. Microglial nodules provide the environment for pathogenic T cells in human encephalitis. *Acta Neuropathologica*, pp.1–17.

Tsou, Y.H. et al., 2017. Drug Delivery to the Brain across the Blood–Brain Barrier Using Nanomaterials. *Small*, 13(43), pp.1–17.

Ulevitch, R.J. & Tobias, P.S., 1999. Recognition of Gram-negative bacteria and endotoxin by the innate immune system. *Current Opinion in Immunology*, 11(1), pp.19–22.

Upadhyay, R.K., 2014. Drug delivery systems, CNS protection, and the blood brain barrier. *BioMed research international*, 2014, p.869269.

van der Valk, J. et al., 2004. The humane collection of fetal bovine serum and possibilities for serum-free cell and tissue culture. *Toxicology in Vitro*, 18(1), pp.1–12.

Varnum, M.M. & Ikezu, T., 2012. The classification of microglial activation phenotypes on neurodegeneration and regeneration in Alzheimer's disease brain. *Archivum immunologiae et therapiae experimentalis*, 60(4), pp.251–66.

Vecil, G.G. et al., 2000. Interleukin-1 is a key regulator of matrix metalloproteinase-9 expression in human neurons in culture and following mouse brain trauma in vivo. *Journal of Neuroscience Research*, 61(2), pp.212–224.

Veerhuis, R., Nielsen, H.M. & Tenner, A.J., 2011. Complement in the brain. *Molecular immunology*, 48(14), pp.1592–603.

Verge, G.M. et al., 2004. Fractalkine (CX3CL1) and fractalkine receptor (CX3CR1) distribution in spinal cord and dorsal root ganglia under basal and neuropathic pain conditions. *European Journal of Neuroscience*, 20(5), pp.1150–1160.

Verrecchia, T. et al., 1995. Non-stealth (poly(lactic acid/albumin)) and stealth (poly(lactic acid-polyethylene glycol)) nanoparticles as injectable drug carriers. *Journal of Controlled Release*, 36(1–2), pp.49–61.

Vinet, J. et al., 2012. Neuroprotective function for ramified microglia in hippocampal excitotoxicity. *Journal of neuroinflammation*, 9(1), p.27.

Vitkovic, L. et al., 2000. Cytokine signals propagate through the brain. *Molecular Psychiatry*, 5(6), pp.604–615.

Vukic, V. et al., 2009. Expression of inflammatory genes induced by beta-amyloid peptides in human brain endothelial cells and in Alzheimer's brain is mediated by the JNK-AP1 signaling pathway. *Neurobiology of Disease*, 34(1), pp.95–106.

Walker, D.G. & Lue, L.-F., 2015. Immune phenotypes of microglia in human neurodegenerative disease: challenges to detecting microglial polarization in human brains. *Alzheimer's research & therapy*, 7(1), p.56.

Wang, A.L. et al., 2005. Minocycline inhibits LPS-induced retinal microglia activation. *Neurochemistry International*, 47(1–2), pp.152–158.

Wang, X. et al., 2009. Inducible nitric-oxide synthase expression is regulated by mitogen-activated protein kinase phosphatase-1. *The Journal of biological chemistry*, 284(40), pp.27123–34.

Wang, Y. et al., 2011. Microglial activation, recruitment and phagocytosis as linked phenomena in ferric oxide nanoparticle exposure. *Toxicology Letters*, 205(1), pp.26–37.

Webster, S.D. et al., 2000. Complement component C1q modulates the phagocytosis of Abeta by microglia. *Experimental neurology*, 161(1), pp.127–38.

Wei, J. et al., 2013. Differences in microglia activation between rats-derived cell and mice-derived cell after stimulating by soluble antigen of IV larva from Angiostrongylus cantonensis in vitro. *Parasitology Research*, 112(1), pp.207–214.

Welch, J.S. et al., 2002. TH2 Cytokines and Allergic Challenge Induce Ym1 Expression in Macrophages by a STAT6-dependent Mechanism. *Journal of Biological Chemistry*, 277(45), pp.42821–42829.

Wessman, S.J. & Levings, R.L., 1999. Benefits and risks due to animal serum used in cell culture production. *Developments in biological standardization*, 99, pp.3–8.

Who & Alzheimer's, 2012. WHO | Dementia: a public health priority. *who*.

Williams, K., 1997. Interactions of polyamines with ion channels. *The Biochemical journal*, 325 (Pt 2)(Pt 2), pp.289–97.

Williams, K.C. et al., 1995. Antigen presentation by human fetal astrocytes with the cooperative effect of microglia or the microglial-derived cytokine IL-1. *The Journal of neuroscience : the official journal of the Society for Neuroscience*, 15(3 Pt 1), pp.1869–1878.

Winblad, B. et al., 2016. Defeating Alzheimer's disease and other dementias: a priority for European science and society. *The Lancet. Neurology*, 15(5), pp.455–532.

Witcher, K.G., Eiferman, D.S. & Godbout, J.P., 2015. Priming the Inflammatory Pump of the CNS after Traumatic Brain Injury. *Trends in Neurosciences*, 38(10), pp.609–620.

Wolf, S.A., Boddeke, H.W.G.M. & Kettenmann, H., 2017. Microglia in Physiology and Disease. *Annual Review of Physiology*, 79(1), pp.619–643.

Wong, M.L. & Medrano, J.F., 2005. Real-time PCR for mRNA quantitation. *BioTechniques*, 39(1), pp.75–85.

Woodroofe, M.N. et al., 1991. Detection of interleukin-1 and interleukin-6 in adult rat brain, following mechanical injury, by in vivo microdialysis: evidence of a role for microglia in cytokine production. *Journal of Neuroimmunology*, 33(3), pp.227–236.

Wu, D.-C. et al., 2006. The inflammatory NADPH oxidase enzyme modulates motor neuron degeneration in amyotrophic lateral sclerosis mice. *Proceedings of the National Academy of Sciences of the United States of America*, 103(32), pp.12132–7.

Wu, T. et al., 2016. Facile Hydrothermal Synthesis of Fe_3O_4/C Core–Shell Nanorings for Efficient Low-Frequency Microwave Absorption. *ACS Applied Materials & Interfaces*, 8(11), pp.7370–7380.

Wuchert, F. et al., 2008. Rat area postrema microglial cells act as sensors for the toll-like receptor-4 agonist lipopolysaccharide. *Journal of Neuroimmunology*, 204(1–2), pp.66–74.

Xue, Y., Wu, J. & Sun, J., 2012. Four types of inorganic nanoparticles stimulate the inflammatory reaction in brain microglia and damage neurons in vitro. *Toxicology Letters*, 214(2), pp.91–98.

Yang, J. et al., 2009. Adult neural stem cells expressing IL-10 confer potent immunomodulation and remyelination in experimental autoimmune encephalitis. *Journal of Clinical Investigation*, 119(12), pp.3678–3691.

Yang, X. et al., 2017. Resveratrol regulates microglia M1/M2 polarization via PGC-1α in conditions of neuroinflammatory injury. *Brain, Behavior, and Immunity*, 64, pp.162–172.

Yankner, B.A., DUFFY, L.K. & Kirschner, D.A., 1990. Neurotrophic and neurotoxic effects of amyloid beta protein: reversal by tachykinin neuropeptides. *Science*, 250(4978), pp.279–282.

Yao, S. et al., 2006. Long-term self-renewal and directed differentiation of human embryonic stem cells in chemically defined conditions. *Proceedings of the National Academy of Sciences*, 103(18), pp.6907–6912.

Ye, S.-M. & Johnson, R.W., 2001. An Age-Related Decline in Interleukin-10 May Contribute to the Increased Expression of Interleukin-6 in Brain of Aged Mice. *Neuroimmunomodulation*, 9(4), pp.183–192.

Yousif, N.M. et al., 2018. Activation of EP $_2$ receptor suppresses poly(I: C) and LPS-mediated inflammation in primary microglia and organotypic hippocampal slice cultures: Contributing role for MAPKs. *Glia*, 66(4), pp.708–724.

Zawadzka, M. et al., 2012. Early steps of microglial activation are directly affected by neuroprotectant FK506 in both in vitro inflammation and in rat model of stroke. *Journal of molecular medicine (Berlin, Germany)*, 90(12), pp.1459–71.

Zeiadeh, I. et al., 2018. Strategies for Enhancing the Permeation of CNS-Active Drugs through the Blood-Brain Barrier: A Review. *Molecules*, 23(6), p.1289.

Zhang, G. et al., 2013. Hypothalamic programming of systemic ageing involving IKK-β, NF-κB and GnRH. *Nature*, 497(7448), pp.211–216.

Zhang, Q.-S. et al., 2017. Pathological α-synuclein exacerbates the progression of Parkinson's disease through microglial activation. *Toxicology Letters*, 265, pp.30–37.

Zhang, S. et al., 2011. CD200-CD200R dysfunction exacerbates microglial activation and dopaminergic neurodegeneration in a rat model of Parkinson's disease. *Journal of neuroinflammation*, 8, p.154.

Zhang, S.C. et al., 2001. Reactive microglia in dysmyelination and demyelination. *Glia*, 34(2), pp.101–9.

Zhang, W. et al., 2005. Aggregated α-synuclein activates microglia: a process leading to disease progression in Parkinson's disease. *The FASEB Journal*, 19(6), pp.533–542.

Zhang, X. & Morrison, D.C., 1993. Lipopolysaccharide-induced selective priming effects on tumor necrosis factor alpha and nitric oxide production in mouse peritoneal macrophages. *Journal of Experimental Medicine*, 177(2), pp.511–516.

Zhang, Y. et al., 2003. Intravenous Nonviral Gene Therapy Causes Normalization of Striatal Tyrosine Hydroxylase and Reversal of Motor Impairment in Experimental Parkinsonism. *Human Gene Therapy*, 14(1), pp.1–12.

Zhang, Y., Kohler, N. & Zhang, M., 2002. Surface modification of superparamagnetic magnetite nanoparticles and their intracellular uptake. *Biomaterials*, 23(7), pp.1553–1561.

Zhao, W. et al., 2006. Protective effects of an anti-inflammatory cytokine, interleukin-4, on motoneuron toxicity induced by activated microglia. *Journal of Neurochemistry*, 99(4), pp.1176–1187.

Zhou, X. et al., 2012. TGFβ signalling plays an important role in IL4-induced alternative activation of microglia. *Journal of Neuroinflammation*, 9(1), p.210.

Zhu, B.C.-R. & Laine, R.A., 1989. Purification of Acetyllactosamine-Specific Tomato Lectin by Erythroglycan-Sepharose Affinity Chromatography. *Preparative Biochemistry*, 19(4), pp.341–350.

Zhu, J.Y. et al., 2016. Preferential Cancer Cell Self-Recognition and Tumor Self-Targeting by Coating Nanoparticles with Homotypic Cancer Cell Membranes. *Nano Letters*, 16(9), pp.5895–5901.

Zhu, X. et al., 2017. Surface De-PEGylation Controls Nanoparticle-Mediated siRNA Delivery In Vitro and In Vivo. *Theranostics*, 7(7), pp.1990–2002.

Ziebell, J.M. et al., 2016. Aging with a traumatic brain injury: Could behavioral morbidities and endocrine symptoms be influenced by microglial priming? *Brain, behavior, and immunity*, 59, pp.1–7.

Zielasek, J. et al., 1992. Production of nitrite by neonatal rat microglial cells/ brain macrophages. *Cellular Immunology*, 141(1), pp.111–120.

Zielasek, J. & Hartung, H.-P., 1996. Molecular mechanisms of microglial activation. *Advances in Neuroimmunology*, 6(2), pp.191–222.

Zitvogel, L., Kepp, O. & Kroemer, G., 2010. Decoding cell death signals in inflammation and immunity. *Cell*, 140(6), pp.798–804.